SYNTHESIS OF BIOLOGICALLY ACTIVE COMPOUNDS

A Thesis submitted to the

University of Mumbai

for the

Ph. D. Degree in Organic Chemistry

Submitted by

VIVEKANAND VIDYADHAR BHAGWAT

Under the Guidance of

Dr. Mukund K. Gurjar

Division of Organic Chemistry: Technology,

National Chemical Laboratory, Pune

March 2007

DEDICATED TO

MY PARENTS

AND ***FAMILY***

NATIONAL CHEMICAL LABORATORY

Dr. Homi Bhabha Road, PUNE - 411 008 INDIA.

Dr. M. K. Gurjar

Telephone and Fax: + 91-20-5893614
+ 91-20-5882456

Deputy Director & Head,
Division of Organic Chemistry: Technology.

E-mail: mk.gurjar@dalton.ncl.res.in
Website: http://www.ncl-india.org

CERTIFICATE

The research work presented in this thesis entitled **"*Synthesis of Biologically Active Compounds*"** has been carried out under my supervision and is bonafide work of **Mr. Vivekanand Vidyadhar Bhagwat**. This work is original and has not been submitted for any other degree or diploma of this or any other University.

Pune-8
Date:

(Dr. M. K. Gurjar)
(Research Guide)

STATEMENT BY THE CANDIDATE

As required by the University Ordnance 770, I wish to state that the work embodied in this thesis titled "**Synthesis of Biologically Active Compounds**" forms my own contribution to the research work carried out under the guidance of **Dr. Mukund K. Gurjar** at the **Division of Organic Chemistry: Technology, National Chemical Laboratory, Pune**. This work has not been submitted for any other degree of this or any other University. Whenever references have been made to previous works of others it has been clearly indicated as such and included in the bibliography.

(V.V. Bhagwat)

Candidate

Certified by

Dr. M.K.Gurjar

Abbrevations

Ac	Acetyl
Ac_2O	Acetic anhydride
Bn	Benzyl
BnBr	Benzyl bromide
BnCl	Benzyl chloride
Boc	tert-Butoxy Carbonyl
BTAC	Benzyl Triethyl Ammonium Chloride
CBz	Benzyl Oxy Carbonyl
CSA	(±)-Camphor-10-Sulfonic Acid
DBTO	Di n-Butyl Tin Oxide
DCC	Dicyclohexylcarbodiimide
DIBAL-H	Diisobutylaluminium hydride
DIPEA	Diisopropylethylamine
DMAP	N, N'-Dimethylaminopyridine
DMF	N, N'-Dimethylformamide
DMP	2,2-Dimethoxypropane
DMSO	Dimethyl sulfoxide
Et	Ethyl
EtOAc	Ethyl acetate
EtOEt, Et_2O	Diethylether
EtOH	Ethanol
F-MOC	Fluorenyl Methoxy Carbonyl
Im	Imidazole
LAH	Lithium Alluminium Hydride
mCPBA	m- chloro per benzoic acid
MeOH	Methanol
MOM	Methoxy Methyl
MOM chloride	Chloro Methyl Methyl Ether

NMR	Nuclear Magnetic Resonance
Pd/C	Palladium on carbon
PDC	Pyridiniumdichromate
PMB	para-Methoxy benzyl
PMR	Proton Magnetic Resonance
pTSA	para-Toluenesulfonic acid
Py	Pyridine
TBAF	Tetrabutylammonium fluoride
TBDPS-Cl	tert-Butyldiphenylchlorosilane
TEA	Triethyl amine
THF	Tetrahydrofuran
TPS	tert-Butyldiphenyl silyl
TS-1	Titanium oxide on silica
TsCl	p-Toluenesulphonylchloride
UAA	Unnatural Amino Acid

General Remarks

- Melting points were recorded on Buchi 535 melting point apparatus and are uncorrected.
- Optical rotations were measured with a JASCO DIP 370 digital polarimeter.
- Infrared spectra were scanned on Shimadzu IR 470 and Perkin-Elmer 683 or 1310 spectrometers with sodium chloride optics and are measured in cm-1.
- Proton magnetic resonance spectra were recorded on AC-200 MHz spectrometer with $CDCl_3$ as a deuterated solvent containing tetra methyl silane (TMS) as an internal standard. Chemical shifts have been expressed in ppm units downfield from TMS.
- ^{13}C Nuclear magnetic spectra were recorded on AC-50 MHz, MSL-75 MHz and Bruker-125 MHz spectrometer.
- Mass spectra were recorded on a Finnigan Mat 1210 spectrometer at 70 eV using a direct inlet system.
- All reactions are monitored by Thin Layer chromatography (TLC) carried out on 0.25 mm. E-Merck silica gel plates (60F-254) with UV, I_2 and anisaldehyde in ethanol as development reagents.
- All evaporations were carried out under reduced pressure on Buchi rotary evaporator below 50°C.
- All solvents and reagents were purified and dried by according to procedures given in Vogel's Text Book of Practical Organic Chemistry.
- Silica gel (60-120) used for column chromatography was purchased from ACME Chemical Company, Bombay, India.

Contents

Chapter 3 Hydrogen Bonding in Various Hexose Sugar 3-C Alkynols

ACKNOWLEDGEMENT

I thank the galaxy of great minds, which came across my research career and left permanent impression through their good words and support.

I take this opportunity with immense pleasure to express my deep sense of gratitude to my teacher and research guide Dr. Mukund K. Gurjar, who has helped me a lot to learn and think more about chemistry. I thank him for his excellent guidance, constant encouragement, sincere advice and unstinted support during all the tough times of my Ph. D. life. I do sincerely acknowledge the freedom rendered to me by him for independent thinking, planning and executing the research. I consider very fortunate for my association with him which has given a decisive turn and a significant boost in my career.

I thank Dr. C.V. Ramana who introduced me to the early school of research with meritorious teaching, so-friendly attitude, spectacular support, distinct advice and conducive environ for my research.

I thank Dr. M.K. Dongare and Dr. C.V. Rode for their keen interest, constant encouragement and moralsupport during my research work.

I thank Dr. R.A. Joshi, Dr. Mrs. R.R. Joshi, Dr. M.N. Deshmukh, and Dr. U.R. Kalkote for timely help and discussion. The help of Mr. I. Siva Kumar is gratefully acknowledged.

I wholeheartedly thank my adorable off and on campus comrades in Pune who made the life memorable and pleasant. It is difficult to phrase their boundless love and rock steady support.

I extend my thanks to technical staff of NCL for their multifarious assistance.

Thanks to DNCL for providing the facilities and CSIR, New Delhi for financial support.

I thank my beloved wife for constant help and moral boost throughout the tough times during my research career. Her keen interest during this time has brought me up to this stage. Her devotion is duly acknowledged.

Last, thanks to my parents who shaped me to this status with their bluntless vision and selfless agenda. Here I take this opportunity to thank my uncle, and aunty for their help and encouragement. My dear Grandfather needs special mention here.

Vivekanand Bhagwat

CHAPTER I:
SOLID ACID CATALYSTS MEDIATED ORGANIC TRANSFORMATIONS

1.1 SYNTHESIS OF CHIRAL MORPHOLINES USING BECKMANN REARRANGEMENT

1.1.1 INTRODUCTION

1.1.2 PRESENT WORK

1.2 EPOXIDATION OF INTERNAL OLEFINS CATALYZED BY SOLID ACID CATALYSTS: A SYSTEMATIC INVESTIGATION

1.2.1 INTRODUCTION

1.2.2 PRESENT WORK

1.3 CATALYST CHARACTERIZATION

1.4 EXPERIMENTAL PROCEDURE

1.5 REFERENCES

Introduction

Morpholines are widely used in organic synthesis; however their use is most frequently restricted to application as a simple base or as a N-alkylating agent. A much less explored field is the synthesis of *C*-functionalized morpholine derivatives, a compound class that may have important applications in the ongoing search for new pharmaceutically active compounds. *C*-Functionalized morpholines are found in various natural products as well as in drugs. Since morpholines are often derived from amino alcohols and amino acids, introduction of chirality is often achieved starting from the corresponding enantiopure amino alcohols or amino acids or other sources from the chiral pool. In 1956 the first synthesis of an enantiomerically pure morpholine[1] was reported. L-Ephedrine was reacted with chloroethanol to give phendimetrazine (fig. 1).

Fig. 1 First synthesis of chiral morpholine reported

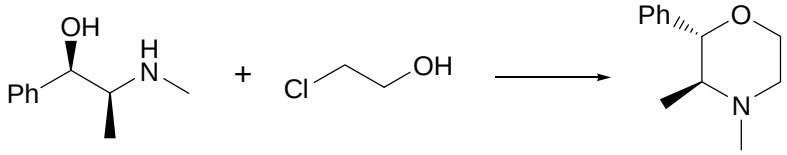

A **B**

C-Alkylated morpholines constitute an important compound class considering their frequent occurrence in natural products and biologically active compounds. *C*-alkylated morpholines and morpholinones have been often applied as synthetic tools in various

Fig. 2 Structure of Polygonapholin

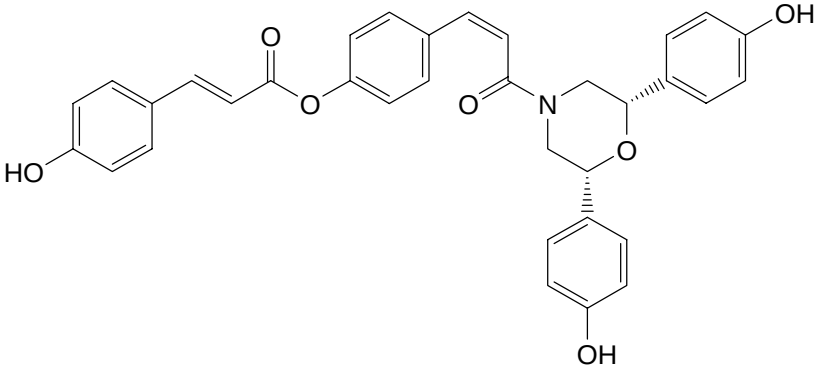

syntheses[2], of which a series of literature examples has been summarized.

Lin and co-workers have reported the isolation of polygonapholine (fig. 2) from a methanol extract of the rhizome of *Polygonatum alte-lobatum*, which had been used as a tonic drug in Taiwan.[3] The structure of this novel alkaloid, was determined by using spectroscopic methods in combination with molecular modeling. Both morpholine *C*-substituents are *cis*-oriented so that they are occupying equatorial positions in the six-membered ring.

Fig. 3 Structures of various alkaloids isolated from Marine sponge *Chelonaplysilla* sp.

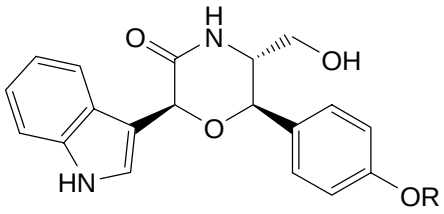

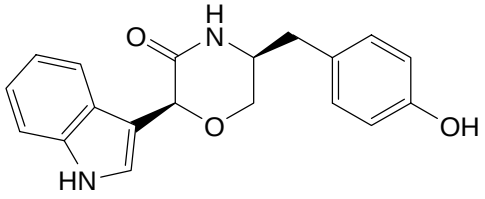

A R = -$(CH_2)_2CN$ **C**

B R = -H

Three novel compounds (shown in fig. 3) are isolated from the digestive glands of toxic mussels *Mytilus galloprovincialis* from the North Adriatic Sea.[4] The structures of these compounds were elucidated using extensive 2D NMR studies combined with molecular mechanics calculations. Of these three compounds, **A** was the only one that proved to be active in a cytotoxicity analysis.

Fig. 4 Bupropion and its derivatives

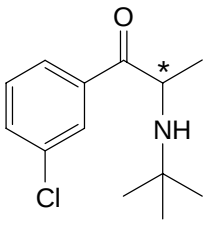

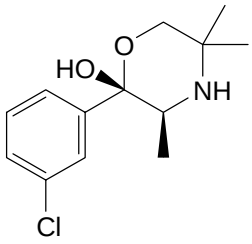

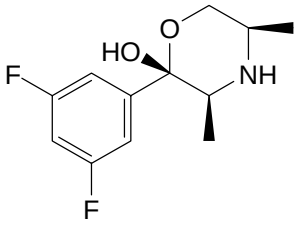

Bupropion **Hydroxybupropion** **1555U88**

Racemic bupropion is the active ingredient of Wellbutrin® (Glaxo Wellcome) marketed for the treatment of depression. Recently, it has also been approved as an aid to smoking cessation under the brand name of Zyban® (Glaxo Wellcome). Bupropion is extensively metabolized in the body and the major active metabolite is hydroxybupropion.[5] Enantiopure bupropion has been prepared by chemical synthesis and hydroxybupropion has been separated by chiral columns.[6] Studies have shown that α-aminoketones readily racemize in neutral and basic media.[7] It has been reported that bupropion's therapeutic activity may result from the active hydroxylated metabolite (hydroxybupropion)[8] and structure–activity relationship studies of 2-phenylmorpholinols led to the discovery of 155U888.[9]

Beckmann Rearrangement

The rearrangement of oximes in presence of an acid to form substituted amides is the well known Beckmann rearrangement.[10] Various mineral acids as well as acidic reagents have been tried for this reaction so far. Generally, strong Brønstead/Lewis acids ranging from stoichiometric to catalytic amounts are employed in order to accomplish the Beckmann rearrangement. Among other reagents used have been concentrated H_2SO_4, formic acid, liquid SO_2, $SOC1_2$,[11] HCl-HOAc-Ac_2O, $POC1_3$,[12] and polyphosphoric acid.[13] Heating an oxime of a cyclic ketone, neat, with $A1C1_3$ also leads to the lactam.[14] Treatment of a cyclic ketone with NH_2OSO_3H on silica gel followed by microwave irradiation also gives the lactam.[15] Microwave irradiation of an oxime on Montmorillonite K10 clay gives the amide.[16]

Fig. 5 *General example of Beckmann Rearrnagement*

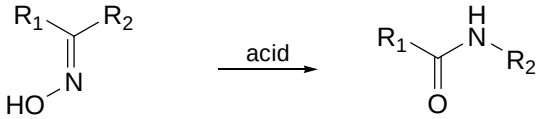

The group that migrates is generally the one anti to the hydroxyl, and this is often used as a method of determining the configuration of the oxime. However, it is not unequivocal. It is known that with some oximes the syn group migrates and that with others, especially where R and R' are both alkyl, mixtures of the two possible amides are obtained. However, this behavior does not necessarily mean that the syn group actually undergoes

migration. In most cases, the oxime undergoes isomerization under the reaction conditions before migration takes place.[17] *The migrating group retains its configuration.*

If there are two or more potential migrating groups, but which migrates is settled by the geometry of the molecule. Only the group trans to the OH migrates. In compounds whose geometry is not restricted in this manner, there still may be eclipsing effects so that the choice of migrating group is largely determined by which group is in the right place in the most stable conformation of the molecule.[18] *However, in some reactions, the molecule may contain several groups that, geometrically at least, have approximately equal chances of migrating. As we know, carbocation stability is enhanced by groups in the order aryl>alkyl>hydrogen, and this normally determines which side loses the OH group. However, exceptions are known, and which group is lost may depend on the reaction conditions.*

Fig. *6 Proposed Mechanism for Beckmann rearrangement*

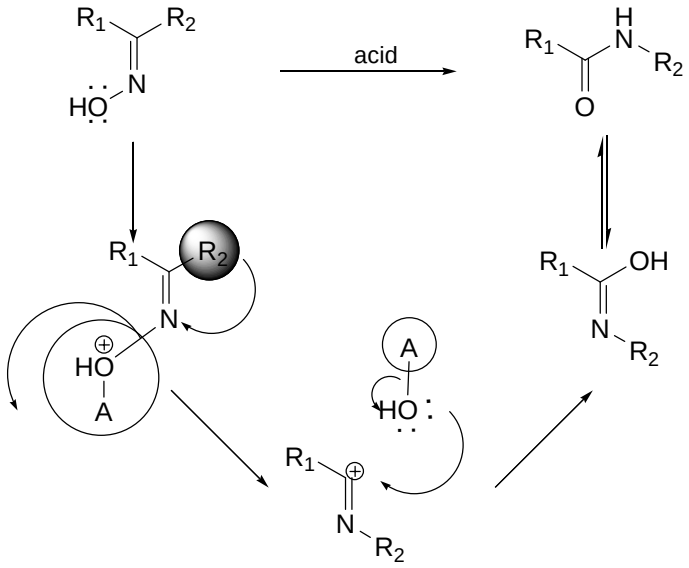

Apart from the question of possible conformational effects, already mentioned, there is also the fact that whether the group R or R' migrates is determined not only by the relative inherent migrating abilities of R and R' but also by whether the group that does not migrate is better at stabilizing the positive charge that will now be found at the migration origin.[19] *It is possible that in a given case R might be found to migrate less than R', not because it*

actually has a lower inherent migrating tendency, but because it is much better at stabilizing the positive charge. Migrating ability of a group is also related to its capacity to render anchimeric assistance to the departure of the nucleophyle.[20] *More often than not, migratory aptitudes are in the order aryl >alkyl, but exceptions are known, and the position of hydrogen in this series is often unpredictable. In some cases, migration of hydrogen is preferred to aryl migration; in other cases migration of alkyl is preferred to that of hydrogen. Mixtures are often found, and the isomer that predominates often depends on conditions. For example, the comparison between methyl and ethyl has been made many times in various systems, and in some cases methyl migration and in others ethyl migration has been found to predominate.*[21]

However, it can be said that among aryl migrating groups, electron-donating substituents in the para and meta positions increase the migratory aptitudes, while the same substituents in the ortho positions decrease them. Electron-withdrawing groups decrease migrating ability in all positions. The following are a few of the relative migratory aptitudes determined for aryl groups by Bachmann and Ferguson:[22] *p-anisyl, 500; p-tolyl, 15.7; m-tolyl, 1.95; phenyl, 1.00; p-chlorophenyl, 0.7; o-anisyl, 0.3. For the o-anisyl group, the poor migrating ability probably has a steric cause, while for the others there is a fair correlation with activation or deactivation of electrophilic aromatic substitution, which is what the process is with respect to the benzene ring. It has been reported that at least in certain systems acyl groups have a greater migratory aptitude than alkyl groups.*[23]

The scope of the reaction is quite broad. Both R and R' may be alkyl, aryl, or hydrogen. However, hydrogen very seldom migrates, so the reaction is not generally a means of converting aldoximes to unsubstituted amides $RCONH_2$. When the oxime is derived from an alkyl aryl ketone, it is generally the aryl group that preferentially migrates. The oximes of cyclic ketones give ring enlargement.

Morpholines have been widely applied as chiral auxiliaries.[24] Both the Boc- and Cbz-protected systems were shown to be useful templates. The synthesis of one of such templates is shown in fig. 7.[25] Reduction of the oxime, resulting from reaction of benzoin with hydroxylamine, furnished racemic intermediate, which was resolved using L-glutamic acid giving both the distereoisomers with more than 98% ee. Subsequent N-alkylation with ethyl

bromoacetate, N-protection with either $(Boc)_2O$ or CbzCl, followed by acid-mediated cyclization yielded the templates in 62– 65%. Apart from their use as chiral auxiliaries in asymmetric synthesis, morpholines and morpholinones are widely used scaffolds in the medicinal chemistry. There are several methods for the syntheses of chiral morpholinones and in general are synthesized from respective amino acids.

Fig. 7 Synthesis of morpholine derivative used as a chiral auxiliary

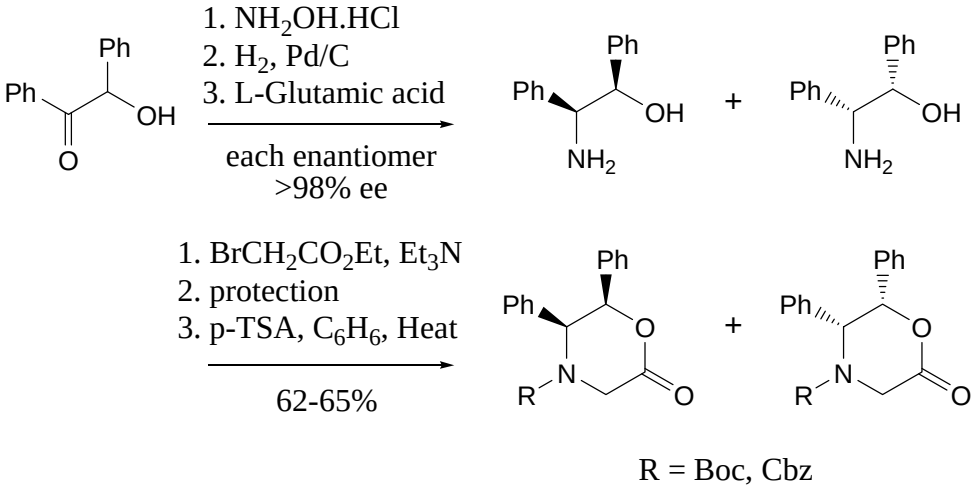

It should be quite clear by now that so far morpholins or morpholinones that have been synthesized are mainly either from amino acids or from the respective amino alcohols. This limit functional and stereochemical diversity of these skeletons, as one can have either one or a maximum of two chiral centers by using amino acids or their corresponding alcohols. Apart from very few examples encountered so far not much work has been done in developing the chiral side chain analogues of morpholins. Various attempts to synthesize the chiral morpholins have resulted into the open chain or ring contraction products.[5b] Thus it seems quiet difficult to synthesize the highly functionalized morpholin analogues in a very cost effective manner. Considering the rich stereochemical diversity available with carbohydrate chiral pool, we have initiated a program to convert the carbohydrate derived building blocks to chiral morpholins and morpholinones which is the focus of present chapter.

Present Work

So far there have been various methods known for synthesis of chiral morpholine derivatives. Chiral morpholinone analogues find importance in various organic transformations and have well applied in medicinal chemistry. Oximes derived from erythronolides and cyclohexitol derivatives have been shown to undergo the Beckmann rearrangement yielding valuable drug candidates such as azythromycin, and polyhydroxycyclic lactams with varying ring sizes. Nonetheless, the use of catalytic methods is scarce. However, the availability of densely functionalized morpholinones with multiple chiral centers is limited and methods available in this regard are very few. Considering the rich stereochemical diversity and easy availability of various carbohydrates, we planned to convert suitably functionalized carbohydrate templates to the highly functionalized morpholine analogues. As indicated in the Scheme 1, we are interested to explore the possibility of Beckmann rearran1.1.2gement on sugar ketoximes where in one can address the synthesis of chiral morpholinones. To the best of our knowledge, there is no report concerning the Beckmann rearrangement of sugar oximes. However, the possibility of formation of a regiomeric product during the Beckmann process is not ruled out.

Scheme 1. Intended Beckmann Rearrangement on Sugar Oximes

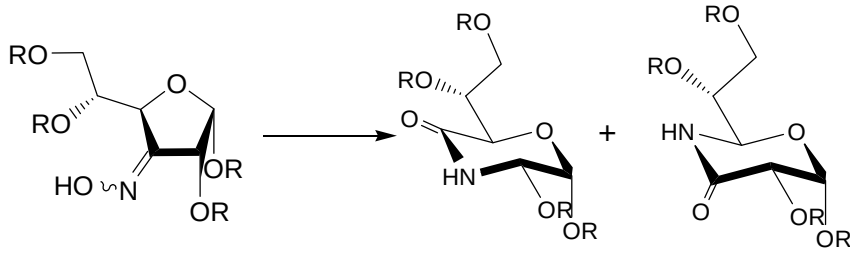

The Beckmann rearrangement is a well-known transformation of keto-oximes to *N*-substituted amides in the presence of an acid. Generally, strong Brønstead/Lewis acids ranging from stoichiometric to catalytic amounts are employed in order to accomplish the Beckmann rearrangement. Various ring expansions have already been studied. The very well known synthesis of ε-caprolactum is one such example.

In case of furanose systems of monosaccharides, the generation of an oxime at appropriate position and its rearrangement can lead to synthesis of a morpholine analogue which can be functionalized at any position of interest. As we all know that Beckmann rearrangement is an acid catalyzed reaction and the acid sensitive protecting groups generally employed for the free hydroxyl groups in sugars can lead to some problems.

To circumvent the harsh reaction conditions generally used for the Beckmann rearrangement coupled with a desire to use clean and environmentally benign reusable catalysts, we selected two different catalyst conditions i.e. Beta zeolite cat. **1** and MoO_3 on SiO_2 with 20% molybdenum cat. **2**. The TPD graph for these two catalysts is given in fig. 1 for comparison. It is quiet evident from this graph that at a temperature range of 100 – 200^{0}C, both these catalysts show increasing acidity (confirmed by increasing concentration of ammonia). In other words, at elevated temperature both these catalysts show large no. of *Lewis* acid sites inside the pores. For the systems of interest we thus selected these two catalysts.

Fig. 1 NH_3- TPD of a) Mo/SiO_2 b) Beta zeolite

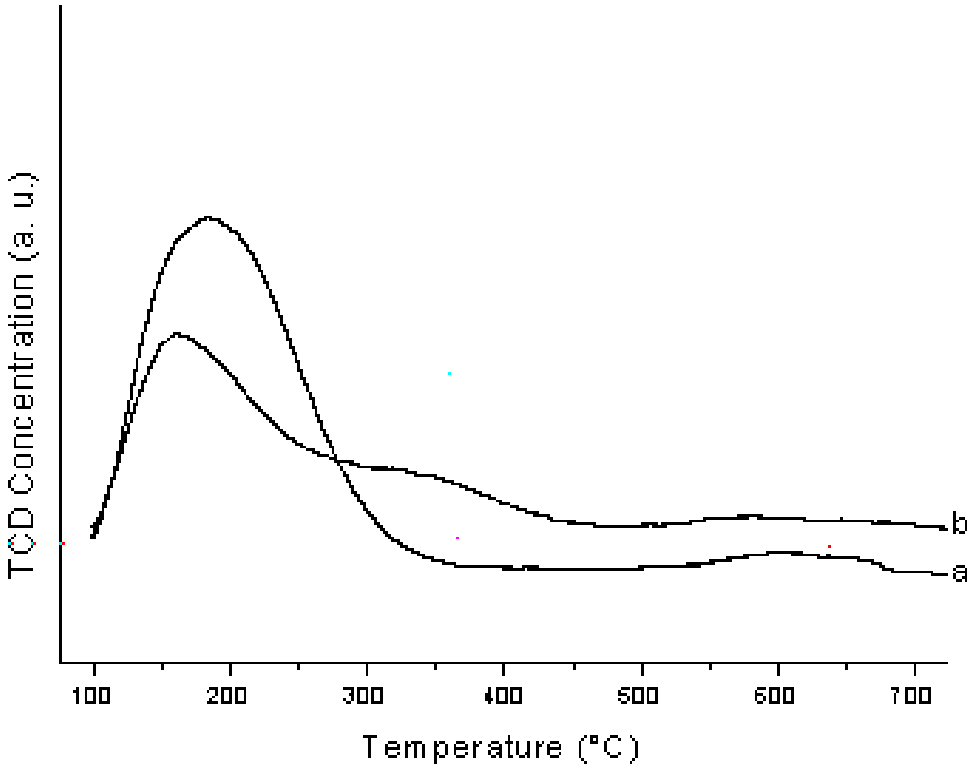

To check the application of the new and unexplored catalysts, initially it was decided to test these catalyst systems with the known substrates. These substrates are selected such that either they are easily available or can be synthesized in some very simple steps. A comprehensive listing of various substrates and the yields with respect to the two different catalysts used in this regard is given in Table 1.

Table 1 Beckmann rearrangement using solid acid catalysts 1 and 2

Entry	Starting Material	Product	Yield (%)	
			Beta-Zeolite	MoO_3/ SiO_2
1	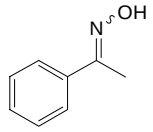	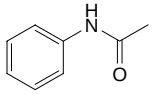	92	95
2	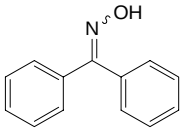	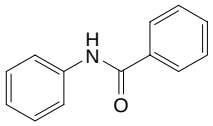	94	97
3	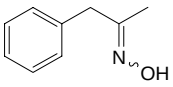	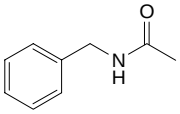	81	91
4	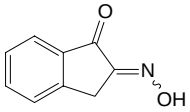	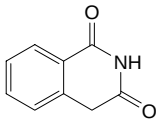	83	87
5	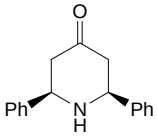	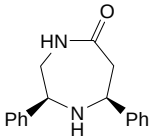	79	89
6	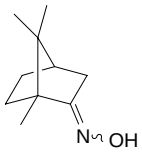	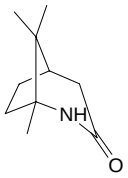	83	96

In order to apply the scope of these reagents to the synthesis of chiral morpholinones, the oximes **3** – **6** which can be easily derived from glucose (Table 2; **3** and **4**) and xylose (Table 2; **5** and **6**) are selected. The rearrangement of sugar-oxime **3** was carried out in the presence of catalyst **1** as well as **2** in refluxing ethanol. With both catalysts, the reactions are

clean and resulted in an inseparable regioisomeric mixture. The amides **7** and **8** are obtained in very good yields and with moderate regioselectivity (3: 2).

Structural Characterization of compounds 7 and 8.

Although we could see well separated peaks for two products in ^{1}H and ^{13}C NMRs, however, attempts to isolate and characterize them separately were met with failure. In order to establish the constitution of the major and minor products in the resulting mixture, a systematic structural investigation with the help of 1D and 2D NMR was carried out. Considering the fact that Beckmann rearrangement is stereospecific and occurs with retention of configuration at the migrating carbon center, one can assume that these two are the regiomeric products **A** and **B**. However, with out ignoring the possibility of epimerization we have considered the two possible epimeric structures **C** and **D** for structural identification (fig.2).

Fig. 2 Different compounds possible during the course of rearrangement of **3**

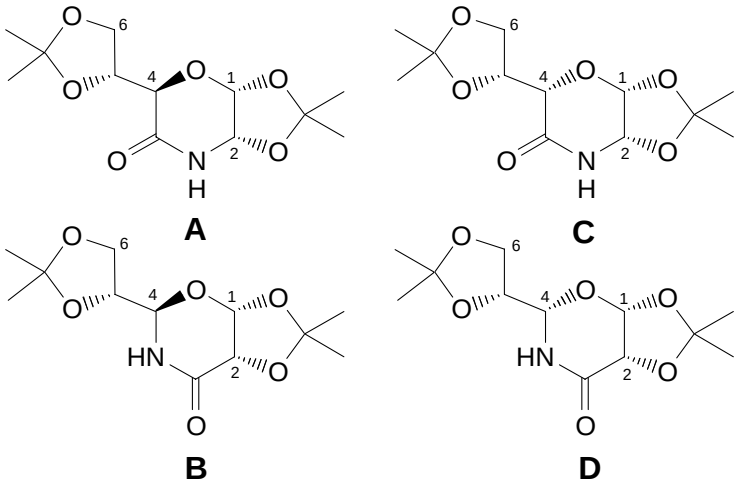

The regioisomer **A** can be anticipated by migration of C-2 with net retention of configuration at C-4. The possibility of epimerization in compound A is only at C4 as C1 and C2 are part of a dioxolane ring which prefers a *cis*-fusion in general. The regioisomer **B** can be concluded by migration of C-4 with retention of configuration at C-4. The possibility of epierization in case of B could be only at C-4 again on the same strain grounds. From the spectroscopic methods it is very clear that only two of these isomers are present. So to

determine those two isomers, it was decided to carry out various decoupling experiments of the proton NMR obtained for the rearrangement of 3-deoxy, 3-ketoxime 1,2,5,6 di-*O*-isopropylidine-α-D-ribofuranoside **3**.

Fig. 3 Irradiation of a signal at δ 8.87

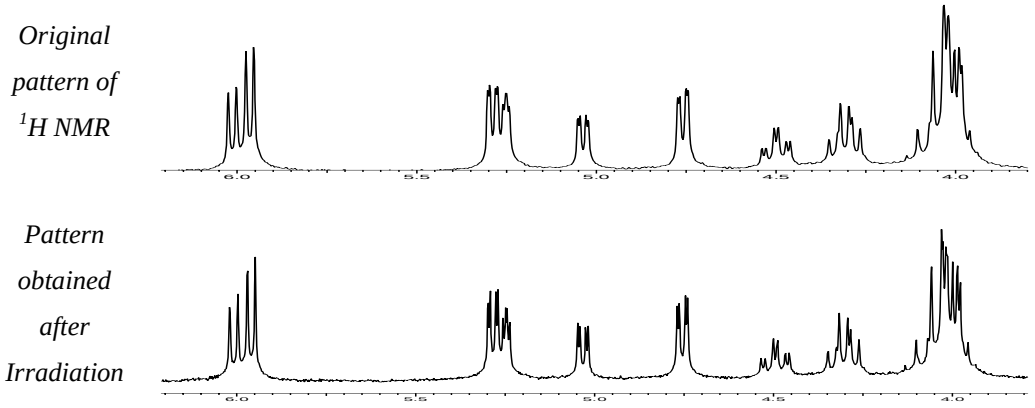

When the signal at δ 8.87 value was irradiated, we observe no change in NMR, which was expected. This confirms that, this signal is observed for the amide proton of both isomers which does not couple with any of the nearby protons. This decoupling experiment is shown in fig.3 above.

Fig. 4 Irradiation of a signal at δ 5.98

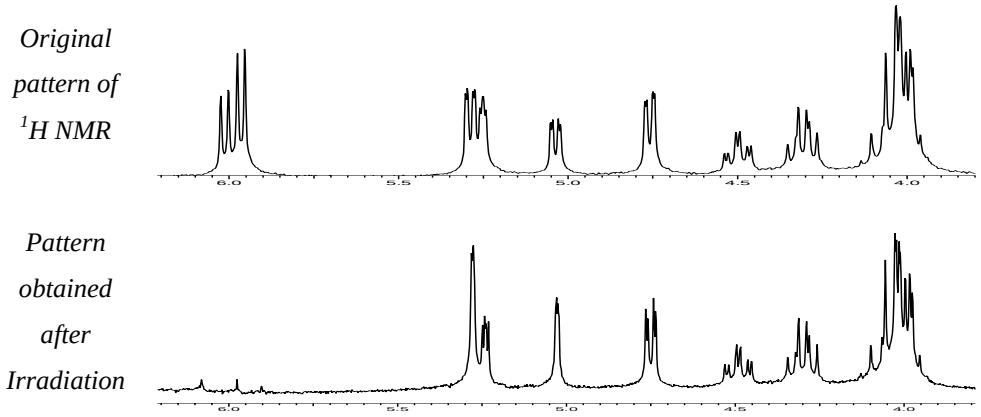

When the irradiation was carried out at around δ 5.98, we observe a peak at δ 5.28 changes to doublet (*J* = 1.2 Hz). Also a peak at δ 5.03 changes to doublet (*J* = 1.3 Hz). This confirms that, this particular signal is observed for H-1 of both isomers and the signal at δ 5.28 value is assigned for H-2 of major isomer and the signal at δ 5.03 value is assigned for H-2 of minor isomer. The major isomers are the ones that show the taller peaks in comparison to minor isomers. This decoupling experiment is shown in fig.4.

Fig. 5 Irradiation of a signal at δ 5.25

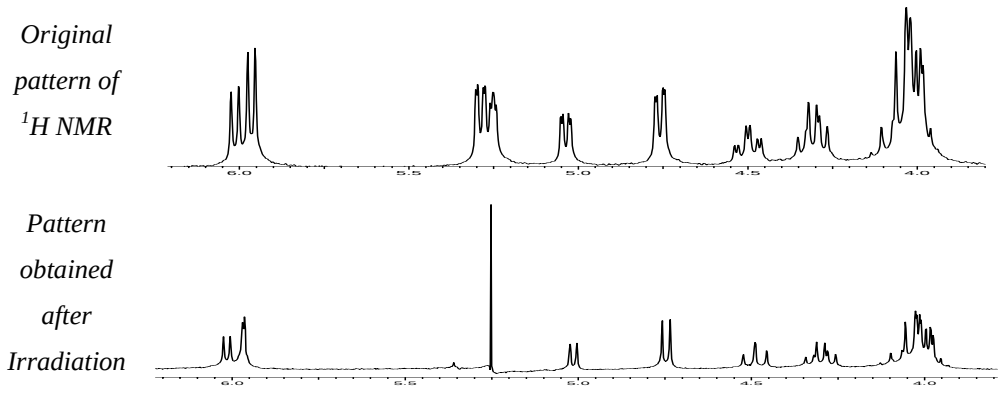

When the signal at δ 5.25 was irradiated, we observe a peak at δ 5.94 changes to doublet (*J* = 1.18 Hz) which is previously assigned as H-1 of the major isomer. A peak at δ 5.03 changes to doublet (*J* = 4.1 Hz), a peak at δ 4.76 changes to doublet (*J* = 4.7 Hz) and a peak at δ 4.49 changes to triplet (*J* = 6.7 Hz). The signals at δ 5.03 and δ 4.49 are accounted for minor isomer and the signal at δ 4.76 is accounted for major isomer. Thus confirms that, this particular signal is observed for H-2 of major isomer and H-4 of the minor isomer. The signal at δ 5.03 value is assigned for H-2 of minor isomer, the signal at δ 4.76 value is assigned for H-4 of major isomer and the signal at δ 4.49 value is assigned for H-5 of the minor isomer. A long range coupling i.e. 1–5 coupling (*J* = 1.2 – 1.3 Hz) between H-2 and H-4 is observed in case of both the isomers of this mixture. This decoupling experiment is shown in fig.5 above.

When the signal at δ 5.03 value was irradiated, we observe a peak at δ 6.01 changes to singlet which is previously assigned as H-1 of the minor isomer. Also a peak at δ 5.24 changes to doublet (*J* = 2 Hz) which is previously assigned as H-4 of the minor isomer. This

confirms that this signal arise from the minor isomer and is assigned for H-2. This decoupling experiment is shown in fig. 6.

Fig. 6 Irradiation of a signal at δ 5.03

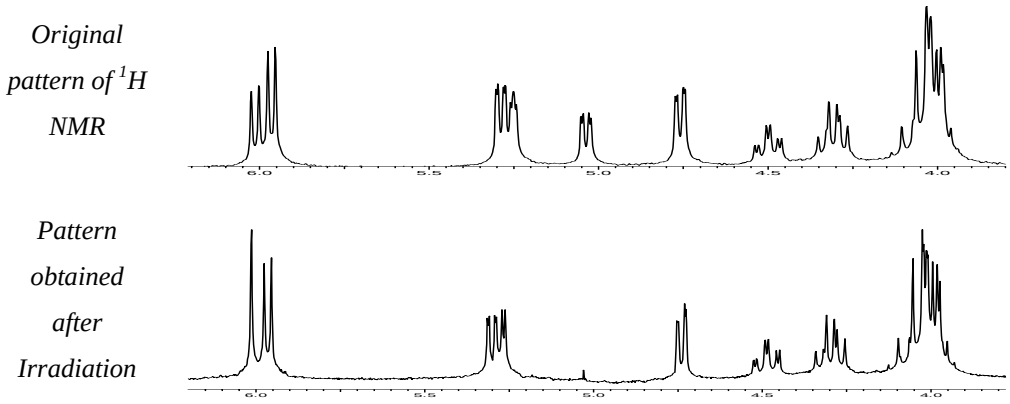

When the irradiation of a signal at δ 4.75 was carried out, we observe a peak at δ 5.28 changes to doublet (J = 4.3 Hz) which is previously assigned as H-1 of the major isomer. Also a peak at δ 4.3 changes to triplet (J = 6.3 Hz). This confirms that this signal arise from the major isomer and is assigned for H-4. This decoupling experiment is shown in fig. 7 below.

Fig. 7 Irradiation of a signal at δ 4.75

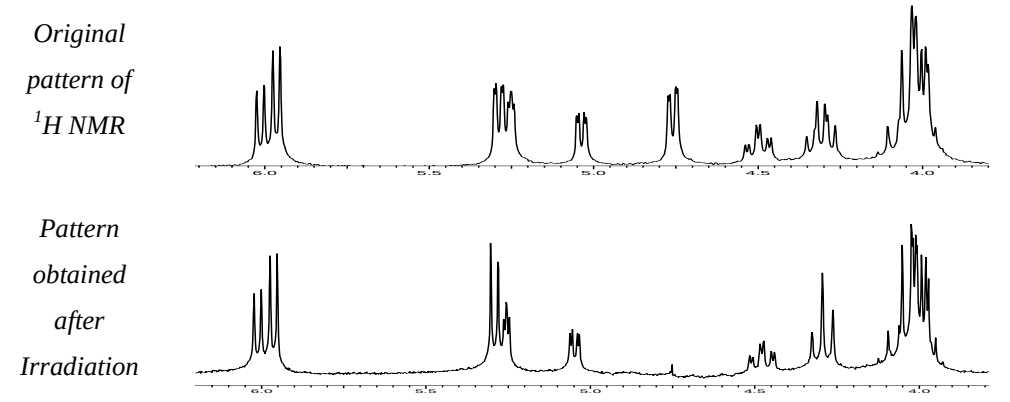

The observation of H-2 of major and H-4 of minor isomers close to each other confirms the formation of regioisomeric mixture of compounds. Because, the environment of

both these protons is similar. Both these protons are bared by a carbon which is attached to a nitrogen as well as an oxygen atom. The long range coupling is observed between H-2 and H-4 for both the isomers. This is possible only for the isomers, which orient themselves in space baring relatively *trans* geometry. Had it been the case of a mixture of epimers then in any case such coupling should not have been observed since these protons in both the case bare relatively *cis* geometry. This study confirms the presence of regioisomers.

Fig. 6 Three dimensional conformations of structures **A** and **B**

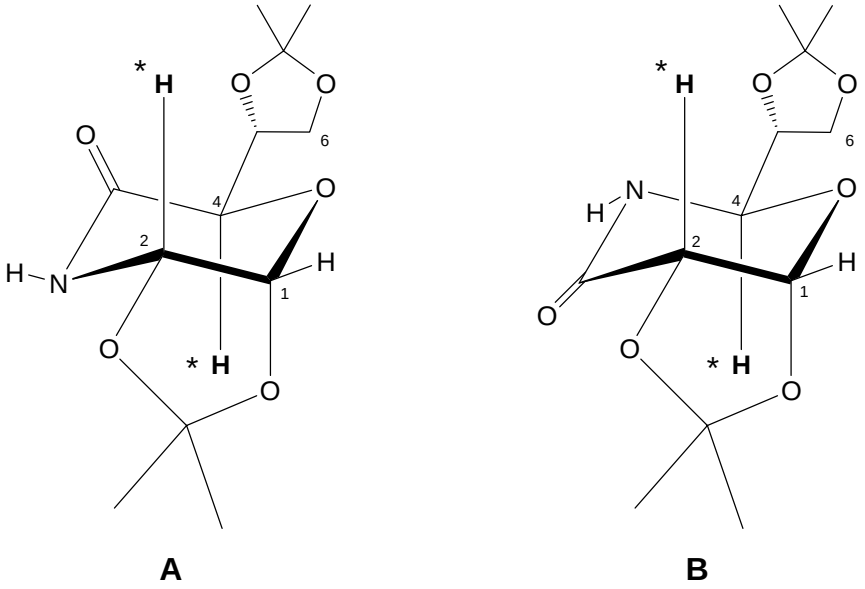

We next focused on oximes **4** – **6**. As indicated in Table 2, with oximes **4** and **5**, the rearrangement was smooth and resulted in regiomeric mixtures. In case of 6 we encounterd a complex reaction mixture observed may be due to the deprotection of the silyl protecting group during the course of reaction. Otherwise the sequence worked well and the mixture of isomers was obtained in fairly good yields. The catalysts show fairly good activity even after recycled up to three times. In case of MoO_3 on SiO_2 leaching of catalyst is observed and the catalyst looses the *Lewis* acidity slowly, when used after fourth time. Otherwise the regioselectivity for oximes **3** – **5** was found to be independent of the catalyst used. This indicated that both catalysts can facilitate the rearrangement but the regioselectivity is governed by stereoelectronic factors. Also, the protecting groups employed *i.e* ketals

(isopropylidine and cyclohexylidine) and benzyl ether are stable under the reaction conditions. The individual ratio of isomers obtained is shown in table no. 2.

Table 2 Beckmann rearrangement of sugar oximes

Sr. No.	Starting Material	Products	Yield (%) Beta-Zeolite	Yield (%) MoO_3/SiO_2
1	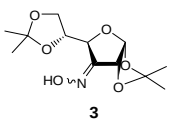 3	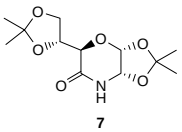 7 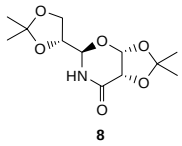 8	85 (3: 2)	82 (3: 2)
2	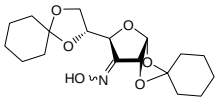 4	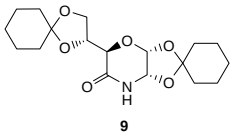 9 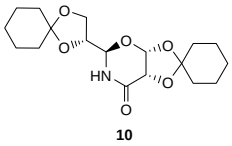 10	84 (3: 2)	87 (3: 2)
3	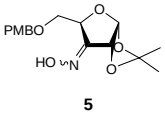 5	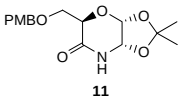 11 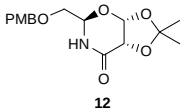 12	71 (3: 1)	70 (3: 1)
4	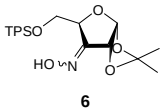 6	Complex Reaction Mixture		

To conclude, a simple and convenient method for the synthesis of densely functionalized chiral morpholinonones from easily available carbohydrate starting materials was developed. Application and comparisons of two different solid acids (beta-zeolite and MoO_3/SiO_2) for a catalytic Beckmann rearrangement is accomplished in sufficiently good to moderate yields. Ours is the first example of a Beckmann rearrangement on carbohydrate templates and importantly using solid catalysts. Commonly employed protecting groups in carbohydrate chemistry such as isopropylidene and cyclohexylidene systems and benzyl ethers were found to be stable under the conditions employed thus establishing the generality of the method employed. The starting compound used for the synthesis is commercially available dextrose (D-Glucose) which is quiet cheap and easily available material. Work in the direction of exploring the potential of the resulting [1,3]-oxazinone and morpholinone derivatives as chiral intermediates is in progress.

Introduction

Epoxidation of alkenes is known with a number of peroxyacids[26], of which *m-chloroperoxybenzoic* has been the most often used. The reaction, called the *Prilezhaev* reaction, has wide utility.[27] Alkyl, aryl, hydroxyl, ester, and other groups may be present, though not amino groups, since these are affected by the reagent. Electron donating groups increase the rate, and the reaction is particularly rapid with tetraalkyl alkenes. Conditions are mild and yields are high. Other peroxyacids, especially peroxyacetic and peroxybenzoic, are also used; trifluoro-peroxyacetic acid[28] and 3,5-dinitro-peroxybenzoic acid[29] are particularly reactive ones.

The mechanism for this reaction was proposed by Bartlett[30], shown in scheme 1. Evidence for this mechanism is as follows

Scheme 1

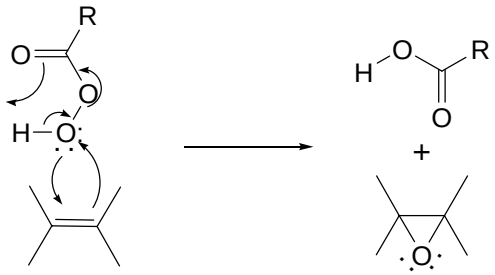

- The reaction is second order. If ionization was the RDS (rate determining step), it would be first order in peroxyacid.
- The reaction readily takes place in non-polar solvents, where formation of ions is inhibited.
- Measurements of the effect on the reaction rate of reaction show that there is no carbocation character in the transition state.[31]
- The addition is stereospecific (i.e., a *trans* alkene gives a *trans* epoxide and a *cis* alkene a *cis* epoxide) even in cases where electron-donating substituents would stabilize a hypothetical carbocation intermediate.

However, where there is a hydroxyl group in the allylic or homoallylic position, the stereospecificity diminishes or disappears, with both *cis* and *trans* isomers giving predominantly or exclusively the product where the incoming oxygen is syn to the hydroxyl group. This probably indicates a transition state in which there is hydrogen bonding between the hydroxyl group and the peroxy acid. Conjugated dienes can be epoxidized (1,2 addition), though the reaction is slower than for corresponding alkenes, but α,β-unsaturated ketones do not generally give epoxides when treated with peroxyacids.[32]

The synthesis of these peracids is achieved from corresponding acids in presence of hydrogen peroxide.[33] This is probably the best known method during the early ages of organic synthesis. For aromatic acids the best catalyst used to achieve peracids is methane sulfonic acid while for aliphatic analogues strong mineral acids are employed.[34] Thus as far as epoxidation of olefins using peracids can be stated as migration of oxygen from the hydrogen peroxide through an organic support i.e. carboxylic acid. Thus various attempts to achieve this reaction with inorganic support resulted successful.

Hydrogen peroxide is probably the best terminal oxidant after dioxygen with respect to environmental and economic considerations.[35] Indeed, in certain circumstances, it is better than oxygen insofar as O_2/ organic mixtures can sometimes spontaneously ignite. As a result, epoxidation systems that use hydrogen peroxide in conjunction with catalytic amounts of cheap, relatively nontoxic metals are potentially viable for large-scale production of inexpensive products, and for specialized applications in development, process, and research. The literature in this area is extensive and difficult to segregate into sharply delineated categories.

Homogeneous coordination complexes: The application of titanium complexes in presence of various chiral or achiral ligands has been a successful attempt in this connection. Various metals in competition to titanium e.g. vanadium, molybdenum, iron, manganese etc. have been attempted to carryout asymmetric epoxidation using different chiral ligands. Various complexes e.g. Mn-Salen complex (HKR catalyst) are available in the market now a days which are used for a variety of applications. Following are a few examples in this regards.

Sharpless Epoxidation: The reaction of an allylic alcohol with tert-butyl hydroperoxide (TBHP) in the presence of $Ti(O\text{-}^{i}Pr)_4$ and diethyl tartrate (DET) to form an

epoxy alcohol of high enantiomeric purity was introduced in 1980.[36] Since then, much has been learned about this asymmetric epoxidation process. The epoxidation as initially described employs a stoichiometric amount of catalyst, even though, as noted in one of the footnotes to the original report, reactions of certain substrates can be carried out with as little as 10% catalyst with little loss of enantioselectivity and some increase in yield. In 1981, the same group reported that, with slight modifications, the same procedure also effects the kinetic resolution of secondary allylic alcohols.[37] Again, it was noted that for certain substrates just 0.25 equiv of catalyst can be effective. Over the next 4 years, no major modifications to the procedure were introduced. The asymmetric epoxidation reaction has proven to have wide applicability, even with use of a stoichiometric amount of catalyst, and has been the subject of an Organic Syntheses preparation.[38] The use of 3Å or 4Å molecular sieves (zeolites) substantially increases the scope of the titanium(IV) catalyzed asymmetric epoxidation of primary allylic alcohols. Whereas without molecular sieves epoxidations employing only 5 to 10 mol % Ti(*O*-^{i}Pr)$_4$ generally lead to low conversion or low enantioselectivity, in the presence of molecular sieves such reactions generally lead to high conversion (>95%) and high enantioselectivity (90-95% ee).[39]

Scheme 2 Sharpless Epoxidation

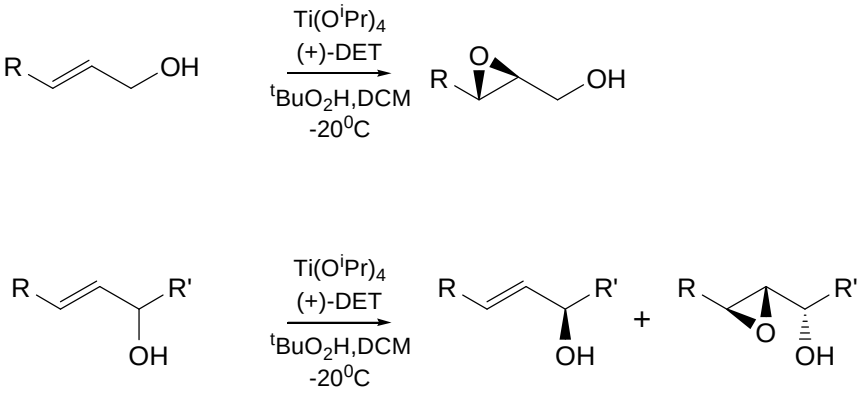

The effect of molecular sieves can be quite dramatic. Several experiments are designed to determine the effect of water and the role of sieves in the catalytic reaction. In one experiment, 10 mol % water was added to a solution of the 10/12% catalyst in dichloromethane at 2°C. After being stirred for 30 min, the homogeneous solution was cooled to -10°C and treated with TBHP and (E)-2-undecen-l-ol. After 20h the reaction was

only 30% complete. Product of 4% ee was obtained, indicating that just 1 equiv. of water is enough to destroy the catalyst in the absence of molecular sieves. In an otherwise identical experiment, powdered 4Å molecular sieves were added just prior to the addition of TBHP. The reaction proceeded to greater than 90% completion after 20 h. Material of 88% ee was obtained.[39]

These results indicate that water does react with the titanium complex, but not initially in an irreversible manner. The fact that catalysis is to a great extent revived after addition of molecular sieves suggests both that (a) the interaction of water with the catalyst is initially reversible, molecular sieves being capable of shifting this equilibrium toward the water-free state, and (b) the reaction of water with the catalyst is eventually irreversible, molecular sieves not being capable of fully regenerating the active system. Thus, it was proposed that the main function of molecular sieves in these reactions is the protection of the catalyst from adventitious water in the reaction medium. The hypothesis that molecular sieves protect the catalyst from water is also supported by the finding that 3Å, 4Å, and 5Å molecular sieves are equally effective in the reaction. If such is the case, then it should be possible by careful technique to avoid exposure of the catalyst to water and thus avoid the use of molecular sieves altogether. Nevertheless, in all cases studied thus far, catalytic reactions with sieves have given higher conversions and/or higher selectivities than the same reactions carried out without molecular sieves.

Jacobsen Epoxidation: Manganese complexes of chiral Schiff bases catalyze epoxidation of alkyl and aryl-substituted olefins with the highest enantioselectivities reported to date for nonenzymatic catalyst.[40] Epoxidations with the chiral Mn(II1) salen complexes afford higher ee's with a wide range of substrate substitution patterns, as monosubstituted**,** disubstituted, and trisubstituted prochiral olefins all react with good or moderate selectivity. The sense and degree of enantioselection in the epoxidation of each substrate is well explained by a side-on perpendicular approach of olefin to the manganese-oxo bond of the putative Mn(V) intermediate.[41]

Fig. 1 Different salen complexes used

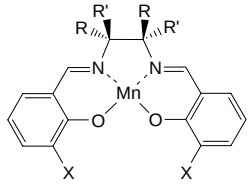

(S,S)-l: R = Ph, R' = H, X = H

(R,R)-l: R = H, R' = Ph, X = H

(R,R)-2: R = H, R' = Ph, X = ^{t}Bu

The aptitude for *cis* olefins is an attractive feature given that these substrates have been noted to afford the poorest results in several previously described highly enantioselective oxidation reactions.[42] The salen-based catalysts offer important advantages over known chiral porphyrin systems.[43] Their superior enantioselectivity can be attributed to the fact that the complexes bear chirotopic carbons in the vicinity of the metal, resulting in better stereochemical communication in the epoxidation step. The synthesis of the salen catalysts is also much simpler, and their steric properties can be fine tuned in a straightforward manner by choosing the appropriate diamine and salicyldehyde precursors.

Heterogenous catalysts (Zeolites):

Zeolites most commonly used for alkene oxidations feature four-coordinate titanium centers in microporous siliceous frameworks.[44] The first Ti-containing silicalite zeolite, TS-1, has a relatively small pore size of 5.5 Å. The small pore size of TS-1 precludes reactions of larger substrates[35d] though the isomorph ZSM-5 or zeolites with larger pore sizes, such as Ti-β, have less severe limitations in this regard.[45] Zeolites such as TS-1 are most reactive toward terminal alkenes and less reactive to *Z*-alkenes, and modified forms can allow for epoxidation of *E*-isomers.[46] For instance, Ti-MWW (a zeolite having large, 10-membered ring, channels in the siliceous framework, also known as MCM-22) mediates epoxidation of C6-C8 linear aliphatic alkenes with 30% H_2O_2 to produce a 4:1 rate preference in favor of *E*-alkenes over their *Z*-isomers. This preference is related to the larger pore size, which also allows formation of C6-C8 epoxides in 80-85% yield. However, such systems tend to be used at slightly elevated temperatures (e.g., 60-70 °C), which may lead to decomposition of sensitive products. Since TS-1 type zeolites are inherently acidic, they are sometimes modified prior to use to prevent inactivation of the catalyst or epoxide-decomposition. Even with such modifications, zeolites are generally limited to production of small, fairly stable epoxides.

Homogenous Co-ordination complexes attached to solid support

Heterogeneous catalysts may be constructed by attaching or impregnating homogeneous catalysts onto solid supports. This may be achieved by using ion-exchange resin to bind anionic catalysts,[47] encapsulating inorganic complexes onto chemically modified silica or zeolites,[48] or covalently binding coordination complexes onto modified silica. Supported homogeneous catalysts tend to have reduced activities relative to their truly

homogeneous analogues. However, this drawback can be offset by the advantages of easy catalyst recovery, reduction of trace metal contamination, and facile methods for parallel screening. Recent work illustrates how solid phase techniques can be used to prepare supported, peptide-derived transition metal complexes (particularly Mn and Fe), which may then be screened for potential catalytic activities.[49]

Molybdenum catalysts (e.g., $[NMe_4]_2[(PhPO_3)\{MoO(O_2)_2\}_2\cdot\{MoO(O_2)_2(H_2O)\}]$, $[(NH_4)_6Mo_7O_{24}\cdot 4H_2O]$, etc.) have been prepared and investigated for the epoxidation of alkenes with H_2O_2.[50] They give low turnovers and selectivities for the desired products, and their reactions are performed under harsh conditions. Soluble molybdenum oxide complexes are often used in stoichiometric quantities in which an active oxidant is generated from 30% H_2O_2 and commercially available ammonium molybdate. Some peroxomolybdate complexes bearing a chiral bidentate R-hydroxyamide or a chiral monodentate amine N-oxide ligand have been prepared and tested in asymmetric epoxidations,[51] but the resulting complexes have to be used in stoichiometric quantities to afford low enantioselectivity and yields.

The selective epoxidation of olefins with tertiary alkyl hydroperoxides, catalyzed by molybdenum complexes, is a synthetic reaction of great significance which is used to produce industrial organic chemicals.[52] However, the nature of the actual oxidizing species is not clearly established. In particular, the requirement for olefin activation through its coordination to the metal center prior to the oxygen-transfer step is still a matter of controversy.[52,53] In this context investigation of catalytic property of Molybdenum porphyrins complexes is done by Ledon etal.[54]

The catalytic activity of molybdenum porphyrins strongly supports the mechanism of olefin epoxidation proposed by Sheldon[53a] and Sharpless[53b] direct attack of the olefin on the electrophilic oxygen of the activated hydroperoxide, without requiring coordination to the metal center. This metalloporphyrin- catalyzed peroxy-bond heterolysis is the first example of a simple chemical model for hydroperoxide-supported oxidation of a substrate by cytochrome P-450.

Present Work

Oxidation reactions of olefins to give epoxides are of major importance for organic synthesis. Nowadays, especially asymmetric epoxidation reactions are in the focus of methodological developments.[55] However, the synthesis of racemic epoxides is still important on laboratory as well as industrial scales. More traditionally, epoxides are synthesized by the reaction of olefins with hydrogen peroxide in the presence of acetic, formic, *m*-chloro-benzoic acid. This convenient method involves in-situ formation of the corresponding peracid, which easily undergoes epoxidation reaction. The drawbacks of this method are potential side-reactions of the acid. Hence, the method is only limited for acid-labile olefins or epoxides.

The most convenient method for the synthesis of epoxides is the oxidation of olefins with hydrogen peroxide or alkyl peroxides in the presence of transition metal complexes.[56] However for homogenous complex catalysts, the application of these catalysts is limited due to difficult recovery of the catalysts from the reaction mixture. Nevertheless, significant advances have been made in metal-catalyzed epoxidation reactions in the last decade.[57] For example, polyoxo tungstate such as $PW_{12}O_{24}^{-3}$ has been found to catalyze the epoxidation of olefins in the presence of quaternary ammonium salts.[58] Also optically active molybdenum peroxo complexes catalyzed epoxidation of olefins has reported to provide the corresponding epoxides up to 50% chemical yield and 40% enantiomeric excess.[59] Furthemore, transition metaloxo species such as methyltrioxorhenium (MTO) has been found to catalyze olefin epoxidations using H_2O_2 as an oxidant.[60]

One of the main advantages of catalytic epoxidation is to adopt acid-free material as epoxidizing agent and thus avoid side reactions due to acid catalyzed oxirane ring opening. Kosel[61] investigated for the first time the epoxidation of low-molecular-weight cis-polybutadiene using dioxomolybdenum-bis(acetylacetonate) as catalyst and tert.-butyl hydroperoxide as an oxidant. But, the conversion of double bonds of the polybutadiene was less than 30%. Hay et al.[62] claimed that diene polymers can be epoxidized with hydrogen peroxide in the presence of methyl-trioctyl-ammonium-tetrakis-(diperoxo-tungsto)-phosphate as the phase transfer catalyst in a biphasic system. Coustsolelos's group[63] reported the epoxidation of diene polymers using metalloporphyrins as catalyst and sodium hypochloride

or iodosobenzene as oxygen donor. These catalytic epoxidation systems of diene polymers either have the disadvantage of low conversion of double bonds or suffer from tedious synthetic procedure for catalyst. Zhang et al. found that ethylene propylene diene monomer (EPDM) could be effectively epoxidized by a simple and commercially available system, which is composed of molybdenum oxide and tert.-butyl hydroperoxide.

A novel method for the epoxidation of olefins catalyzed by transition metal compounds, e.g. hexacarbonyl-molybdenum, octacarbonyl-dicobalt or tungsten acid etc., in association with oxygen donor (such as hydrogen peroxide, alkyl hydroperoxides, sodium hypochloride or iodosobenzene etc.) was discovered recently.[64] Heterogeneous systems for epoxidation of alkenes with H_2O_2 are typically mineral-type catalysts, including zeolites[46,65] or hydrotalcites.[66] Neither the homogeneous nor the heterogeneous Ti^{IV}/ SiO_2 catalysts are effective with hydrogen peroxide as the oxygen donor. Indeed, they are seriously inhibited by strongly coordinating molecules such as alcohols and particularly water.[56c] In the mid-eighties two approaches were followed to achieve this goal. Enichem scientists developed a Ti(IV)-silicalite catalyst (TS-1) that is extremely effective for a variety of synthetically useful oxidations, including epoxidation with 30% aq. H_2O_2.[67] The unique activity of TS-1 derives from the fact that silicalite is a hydrophobic molecular sieve in contrast to Ti^{IV}/SiO_2 which is hydrophilic. Consequently, hydrophobic substrates are preferentially adsorbed by TS-1 thus precluding the strong inhibition by water observed with Ti^{IV}/SiO_2.

However, a serious limitation of TS-1 in organic synthesis is that its scope is restricted to relatively small molecules, e.g., linear olefins that are able to access the micropores (5.3X5.5 Å). This provoked to flourish the activity aimed at developing titanium substituted molecular sieves with larger pores and amorphous titania–silica mixed oxides which, as yet, has not shown the activity comparable to TS-1.[68] The small pore size of TS-1 precludes reactions of larger substrates though the isomorph ZSM-5 or zeolites with larger pore sizes, such as Ti-β, have less severe limitations in this regard.[45] Zeolites such as TS-1 are most reactive toward terminal alkenes and less reactive to *Z*-alkenes, and modified forms can allow for epoxidation of *E*-isomers.[46] For instance, Ti-MWW (a zeolite having large, 10-membered ring, channels in the siliceous framework, also known as MCM-22) mediates epoxidation of C6-C8 linear aliphatic alkenes with 30% H_2O_2 to produce a 4:1 rate preference in favor of *E*-alkenes over their *Z*-isomers. This preference is related to the larger

pore size, which also allows formation of C6-C8 epoxides in 80-85% yield. However, such systems tend to be used at slightly elevated temperatures (e.g., 60-70 °C), which may lead to decomposition of sensitive products. Since TS-1 type zeolites are inherently acidic, they are sometimes modified prior to use to prevent inactivation of the catalyst or epoxide decomposition. Even with such modifications, zeolites are generally limited to production of small, fairly stable epoxides.

Hydrotalcite systems are more widely applicable than zeolites in so far as they can be used with a greater variety of substrates. These synthetic anionic clays are basic; in fact, they are basic enough to promote some nucleophilic epoxidations.[69] $Mg_{10}Al_2(OH)_{24}CO_3$ hydrotalcite system developed by Kaneda gives high conversions and selectivities for electrophilic epoxidations, even when acid sensitive epoxides are produced. Unfortunately, this system requires more than one equivalent of an amide[66a] or nitrile[66b] additive to act as a peroxide carrier. This additive is converted into a carboxylic acid byproduct, which can complicate isolation of the desired epoxide.

There are other important, but subtle properties of catalysts that must often be optimized to obtain useful reactivities in epoxidation reactions. This is particularly true for coordination complexes where electronic and steric effects of a ligand can have dramatic and unpredictable effects on reactivities.

"Homogeneous Catalysts" attached to solid supports: Heterogeneous catalysts may be constructed by attaching or impregnating homogeneous catalysts onto solid supports. This may be achieved by using ion-exchange resin to bind anionic catalysts,[47] encapsulating inorganic complexes onto chemically modified silica or zeolites,[48] or covalently binding coordination complexes onto modified silica. As shown in the figure 1 illustrates the latter approach in the context of porphyrin or triazacyclononane complexes. Supported homogeneous catalysts tend to have reduced activities relative to their truly homogeneous analogues. However, this drawback can be offset by the advantages of easy catalyst recovery, reduction of trace metal contamination, and facile methods for parallel screening. Recent work illustrates how solid phase techniques can be used to prepare supported, peptide-derived transition metal complexes (particularly Mn and Fe), which may then be screened for potential catalytic activities.[49]

Figure 1. Strategies for attaching coordination complexes to modified silica.

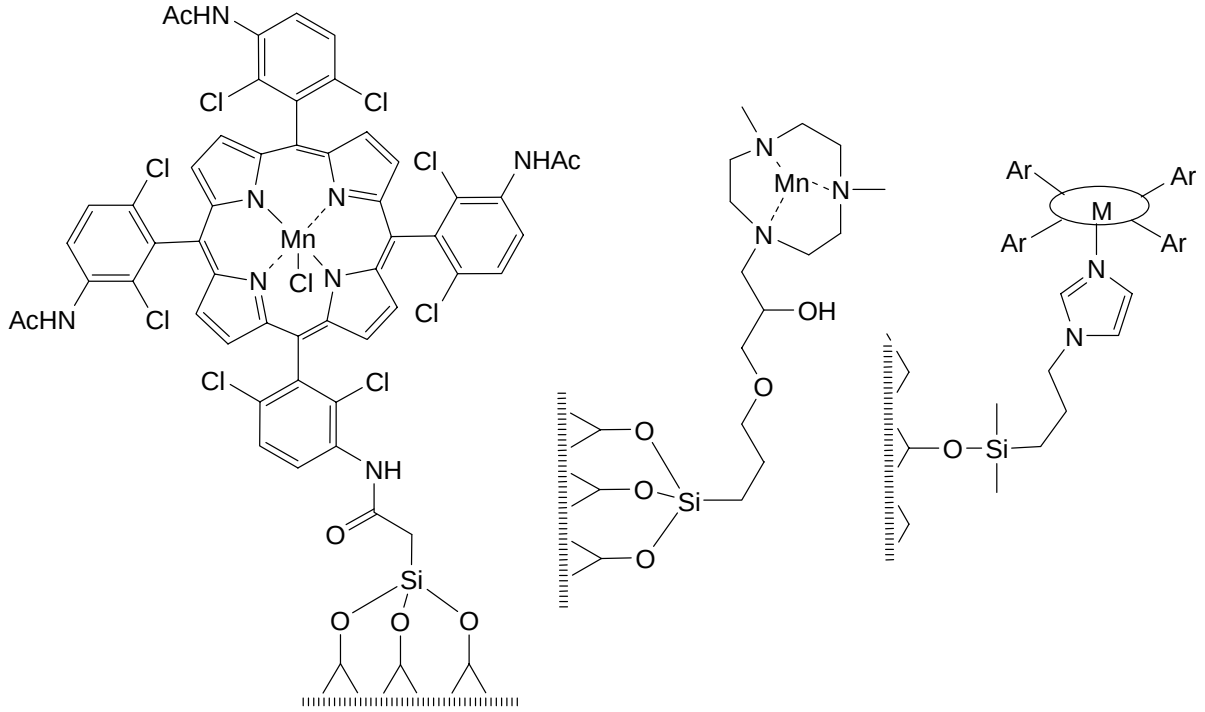

Mo-catalysts (e.g. $[NMe_4]_2[(PhPO_3)\{MoO(O_2)_2\}_2\cdot\{MoO-(O_2)_2(H_2O)\}]$, $[(NH_4)_6Mo_7O_{24}\cdot 4H_2O]$) have been prepared and investigated for the epoxidation of alkenes with H_2O_2.[50] They give low turnovers and selectivities for the desired products, and their reactions are performed under harsh conditions. Soluble molybdenum oxide complexes are often used in stoichiometric quantities in which an active oxidant is generated from 30% H_2O_2 and commercially available ammonium molybdate. Some peroxomolybdate complexes bearing a chiral bidentate R-hydroxyamide or a chiral monodentate amine N-oxide ligand have been prepared and tested in asymmetric epoxidations,[51] but the resulting complexes have to be used in stoichiometric quantities to afford low enantioselectivity and yields. Good epoxidation catalysts must activate H_2O_2 without radical production.

Apart from different catalysts used various studies involving different solvents have been done for epoxidation of internal olefins. Various N-substituted 1,4,7-triazacyclononanes (TACN) Mn(IV) complexes have been used as catalysts by Koek et al.[70] for the epoxidation of styrene with hydrogen peroxide in a two phase system (H_2O–CH_2Cl_2). Manganese complexes with similar structure and with similar ligands were used for epoxidations with H_2O_2 in acetone solution. Thus, Bolm et al.[71] found that the reaction of styren catalyzed by

$[L'2Mn^{III}(\mu\text{-}O)(\mu\text{-}AcO)_2](PF_6)_2$ (L' is an enantiopure C3-symmetric TACN derived from L-proline) proceeds at -25°C with 28% conversion and gives the S-enantiomer of the epoxide with 24% ee.

Most homogeneous epoxidation systems are greatly enhanced by adding molecules that can coordinate to the reaction mixture. These additives are often tertiary heterocyclic amines (i.e., pyridines, pyrazoles, and imidazoles) or carboxylates (i.e., acetates, benzoates, or glyoxylates). Useful additives favorably change catalytic efficiencies, selectivities, and reactivities and do not complicate isolation of the epoxide products. Additives facilitate catalyst tuning without re-designing the ligand, and their value may be underappreciated in the field. The process of discovering which additive to use, however, clearly requires trial and error and cannot be predicted reliably; modern high-throughput screening techniques are therefore valuable in this regard.

There is no single method for epoxidations using hydrogen peroxide that is uniformly better than the rest. The best method available depends on desired substrate and reaction scale. Zeolites can be superior for large-scale production of small, stable epoxides; these catalysts are cheap, robust, and easily removed from the products. Methyltrioxorhenium or manganese sulfate systems allow convenient production of racemic, acid-sensitive epoxides using commercially available reagents. Phosphate/tungstic acid systems are more Lewis acidic and require elevated temperatures. Each of these systems has attributes and limitations that are to some extent complementary.

There are no satisfactory conditions for certain catalytic epoxidations with hydrogen peroxide. For instance, large-scale epoxidation of a high molecular mass, cis-alkene at the late stages of a pharmaceutical synthesis might be very challenging. Heterogeneous catalysts are inappropriate for nonvolatile, high molecular mass alkenes that do not fit in molecular pores, the requirement for stereospecific formation of cis-epoxide would rule out several possibilities, and environmental/toxicity issues might well rule out all the remaining alternatives. Such challenging cases are rare, but they can arise. Nontoxic catalysts that stereospecifically mediate epoxidation of a broad range of alkenes under mild conditions with very efficient use of hydrogen peroxide have yet to be developed.

Keeping a view on all these extensive discussions so far we planned ourselves to study in detail the epoxidation of one such internal olefin i.e. 1,4-di-*O*-Benzyloxy-2-butene.

Figure 2 Structure of 1,4-di-*O*-Benzyloxy-2-butene

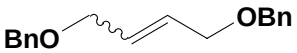

The selection of this butene was done such that this olefin carries both the terminal hydroxy functionalities to be protected as benzyl ethers. Thus incorporation of the oxygen without forming any oxide could be studied. The next significant feature with this olefin being the symmetry, thus the quest of chirality being eliminated. The third feature being the benzyl protection as we needed a chromophoric group for convenient analytical identification with significant bulk at the terminal end.

The next feature being the selection of the catalysts. Rode et.al. have shown that alkali promoted TS-1 catalyst system is one of the potent viable epoxidation catalysts system for styren (terminal olefin). More over as discussed earlier this is one of the best catalyst systems used so far for the epoxidation of olefins. Thus we planned to test this catalyst and compare these results with the catalyst we developed in our laboratory i.e 20% MoO_3 on SiO_2. These two systems being the supported catalysts we tested one homogenous catalyst i.e. $[(NH_4)_6Mo_7O_{24}{\cdot}4H_2O]$ (ammonium Molybdate).

Dichloromethane has been proved to be one of the solvents of choice. As this is the solvent which is commonly employed for different asymmetric epoxidation reactions (*Sharpeless epoxidation, She epoxidation, Jacobsen epoxidation*, etc.). Moreover during the epoxidation of olefins using peracids dichloromethane has been proved to be a solvent of choice. Thus we selected this solvent and compared the results with one comparatively polar solvent system i.e. Methanol:Acetonitrile (3:1).

Scheme 1

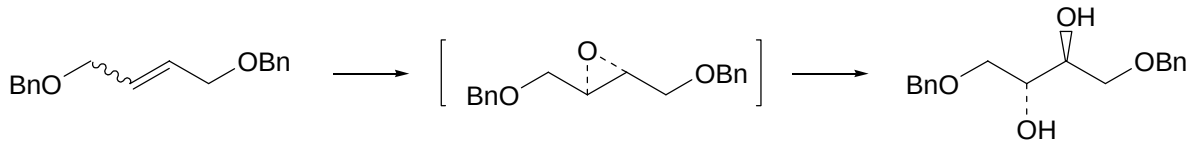

We need to achieve the epoxidation of olefins in presence of inorganic catalyst systems with hydrogen peroxide as the co-oxidant (water based). The solvents selected are organic and the olefin is in the organic medium. Thus to achieve we need to select some phase transfer catalyst or some promoter that might bring about this reaction in short span of time. Thus two different systems were selected i.e Benzyl Triethyl Ammonium chloride (BTAC) and is

compared with DiButyl Tin Oxide (DBTO). One being proved phase transfer catalyst, while other being known promoter in a variety of organic reactions.

Table 1 Epoxidation of olefin 1,4-di-*O*-Benzyloxy-2-butene

Ent. No.	Additive	H_2O_2	Solvent	Time h	Conv. %	Select. % Diol	Select. % Epo.	TOF h^{-1}	Remarks
1	-	*Absent*	*DCM*	*4*	*17.46*	*45.55*	*54.45*	*0.04*	Amm. Molyb. Soln. in catalytic amount
2	-	*Absent*	*MeOH:AcCN*	*4*	*11.12*	*59.63*	*40.33*	*0.02*	
3	-	*Present*	*DCM*	*4*	*2*	*60.81*	*39.19*	*0.004*	
4	-	*Present*	*MeOH:AcCN*	*4*	*18.88*	*75.34*	*24.64*	*0.04*	
5	*DBTO*	*Absent*	*DCM*	*4*	*15.29*	*26.61*	*73.39*	*0.03*	
6	*DBTO*	*Absent*	*MeOH:AcCN*	*4*	*12.20*	*72.68*	*27.32*	*0.027*	
7	*BTAC*	*Absent*	*DCM*	*4*	*29.56*	*53.21*	*46.79*	*0.065*	
8	*BTAC*	*Absent*	*MeOH:AcCN*	*4*	*63.63*	*36.36*	*4.3*	*0.01*	
9	*DBTO*	*Present*	*DCM*	*4*	*57.09*	*12.38*	*87.62*	*2.55*	MoO_3/ SiO_2 in catalytic amount
10	*DBTO*	*Present*	*MeOH:AcCN*	*4*	*38.59*	*12.26*	*87.74*	*1.73*	
11	*DBTO*	*Absent*	*DCM*	*4*	*29.03*	*69.2*	*30.8*	*1.3*	
12	*DBTO*	*Absent*	*MeOH:AcCN*	*4*	*25.81*	*27.55*	*72.45*	*1.15*	
13	-	*Present*	*DCM*	*4*	*77.73*	*81.63*	*18.37*	*3.47*	
14	-	*Present*	*MeOH:AcCN*	*4*	*56.98*	*41.3*	*58.07*	*2.54*	
15	**DBTO**	**Present**	**DCM**	**8**	**98.94**	**10.91**	**89.08**	**2.2**	TS-1 in catalytic ammount
16	*DBTO*	*Present*	*MeOH:AcCN*	*8*	*50.14*	*4.58*	*95.42*	*0.75*	
17	*BTAC*	*Present*	*DCM*	*8*	*33.74*	*44.07*	*55.93*	*1.5*	
18	*BTAC*	*Present*	*MeOH:AcCN*	*8*	*54.42*	*49.44*	*50.56*	*0.81*	
19	-	*Present*	*DCM*	*4*	*16.21*	*56.74*	*43.25*	*0.72*	
20	-	*Present*	*MeOH:AcCN*	*4*	*52.12*	*79.48*	*20.51*	*2.32*	
21	*DBTO*	*Absent*	*DCM*	*8*	*8.44*	*23.3*	*76.7*	*0.18*	
22	*DBTO*	*Absent*	*MeOH:AcCN*	*8*	*11.52*	*22.34*	*77.66*	*0.25*	

We carried out several reactions changing the solvent system, catalysts and the additives in a systematic manner to understand and optimize process. The results obtained in different conditions are tabulated in table 1.

As far as catalysts are concerned TS-1 catalyst shows the best conversion (99%) with moderate selectivity towards the intermediate epoxide (89%). Under similar conditions, the catalyst developed by us shows moderate conversion (57%) and selectivity (87%) while the homogenous system as expected shows very poor results. The TOF (Turn Over Frequency) calculation results in case of both heterogeneous systems seems to be enhanced almost 50 times compared to homogenous system (in case of homogenous system TOF ranges from 0.004 –0.065 while in case of heterogeneous system, from 1.5 – 2.32). Thus for 20 mole % loading of the catalyst per batch the heterogeneous catalyst system proves to be the system of choice in comparison to homogenous system.

Mechanism 1

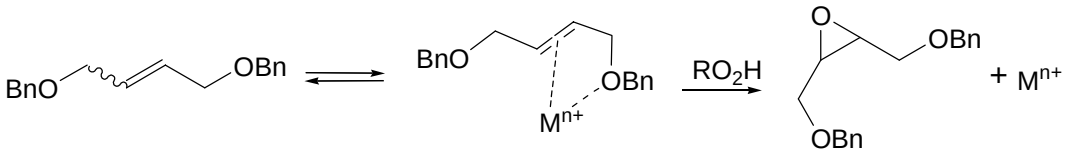

As reported earlier for vanadyl complexes by Sheng et.al.[72] there are three different possible mechanisms operating as far as different conditions are considered. In mechanism 1, the metal forms a π-complex with the double bond as well as the oxygen at the allylic position along with the peroxy oxygen and transfers the oxygen on the surface of the catalyst resulting the epoxide formation.

Mechanism 2

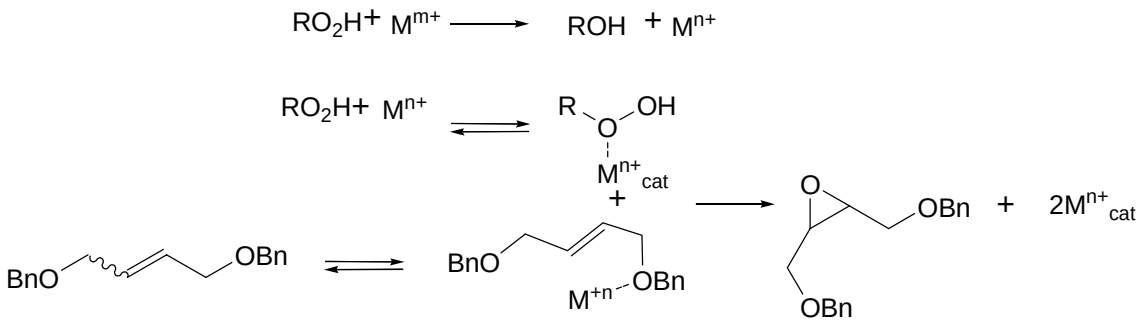

In mechanism 2, the metal might change its oxidation state getting oxidized with the peroxide. Further half of the oxidized metal ion complexes with the peroxy oxygen while

remaining half complexes with the protected allylic alcohol as in case of scheme 1. Then these two species react together to form the epoxide and the oxidized metal gets free. This mechanism is proposed considering the leeching of the catalyst from the solid support (for heterogeneous system).

Mechanism 3

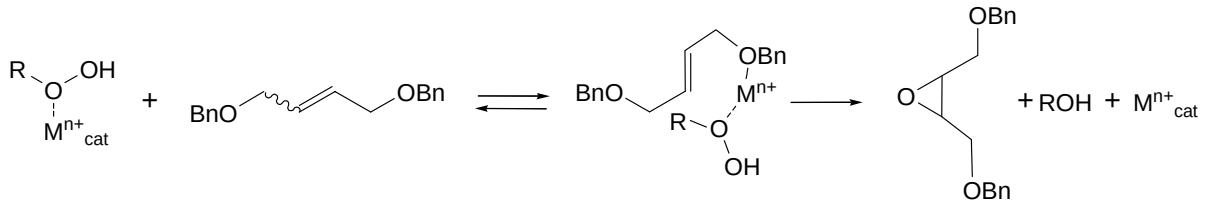

In case of mechanism 3, it is considered that the metal ion complexes with the peroxy oxygen as well as the olefin resulting into the epoxide.

The role of solvent and the additive is very clear from all these mechanisms. In all cases the chlorinated solvent Dichloromethane serves to be the better solvent for selectivity towards epoxide while the polar solvent shows selectivity towards diol. This is true because in all the cases the intermediate complex with the metal atom due to solvation results into diol formation which is possible in case of polar solvents, because the non polar (hydrophobic) solvent will separate the water molecules from the epoxide.

The role of additives is also quiet clear from this discussion. DBTO used shows enhancement in the conversion compared to the phase transfer catalyst BTAC. Because apart from the metal from the catalyst (titanium in case of TS-1 and molybdenum in remaining two cases) tin also complexes in similar fashion thus promoting the reaction. (Probably the half life of the catalyst is not good enough, thus not being used as a catalyst.)

The key to clean activation seems to be that the O-O bond must be cleaved heterolytically; homolytic cleavage generates free radicals in solution (Fenton-type chemistry), leading to spurious reactions that can degrade the catalyst, and unproductive consumption of the substrate and product. Once the activated catalyst-peroxide adduct has been formed, efficient transfer of oxygen to the alkene substrate is important. Oxygen-transfer from a metal can be achieved directly, or in two steps. Clearly, direct transfer is better with respect to minimization of reaction byproducts. Often, the physical properties of

catalysts are critical for developing epoxidation conditions. Partition coefficients between two solvents, or the solubilities in homogeneous media, can differentiate well from poor epoxidation systems. In conclusion, TS-1 is the better catalyst system for epoxidation overall giving 99% conversion with 93% selectivity towards epoxide. Chlorinated solvents are better solvents for epoxidation. DBTO is used as a promoter in this reaction and is found to be better additive over BTAC.

Catalyst Characterization

The XRD patterns of 1, 10, 20 and 30 mol% MoO_3/SiO_2 catalysts prepared by sol-gel technique are shown in Fig. 1. For comparison, the XRD pattern of pure silica is also included in the figure (Fig 1a). The patterns show the amorphous nature of the material at lower Mo loading (Fig. 1b, & 1c). Catalysts with 20 % Mo loading (Fig. 1d) show crystalline nature with intense peaks at 2θ = 12.9, 23.4, 25.8 and 27.4º corresponding to α-MoO_3 in the orthorhombic phase. No β- MoO_3 phase is observed in the structure because the samples are calcined at 500 ºC, a temperature at which β- MoO_3 phase is not stable.[73] It is interesting to note that even though the MoO_3 is in the crystalline form at higher Mo loading, the silica support still retains its amorphous nature leading to the high surface area of the catalysts.[74]

Fig. 1 XRD of a = silica and MoO_3/SiO_2 with b = 1, c = 5, d = 10, e = 15, f = 20 % MoO_3/SiO_3 loading

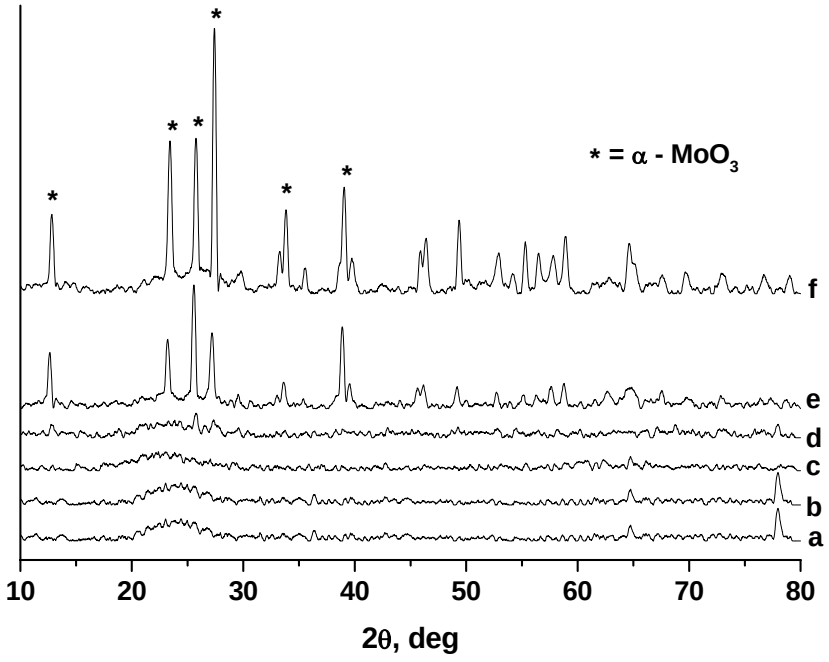

In case of 30 mol% MoO_3/SiO_2, very clear crystalline α-MoO_3 phase is observed, (Fig. 1e) however absence of the hump in the 2θrange of 20-30^0 for amorphous silica

indicates the formation of bulk molybdenum oxide as 30 mol% (~52 wt%) MoO_3 is quite high and forms mixed oxide phase with amorphous silica. Upto 20 mol% MoO_3 loading there is uniform distribution of MoO_3 on silica support, however with still higher loading MoO_3 becomes bulk phase.

The surface areas of all the catalysts determined using BET method are given in Table 1. As expected, a very high surface area of 606 m^2/g has been observed in case of pure silica because of sol-gel synthesis using ethyl silicate-40 as the silica source. Ethyl silicate-40 is a polymeric form (trimeric and tetrameric) of tetraethyl orthosilicate monomer, which on controlled hydrolysis yields the silica of a very high surface area .[75] On controlled hydrolysis of ethyl silicate-40; the trimeric and tetrameric species form corresponding trimeric and tetrameric silica structure. The trimeric and tetrameric silica structures restrict the growth of large particles. The surface area is found to decrease with increase in MoO_3 loading. During the sol-gel synthesis, an aqueous solution of AHM (Ammonium Hexa Molybdate) is added to ethyl silicate-40, which hydrolyzes ethyl silicate-40. However the control of the rate of hydrolysis is difficult, because of the use of excess water for dissolving AHM, which leads to a decrease in the surface area. The basic pH of the solution due to NH_3 liberated during hydrolysis of AHM also leads to the formation of the product with lower surface area. It is expected that, as MoO_3 loading is increased, the crystalline molybdenum oxide clusters are formed that cover the amorphous silica support, reducing the total surface area of the catalyst.

Table 1 Surface area and acidity of the MoO_3/SiO_2 catalysts

Catalyst	Surface area, m^2/g	Pore volume, cc/g	Average pore diameter, Å	NH_3 desorbed, mmol/g
Silica	606	0.6132	50.49	0.0317
1 % MoO_3/SiO_2	583	0.5934	40.69	0.1830
10 % MoO_3/SiO_2	284	0.5656	40.56	0.7056
20 % MoO_3/SiO_2	180	0.2327	51.64	0.9370

The mesoporosity of the catalysts is evident from the nitrogen adsorption-desorption isotherms of all the catalysts including silica, which shows the H4 type of hysteresis. The

average pore diameter for all the catalysts is given in the Table 1. Since no template is used during the synthesis of pure silica as well as MoO_3/SiO_2, the pore size distribution does not show any specific trend. During the preparation of all the catalysts by sol-gel method it is difficult to maintain identical process parameters. Amount of water used varies as amount of water for dissolving AHM varies. Due to ammonia liberated during the hydrolysis of AHM, the pH of the medium is not constant. Also due to change in amount of water and different basicity of the medium, rate of hydrolysis is not same for all the catalysts. Due to all these factors, there is no specific trend observed in average pore diameter and pore volume of the catalysts. However pore diameters are in the range of 40-80 Å, which confirms its mesoporous nature.

Fig. 2 NH_3 TPD of a = silica and MoO_3/SiO_2 with b = 1, c = 5, d = 10, e = 15, f = 20 % MoO_3/SiO_3 loading by sol gel technique

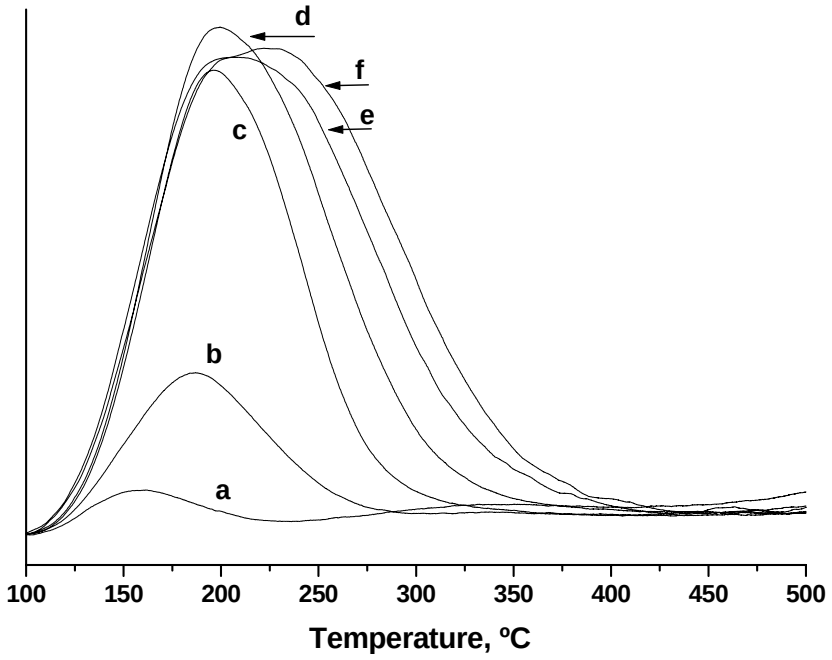

Ammonia -TPD experiments are carried out to determine the acid strength of the catalyst. The results are shown in Figure 2, and the amount of NH_3 desorbed is given in Table 1. The pure silica catalyst show the lowest acidity, with 0.0317 mmol/g of ammonia desorbed at comparatively lower temperature, indicating the presence of few weaker acid sites. Addition of 1 % MoO_3 to the silica support by sol-gel increases the acidity almost six

times (0.183 mmol/g) with respect to the number of acid sites as well as the acid strength. The temperature for total desorption of ammonia increased (275 to 400 ºC) with increase in MoO_3 loading upto 20 mol% MoO_3/SiO_2 showing the increase in acid strength as well as in the number of acid sites. The catalyst with 20 % Mo loading showed maximum number of acid sites (NH_3 desorbed: 0.937 mmol/g) as well as the highest acid strength.

Pyridine adsorption studies for the determination of the nature of acidity reveal the presence of Lewis acidity in all catalysts.[74] Figure 3 shows the IR spectra of adsorbed pyridine on catalyst surface. The spectrum of pure silica (Fig. 3a) shows the presence of only Lewis acidity (peak at 1450 cm^{-1}) with low acidity and 1 % MoO_3/SiO_2 sample (Fig 3b) shows increase in Lewis acidity as well as acid strength. As the MoO_3 loading is further increased, the samples show the presence of both Brønsted (peak at 1540 cm^{-1}) as well as Lewis acid sites. The generation of Brønsted acidity may be correlated to the formation of polymolybdate *Keggin* structures.[76]

Fig. 3 FTIR spectra of adsorbed pyridine on a = Silica, b = 1, c = 5, d = 10, e = 15, f = 20 % MoO_3/SiO_3

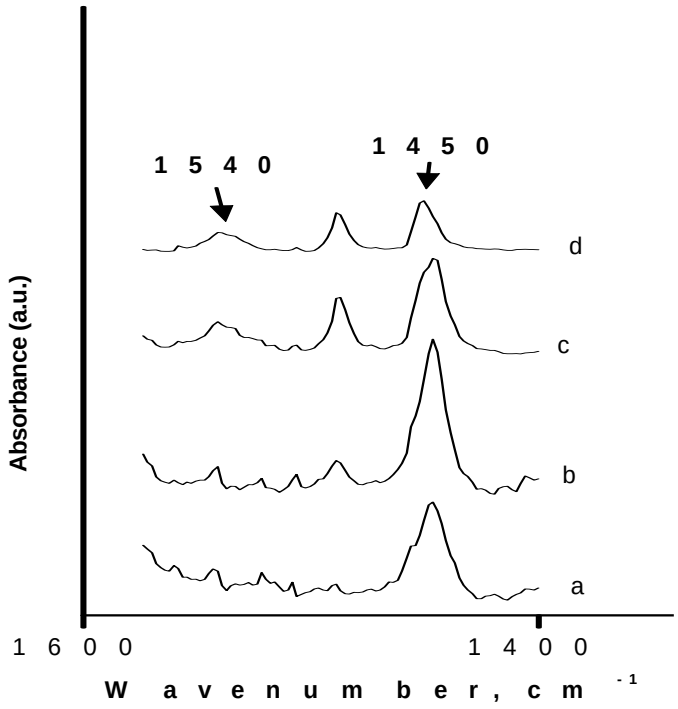

The IR spectra of the catalyst in the framework region shows the presence of peaks at 959 and 914 cm^{-1}, which corresponds to polymolybdate *Keggin* structures, which is reported to exhibit Brønsted acidity. At temperatures of about 500 ºC transformation of hexagonal form of molybdenum trioxide into its orthorhombic form takes place. The oxide becomes hydrated and subsequently converted into polymolybdenic trimers.[77] Such structural units are expected to show Brønsted acidity. The ratio of Brønsted to Lewis (B/L) acidity increases with increase in Mo loading. Though the Lewis acidity is found to

decrease with increase in Mo loading, the Brønsted acidity observed at higher Mo loading contributes to overall increase in the total acidity, which is seen by NH_3-TPD. The MoO_3/SiO_2 catalysts prepared by impregnation technique are reported to show the presence of only Lewis acid sites without any Brønsted acidity. Ma etal[78] have prepared a series of MoO_3/SiO_2 catalyst (1-16 wt %) by impregnation method and the NH_3 TPD shows desorption at much lower temperature (<250ºC) indicating presence of weak acidity. Amount of ammonia desorbed for 1% MoO_3/SiO_2 is reported to be only 0.056 mmol/g which is increased to 0.102 mmol/g for 16% MoO_3/SiO_2, this shows that acidity of impregnation catalysts is significantly low, compared to the catalysts prepared by sol-gel.

Experimental Work

Catalyst preparation

MoO_3/SiO_2 catalysts with varying molybdenum oxide molar concentrations (1, 10, 20 and 30 mol %) are prepared by sol-gel technique. Ammonium heptamolybdate (AHM) and ethyl silicate-40 (CAS registry no. 18945-71-7) are used as molybdenum and silica source, respectively.

In a typical procedure 20 mol % MoO_3/SiO_2 catalyst is synthesized by dissolving 14.11 g AHM in 40 ml water at 80 ºC. This hot solution is added dropwise to the dry isopropyl alcohol solution of ethyl silicate-40 (48.0 g) with constant stirring. The resultant transparent greenish gel is air dried and calcined at 500ºC in air in a muffle furnace for 12 h. Similarly catalysts with 1, 10 and 30 mol % molybdenum oxide loading are prepared.

Pure high surface area silica catalyst is prepared for comparison by adding 52 g ethyl silicate-40 to 30 cc dry isopropyl alcohol; to this mixture 0.02 g ammonia solution (25 %) is slowly added with constant stirring. The transparent white gel thus obtained is air-dried and calcined in a muffle furnace at 500ºC for 12 h.

Representative procedure for the rearrangement:

A suspension of the catalyst (12.3 mg) and starting material (5.0 mmol) in ethanol (10 mL) under argon is heated under reflux for 18 h. The reaction mixture is diluted with water and repeatedly extracted with ether. The combined organic layer is washed with brine, dried (magnesium sulphate), and concentrated. The residue is purified by flash column chromatography on silica gel to give product.

Rearrangement of 3-deoxy, 3-ketoxime 1,2,5,6 di-*O*-isopropylidine-α-D-ribofuranoside

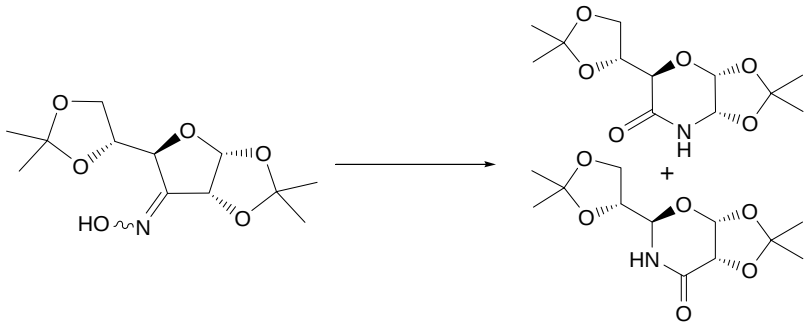

Major Isomer: **IR** ($CHCl_3$) 1740 cm^{-1};

^{1}H NMR (300 MHz, $CDCl_3$): δ 1.35 (s, 3 H), 1.41 (s, 3 H), 1.43 (s, 3 H), 1.51 (s, 3 H), 3.96 – 4.10 (m, H-8, H-8'), 4.30 (dt, H-7, *J* = 6.3, 4.9 Hz, *Irrdn. at* 4.77 → t, *J* = 6.3 Hz), 4.76 (dd, H-6, *J* = 4.7, 1.2 Hz, *Irrdn. at* 5.28 → d, *J* = 4.7 Hz), 5.28 (dd, H-3, *J* = 4.4, 1.2 Hz, *Irrdn. at* 4.76 → d, *J* = 4.3 Hz, *Irrdn. at* 5.94 → d, *J* = 1.2 Hz), 5. 94 (d, H-2, *J* = 4.4 Hz, *Irrdn. at* 5.28 → br.s), 8.87 (br.s, H-N)

^{13}C NMR (75 MHz, $CDCl_3$): δ 25.3, 26.3, 27.4, 65.4, 74.3, 76.9, 77.4, 104.8, 110.2, 113.8, 157.9 ppm

Minor Isomer: **IR** ($CHCl_3$) 1740 cm^{-1}

^{1}H NMR (300 MHz, $CDCl_3$): δ 1.33 (s, 3 H), 1.39 (s, 3 H), 1.44 (s, 6 H), 3.96 – 4.10 (m, H-8, H-8', *Irrdn. at* 5.24 → change), 4.49 (dt, H-7, *J* = 6.9, 2.3 Hz, *Irrdn. at* 5.24 → t, *J* = 6.7 Hz), 5.03 (dd, H-3, *J* = 4.4, 1.3 Hz, *Irrdn. at* 5.24 → d, *J* = 4.1 Hz, *Irrdn. at* 6.01 → d, *J* = 1.3 Hz), 5.24 (dd, H-6, *J* = 2.4, 1.3 Hz, *Irrdn. at* 5.03 → d, *J* = 2.0 Hz, *Irrdn. at* 4.49 → d, *J* = 1.3 Hz, *Irrdn. at* 6.01 → no change), 6.01 (d, H-2, *J* = 4.4 Hz, *Irrdn. at* 5.03 → s), 8.80 (br.s, H-N)

^{13}C NMR (75 MHz, $CDCl_3$): δ 26.1, 27.4, 27.6, 64.9, 77.4, 77.7, 79.1, 104.6, 109.8, 114.1, 158.5 ppm.

MS-ESI: 274.2 (49%, $[M+1]^+$).

Anal. Calcd. for $C_{12}H_{19}NO_6$: C, 52.74; H, 7.01; N, 5.13 Found : C, 51.65; H, 6.99; N, 4.64.

Rearrangement of 3-deoxy, 3-ketoxime 1,2,5,6 di-*O*-cyclohexylidine-α-D-ribofuranoside

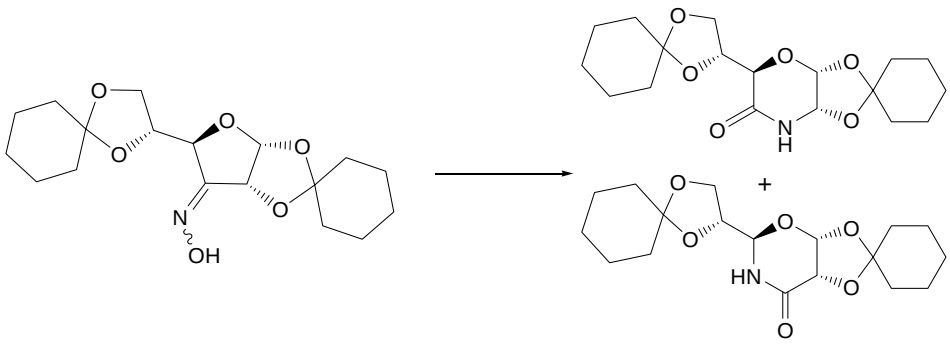

Major Isomer: **IR** ($CHCl_3$) 1740 cm^{-1}

^{1}H NMR (300 MHz, $CDCl_3$): δ 1.61 (bs, 20 H), 3.93 – 4.14 (m, 2H), 4.30 (dt, J= 4.79, 6.31 Hz, 1H), 4.76 (dd, *J* = 4.40, 0.98 Hz 1H), 5.28 (dd, *J* = 4.4, 1.46 Hz, 1H), 5. 94 (d, *J* = 4.4 Hz, H-2), 8.87 (bs, 1H)

^{13}C NMR (75 MHz, $CDCl_3$): δ 23.44, 24.62, 34.43, 35.57, 36.64, 64.54, 76.85, 78.25, 104.16, 110.52, 114.60, 157.10 ppm

Minor Isomer: **IR** ($CHCl_3$) 1740 cm^{-1}

^{1}H NMR (300 MHz, $CDCl_3$): δ 1.61 (bs, 20 H), 3.96 – 4.10 (m, 2H), 4.49 (dt, *J* = 7.7, 1.93 Hz), 5.03 (dd, *J* = 4.88, 0.98 Hz, 1H), 5.24 (dd, *J* = 2.06, 1.37 Hz, 1H), 6.01 (d, *J* = 4.88 Hz, 1H), 8.80 (bs, 1H)

^{13}C NMR (75 MHz, $CDCl_3$): δ 23.59, 24.84, 34.58, 35.39, 36.49, 64.25, 73.62, 77.18, 103.98, 110.01, 114.60, 157.90 ppm.

MS-ESI: 354.18 (20%, $[M+1]^+$).

Anal. Calcd. for $C_{18}H_{27}NO_6$: C, 61.17; H, 7.70; N, 3.96 Found : C, 61.16; H, 7.36; N, 3.23

Rearrangement of 3-deoxy, 3-ketoxime 5-(4-methoxy phenyl) methoxy, 1,2 -*O*-isopropylidine-α-D-erythreofuranoside

IR ($CHCl_3$) 1740 cm^{-1}

^{1}H NMR (300 MHz, $CDCl_3$): δ 1.43 (s, 3H), 1.50 (s, 3H), 3.56 (dd, J= 4.42, 10.54 Hz, 1H), 3.72 (dd, J= 2.75, 10.54 Hz, 1H), 3.80 (s), 4.49 (s, 2H), 4.86 (bs, 1H), 5.22 (d, J= 3.67 Hz, 1H), 5.95 (d, J= 4.13 Hz, 1H), 6.83 (d, J= 8.25 Hz, 2H), 7.20 (d, J= 8.25 Hz, 2H), 7.79 (bs, 1H)

^{13}C NMR: δ 14.33, 21.05, 27.47, 29.79, 55.17, 60.33, 71.14, 73.32, 74.16, 77.00, 78.85, 105.04, 105.36, 113.56, 113.85, 129.06, 129.26, 129.87, 158.73, 159.34

MS-ESI: 324.13 (50%, $[M+1]^+$).

Anal. Calcd. for $C_{16}H_{21}NO_6$: C, 59.43; H, 6.55; N, 4.33 Found : C, 60.17; H, 6.76; N, 3.97

Rearrangement of Camphor oxime

IR ($CHCl_3$) 1740 cm^{-1}

^{1}H NMR (300 MHz, $CDCl_3$): δ 0.84 (s, 3H), 0.91 (s, 3H), 0.96 (s, 3H), 1.33 (dd, J= 2.93, 9.28 Hz, 1H), 1.38 (d, J= 1.46 Hz, 1H), 1.43 (dd, J= 8.86, 3.53 Hz, 1H), 1.63 (dd, J= 8.64, 2.0 Hz, 1H), 1.73 (dd, J= 12.49, 3.41 Hz, 1H), 1.84 (d, J= 18.06 Hz, 1H), 1.94 (dt, J= 11.23, 3.42 Hz, 1H), 2.09 (t, J= 4.40 Hz, 1H), 2.35 (ddd, J= 3.56, 4.48, 17.97 Hz, 1H), 7.36 (bs, 1H)

^{13}C NMR: δ 8.96, 18.85, 19.47, 26.79, 29.55, 42.85, 46.38, 57.19, 95.82, 159.56

Rearrangement of (2R,6S)-2,6-diphenylpiperidin-4-oxime

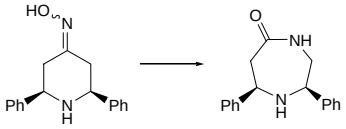

IR ($CHCl_3$) 1740 cm^{-1}

^{1}H NMR (300 MHz, $CDCl_3$): δ 2.03 (m, 1H), 2.37 (m, 1H), 2.58 (m, 2H), 3.88 (dt, J= 10.75, 2.93 Hz, 1H), 4.07 (dd, 10.29, 3.91 Hz, 1H), 7.35 (m, 12H)

References

1. Otto, W. G. *Angew. Chem.* **1956**, *68*, 181.
2. Wijtmans, R.; Vink, M. K. S.; Schoemaker, H. E.; van Delft, F. L.; Blaauw, R. H.; Rutjes F. P. J. T. *SYNTHESIS* **2004**, 641.
3. Lin, C.; Huang, P.; Lu, C.; Wu, R.; Hu, W.; Wang, J. *Tetrahedron* **1997**, *53*, 2025.
4. Ciminiello, P.; Dell'Aversano, C.; Fattorusso, E.; Forino, M.; Magno, S.; Ianaro, A.; Di Rosa, M. *Eur. J. Org. Chem.* **2001**, 49.
5. (a) Welch, R. F.; Lai, A. A.; Schroeder, D. H. *Xenobiotica* **1987**, 17, 287. (b) Fang, Q. K.; Han, Z.; Grover, P.; Kessler, D.; Senanayake C. H.; Wald S. A. *Tetrahedron* Asymmetry **2000**, *11*, 3659.
6. (a) Kelley, J. L.; Musso, D. L.; Boswell, G. E.; Soroko, F. E.; Cooper, B. R. *J. Med. Chem.* **1996**, 39, 347–349. (b) Musso, D. L.; Mehth, N. B.; Soroko, F. E.; Ferris, R. M.; Hollingsworth, E. B.; Kenney, B. T. *Chirality* **1993**, 5, 495. (c) Musso, D. L.; Mehth, N. B.; Soroko, F. E. *Bioorg. Med. Chem. Lett.* **1997**, 1.
7. Mey, B.; Paulus, H.; Lamparter, E.; Blaschke, G. *Chirality* **1998**, 307.
8. Suckow, R. F.; Zhang, M. F.; Cooper, T. B. *Biomed. Chromatogr.* **1997**, 11, 174.
9. Boswell, G. E.; Musso, A. O.; Davis, D. L.; Kelley, J. L.; Soroko, F. E.; Cooper, B. R. *J. Heterocycl. Chem.* **1997**, 34, 1813.
10. (a) Nubbemeyer, U. *Top. Curr. Chem.* **2001**, *216*, 125 – 196. (b) Craig, D. *Comp. Org. Synth.* **1999**, *7*, 689 – 702. (c) Abele, E.; Lukevics, E. *Heterocycles* **2000**, *53*, 2285 – 2336. (d) Smith, M. B.; March, J. *March's Advanced Organic Chemistry: reactions, mechanisms and structures*, 5th ed. John Willy and sons **2001**, 1415.
11. Butler, R. N.; O'Donoghue, D. A. *J. Chem. Res. (S)*, **1983**, 18.
12. Majo, V. J.; Venugopal, M.; Prince, A. A. M.; Perumal, P. T. *Synth. Commun.* **1995**, *25*, 3863.
13. Beckwith, A. L. J. in *Zabicky The Chemistry of Amides*; Wiley. NY, **1970**, 131.
14. Ghiaci, M; Imanzadeh, G. H. *Synth. Commun.* **1998**, *28*, 2275.
15. Laurent, A.; Jacquault, P.; DiMarino, J. L.; Hamelin, J. *J. Chem. Soc, Chem. Commun.* **1995**, 1101.

16. Bosch, A. I.; de la Cruz, P.; Diez-Barra, E.; Loupy, A.; Langa, F. *Synlett*. **1995**, 1259.
17. Lansbury, P. T.; Mancuso, N. R. *Tetrahedron Lett.* **1965**, 2445.
18. (a) Cram, D. J. *Newman Steric Effects in Organic Chemistry*; Wiley: NY, **1956**, 270. (b) Nickon, A.; Weglein, R. C *J. Am. Chem. Soc.* **1975**, *97*, 1271.
19. (a) McCall, M. J.; Townsend, J. M.; Bonner, W. A. *J. Am. Chem. Soc.* **1975**, *97*, 2743. (b) Brownbridge, P.; Hodgson, P. K. G.; Shepherd, R.; Warren, S. *J. Chem. Soc, Perkin Trans. 1* **1976**, 2024.
20. (a) Fischer, A.; Henderson, G.N. *J. Chem. Soc, Chem. Commun.* **1979**, 279. (b) Palmer, J. D.; Waring, A. J. *J. Chem. Soc, Perkin Trans. 2* **1979**, 1089. (c) Marx, J. N.; Hahn, Y. P. *J. Org. Chem.* **1988**, *53*, 2866.
21. (a) Cram, D. J.; Knight, J. D. *J. Am. Chem. Soc.* **1952**, *74*, 5839. (b) Stiles, M.; Mayer, R. P. *J. Am. Chem. Soc.* **1959**, *81*, 1497. (c) Heidke, R. L.; Saunders Jr.; W. H. *J. Am. Chem. Soc.* **1966**, *88*, 5816. (d) Dubois, J. E.; Bauer, P. *J. Am. Chem. Soc.* **1968**, *90*, 4510. (e) Bundel', Yu. G.; Levina, I. Yu.; Reutov, O. A. *J. Org. Chem. USSR* **1970**, *6*, 1. (f) Pilkington, J. W.; Waring, A. J. *J. Chem. Soc, Perkin Trans. 2* **1976**, 1349. (g) Korchagina, D. V.; Derendyaev, B. G.; Shubin, V. G.; Koptyug, V. A. *J. Org. Chem. USSR* **1976**, *12*, 378. (h) Wistuba, E.; Ruchardt, C. *Tetrahedron Lett.* **1981**, *22*, 4069. (i) Jost, R.; Laali, K.; Sommer, J. *Nouv. J. Chim.* **1983**, *7*, 79.
22. Bachmann, W. E.; Ferguson, J. W. *J. Am. Chem. Soc.* **1934**, *56*, 2081.
23. (a)Le Drian, C.; Vogel, P. *Helv. Chim. Acta*.; **1987**, *70*, 1703. (b) *Tetrahedron Lett.* **1987**, *28*, 1523.
24. (a) Sinclair, P. J.; Zhai, D.; Reibenspies, J.; Williams, R. M. *J. Am. Chem. Soc.* **1986**, *108*, 1103. (b) Van den Nieuwendijk, A. M. C. H.; Warmerdam, E. G. J. C.; Brussee, J.; Van der Gen, A. *Tetrahedron: Asymmtery* **1995**, *6*, 801.
25. Wiliams, R. M.; Sinclair, P. J.; Zhai, D.; Chen, D. *J. Am. Chem. Soc.* **1988**, *110*, 1547.
26. Larock, R.C. Comprehensive Organic Transformations; VCH: NY, **1989**, 450.
27. (a) Hudlicky, M. Oxidations in Organic Chemistry; A.C.S.: Washington, **1990**, p.60. (b) Haines, A.H. Methods for the Oxidation of Organic Compounds; Academic Press: NY, **1985**, p.295. (c) Dryuk, V.G. *Russ. Chem. Rev.;* **1985**, *54*, 986. (d) Plesnicar, B. Trahanovsky Oxidation in Organic Chemistry, pt. C; Academic Press: NY, **1978**, p.

211. (e) Swern, D. Swern Organic Peroxides, vol. 2; Wiley: NY, **1971**, p. 355. (f) Metelitsa, D.I. *Russ. Chem. Rev.* **1972**, *41*, 807. (g) Hiatt, R. Augustine; Trecker Oxidation, vol. 2; Marcel Dekker: NY, **1971**, p. 113. (h) House, H.O. Modern Synthetic Reactions, 2nd ed.; W.A. Benjamin: NY, **1972**, p. 292. (i) Berti, G. *Top Stereochem.* **1973**, *7*, 93-251.

28. Emmons, W.D.; Pagano, A.S. *J. Am. Chem. Soc.* **1955**, *77*, 89.
29. Rastetter, W.H.; Richard, T.J.; Lewis, M.D. *J. Org. Chem.* **1978**, *43*, 3163
30. (a) Bartlett, P.D. *Rec. Chem. Prog.;* **1957**, *18*, 111. (b) Kwart, H.; Hoffman, D.M. *J. Org. Chem.* **1966**, *31*, 419. (c) Hanzlik, R.P.; Shearer, G.O. *J. Am. Chem. Soc.* **1975**, *97*, 5231. (d) Dryuk, V.G. *Tetrahedron* **1976**, *32*, 2855. (e) Finn, M.G.; Sharpless, K.B. Asymmetric Synthesis, vol. 5; Academic Press: NY, **1985**, p. 247. (f) Bach, R.D.; Canepa, C.; Winter, J.E.; Blanchette, R.E. *J. Org. Chem.* **1997**, *62*, 5191. (g) Plesnicar, B. Patai The Chemistry of Peroxides; Wiley: NY, **1983**, p. 521. (h) Ogata, Y.; Tabushi, I. *J. Am. Chem. Soc.* **1961**, *83*, 3440. (i) Woods, K.W.; Beak, P. *J. Am. Chem. Soc.* **1991**, *113*, 6281. (j) Vedejs, E.; Dent III, W.H.; Kendall, J.T.; Oliver, P.A. *J. Am. Chem. Soc.* **1996**, *118*, 3556.
31. (a) Khalil, M.M.; Pritzkow, W. *J. Prakt. Chem.* **1973**, *315*, 58. (b) Schneider, H.; Becker, N.; Philippi, K. *Chem. Ber*. **1981**, *114*, 1562. (c) Batog, A.E.; Savenko, T.V.; Batrak, T.A.; Kucher, R.V. *J. Org. Chem. USSR* **1981**, *17*, 1860.
32. Houk, K.N.; Liu, J.; DeMello, N.C.; Condroski, K.R. *J. Am. Chem. Soc.* **1997**, *119*, 10147.
33. Swern, D. Swern Organic Peroxides, vol. 1; Wiley: NY, **1970**, p. 313.
34. Smith, M.B.; March, J. March's Advanced Organic Chemistry 5th Ed. John Willy & sons. **2001**, p. 1542
35. (a) Jones, C. W. Applications of Hydrogen Peroxide and Derivatives; MPG Books Ltd.: Cornwall, U.K.; **1999**. (b) Jorgensen, K. A. *Chem. Rev.* **1989**, *89*, 431. (c) In Peroxide Chemistry Mechanistic and Preparative Aspects of Oxygen Transfer; Adam, W.; Ed.; Wiley-VCH: Darmstadt, Germany, **2000**. (d) Sanderson, W. R. *Pure Appl. Chem.* **2000**, *72*, 1289.
36. Katsuki, T.; Sharpless, K. B. *J. Am. Chem. Soc.* **1980**, *102*, 5974.

37. Martin, V. S.; Woodard, S. S.; Katsuki, T.; Yamada, Y.; Ikeda, M.; Sharpless, K. B. *J. Am. Chem. Soc.* **1981**, *103*, 6237.
38. Hill, J. G.; Sharpless, K. B.; Exon, C. M.; Regenye, R. *Org. Synth.***1984**, *63*, 66.
39. Gao, Y.; Hanson, R. M.; Klunder, J. M.; KO, S. Y.; Masamune, H.; Sharpless, K. B. *J. Am. Chem. Soc.* **1987**, *109*, 5165-5180.
40. (a) Davis, F. A.; Chattopadhyay, S. *Terrahedron Lett.* **1986**, *27*, 5079. (b) Ben Hassine, B.; Gorsane, M.; Geerts-Evrard, F.; Pecher, J.; Martin, R. H.; Castelet, D. *Bull. SOC. Chim. Belg.* **1986**, *95*, 547. (c) Schurig, V.; Hintzer, K.; Leyrer, U.; Mark, C.; Pitchen, P.; Kagan, H. B. *J. Organomet. Chem.* **1989**, *370*, 81.
41. Zhang, W.; Loebach, J. L.; Wilson, S. R.; Jacobsen, E. N. *J. Am. Chem. Soc.* **1990**, *112*, 2801.
42. (a) Oishi, T.; Hirama. M. *J. Org. Chem.* **1989**, *54*, 5834. (b) Katsuki, T.; Sharpless, K. B. *J. Am. Chem. Soc.* **1980**, *102*, 5974. (c) Gao, Y.; Hanson, R. M.; Klunder, J. M.; Ko, S. Y.; Masamune, H.; Sharpless, K. B. *J. Am. Chem. Soc.* **1987**, *109*. 5765. (d) Wai, J. S. M.; Markb, I. E.; Svendsen, J. S.; Finn, M. G.; Jacobsen. E. N.; Sharpless, K. B. *J. Am. Chem. Soc. 1989*, *111*, 1123.
43. (a) Groves, J. T.; Myers, R. S. *J. Am. Chem. Soc.* **1983**, *105*, 5791. (b) Naruta, Y.; Tani, F.; Maruyama, K. *Chem. Lett.* **1989**, 1269. (c) O'Malley, S.; Kodadek, T. *J. Am. Chem. Soc.* **1989**, *111*, 9116.
44. (a) Munakata, H.; Oumi, Y.; Miyamoto, A. *J. Phys. Chem. B* **2001**, *105*, 3493. (b) Tantanak, D.; Vincent, M. A.; Hillier, I. H. *Chem. Commun.***1998**, 1031. (c) Notari, B. Advances in Catalysis; Eley, D. D.; Ed.; Academic Press: San Diego, **1996**; Vol. 41.
45. (a) Zahedi-Niaki, M. H.; Kapoor, M. P.; Kaliaguine, S. *J. Catalysis* **1998**, *177*, 231. (b) Xia, Q.-H.; Chen, X.; Tatsumi, T. *J. Mol. Catal. A: Chem.* **2001**, *176*, 179. (c) Skowronska-Ptasinska, M. D.; Vorstenbosch, M. L. W.; van Santen, R. A.; Abbenhuis, H. C. L. *Angew. Chem.; Int. Ed. Engl.* **2002**, *41*, 637.
46. Wu, P.; Tatsumi, T. *Chem. Commun.* **2001**, 897.
47. (a) Villa de P.; A. L.; Sels, B. F.; De Vos, D. E.; Jacobs, P. A. *J. Org. Chem.* **1999**, *64*, 7267. (b) Luz Villa de P.; A.; Farla´n Taborda, A.; Montes de Correa, C. *J. Mol. Catal. A: Chem.* **2002**, *185*, 269.

48. (a) Wang, Y.; Zhang, Q.; Shishido, T.; Takehira, K. *J. Catal.* **2002**, *209*, 186. (b) Mandelli, D.; van Vliet, M. C. A.; Arnold, U.; Sheldon, R. A.; Schuchardt, U. *J. Mol. Catal. A: Chem.* **2001**, *168*, 165. (c) Capel-Sanchez, M. C.; Campos-Martin, J. M.; Fierro, J. L. G.; de Frutos, M. P.; Polo, A. P. *Chem. Commun.* **2000**, 855. (d) Sakamoto, T.; Pac, C. *Tetrahedron Lett.* **2000**, *41*, 10009. (e) Gelbard, G.; Gauducheau, T.; Vidal, E.; Parvulescu, V. I.; Crosman, A.; Pop, V. M. *J. Mol. Catal. A: Chem.* **2002**, *182- 183*, 257.
49. Venturello, C.; D'Aloisio, R.; Bart, J. C. J.; Ricci, M. *J. Mol. Catal.* **1985**, *32*, 107.
50. (a) Gresley, N. M.; Griffith, W. P.; Laemmel, A. C.; Nogueira, H. I. S.; Parkin, B. C. *J. Mol. Catal. A: Chem.* **1997**, *117*, 185. (b) Csanyi, L. J.; Jaky, K. *J. Catalysis* **1991**, *127*, 42. (c) Kamiyama, T.; Inoue, M.; Enomoto, S. *Chem. Lett.* **1989**, 1129. (d) Griffith, W. P.; Parkin, B. C.; White, A. J. P.; Williams, D. J. *J. Chem. Soc. Dalton Trans.* **1995**, 3131. (e) Bortolini, O.; Furia, F. D.; Modena, G.; Seraglia, R. *J. Org. Chem.* **1985**, *50*, 2688. (f) Ishii, Y.; Yamawaki, K.; Yoshida, T.; Ura, T.; Ogawa, M. *J. Org. Chem.* **1987**, *52*, 1868. (g) Trost, B. M.; Masuyama, Y. *Isr. J. Chem.* **1984**, *24*, 134.
51. (a) Schurig, V.; Hintzer, K.; Leyrer, U.; C.; M.; Pitchen, P.; Kagan, H. B. *J. Organometallic Chem.* **1989**, *370*, 81. (b) Bortolini, O.; Di Furia, F.; Modena, G.; Schionato, A. *J. Mol. Catal.* **1986**, *35*, 47.
52. (a) Sheldon, R. A,; Kochi, J. K. *Adv. Catal.* **1976**, *25*, 272-413. (b) Lyons, J. E. *Aspects Homogeneous Catal.* **1977**, *3*, 1-136. (c) Parshall, G. W. *J. Mol. Catal.* **1978**, *4*, 243-270. (d) Sheldon, R. A. *Ibid.* **1980**, *7*, 107-126. (e) "Chemical and Physical Aspects of Catalytic Oxidation"; Portefaix, J. L.; Figueras, F.; Eds.; Editions du C.N.R.S.: Lyon, **1980**.
53. (a) Sheldon, R. A.; Van Doorn, J. A. *J. Calal.* **1973**, *31*, 427-437. (b) Chong, A. O.; Sharpless, K. B. *J. Org. Chem.* **1977**, *42*, 1587-1590. (c) Mimoun, H. *J. Mol. Catal.* **1980**, *7*, 1-29. (d) Mimoun, H.; Charpentier, R.; Mitschler, A.; Fischer, J.; Weiss, R. *J. Am. Chem. Soc.* **1980**, *102*, 1047-1054.
54. Ledon, H. J.; Durbut, P.; Varescon F. *J. Am. Chem. Soc.* **1981**, *103*, 3601-3603.
55. (a) Jacobsen, E.; Pfaltz, A. (Eds.), Catalytic Asymmetric Synthesis, Springer, Heidelberg, **1999**. (b) Beller, M.; Bolm, C. (Eds.), Transition Metals for Organic

Synthesis, Wiley-VCH, Weinheim, **1998**. (c) Joergensen, K.A. *Chem. Rev.* **1989**, *89*, 431.

56. (a) Sheldon, R. A.; Kochi, J. K. Metal-Catalyzed Oxidations of Organic Compounds, Academic Press, New York, **1981**. (b) Barf, G. A.; Sheldon, R. A. *J. Mol. Catal.* **1995**, *102*, 23. (c) Arends, I. W. C. E.; Sheldon, R. A. *Top. Catal.* **2002**, *19*, 133. (d) Ostovic, D.; Bruice, T. C. *Acc. Chem. Res.* **1992**, *25*, 314.
57. (a) Sato, K.; Aoki, M.; Ogawa, M.; Hashimoto, T.; Panyella, D.; Noyori, R. *Bull. Chem. Soc. Jpn.* **1997**, *70*, 905. (b) Sato, K.; Aoki, M.; Ogawa, M.; Hashimoto, T.; Noyori, R. *J. Org. Chem.* **1996**, *61*, 8310. (c) Duncan, D. C.; Chambers, R. C.; Hecht, E.; Hill, C. L. *J. Am. Chem. Soc.* **1995**, *117*, 681. (d) Ben-Daniel, R.; Khenkin, A. M.; Neumann, R.; *Chem. Eur. J.* **2000**, *6*, 3722. (e) Hoegaerts, D.; Sels, B. F.; de Vos, D. E.; Verpoort, F.; Jacobs, P. A. *Cat. Today* **2000**, *60*, 209. (f) Ishii, Y.; Yamawaki, K.; Ura, T.; Yamada, H. Yoshida, T.; Ogawa, M. *J. Org. Chem.* **1988**, *53*, 3587. (g) Venturello, C.; Daloisio, R. *J. Org. Chem.* **1988**, *53*, 1553. (h) Bosing, M.; Noh, A.; Loose, I.; Krebs, B. *J. Am. Chem. Soc.* **1998**, *120*, 7252. (i) de Vos, D.; Bein, T. *Chem. Commun.* **1996**, 917. (j) Neumann, R.; Gara, M. *J. Am. Chem. Soc.* **1995**, *117*, 5066. (k) Neumann, R.; Gara, M. *J. Am. Chem. Soc.* **1994**, *116*, 5509.
58. Matoba, Y.; Inoue, H.; Akagi, J.; Okabayashi, T.; Ishii, Y.; Ogawa, M. *Syn. Commun*. **1984**, *14*, 645.
59. Chaumette, P.; Mimoun, H.; Saussine, L. *J. Organomet.Chem*. **1983**, *250*, 291.
60. Rudolph, J.; Laxma Reddy, K.; Chiang, J. P.; Sharpless, K. B. *J. Am. Chem. Soc.* **1997**, *119*, 6189.
61. Kosel, N.A. *Polymer Sci. (USSR) Ser. A* **1980**, *22*, 2411.
62. (a) Jian, X.G.; Hay, A.S. *J. Polym. Sci.: Part A Polym. Chem.* **1991**, *29*, 1183. (b) Jian, X.G.; Hay, A.S. *J. Polym. Sci.: Part C* **1990**, *28*, 285.
63. (a) Tornaritis, M.J.; Coustsolelos, A.G. *J. Polym. Sci.: Part A Polym. Chem.* **1992**, *30*, 2791. (b) Tornaritis, M.J.; Coustsolelos, A.G. *Polymer* **1992**, *32*, 1725.
64. (a) Jorgensen, K.A. *Chem. Rev.* **1989**, *89*, 431. (b) Hoveyda, A.H.; Evans, D.A.; Fu, G.C. *Chem. Rev.* **1993**, *93*, 1307.
65. (a) Clerici, M. G.; Bellussi, G.; Romano, U. *J. Catal.* **1991**, *129*, 159. (b) Wang, Y.; Zhang, Q.; Shishido, T.; Takehira, K. *J. Catal.* **2002**, *209*, 186.

66. (a) Yamaguchi, K.; Ebitani, K.; Kaneda, K. *J. Org. Chem.* **1999**, *64*, 2966. (b) Ueno, S.; Yamaguchi, K.; Yoshida, K.; Ebitani, K.; Kaneda, K. *Chem. Commun.* **1998**, 295. (c) Cativiela, C.; Figueras, F.; Fraile, J.; Garcı´a, J.; Mayoral, J. *Tetrahedron Lett.* **1995**, *36*, 4125. (d) Mandelli, D.; van Vliet, M. C. A.; Arnold, U.; Sheldon, R. A.; Schuchardt, U. *J. Mol. Catal. A: Chem.* **2001**, *168*, 165.
67. (a) Notari, B. *Catal. Today* **1993**, *18*, 163. (b) Clerici, M.G.; Ingallina, P. *J. Catal.* **1993**, *140*, 71.
68. Sheldon, R.A.; Wallau, M.; Arends, I.W.C.E.; Schuchardt, U. *Acc. Chem. Res.* 1998, *31*, 485.
69. Reichle, W. T.; Kang, S. Y.; Everhardt, D. S. *J. Catal.* **1986**, *101*, 352.
70. Koek, J.H.; Kohlen, E.W.M.J.; Russell, S.W.; van der Wolf, L.; ter Steeg, P.F.; Hellemons, J.C. *Inorg. Chim. Acta* **1999**, *295*, 189–199.
71. Bolm, C.; Meyer, N.; Raabe, G.; Weyherm¨uller, T.; Bothe, E. *Chem. Commun.* **2000**, 2435–2436.
72. Sheng, M. N.; Zajacek, J. G. *J. Org. Chem.* **1970**, *35*, 1839
73. Kido, A.; Iwamoto, H.; Azuma N.; Ueno, A. *Catal. Surv. Jpn.* **2002**, *6*, 45.
74. Biradar, A. V.; Umbarkar S. B.; Dongare, M. K. *Appl. Catal. A*, **2005**, *285*, 190.
75. (a) Dongare, M. K.; Patil, P. T.; Malshe, K. M. Eur. Pat. 1386907, **2004**. (b) Dongare, M. K.; Patil, P. T.; Malshe, K. M. US Pat. 2004024267, **2004**.
76. Skupinski, W.; Malesa, M. *Appl. Catal. A*, **2002**, *236*, 223.
77. (a) Rocchicioli-Deltcheff, C.; Amirouche, M.; Herve, G.; Fournier, M.; Che, M.; Tabibonet, J. M. *J. Catal.* **1990**, *126*, 591. (b) Rocchicioli-Deltcheff, C.; Amirouche, M.; Herve, G.; Fournier, M.; Che, M.; Tabibonet, J. M. *J. Catal.* **1990**, *125*, 292.
78. Ma, X.; Gong, J.; Wang, S.; Gao, N.; Wang, D.; Yang, X.; He, F. *Catal. Comm.* **2004**, *5*, 101.

Spectral Data

Proton magnetic resonance spectra were recorded on AC-200 MHz, MSL-300 MHz and Bruker-500 MHz spectrometer using tetra methyl silane (TMS) as an internal standard. Chemical shifts have been expressed in ppm units downfield from TMS.

^{13}C Nuclear magnetic spectra were recorded on AC-50 MHz, MSL-75 MHz and Bruker-125 MHz spectrometer.

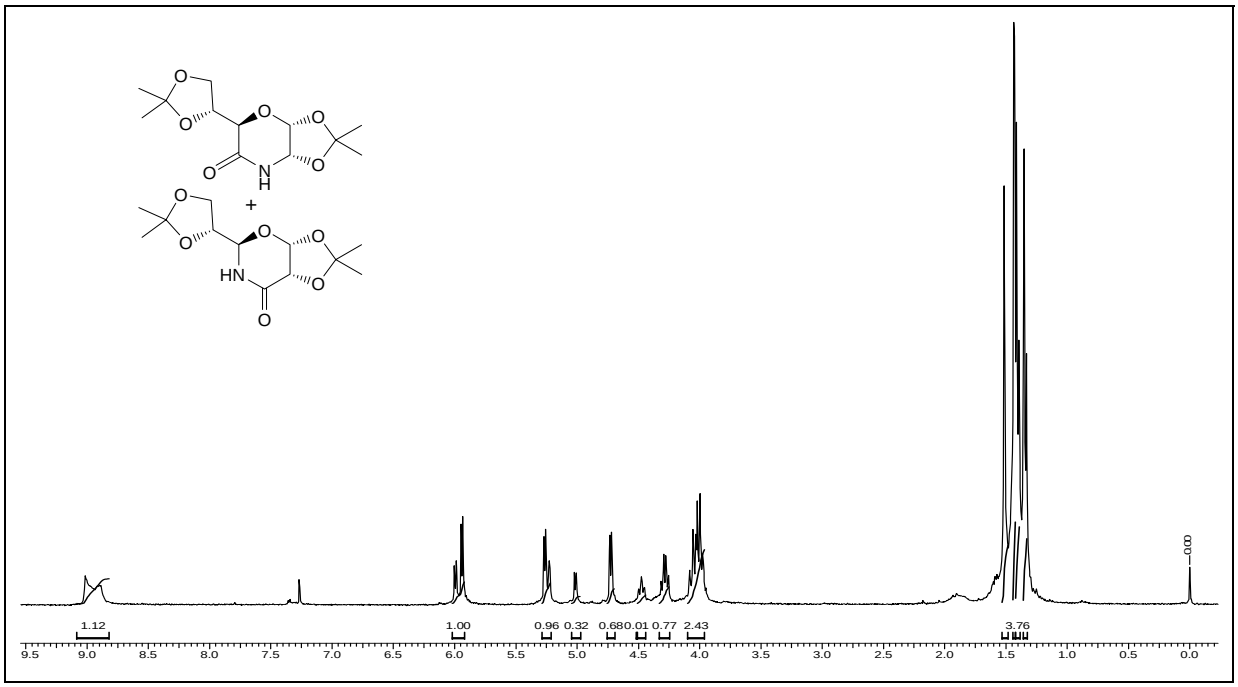

Spectral data for compounds 7 and 8

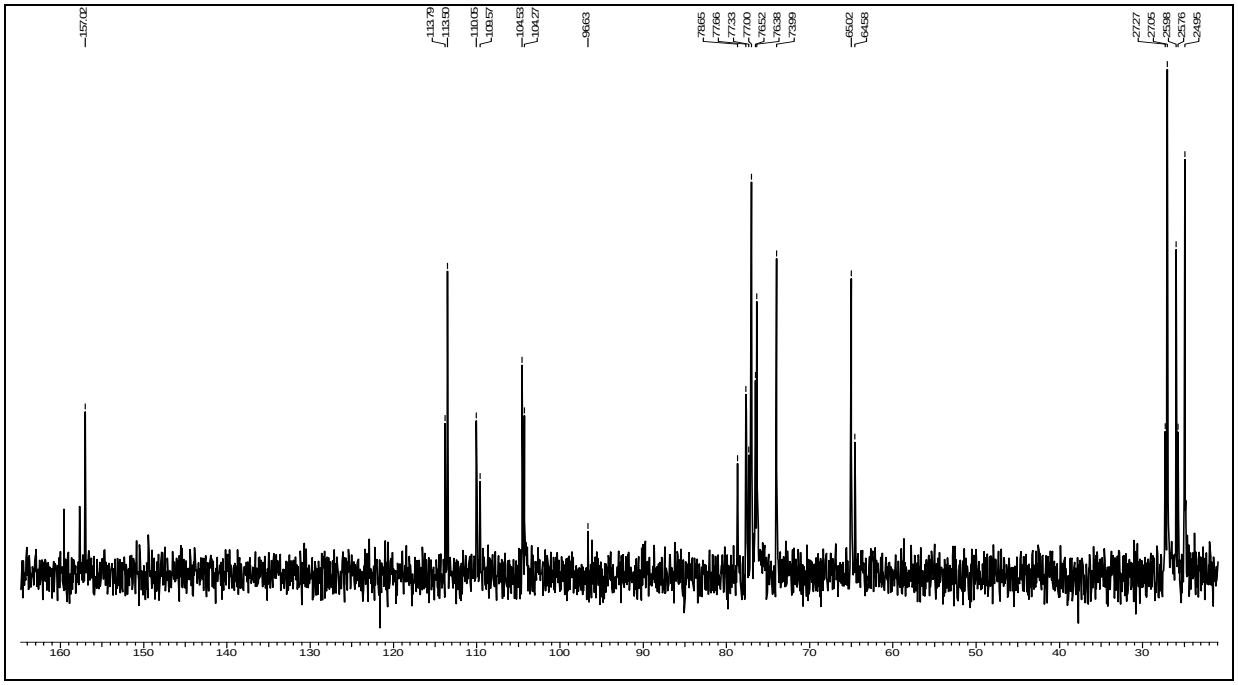

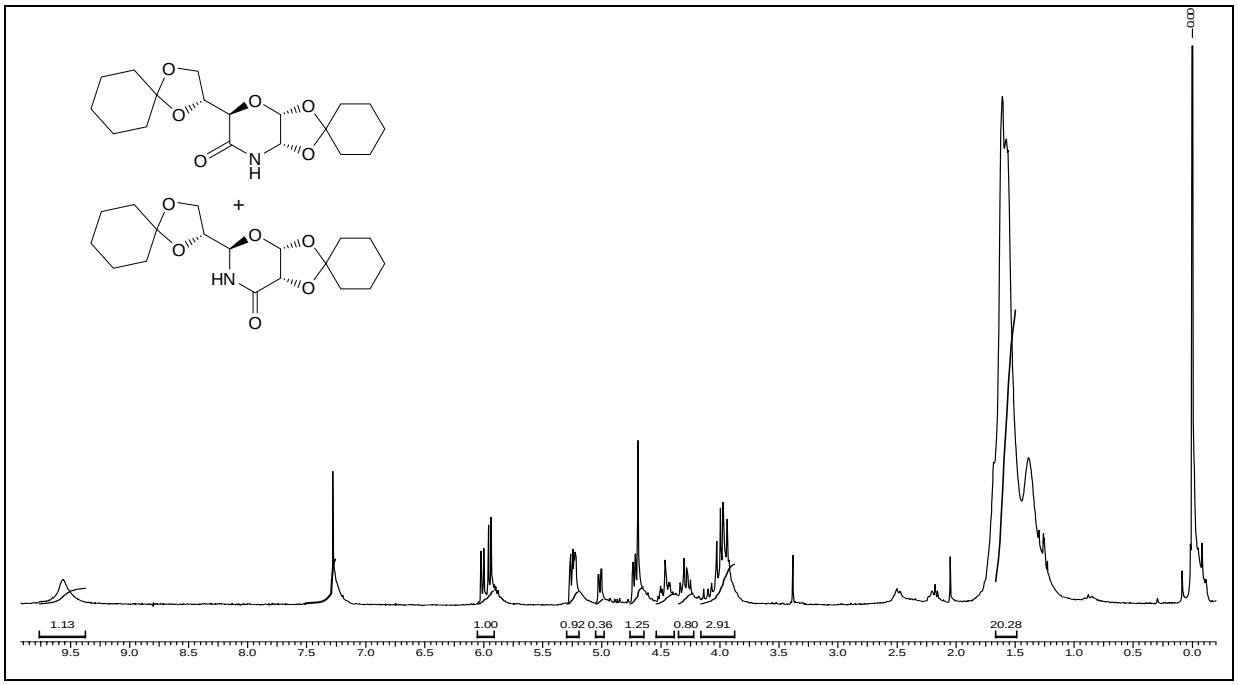

Spectral data for compounds 9 and 10

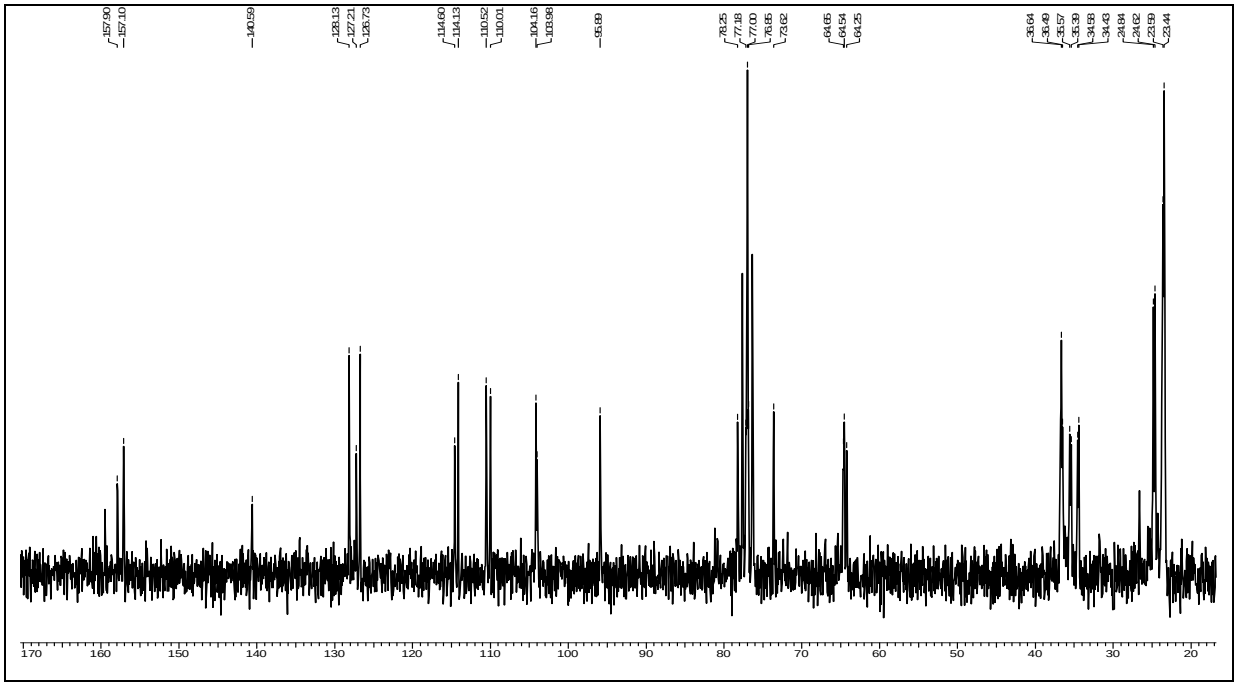

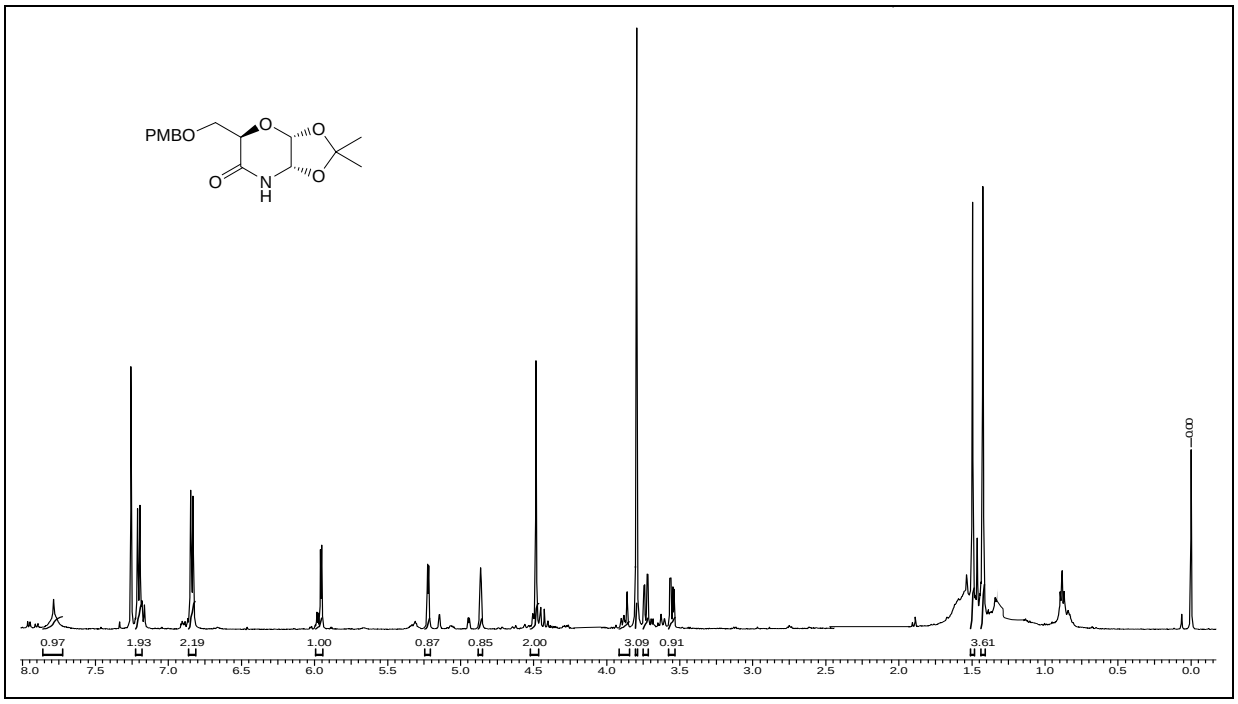

Spectral data for compounds 11 and 12

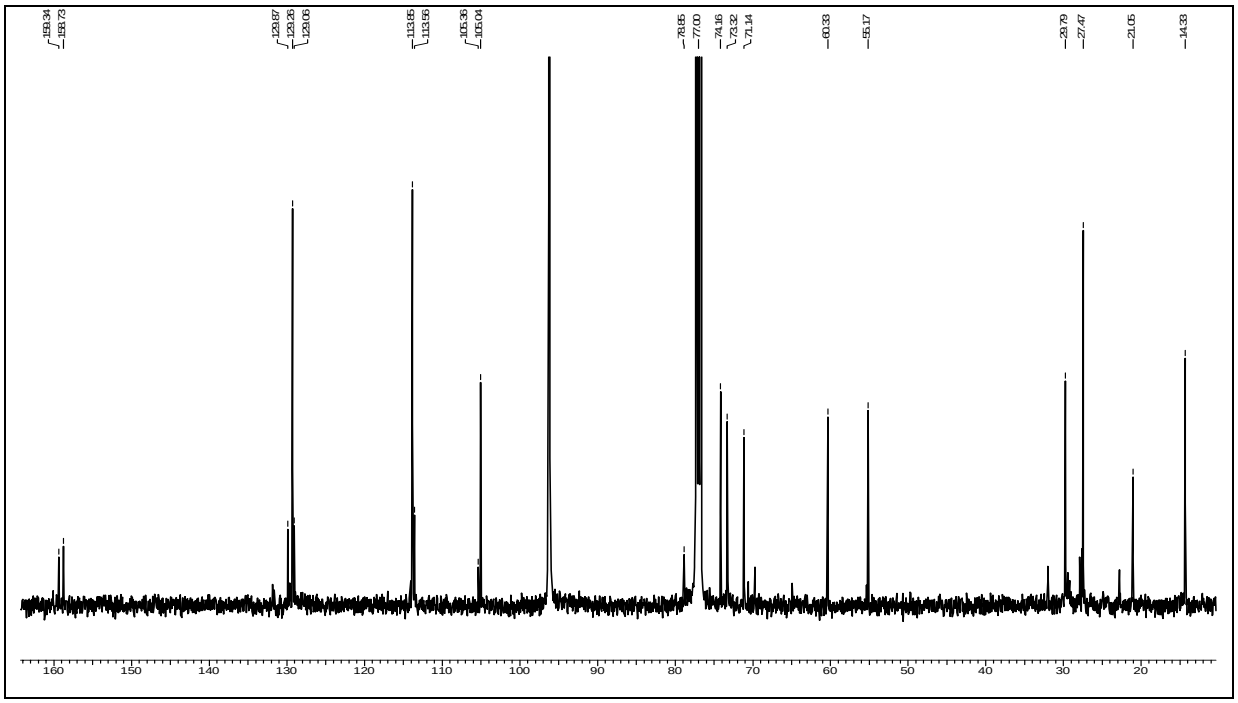

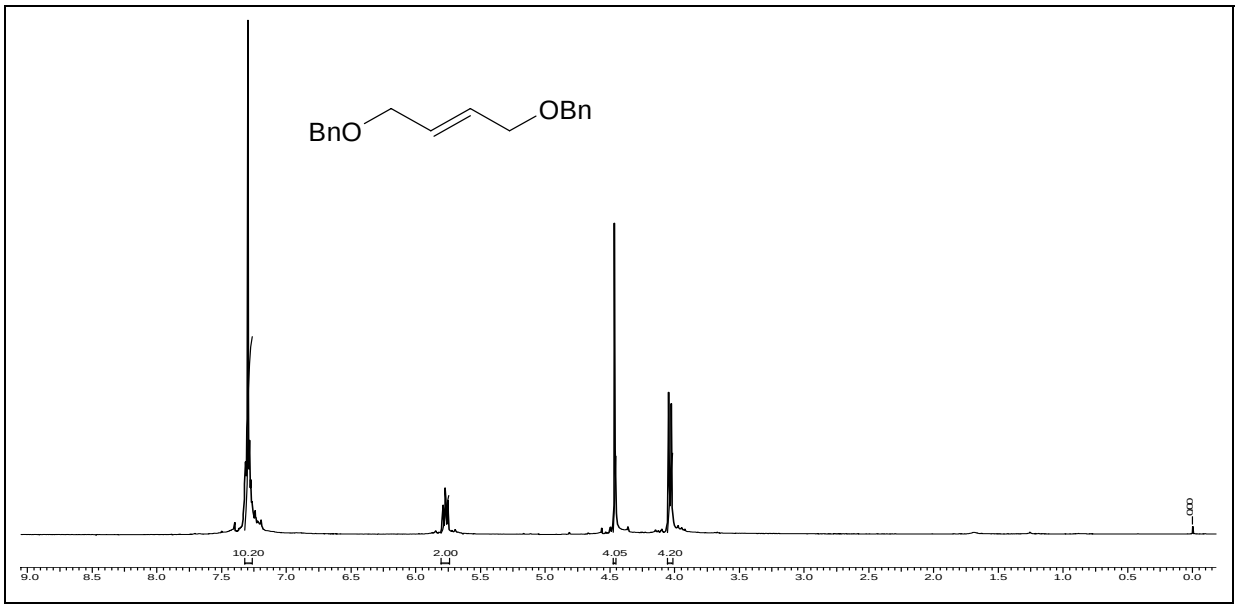

Spectral data for olefin

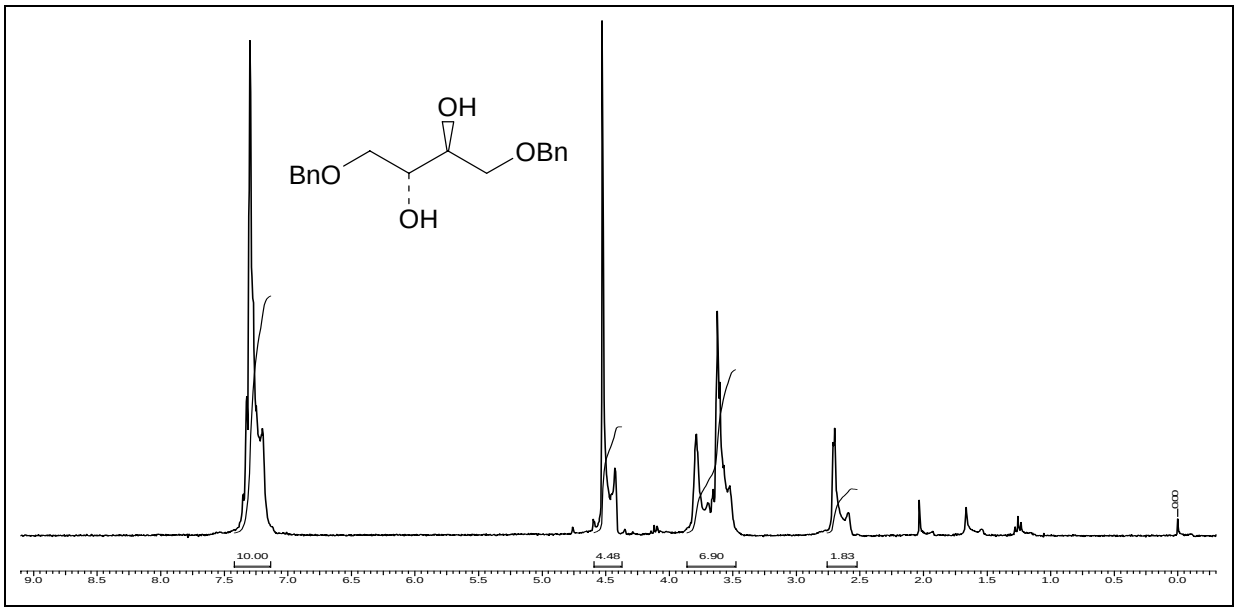

Spectral data for diol

CHAPTER II:

SYNTHESIS OF A NOVEL BIS-FURAN UNNATURAL AMINO ACID (UAA) TEMPLATE FOR PEPTIDO-MIMETIC STUDIES

Introduction

Peptides and proteins play a central role in numerous biological and physiological processes in living organisms; they are involved as hormones and neurotransmitters in intercellular communication, act as antibodies in the immune system to protect organisms against foreign invaders, and are also involved in the transport of various substances through biological membranes. Understanding the control, at the molecular level, of the mechanisms and principles governing structural and functional properties of bioactive proteins is an important objective in biological and medical research. The first requirement for the study of proteins is to assess their ease of availability in terms of purity and quantity. There are three main routes to consider: (i) native protein isolation, (ii) recombinant techniques for the expression of proteins in microorganisms, and (iii) chemical synthesis. Each of these methods has its advantages and disadvantages but only chemical peptide synthesis permits the incorporation of unnatural amino acids and the production of large quantities of pure peptides.

The amino acids are classified on the basis of the position of amino functionality present on the carbon framework i.e. α, β, γ, δ etc. in nature. There are overall twenty-four naturally occurring α-L-amino acids. There are many other β, γ, δ and so on amino acids available in nature. Some natural products even have these amino acids either coupled or inbuilt. The amide bond formed by coupling the NH of one with CO of other amino acid in particular case is called peptide bond and such di, tri, tetra and so on peptides are commonly called as polypeptides. These peptides at times coupled to non amino acid framework for various reasons are called as proteins carrying the name of the non amino acid framework they are attached to e.g. a protein with a peptide linkage attached to carbohydrate moiety is commonly called glycopeptide.

Fig. 1 Synthesis of dipeptide carried out by E. Fischer

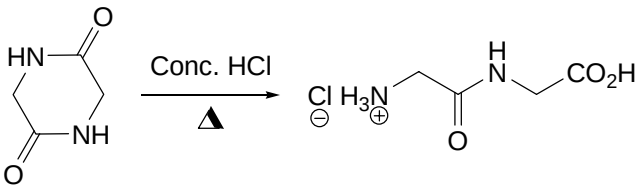

Since the first synthesis of a dipeptide by Emil Fischer[1] in 1901, peptide science has made tremendous progress and with recent innovations it is currently possible to routinely synthesize proteins, well over 200 amino acids in length. The publication in 1901, by E. Fischer[1] of the preparation of the dipeptide glycylglycine by hydrolysis of the diketopiperazine of glycine, is considered to be the beginning of peptide chemistry. However, T. Curtius had synthesized and characterized a related peptide 20 years earlier, during his Ph.D. studies with H. Kolbe, preparing the first N-protected dipeptide, benzoylglycylglycine, by treatment of the silver salt of glycine with benzoylchloride[2]. Some of the first synthetic biologically active peptides are shown in figure 2.

Fig.2 Some of the first synthetic biologically active peptides

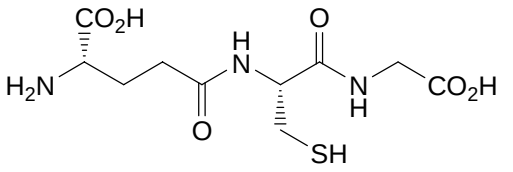

Glutathione
C.R. Harington
1935

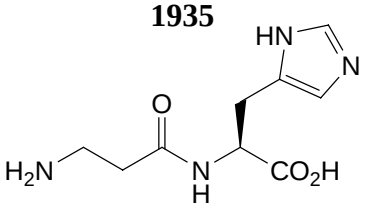

Carnosine
R.H.Siefferd
1935

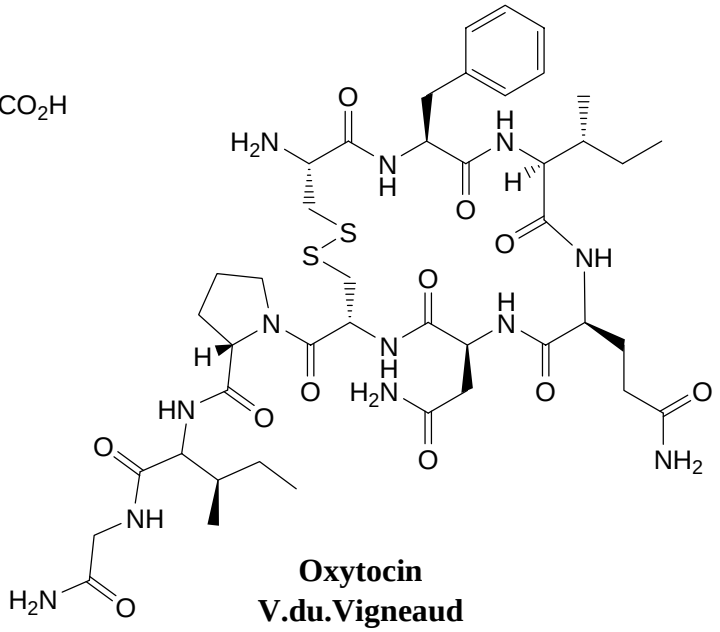

Oxytocin
V.du.Vigneaud
1953

Fig. 3 β-corticotropin Adrenocorticotrophic Hormone (ACTH), a porcine hormone

1 10
H-Ser-Tyr-Ser-Met-Glu-His-Phe-Arg-Tyr-Gly-Lys-Pro-Val-Gly-Lys-Lys-Arg-Arg-Pro-
20 30 39
Val-Lys-Val-Tyr-Pro-Asp-Gly-Ala-Glu-Asp-Glu-Leu-Ala-Phe-Pro-Leu-Glu-Phe-OH

The introduction, in 1957, by L. A. Carpino and F. C. McKay and N. F. Albertson of a new, acid-labile protecting group, the tert-butyloxycarbonyl group (Boc)[3], which is stable toward hydrogenation, Birch reduction, strong alkali and therefore totally orthogonal to the Cbz group and also to benzyl esters and ethers, greatly enhanced the arsenal of protecting groups available to the peptide chemist at the time. The combination of BOC - and CBz - protecting groups was then used for the synthesis of several peptides, the most spectacular example, for this period, being the synthesis of β-corticotropin Adrenocorticotrophic Hormone (ACTH), a 39-residue porcine hormone, in 1963, by R. Schwyzer and P. Sieber[4].

Fig. 4 Coupling reaction through carbodiimide activation: mechanism of racemization via the formation of a 5(4H)-oxazolone.

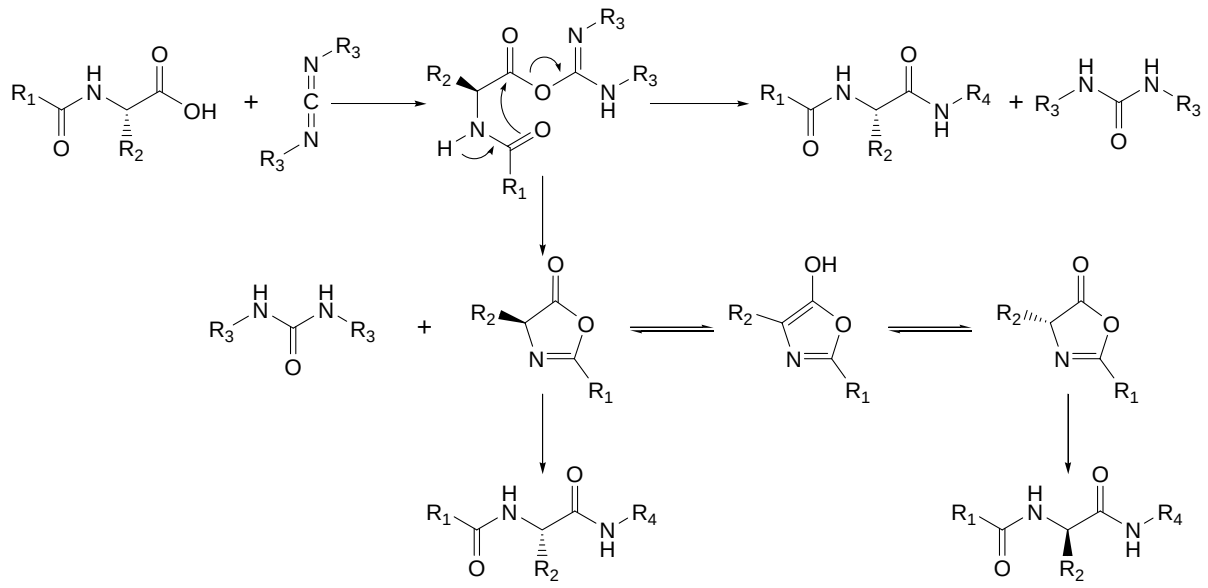

The development of new protecting groups was accompanied by intensive research toward discovering new coupling methods. The most important innovation in this regard was probably the introduction of carbodiimides[5]. The carbodiimide activation method has, however, a high propensity for racemization because of the high reactivity of the O-acyl-isourea, which can lead, through intramolecular cyclization, to the formation of anoxazolone: this cyclic intermediate can easily racemize via an aromatic intermediate.

The racemization mechanism through the formation of the oxazolone has been extensively investigated. In their pioneering work, Goodman and McGahren[6] established all

the factors affecting the optical purity of the oxazolone intermediate during the peptide bond formation, such as the nucleophilicity /basicity ratio of the incoming amino group and solvent effects. However, the introduction of additives such as 1-hydroxybenzotriazole (HOBt) to the reaction mixture was then shown to minimize this by the formation of a less-reactive HOBt ester.

Over the years, numerous other coupling reagents have been developed. The next major breakthrough in peptide chemistry came in 1963 when B. Merrifield published a historic paper describing the principles and the applications of his invention: solid-phase peptide synthesis (SPPS)[7].

Fig. 5 Schematic presentation of the principles of solid-phase peptide synthesis developed by Dr. R.B. Merrifield.

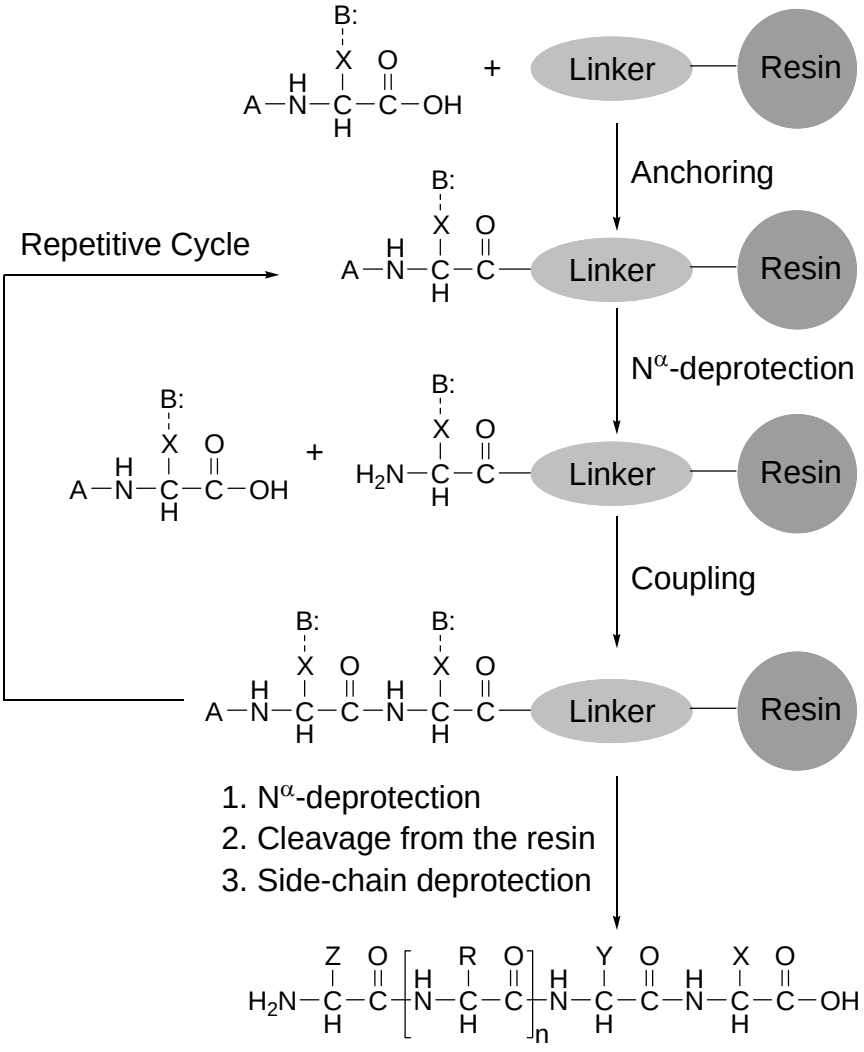

In contrast to the solution-phase methodology, where after each reaction the product has to be isolated and purified before the next step, the growing peptide in the solid-phase approach is linked to an insoluble support and therefore, after each reaction step, the byproducts are simply removed by filtration and washing. Furthermore, because of the repetitive nature of peptide synthesis (deprotection, washing, coupling, washing, deprotection, …), the use of an insoluble support in a single reaction vessel allows for automatization of the processes. In the beginning, the solid support used was a styrene–divinyl benzene co-polymer, functionalized by chloromethylation. The resulting benzyl chloride derivative (the Merrifield resin) was used for anchoring the first amino acid to the resin via an ester linkage. The peptide was then assembled using a carbodiimide as coupling reagent, with a combination of Boc as the protecting group for the N-terminus and benzyl for the side-chain functionalities. Upon completion of the last coupling, the peptide could be cleaved from the resin, with concurrent deprotection of the side-chain-protecting groups, using liquid hydrogen fluoride (HF). The use of liquid HF can, however, lead to numerous side reactions, including catalytic Friedel–Crafts reactions between the aromatic groups of the resin and the side chains of the peptide, and/or promotion of an N→O acyl shift involving the side-chain groups of serine and threonine. These side reactions were minimized by the introduction of a two-stage, low–high HF concentration cleavage protocol by Tam etal[8].

In 1970, L. A. Carpino and G. Y. Han introduced a totally different protecting-group strategy. This was based on the use of the base-labile 9-fluorenyl-methyloxy-carbonyl (Fmoc) group for the protection of the α-amino group, thereby allowing the orthogonal protection of side-chain groups through use of acid-labile protection[9]. The mechanization of the SPPS process permits, in a fully automatic manner, the incorporation of more than 10 amino acid residues per day and since the first introduction of this methodology, has accounted for the synthesis of thousands of peptides. In 1984, B. Merrifield was awarded the Nobel Prize in chemistry for his invention.

There is an important aspect of peptide chemistry that has not been mentioned so far, but which is an essential consideration: the purification and analysis of peptides. Parallel to the intensive development of synthetic methodology for the production of peptides, considerable progress has been made to address these factors. Today, high pressure (high-performance) liquid chromatography (HPLC)[10] is the most widely used method and indeed a

highly effective method for purification, allowing the routine separation of complex product mixtures. Mass spectrometry, on the contrary, is the most powerful tool for product analysis: determining the exact mass of an analytical sample is the best proof that a synthesis was, at least in part, successful or not. The development of new technologies in mass spectrometry permits the sequencing of peptides or proteins and therefore represents a direct analysis of their primary structures[11].

Protein structures mainly comprise of four different classes i.e. primary, secondary, tertiary and quaternary structure. Primary structure is the sequence of amino acids. The secondary structure is the formation of α-helix, β-sheet, β-turn. The folding of secondary structure is determining the tertiary structure and the interaction between various protein subunits is called quaternary structure

Fig. 6 The three main chain torsion angles of a polypeptide

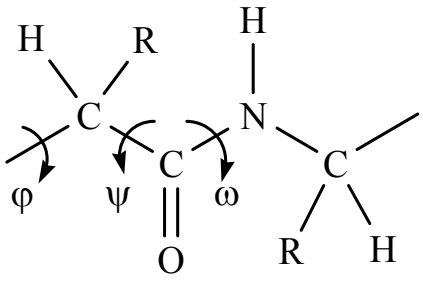

The primary structure of a polypeptide of protein determines its structure at various levels i.e. secondary tertiary and quaternary because for formation of any turn, sheet or helix. The hydrogen bonding that is responsible, achieved by various functionalities of amino acid those form the sequence. Thus systematic investigation of primary structure is the key to study the remaining types of structure of proteins. The secondary structure of protein is the regular arrangement of the polypeptide chain to stabilize the primary structure by hydrogen bonding between the amine and carboxyl group. This type is further divided into three types viz. helix, sheet, turn. The favorable conformations for the formation of either of the forms of secondary structure depend on side chains of the amino acids. They have a tendency for certain φ and ψ bond angles due to steric hindrance either physically or by intra-molecular forces.

In a polypeptide main chain N-C and C-C bonds relatively are free to rotate. These rotations are represented by torsion angles φ and ψ respectively. G.N. Ramchandran used computer models of small polypeptides to symmetrically vary φ and ψ with an objective to find stable conformations.

In the fig.7 the white areas correspond to conformations where atoms in the polypeptide come closer than the sum of their van der Wall's radi. There regions are

sterically disallowed for all amino acids except glycine which is unique in that it lacks a side chain. The grayish region correspond to the conformations where there are no steric clashes i.e. these are the allowed regions namely the α-helical and β-sheet conformations. The yellow areas show the allowed regions if slightly shorter van der Walls radii are used in the calculation i.e. the atoms are allowed to come a little closer together. This brings out an additional region, which corresponds to a left-handed α-helix.

Fig. 7 Ramchandran Plot.

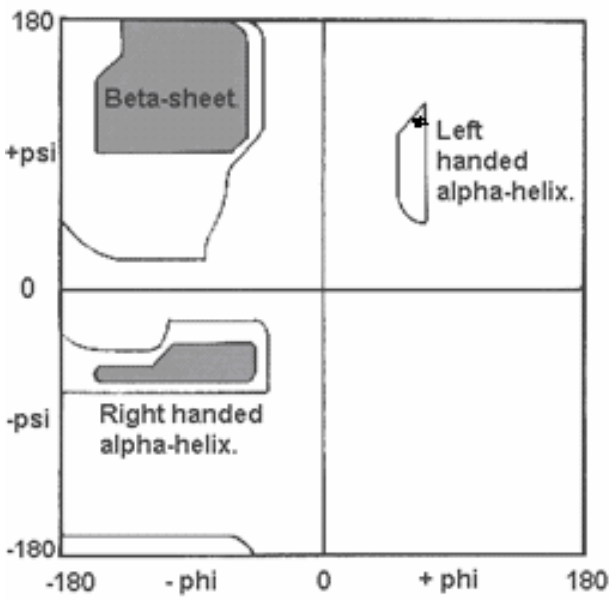

A helical structure of proteins is something similar to a motor winding or a stack of wire or a thread bundle. On the basis of turning in the lining the helical structure are further called α-helix, β–helix and so on. For an anti-clockwise rotation of the peptide sequence the helix is named as *Left-handed helix* and for a clockwise rotation of the peptide sequence the helix is named as *Right-handed helix*. In proteins α-helix conformation is most common. These helices are further divided into 3 major categories α-helix, 3_{10}helix, π-helix.

Linus Pauling, Robert Corey, and Herman Branson first postulated α-helix in 1951 based on the known crystal structure of amino acid and peptide and Pauling's prediction of planer peptide bonds. The general structure of α-helix looks like a screw. The amino acid sequence in an α-helix is arranged in a helical structure about 50 nm (5Å) wide. Each amino acid results in a 100^0 turn in the helix. The helix is tightly packed and there is no free space available in helix. All amino acid chains are arranged at the outside of the helix.

Fig. 8 Toilet role representation of the main chain hydrogen bonding in an α-Helix

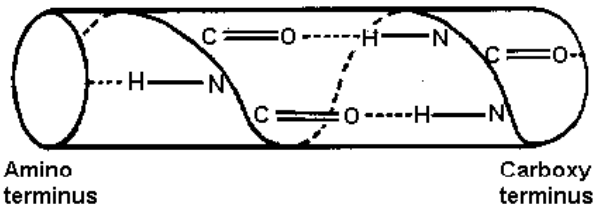

All amino acids don't favor formation of α-helix. Residues that are favorable for the formation of α-helix are alanine, cysteine, leucine, methionine, glutamate, glutamine, histidine, lysine. This means that you can predict the occurrence of α-helix if there are four of six residues that favor the helix form. Hydrogen bonds within an α-helix also display repeating pattern, in which the backbone C=O of residue i hydrogen bonds to the backbone NH of residue i+4.

Fig. 9 Graphical summary of unambiguously assigned NOEs involving sequentially nonadjacent residues for α/β-peptide in CD_3OH.

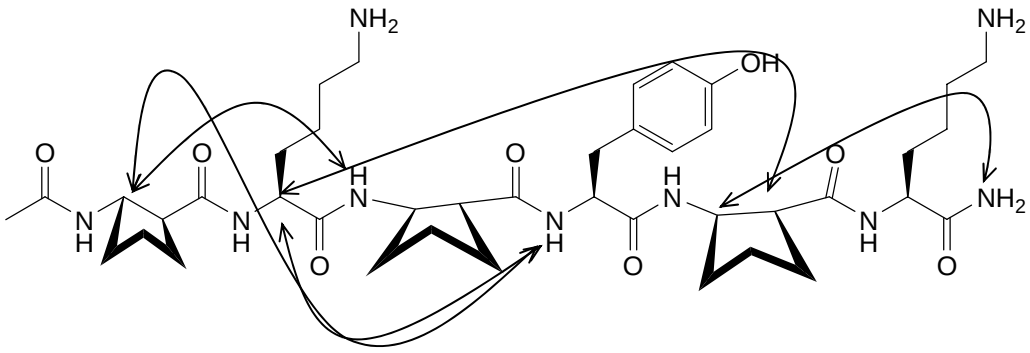

Gellman etal have shown that combining α-amino acid and cyclic β-amino acid residues in a sequentially alternating pattern can lead to helix formation within relatively short hetero oligomers[12]. Structural data suggest that these foldamers have a "split personality," simultaneously populating two different helical conformations. Both helices contain backbone C=O···H-N hydrogen bonds with N→C directionality, but they differ in the sequential spacing between C=O and H-N (i, i+3 in one case and i, i+4 in the other). This behavior parallels closely the split personality observed among peptides composed exclusively of α-amino acid residues, which frequently populate both α- and 3_{10}-helical conformations in solution[13]. These α/β-peptides differ from α-peptides, however, in that folding is observed with fewer residues in the former than in the latter. The different monomer types in the heterogeneous α/β-peptide backbone offer complementary benefits to the new foldamers that have been identified: the constrained β-residues provide conformational preorganization, while the α-residues allow facile introduction of specific side chains at specific positions. The distereoisomer of the compound shown in fig. 9 where

all the α-residues have the opposite configuration does not show similar NOEs marked in fig. 9. Model structures are constructed also for helices defined by hydrogen bonds with the opposite directionality, from carbonyl groups to amide protons in the N-terminal direction (the 9-, 12/13-, and 16-helices). This set of helical conformations could be ruled out because the NOEs predicted for these structures, mostly NH of residue i to H^{α} or H^{β} of residue i+2, i+3, or i+4, were not detected for the particular compound or the oligomers discussed[14].

Fig. 10 Peptide sequences forming α-helix

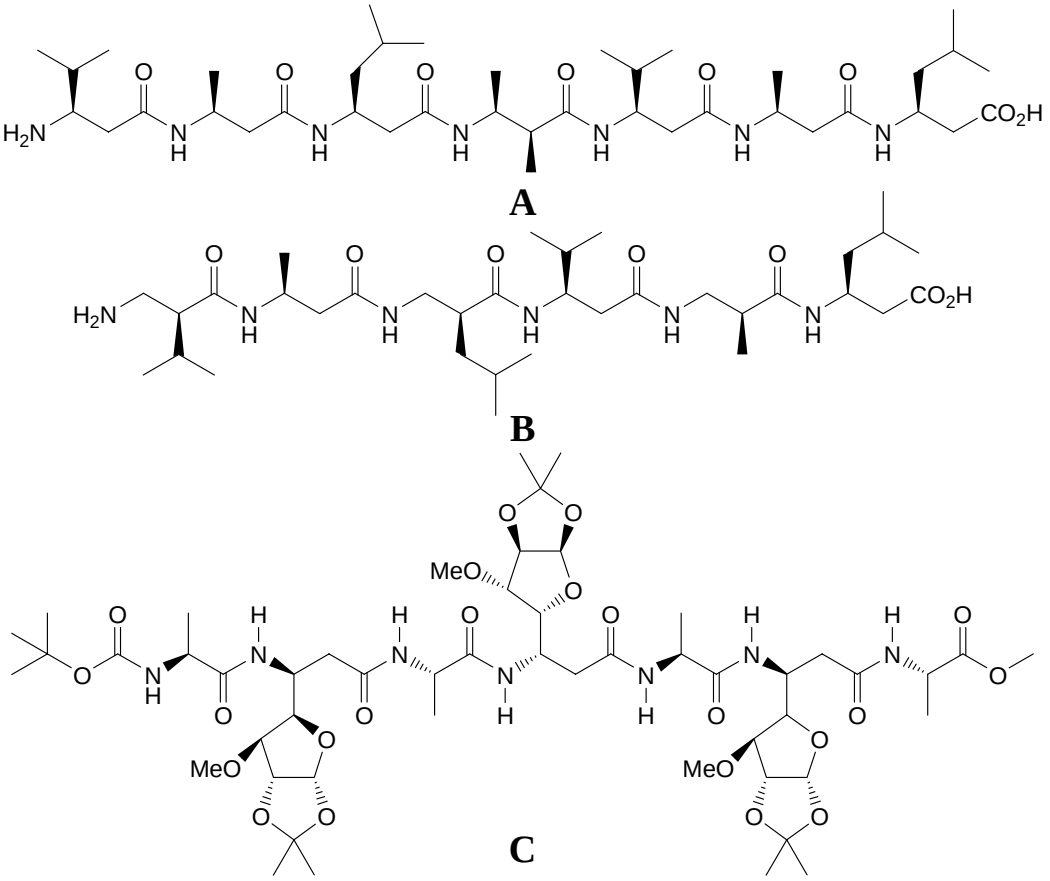

In **A**[15] (fig. 10) all side chains are in position C-3 (except for residue number four, which is methylated at both C-3 and C-2 positions), while in **B**[15, 16] the side chains alternate between positions C-2 and C-3. In methanol and pyridine, **A** adopts a left-handed helix (hydrogen bonds between residues i and i+2) consisting of three residues per turn (3_{10}-helix), in which the amide C=O bonds point in the direction of the N terminus. In the same solvents, **B** predominantly forms a right-handed helix (hydrogen bonds between residues i and i+1, and

between i and i+3) in which the amide C=O bonds point alternately up and down the helix axis. Peptide **C**[17] is synthesized with alternate alanine units coupled with a novel β-amino acid obtained form D-Glucose. This peptide folds itself into α-helix conformation with NH of i forms intramolecular hydrogen bonding with i+4.

The 3_{10} helix is not a common secondary structural element in proteins. Only 3.4% of the residues are involved in 3_{10} helices in the Sander database (1983). α-helix at times begins or ends with a single turn of 3_{10} helix (one hydrogen bond). There are 3 residues present per helical turn in this type. Here even hydrogen bonds also show repeating pattern and the backbone C=O of residue i hydrogen bonds to the backbone NH of residue i+3. The φ and ψ bond angles of a pure 3_{10} helix (-74.0, -4.0) lie at the edge of an allowed minimum energy level region of the Ramchandran (φ, ψ) map.

π-helix is the most rare forms of secondary structure of protein. Hydrogen bonds within π-helix display a repeating pattern in which the backbone C=O of residue i forms hydrogen bonds with backbone residue NH of residue i+5. Similar to 3_{10} helix, π-helix is found at the end of α-helix. The φ and ψ bond angles of the pure π-helix (-57.1, -69.7) also lie at edge of an allowed minimum energy level region of the Ramchandran plot.

β-sheets is another common form of secondary structure of protein first proposed by Linus, Robert Corey in 1951. A β-sheet contains two or more hydrogen bonded β-strands. The two neighboring β-strands may be anti parallel (A) or parallel (B) or mixed (C), this depends on their alignment from N to C terminus. When φ and ψ bond angles are repeated throughout a polypeptide chain (-139, +135) then β-sheet conformation will occur. Residues that favor conformation are Valine, Isoleucine, Phenyl Alanine, tyrosine, tryptophan, threonine. β-sheet will only form if there are minimum of three to five residues of β-sheet favoring.

Fig. 11 Different Types of sheets

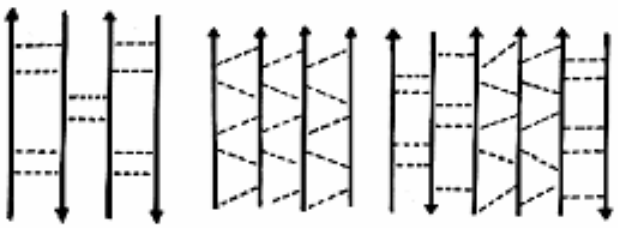

For a β-sheet conformation, the hydrogen bonds are observed between the C=O and HN groups of adjacent chains. van der Waal's repulsions between the α-hydrogens of side

chains cause the chains to rotate with respect to one another to give a rippled effect. Hence the name *pleated β sheet*. The pleated β sheet is an important secondary structure, especially in proteins that are rich in amino acids with small side chains, such as H (glycine), CH_3 (alanine), and CH_2OH (serine). Fibroin, the major protein of most silk fibers, is almost entirely pleated β sheet, and over 80% of it is a repeating sequence of the six-residue unit -Gly-Ser-Gly-Ala-Gly-Ala-.

Fig. 12 The left handed twist of a β-sheet

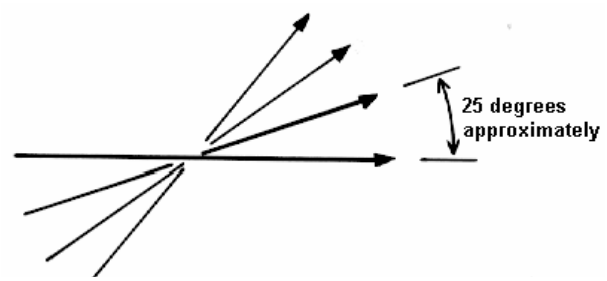

The Pauling-Corey model of the β-sheet is planar. However, most β-sheets found in globular protein X-ray structures are twisted. The overall twisting of the sheet results from a relative rotation of each residue in the strands by 30 degrees per amino acid in a right-handed sense. Parallel sheets are less twisted than anti-parallel and are always buried. In contrast, anti-parallel sheets can withstand greater distortions (twisting and β-bulges) and greater exposure to solvent. This implies that anti-parallel sheets are more stable than parallel ones that are consistent both with the hydrogen bond geometry and the fact that small parallel sheets rarely occur.

The pleated β sheet is flexible, but because the peptide chains are nearly in an extended conformation, it resists stretching. Unlike the pleated β sheet, in which hydrogen bonds are formed between two chains, the helix is stabilized by hydrogen bonds within a single chain. The principal protein components of muscle (myosin) and wool (α-keratiri), for example, contain high percentages of helix. When wool fibers are stretched, the breaking of hydrogen bonds elongates these helical regions. Disulfide bonds between cysteine residues of neighboring α-keratin chains are too strong to be broken during stretching, however, and they limit the extent of distortion. After the stretching force is removed, the hydrogen bonds re-form spontaneously, and the wool fiber returns to its original shape. Wool has properties that are different from those of silk because the secondary structures of the two fibers are different, and their secondary structures are different because the primary structures are different.

Fig. 13 Peptides showing β-sheet formation

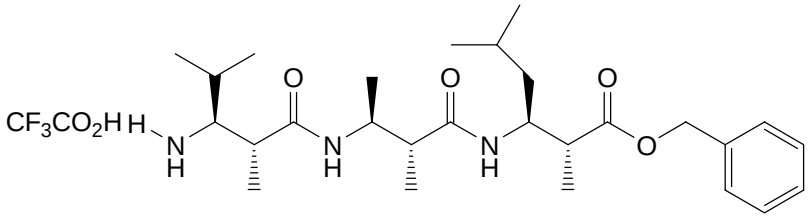

A

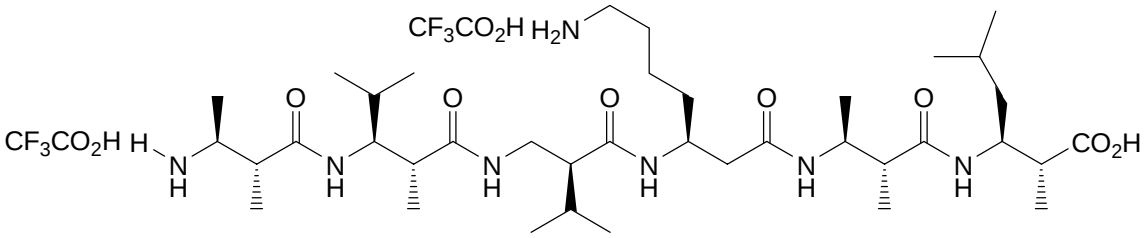

B

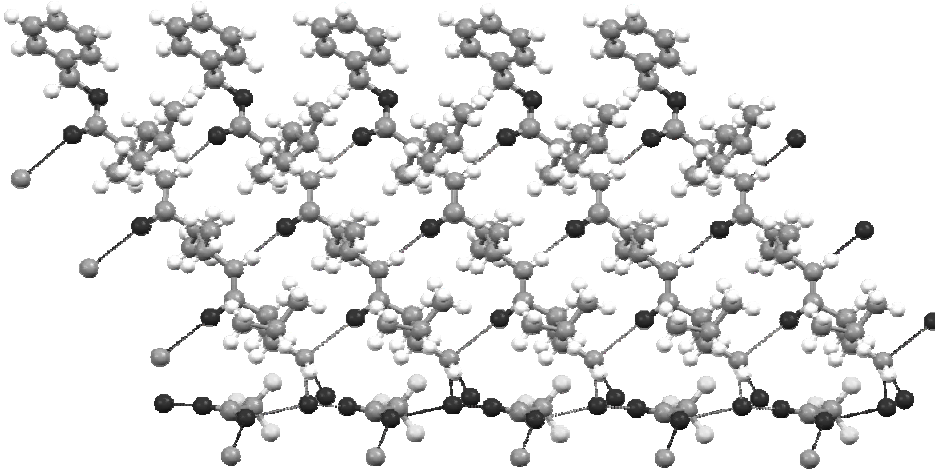

Crystal structure of A

Unsurmountable solubility problems arise upon chain elongation with formation of β-peptides such as **A**, so that attempted dimerizing coupling of **A**[18] (fig. 13) to give a hexapeptide is unsuccessful. The parallel amide planes in the individual strands are connected through CHR-CHMe ethane moieties, in which R and methyl are antiperiplanar as are HN and C=O; 14-membered hydrogen-bonded rings connect the strands in the parallel sheet structure. In contrast to α-peptidic sheets, where neighboring O=C bonds point in opposite directions, these bonds are unidirectional in the β-peptide structure, leading to a polar packing that might be an additional reason for the low solubility of compounds of this

type. In case of **B**, two dipeptide segments of unlike-β-amino acids, which enforce the extended conformation, are attached on each end of this unit and are supposed to form intra- rather than intermolecular hydrogen bonds. In fact, the resulting β-peptide **B** is well soluble, even in water (due to the ω-amino butyl group). The structure of hexapeptide **B** in CD_3OH is determined by 2D NMR spectroscopy[19].

Fig. 14 Backbone-backbone NOEs between nonadjacent residues observed in ROESY analysis for 2.5 mM

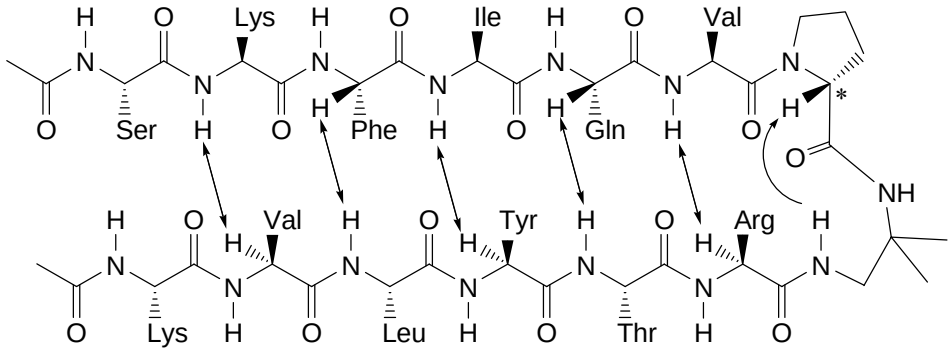

A combination of NMR and CD data shows that compound shown in fig. 14 adopts a two-stranded parallel β-sheet conformation in aqueous solution[20]. As with other secondary structure model systems, folded and unfolded conformations appear to be in rapid equilibrium. Inverting the configuration of the *Pro* residue in the linker segment (marked as *) has a profound effect on conformation, since the distereoisomer appears to be entirely random coil. Similar effects have previouly been observed for antiparallel β-sheet model systems in which Pro – Gly segments are used to link adjacent strands[21].

Turns are first identified by Venkatachalam (1968) who found three types each containing hydrogen bonds between the carbonyl oxygen of residue i and the amide nitrogen of i+3. An alternative requirement for a turn to occur in peptide secondary structure is that, the α-carbons of residue i and i+3 must be within 7Å. These three types of turns are designated as I, II and III. Type I turn occurs most frequently (2-3 times more frequently than II and III). The mirror image type I' and type II' are rare but I' is preferred to formation of β-hairpins. Proline is most favored at position i+1 as its φ angle is restricted to -60 and its amide nitrogen does not require hydrogen bond. Glycine is favored at i+3 in type I and II

turns. Ideally type I' turns have glycine at position i+1 and i+2 and type II' turns have glycine at position i+1.

Fig. 15 Structures showing β-Turn during folding

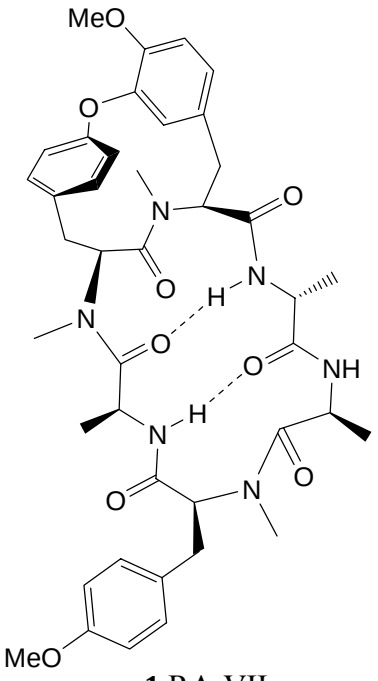

1 RA-VII

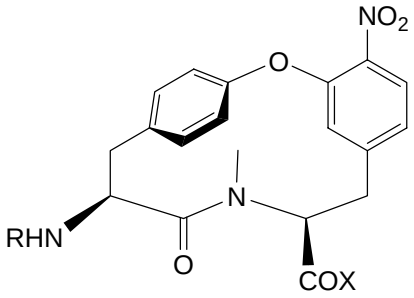

2 R = Me, X = OH
4 R = COMe, X = NHMe

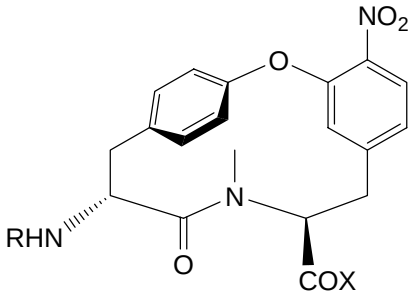

3 R = Me, X = OH
5 R = COMe, X = NHMe

Type I turn: - Hydrogen bonding is observed between C=O of residue i and NH of residue i+3. The backbone dihedral angle of residues are (-60, -30) and (-90, 0) of residues i+1 and i+2 respectively of the type I turns.

Type II turns: - Similar to type I turns here also hydrogen bonding is observed between C=O of residue i and NH of residue i+3. The backbone dihedral angles of residues are (-60, -120) and (80, 0) of residues i+1 and i+2 respectively of type II turn.

Type III turns: - Similar to type I turns here also hydrogen bonding is observed between C=O of residue i and NH of residue i+3. This is a single turn of right hand (III) and left handed (III') 3_{10} helix respectively. The backbone dihedral angles of residues are (-60, -30) and (-60, -30) of residues i+1 and i+2 respectively of the classical type III turn.

Moritta etal have investigated RA-VII (fig. 15 **1**), a natural product with potent anti-tumor activity[22]. Both X-ray and solution NMR spectroscopic analysis of RA-VII indicate the presence of a typical type-II β turn structure for the major conformer. Since it is well known that 18-membered cyclic hexapeptides are prone to adopt a turn-extended-turn conformation[23], it is thus expected that RA-VII contains a β-turn motif within the 18-membered ring. On the other hand, it was unknown whether the 14-membered *m*,*p*-cyclophane alone (**2** or its diastereomer **3**) is able to induce an external β-turn at the outset of this work. Inspection of the X-ray structure of (S_{i+1}, S_{i+2})-cyclophane (**2**) and (R_{i+1}, S_{i+2})-cyclophane (**3**)[24] indicated that only the unnatural (R_{i+1}, S_{i+2})-stereomer **3** is capable of acting as a β-turn inducer[25]. To gain further insight into the conformational properties of these two cyclophanes, molecular modeling of compounds **4** and **5** is carried out. In accord with speculation, only the (R_{i+1}, S_{i+2})-**5**, not the (S_{i+1},S_{i+2})-**4**, adopted a β-turn conformation. Indeed, the values of the torsion angles of the lower energy conformer of **5**, ϕ (*i*+1) 70.8, φ (*i*+1) -117.1, ϕ (*i*+2) -79.1, φ (*i*+2) -7.6, corresponded nicely to that of an ideal type-II′ β-turn.

Fig. 16 Structure of BDT and its amino analogue showing β-Turn activity

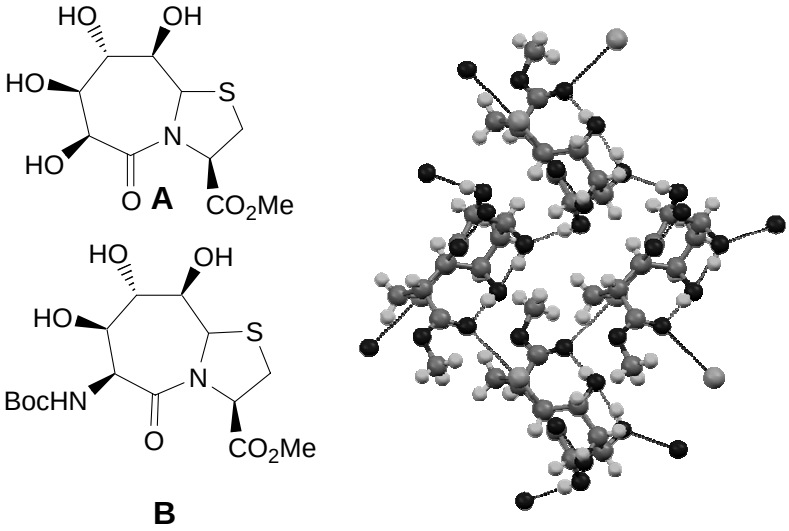

The structure of BDT mimics sequences like Serine – Proline or Threonine - Cystine. Counting the bonds from the amino terminus along the seven-membered ring to the C-terminus, **B** is also the poly-hydroxy analogue of a tripeptide sequence and therefore a so-

called sugar amino acid[26]. Bicyclic thiazolidine lactams induce reverse turns in peptides[27]. BTD fixes the torsions $\psi_{(i+l)}$ and $\phi_{(i+2)}$of a reverse turn to the values of -157° and -66°. 169° (O6-C6-C5-N4) and -88° (C5-N4-C3-CO) were found for **A**[28] and coupling constants and intramolecular NOE buildup rates indicate a similar conformation for **B** in water[29]. BTD was incorporated in numerous peptides and even in proteins[30]. **B** is easier accessible than BTD, it is more hydrophilic and offers functional groups for further derivatisation. The protection of secondary alcohols is not required during peptide synthesis.

Fig. 17 Structures of isosters showing β-turn mimics

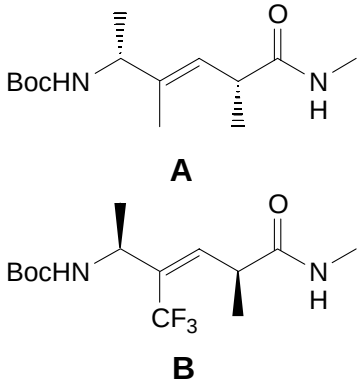

Wipf etal have been able to devise enantioselective synthetic approaches for L-Ala-D-Ala (or enantiomeric) dipeptide alkene isostere sequences that, for the first time, included the preparation of a (trifluoromethyl) alkene isostere[31]. X-ray study has established that methyl- and trifluoromethyl-substituted alkenes provide conformationally considerably more highly preorganized backbone-rigidified peptide mimetics than the parent disubstituted alkenes. The D-L methyl-(*E*)-alkene isostere sequence **A** prefers an intramolecularly hydrogen bonded type-II' β-turn in the solid state. The corresponding trifluoromethyl analogue **B** representing an L-D sequence shows a preference for a type-II β-turn and folds almost perfectly pseudo enantiomeric to **A**. The conformational properties of **A** and **B** follow closely those of regular peptides, since a type II β-turn is generally preferred by an L-Ala-D-Ala sequence and a type-II' by the corresponding D-L dipeptide. Glycine often replaces the non-proteinogenic D-amino acid in these turns.

A β-hairpin is defined as a polypeptide or polynucleotide secondary structure element containing two antiparallel strands connected by a turn. In such peptides the amino acid chain reverses its overall direction and intramolecular hydrogen bonds are formed between the facing amino acids, given rise to pseudo-rings (for example i and i+3 → pseudo-ten; i-1 and i+4 → pseudo fourteen membered ring, fig. 14).[20, 32] In native β-hairpins, the involved β-turn was recognized to be always of type I' or II' conformation, which comprise only 4% and 3%, respectively, of all known classic β-turns.[33] It has been suggested that these, especially type

I', are only favored when stabilized by additional hydrogen bonds, for example in a β-hairpin.[33b] Originally the term β-sheet was defined as a group of hairpins however today it is also used as a synonym for a β-hairpin. Efforts to characterize and mimic β-hairpins have been pursued intensively, most likely motivated by the recognition of their involvement in many vital physiological processes and pathological disorders. Protein-DNA recognition,[34] protein-RNA recognition[35] and protein-protein recognition,[36] Alzheimer's disease,[37] prion diseases,[38] immunoglobulin E mediated allergic response,[39] interaction of bacterial cell surface asspciated protein with immunoglobulin G,[40] and HIV glycoprotein-120 binding to human T-cell surface protein CD4[41] are some examples of the biological occurrence of the β-hairpin secondary structure element.

The direct use of peptides as oral drugs is in general limited by their poor absorption from the gastrointestinal tract, low metabolic stability towards proteolytic enzymes, rapid clearance through the liver and kidneys and a profound antigen character. Efforts to overcome these disadvantages have resulted in development of peptidomimetics, compounds mimicking the biological effects of endogenous peptides while displaying more favorable pharmacological properties. In peptidomimetics, the amino acid considered to be of minor importance for the molecular recognition event are substituted by non-peptidic moieties thereby in the optimal case they provide superior pharmacokinetic properties and simultaneously enforce the formation of a particular secondary structure element.

For β and γ-turns, the amino acid side chains in the turn regions were suggested to be involved in intramolecular interactions.[42] However, in the case of β-hairpins, those positioned in the extended strands is most likely to be responsible for the biological activity.[43] Because of the low significance of the side chains in the turn parts of β-hairpins for molecular recognition, a large number of hairpin mimetics replacting turns by other non-native peptide or non peptide motifs have been reported.[32,44] The recently recognized correlation of biological activity with hairpin conformational stability (antiparallel alignment of the participating peptide strands) in some peptides[45] signifies the impact of well designed, rigid turn mimetics.

The NMR analysis confirms that all of the peptides adopt a β-hairpin structure in equilibrium with random-coil conformations.[46a] Although some of the NOEs are not found in all of the peptides (in some cases due to signal overlapping), the NOEs observed in the six

peptides are consistent with the same β-hairpin structure. In particular, the diagnostic αα (i,i + 5) between Thr 5 and Thr 10, characteristic of the β-hairpin 2:2 structure (following the nomenclature proposed by Sibanda et al. 1989)[46b], is found in aqueous solution in all peptides. A new αα NOE between residues 3 and 12 is observed in aqueous solution. Another NMR parameter that is sensitive to the presence of folded structures is the conformational shift of the Cα protons (differences between a random-coil reference and the experimental values). Downfield chemical shifts are associated to extended populations, whereas upfield values are indicative of helical or turn regions.[46c]

Fig. 18 Structure of BH-KE peptide sequence showing β-hairpin structure

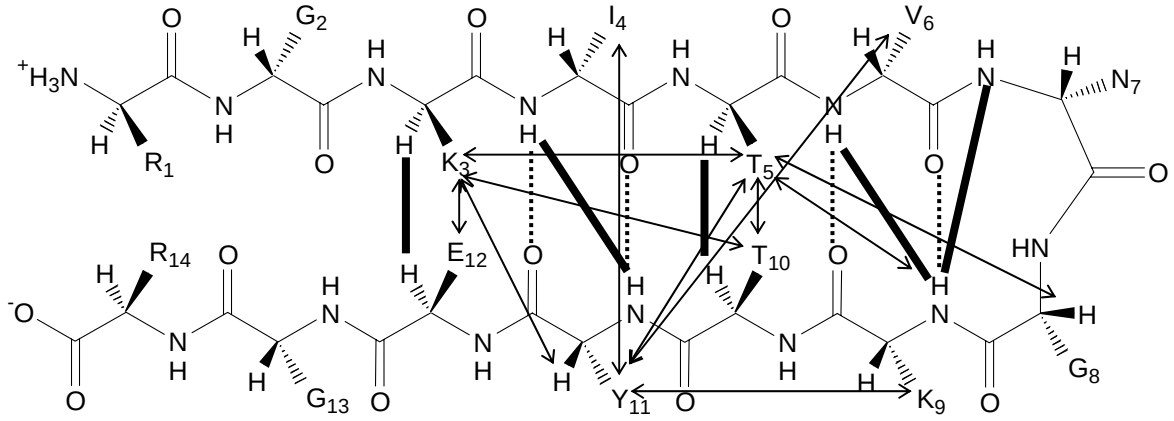

(Thick lines) Main-chain–main-chain NOEs. (Arrows) Side-chain–side chain and side-chain–main-chain NOEs.

In addition to the previously included β-strand residues, the residues added at positions 3 and 12 also exhibit downfield shifts. The $^{3}J_{NH\alpha}$ coupling constants are related to the ϕ dihedral angle[46d] and therefore should also be sensitive to the formation of a β-hairpin structure. The experimental $^{3}J_{NHa}$ coupling constants values in the β-strand regions are generally higher than in the random-coil conformation.[46e] All of these results indicate that the β-hairpin structure is restricted to residues 3–12. Addition of the ionic pair Lys–Glu resulted in the formation of a more stable β-hairpin motif having four residues per strand. When looking at the individual residues, it seems that, similarly to what happens in β-helices, there is some fraying at the first and last positions of the β-hairpin (positions 3 and 12). This fraying is not observed in the shortest peptide BH8.[46f] Fraying at the ends of a β-hairpin has

also been observed in a four-residue β-hairpin analyzed by Rico and coworkers.[46g] The fact that the first and last residues in a four-residue-per-strand β-hairpin are not involved in main chain hydrogen bonds, as it happens in a three-residue per strand β-hairpin, could explain these results. Analysis of peptide BH-KE in 40% TFE supports this hypothesis, because the population estimate with the α-α NOE intensity between residues 3 and 12 seems to be lower than that using residues 5–10.

Fig. 18 Structure of Carboxypeptidase A displayed as a tube model and a ribbon diagram.

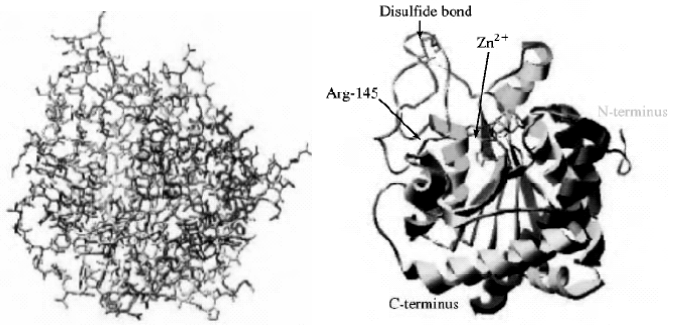

The tertiary structure of a peptide or protein refers to the folding of the chain. The way the chain is folded affects both the physical properties of a protein and its biological function. Structural proteins, such as those present in skin, hair, tendons, wool, and silk, may have either helical or pleated-sheet secondary structures, but in general are elongated in shape, with a chain length many times the chain diameter. They are classed as fibrous proteins and, as befits their structural role, tend to be insoluble in water. Many other proteins, including most enzymes, operate in aqueous media; some are soluble, but most are dispersed as colloids. Proteins of this type are called globular proteins. Globular proteins are approximately spherical. Fig. 18 shows carboxypeptidase A,[47] a globular protein containing 307 amino acids. A typical protein such as carboxypeptidase A incorporates elements of a number of secondary structures: some segments are helical; others, pleated sheet; and still others correspond to no simple description. The shape of a large protein is influenced by many factors, including, of course, its primary and secondary structure. The disulfide bond shown in fig. links Cys- 138 of carboxypeptidase A to Cys-161 and contributes to the tertiary structure. Car- boxypeptidase A contains a Zn^{2+} ion, which is essential to the catalytic activity of the enzyme, and its presence influences the tertiary structure. The Zn^{2+} ion lies

near the center of the enzyme, where it is coordinated to the imidazole nitrogens of two histidine residues (His-69, His-196) and to the carboxylate side chain of Glu-72.

Fig. 19 Proposed mechanism of hydrolysis of a peptide catalyzed by carboxypeptidase A.

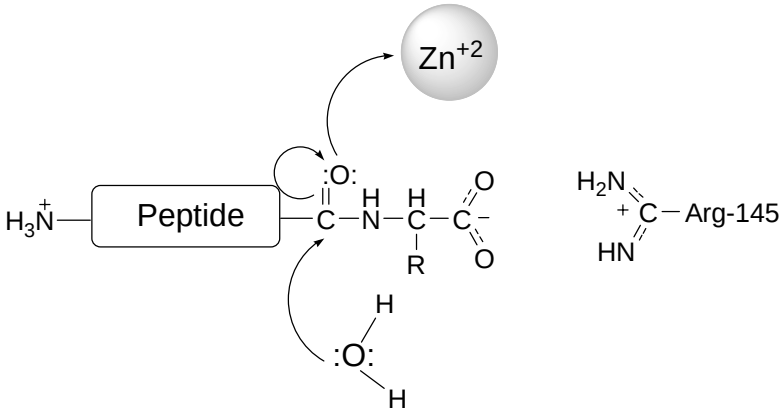

Protein tertiary structure is also influenced by the environment. In water a globular protein usually adopts a shape that places its hydrophobic groups toward the interior, with its polar groups on the surface, where they are solvated by water molecules. About 65% of the mass of most cells is water, and the proteins present in cells are said to be in their native state, the tertiary structure in which they express their biological activity. When the tertiary structure of a protein is disrupted by adding substances that cause the protein chain to unfold, the protein becomes denatured and loses most, if not all, of its activity. Evidence that supports the view that the tertiary structure is dictated by the primary structure includes experiments in which proteins are denatured and allowed to stand, whereupon they are observed to spontaneously readopt their native-state conformation with full recovery of biological activity. Most protein tertiary structures are determined by X-ray crystallography. The first, myoglobin, the oxygen storage protein of muscle, was determined in 1957. Since then thousands more have been determined. The data are deposited as a table of crystallographic coordinates in the Protein Data Bank and are freely available. At present, the Protein Data Bank averages about one new protein structure per day.

Knowing how the protein chain is folded is a key ingredient in understanding the mechanism by which an enzyme catalyzes a reaction. Take carboxypeptidase A for exam-example. This enzyme catalyzes the hydrolysis of the peptide bond at the C terminus. It is

believed that an ionic bond between the positively charged side chain of an arginine residue (Arg-145) of the enzyme and the negatively charged carboxylate group of the substrate's C-terminal amino acid binds the peptide at the active site, a cavity on the enzyme's surface where the catalytically important functional groups are located. There, the Zn^{2+} ion acts as a Lewis acid toward the carbonyl oxygen of the peptide substrate, increasing its susceptibility to attack by a water molecule. Living systems contain thousands of different enzymes. As we have seen, all are structurally quite complex, and no sweeping generalizations can be made to include all aspects of enzymic catalysis. The case of carboxypeptidase A illustrates one mode of enzyme action, the bringing together of reactants and catalytically active functions at the active site.

Fig. 20 Structure of sperm-whale myoglobin displayed as a tube model and a ribbon diagram.

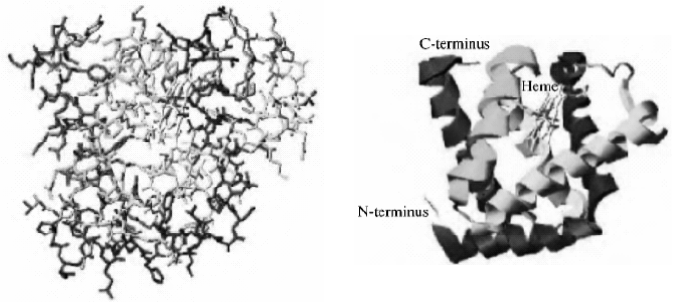

Rather than existing as a single polypeptide chain, some proteins are assemblies of two or more chains. The manner in which these subunits are organized is called the quaternary structure of the protein. Quaternary structure describes the assembly of different tertiary structures. They are formed by non-covalent interactions between more than one chain in protein. Different tertiary structures associate to form a quaternary structure.[48] Hemoglobin is the oxygen-carrying protein of blood. It binds oxygen at the lungs and transports it to the muscles, where it is stored by myoglobin. Hemoglobin binds oxygen in very much the same way as myoglobin, using heme as the prosthetic group. Hemoglobin is much larger than myoglobin, however, having a molecular weight of 64,500, whereas that of myoglobin is 17,500; hemoglobin contains four heme units (myoglobin only 1). Hemoglobin is an assembly of four hemes and four protein chains, including two identical chains called the α chains and two identical chains called the β chains.

Fig. 21 Structure of Heam unit

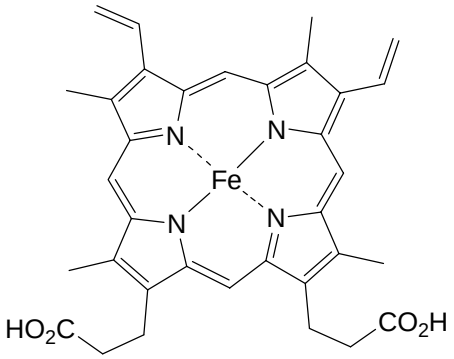

Some substances, such as CO, form strong bonds to the iron of heme, strong enough to displace O_2 from it. Carbon monoxide binds 30-50 times more effectively than oxygen to myoglobin and hundreds of times better than oxygen to hemoglobin. Strong binding of CO at the active site interferes with the ability of heme to perform its biological task of transporting and storing oxygen, with potentially lethal results. How function depends on structure can be seen in the case of the genetic disorder sickle cell anemia. This is a debilitating, sometimes fatal, disease in which red blood cells become distorted ("sickle-shaped") and interfere with the flow of blood through the capillaries. This condition results from the presence of abnormal hemoglobin in affected people. The primary structures of the beta chain of normal and sickle cell hemoglobin differ by a single amino acid out of 146; sickle cell hemoglobin has valine in place of glutamic acid as the sixth residue from the N terminus of the C chain. A tiny change in amino acid sequence can produce a life-threatening result! This modification is genetically controlled and probably became established in the gene pool because bearers of the trait have an increased resistance to malaria.

Sugar Amino Acids (SAAs)

Carbohydrates as well as peptides and proteins are essential biopolymers of life. They are involved in complex biological processes such as catalysis and highly selective molecular recognition. In order to perform these functions, the correct folding of the biopolymers creating the active site is crucial, since any kind of interaction is observed only if the reactive groups are positioned in the correct spatial orientation to each other. Thus, the development of small, easy-to-functionalize building blocks and oligomers with backbones of discrete and predictable folding patterns ("foldamers") is required in order to design and develop molecules with useful biological functions. Nevertheless, for a successful application, their structural properties have to be scrutinized.

Fig. 1 Sugar amino acids as structural scaffolds, as carbohydrate mimetics, and as peptide mimetics.

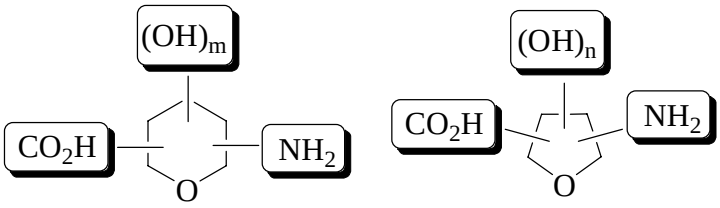

Among the major classes of biomolecules carbohydrates, allow almost unlimited structural variations due to their chiral diversity and high density of easy to functionalize groups. The molecular diversity of carbohydrates offers a valuable tool for drug discovery in the areas of biologically important oligosaccharides, glycoconjugates and molecular scaffolds by investigating their structural and functional impact. However, **S**ugar **A**mino **A**cids (SAAs) and their oligomers, which bridge carbohydrates and proteins, have only recently been investigated.[49]

SAAs are sugar moieties containing at least one amino as well as at least one carboxyl group. Thus, they may be considered as monomeric building blocks of chimeras between carbohydrates and proteins. They allow among other modifications the replacement of the naturally occurring, but synthetically difficult to generate, O/N- glycosidic bonds by

peptidic bonds. This not only increases the enzymatic stability, but facilitates the assembly of large, diverse oligomer carbohydrate or peptidomimetic libraries by solid phase techniques as well. Their use as structural templates in peptides, is a very attractive application of SAAs. Besides their immediate intrinsic different pharmacological properties, SAAs can be used as building blocks for the preparation of modified analogs of biologically active peptides and/or oligosaccharides. The difference in ring size allows modification of the conformations of the peptides and carbohydrates. SAAs can as well be used as starting compounds for different oligomers. They are potential pharmaceutical compounds, are valuable for the synthesis of natural products or analogs, and also as building blocks in drug design and drug research.

Fig. 2 Various Naturally occurring Sugar Amino acids

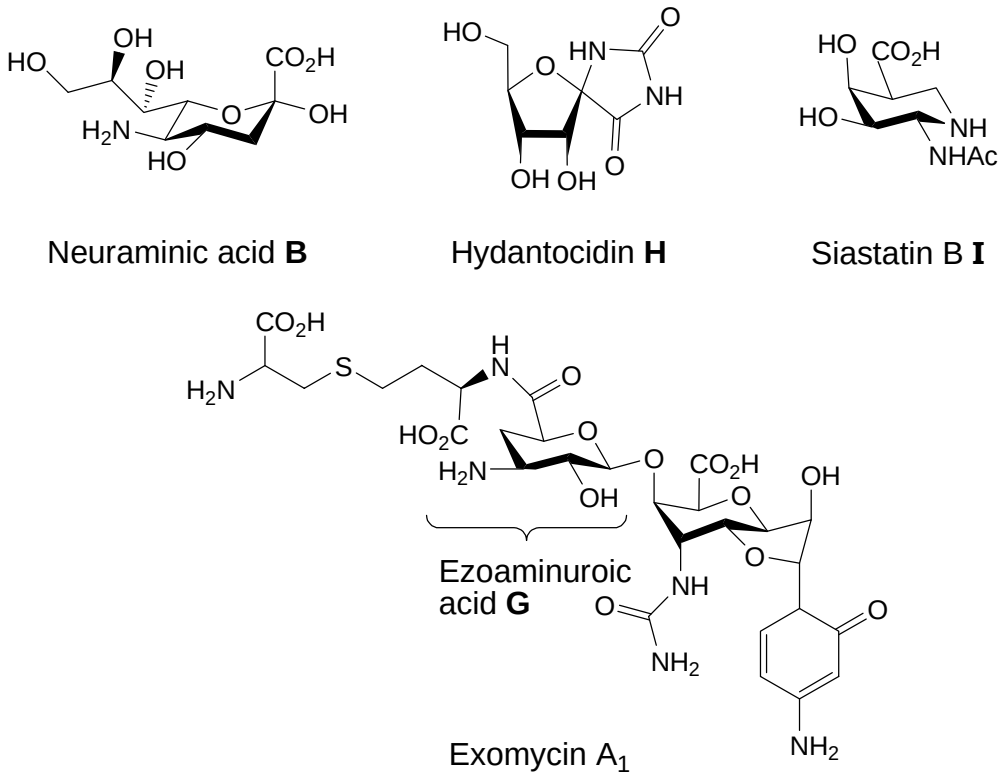

Some sugar amino acids can be found in nature largely as construction elements. The most prominent and abundant example is sialic acid **A** often located peripherically on glycoproteins. This family of natural SAAs consists of *N*- and *O*- acyl derivatives of neuraminic acid **B**. The main substituents on nitrogen are the N-acetyl and N-glycosyl groups. Glycosaminuronic acids (**C**-**F)** are more common in form of their derivatives. For

instance 2-acetamido-2-deoxy-glucuronic acid is found in bacterial cell walls[50] and 2-acetamido-2-deoxygalacturonic acid is one component of bacterial Vi antigen of *Escherichia coli*.[51] Derivatives of glucosaminuronic acid were also detected in the *cancomycin* family of antibiotics similar to *Vancomycin*.

Fig.3 Structures of Glycosaminuronic acids

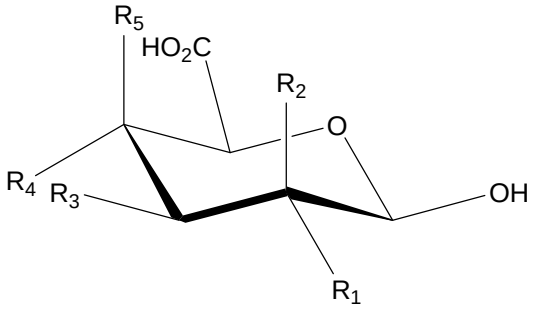

Glycosaminuronic acids		R_1	R_2	R_3	R_4	R_5
Glucosaminuronic acids	**C**	NH_2	H	OH	OH	H
Galactosaminuronic acids	**D**	NH_2	H	OH	H	OH
Mannosaminuronic acids	**E**	H	NH_2	OH	OH	H
4-amino-4-deoxy-glucuronic acid	**F**	OH	H	OH	NH_2	H

Interestingly, natural SAAs can be found in nucleoside antibiotics.[52] Two different 3-amino-3-deoxy uronic acids, derivatives of 3-amino-3-deoxy-D-gulopyranuronicacid and 3-amino-3,4-dideoxy-D-xylohexopyranuronic acid, were found in *ezomycin* A[53] **G**. 4-amino-4-deoxy-glucuronic acid **F**, can be found in *gougerotin*[54], a antibiotic from *Streptomyces* bacteria, as the carbohydrate residue of the nucleoside. The naturally occurring furanoid SAA *(+)-hydantocidin* **H**, which represent a spiro-hydanthion derivative[55], exhibits herbicidal activity. *Siastatin* B **I** is among the class of SAAs, in which the nitrogen is located within the pyranoid ring structure. This inhibitor for both β-glucuronidase and N-acetyl neuraminidase was isolated from a *Streptomyces* culture.[56]

Radiolabeled octreotide and octreotate derivatives conjugated with glucose, maltose or maltotriose glycosylated tracers[57] showed reduced liver and increased tumor uptake resulting in excellent tumor-to-background ratios which allows imaging of SSTR-positive tumors with high contrast. Glycosylation of RGD-peptides using a sugar amino acid is easy

to accomplish via standard peptide chemistry protocols. Subsequently, radiolabeling with [^{18}F] NFP results in [^{18}F] Galacto-RGD in high radiochemical yields and radiochemical purity. Introduction of the sugar moiety in combination with this prosthetic group leads to a hydrophilic tracer with fast predominantly renal excretion and suitable metabolic stability in vivo which allows noninvasive determination of $\alpha v\beta_3$- expression in different murine tumor models. The route described enables production of a standard amount of [^{18}F] Galacto-RGD sufficient for patient studies, starting with approximately 2.2 GBq of [^{18}F] fluoride. The estimated radiation dose is in the same range as found for [^{18}F] FDG.

Fig. 4 [^{18}F] FDG

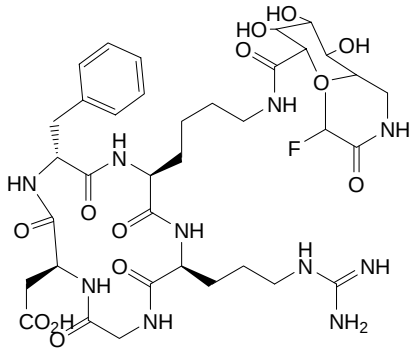

The classification of sugar amino acids is based on position of amino functionality from C-terminus. The synthesis of sugar amino acids is accomplished starting from commercially available, or easy accessible monosaccharides, i.e., glucose, glucosamine, galactose, etc. The amino functionality of the SAA is usually introduced as an azide, cyanide, oxime or nitromethane equivalent, followed by subsequent reduction. The carboxylic function is introduced directly as CO_2, or as hydrolyzable cyanide, by a Wittig reaction and subsequent oxidation or by selective oxidation of a primary alcohol.

α-SAAs: Several derivatives with an α-amino acid moiety at the anomeric position of the sugar were synthesized by Fleet et al. including glucose,[58] rhamnose,[59] galactose,[60] and mannose[61] derivatives. The various routes developed by Fleet's group and Dondoni's group have recently been summarized.[62] Fleet's azide precursors and N-protected SAAs are stable against epimerization; however, all free SAAs (also the pyranoid derivatives) and their respective esters equilibrate to a mixture of α- and β-anomers in solution.

Fig. 5 Some of Fleet's α-SAAs

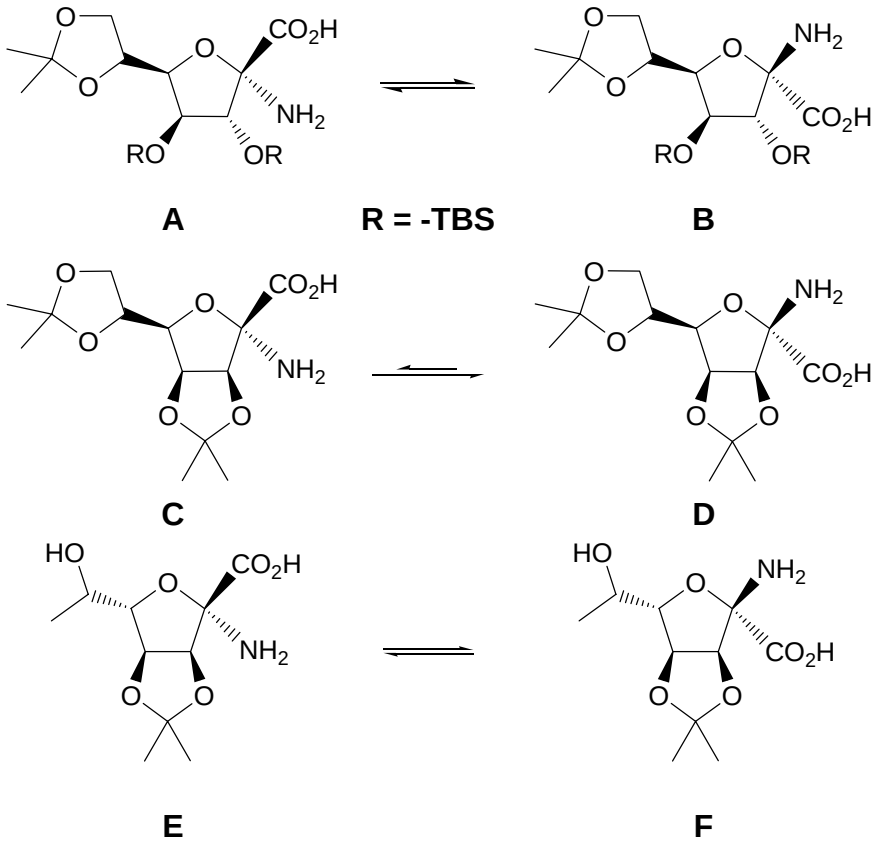

This class of SAAs has also been employed as precursors to five- and six-membered spiro-heterocyclic derivatives of carbohydrates such as the rhamnose functionality, required for enhanced activity analogs of hydantocidin.[63] The naturally occurring (+)-hydantocidin[55] (fig. 2, **H)** exhibits herbicidal activity. Those spirodiketopiperazine derivatives are considered as potential inhibitors of carbohydrate processing enzymes and thus might be useful in elucidating the biosynthesis of the cell walls of mycobacteria.

β- and γ-SAAs: Fleet et al. published the synthesis of several azide precursors to β- and γ-SAAs shown in Figure 6.[64] They synthesized the β-SAA precursor **E** and the γ-SAA precursors **F** and **G** via **Q**, which was obtained by the route described in Scheme 1.[64b, 65] Key step of the synthesis of **Q** was the hydrolysis of the side-chain acetonide of **M** and methanolysis of the lactone with intramolecular displacement of the triflate at C-2 by 5-OH.[65]

Fig. 6 Some of Fleets large collection azides used as β- and γ-SAA precursors

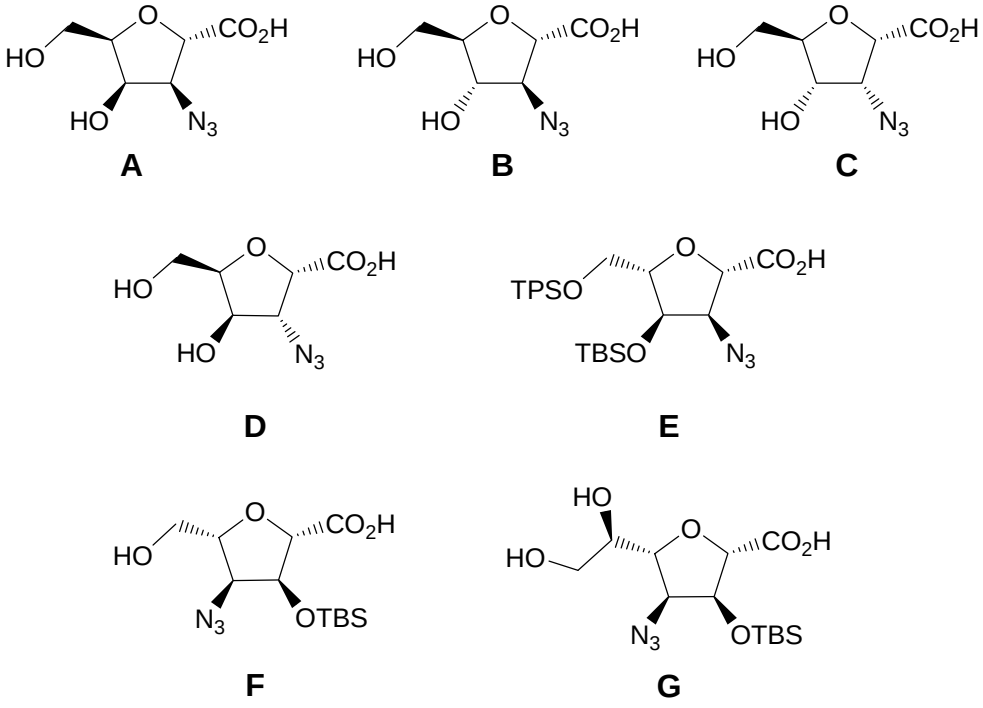

Side-chain hydrolysis of the acetonide of **Q** afforded the γ-SAA precursor **G**, subsequent periodate cleavage, followed by immediate cyanoborohydride reduction of the resulting aldehyde in acetic acid yielded the γ-SAA precursor **F**. Overall yields for **F** and **G**, starting from D-*glycero*-D-*gulo*-heptono-1,4-lactone **J**, were 10 % and 13 %, respectively. Sodium borohydride reduction of the ester function in **Q**, followed by a series of protection deprotection steps and subsequent oxidation of the diol moiety with sodium periodate in the presence of catalytic amounts of ruthenium(III) chloride led to the β-SAA precursor **E** in an overall yield starting from **J** of about 3%.

δ-SAAs: As dipeptide isosteres for the incorporation into peptide based drugs Le Merrer and co-workers synthesized **A** and **B** (Figure 7).[66] The benzylated derivatives were designed as mimics for hydrophobic, the unprotected SAAs as mimics for hydrophilic amino acids.

Key step of their synthesis was the one-pot silica gel assisted azidolysis followed by *O*-ring closure of the bis-epoxides **H** and **I** (Scheme 2) to yield **J** and **K** respectively. Sodium dichromate oxidation of the primary hydroxyl group, treatment with an excess of diazomethane, followed by a one pot conversion of the respective azidoesters by

hydrogenolysis in presence of di-*tert*-butyldicarbonate, yielded the N-Boc protected, fully benzylated SAA methylesters of **A** and **D**. SAA **A** was also synthesized by Chakraborty's and Fleet's groups, using different reaction pathways.[67]

Scheme 1 Synthesis of protected γ-SAA precursor

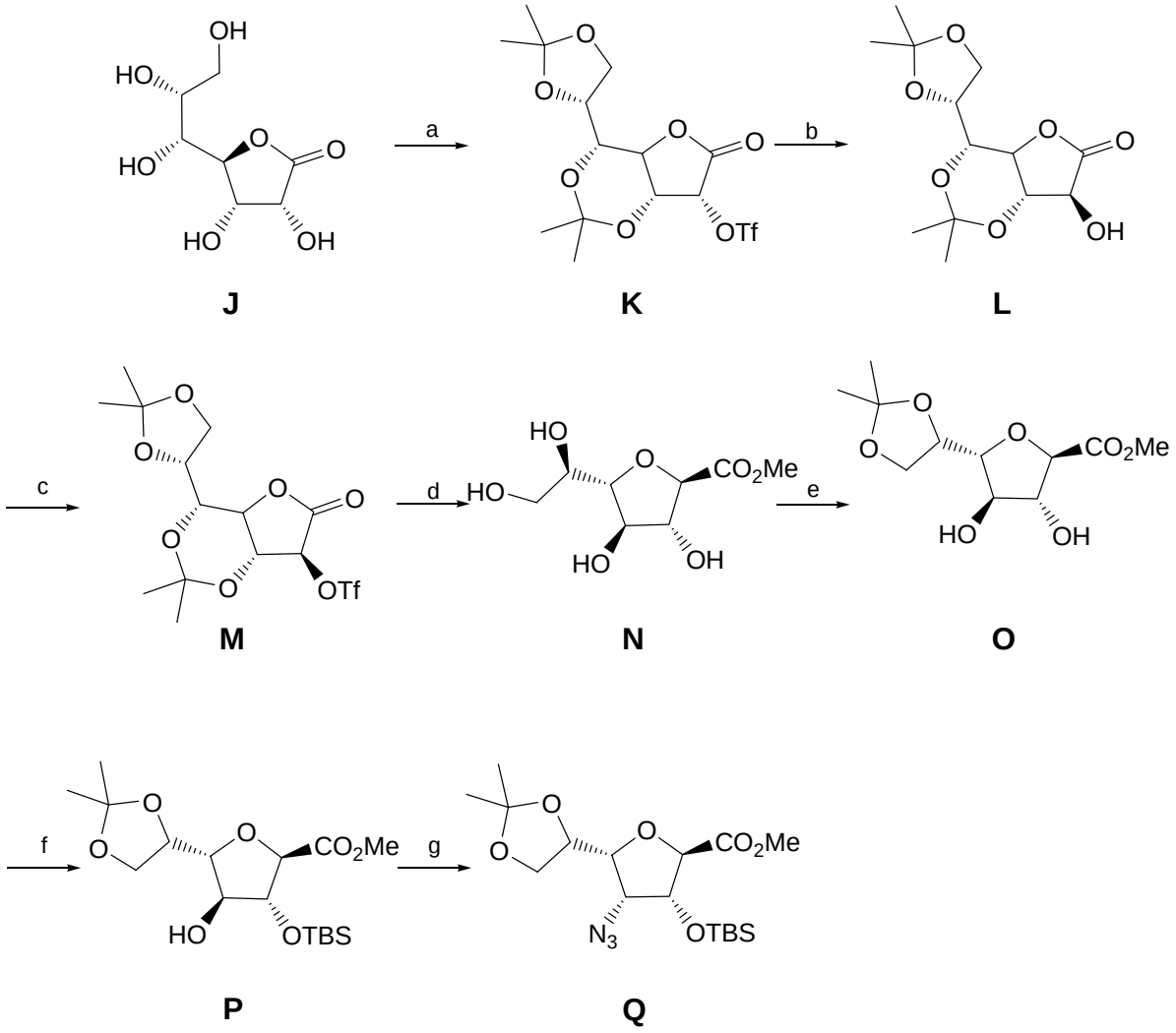

Reagents and conditions: (a) *i*. Conc. H_2SO_4, Acetone, *ii*. Tf_2O, Py 70%, (b) $NaCO_2CF_3$, MeOH, 81% , (c) Tf_2O, Py 89%, (d) AcCl, MeOH, 95%, (e) DMP, CSA, 61%, (f) TBS-Cl, Im, 72%, (g) i. Tf_2O, Py, ii. NaN_3 65%.

Furthermore, also for the use as dipeptide isosteres, Chakraborty et al. synthesized several new δ-SAAs (Figure 7).[67 a,b]

Fig. 7 Some of Le Merrer's, Fleet's and Charkraborty's furanoid δ-SAAs.

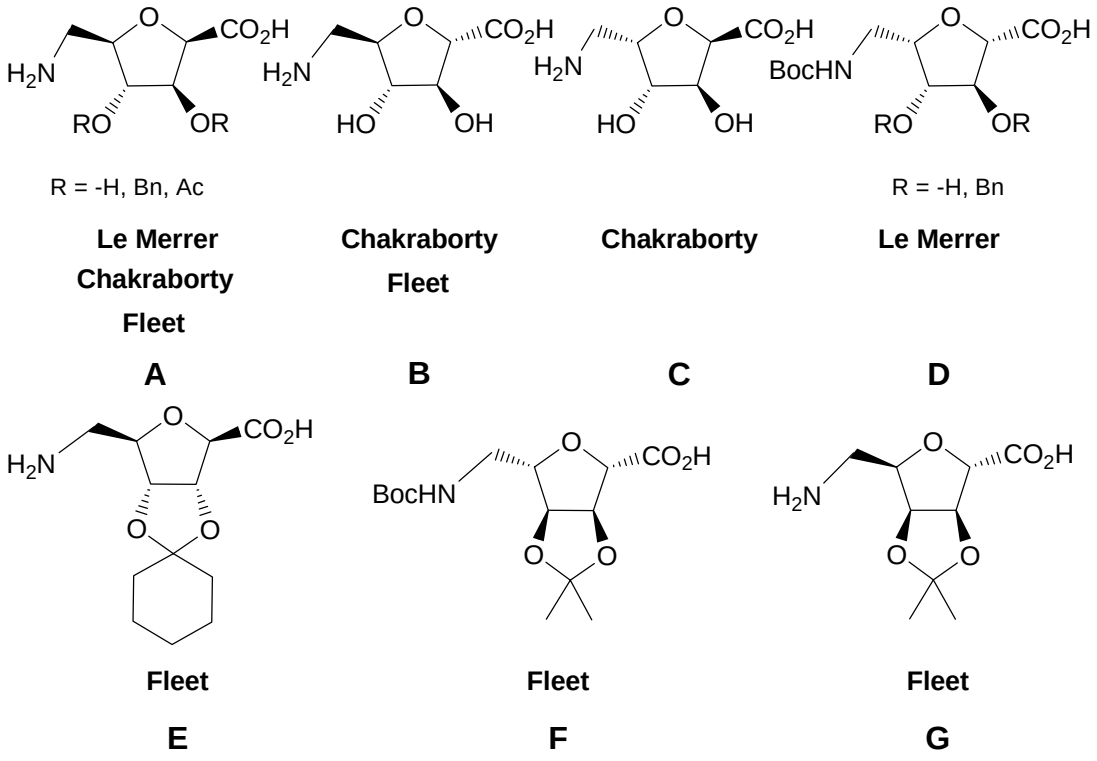

Scheme 2 Key step of Le Merrer's synthesis of **A** and **D**.

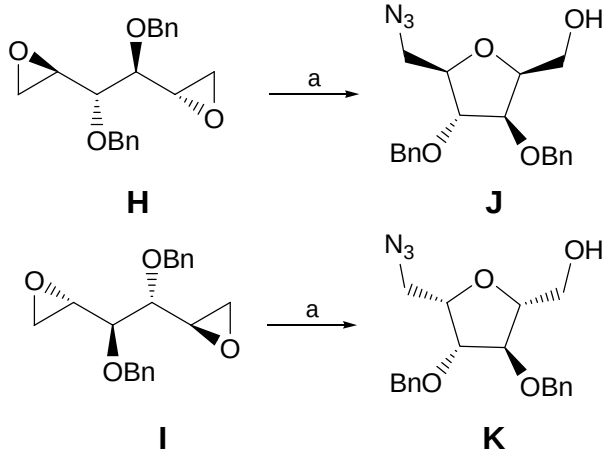

Reagents and conditions: (a) NaN_3 (10 eq.), CH_3CN, SiO_2, 80%

The key step of their synthesis of SAA **A** and SAA **B** followed a different reaction path, in which an intramolecular 5-*exo* opening of the terminal aziridine ring (Scheme 3) of the hexose-derived substrate **L** (with the respective stereochemistry) by the γ-benzyloxy oxygen with concomitant debenzylation occurred during pyridinium dichromate (PDC)

oxidation of the primary hydroxyl group with complete stereocontrol. At about the same time Fleet et al. synthesized a wide range of different δ-SAAs including also **A**, to study the influence of the SAA's stereochemistry and that of the hydroxyl protecting groups on the secondary structure of their linear homooligomers.[67c,d, 68] A few representative examples are shown in Figure 7.

Scheme 3 Synthesis of **A** and **B** starting from **L**. The stereochemistry of **L** determines, if the synthesis results in **A** or **B**.

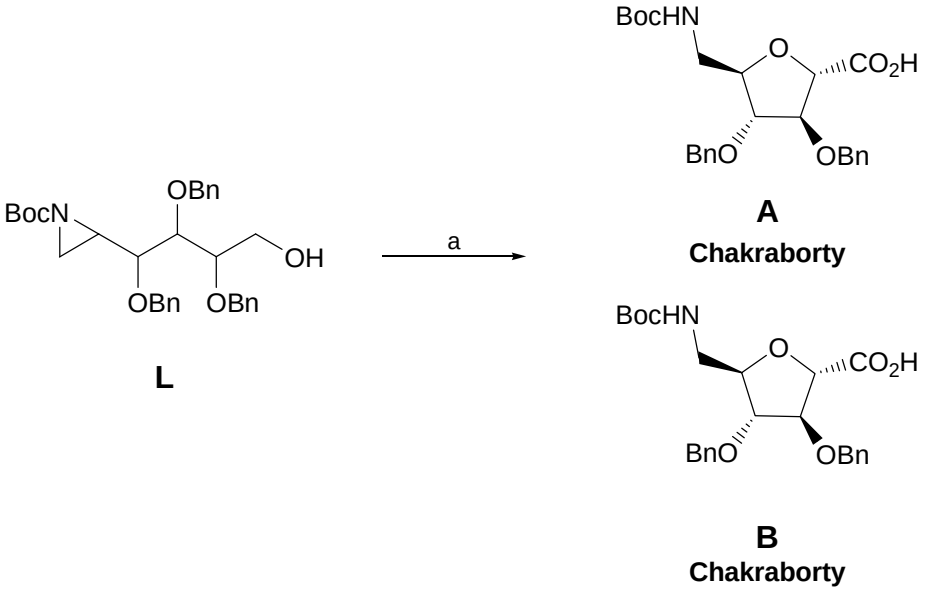

Reagents and conditions: (a) PDC, DMF

SAAs have been used as analogs of biopolymer building blocks to mimic oligo and polysaccharide structures via amide bond linkages.[69] In fact, the assembly of synthetic polysaccharide libraries in solution or on solid-phase is difficult in spite of the recent progresses using chemical and enzymatic techniques.[70] Taking advantage of the well-established chemistry of peptides many homo oligomers from SAAs and hybrid sequences containing natural amino acids (AAs), carbohydrates and SAAs have been synthesized. The resultant oligomers represent useful drug candidates, since they may overcome the problems associated with oligosaccharide and peptide libraries such as the susceptibility towards glycosidases due to the altered peptide backbone, and such as their resistance to many proteases due to their resemblance to carbohydrates.

Linear Oligomers: The first oligomers were synthesized in solution by Fuchs and Lehmann, although they only characterized the individual products by mass spectroscopy.[71] The first dimers were synthesized from D-glucosaminuronic acid and D-mannosaminuronic acid by coupling with DCC by Tsuchida et al. in 1976.[72] More recently oligomers were synthesized both in solution[49a,c, 73] and on solid phase[74], and have been proposed to mimic oligosaccharides[49b] and oligonucleotides (so called GNA, Glucopyranosyl Nucleic Amide) (Figure 8).[75] The aim of GNA development was to improve the properties of the presently most useful class of antisense agents, the phosphorothioates. After the discovery, that peptide nucleic acid (PNA) is a selective binder of DNA and RNA, the idea of replacing the phospho-diester linkages with amide bonds was advisable.

Fig. 8 Oligomers of Gum; R=Me, R=Bn and with nucleobases

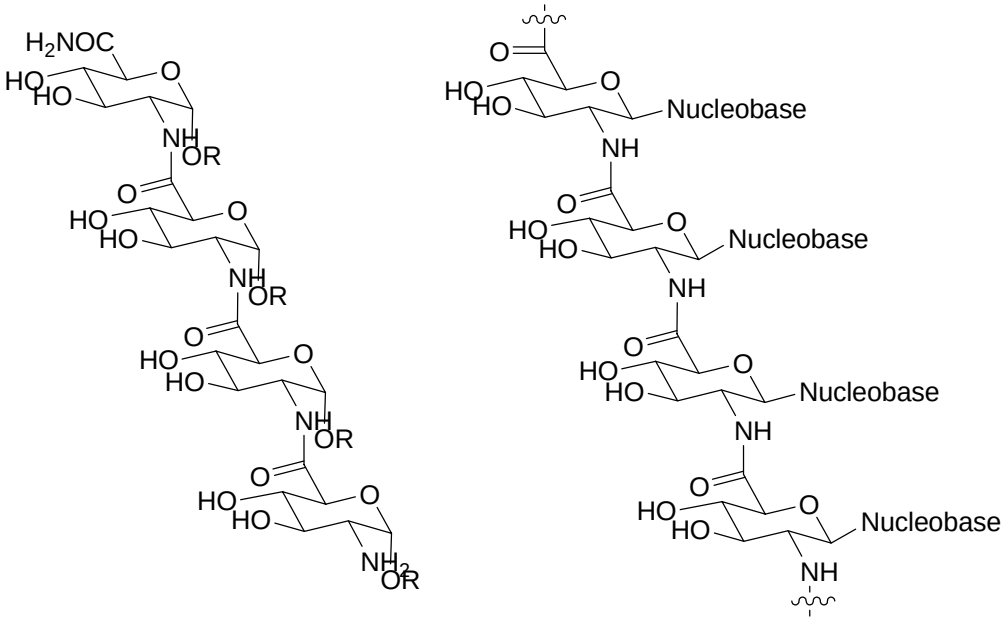

Wessel and co-workers, who first introduced in 1995 the synthesis of amide-linked oligomers in solution (Figure 8), used a [2+2] block synthesis.[49a] In their synthetic protocol benzyloxycarbonyl (Z) was employed as amine protecting group and carboxylic acids were protected as tert-butyl ester. The two monomer building blocks were coupled via mixed anhydrides and the so obtained dimer after tert-butyl deprotection was activated via 2-chloro-4,6-dimethoxy-1,3,5-triazine (CDMT). No protection of the hydroxyl groups was needed.

Fügedi et al. presented several oligomers, which were evaluated in glycosidase inhibitor assays with moderate activities (Figure 9).[76]

Fig. 9 Oligomers by P. Fügedi's group.

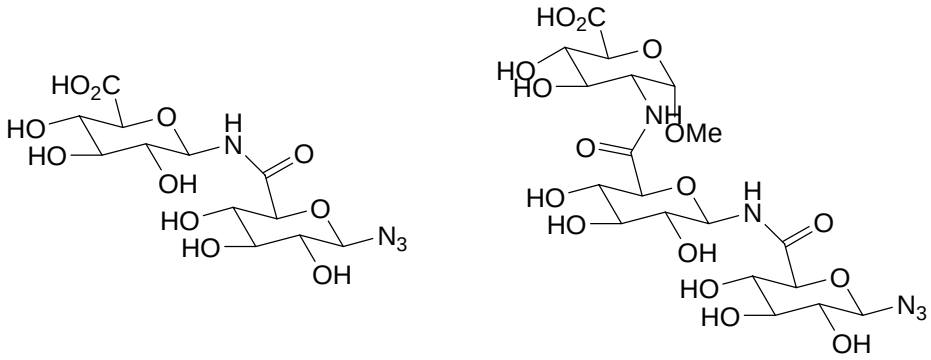

Recently, mixed cyclic oligomers containing SAAs have been proposed by van Boom et al.[77] and by us as potential molecules for host guest chemistry (Figure 10).[78] 2D NMR data suggests preferred secondary conformations for oligomers **A**[77] and **B**.[78] The parallel solid-phase synthesis of cyclic sugar amino acid/amino acid hybrid molecules containing furanoid SAAs was carried out by van Boom et al. using Boc *N*-protection strategy and BOP/DIPEA as coupling reagents.[77]

Figure 10 Mixed cyclic oligomers **A** and **B**.

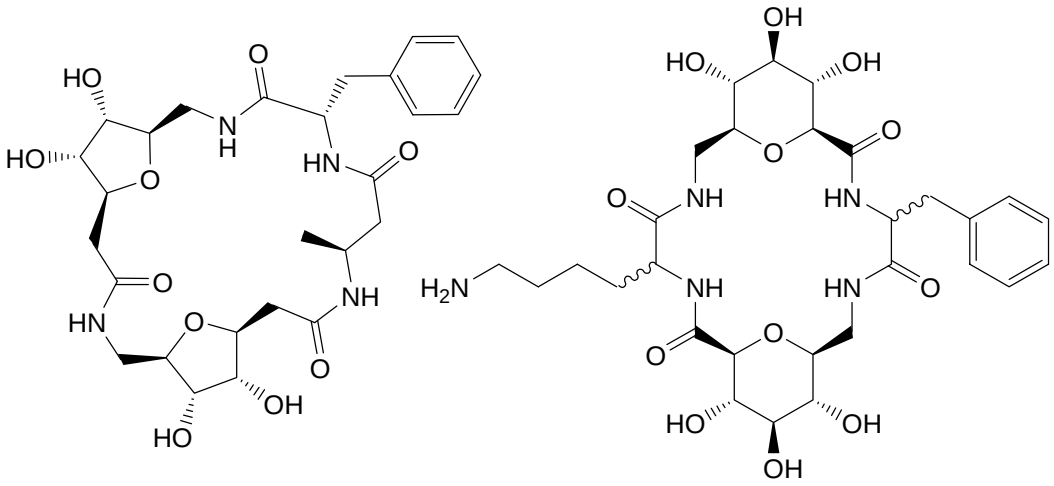

A **B**

The first amino acid was anchored on an oxime resin in order to employ acid catalyzed cyclization and cleavage from the resin. By exploiting standard solid and solution phase coupling procedures linear and cyclic homooligomers containing Gum were synthesized.[79] High yields and very short coupling times for the oligomerization and cyclization of sequences containing 2, 3, 4 and 6 units were achieved. The conformational preferences in aqueous solution of the cyclic derivatives and their applications as potential host molecules were described. Taking into consideration the trans configuration of the amide bonds and the $^4C_1$ conformation of the pyranoid ring, confirmed *via* coupling constants and ROE data, two low energy structures were found for the SAA unit which differ in the relative orientation (*syn* or *anti*) of the C-H[49c] and C=O bonds. The molecular structure of the cyclic oligomers in the all-*syn* conformation generates a hydrophilic exterior surface and a nonpolar interior cavity which resemble the cyclodextrin molecular shape. Indeed, the complexation of the cyclic hexamer with two model guest molecules (*p*-nitrophenol, benzoic acid) was proved from titration studies using NMR the spectroscopic parameters: chemical shifts, longitudinal relaxations (T1) and diffusion coefficients. All of them showed different values for host and guest molecules measured independently and in the presence of each other.

Present Work

Understanding the control, at the molecular level, of the mechanisms and principles governing structural and functional properties of biopolymers is an important objective in biological and medical research. The importance of secondary and tertiary structure in macromolecules has long been appreciated as critical to their cellular roles. Much effort has been expended in x-ray crystallography, nuclear magnetic resonance, and computational analysis to understand, qu*anti*fy, and describe the conformations adopted by biologically relevant nucleic acids, peptides, and proteins. These biopolymers have been and are continuing to be attractive targets for those interested in structural issues because of the central role that they play as both catalysts and substrates for biological processes. In this regard, to reproduce activities of the biopolymers using smaller molecular structures has been one of the challenges in chemistry.

Fig. 1 Some of the available templates for mimicking the α-helices

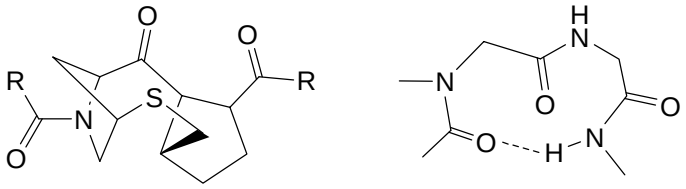

Biopolymers such as polypeptides, nucleic acids and to some extent oligo/polysaccharides are characterized by the occurrence of conformationally defined secondary structures helping overall tertiary structure. As these biopolymers are elusive for an organic chemist to *syn*thesize in flask, in the quest to understand, control, and mimic the actions of biopolymers, many chemists have first turned to the more basic idea of mimicking secondary structures. As the focus in molecular *syn*thesis is shifts increasingly from structure to function, there is always a need for qualitative as well as qu*anti*tative understanding of various secondary interactions in detail, which will allow a precise selection of the desired function before going for more complex *syn*thesis.

There are several strategies that have been reported in this context. One being tough, involves the *syn*thesis of portions of these bio-polymers, and study the secondary structure in

detail either by using indirect methods (like NMR, IR, UV and CD) and molecular modeling or by direct *X*-ray crystallographic studies and subsequent qualitative as well as qu*anti*tative description of weak interactions. The second strategy simplifies this by attempting to mimic secondary structural elements that participate in protein-carbohydrate interactions,[80] like mimicking α-helices[81] β-sheets[81a,c] and β-turns[81b, 82] in proteins, α-helices, major groove, minor groove of nucleic acids,[83] and mimicking naturally available polymorphs of polysaccharides, like native cellulose[84] which is one of the abundant biopolymer and is available in different polymorphs. In this context, Balaram and co-workers have well established the use of α-amino-isobutyric acid,[85] also other higher alkyl analogues[86] and non-protein amino acids to act as a stereochemical director of polypetide chain folding for the modular construction of synthetic protein mimics. In pioneering studies, the Gellman[87] and Seebach [88] groups independently produced helical oligomers based upon β-peptides.

Fig. 2 Some of the available templates for mimicking the β-turns

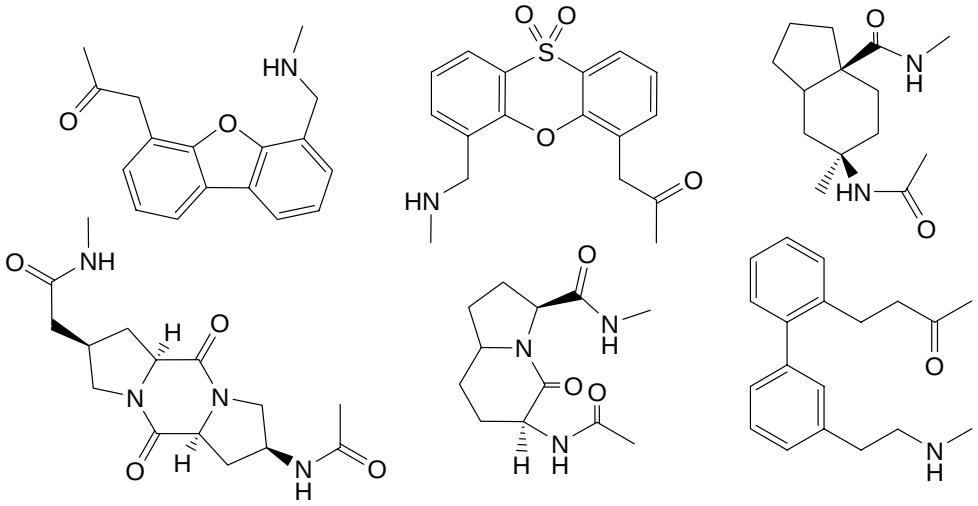

The research groups of Hanessian[89] and Seebach[90] have also shown that peptides derived from longer amino acids[91] are also capable of forming stable helical structures. Non-protein amino acids having cyclic structures (ex. bicycliclactams,[92] bicyclichydrazides[93]) or very often templated on rigid aromatic rings (ex. anthracene, dibenzofuran,[94] phenoxanthin[95]), bicyclic rings (ex. *cis*-norbornyl esters[96]), even acyclic olefinic chains[97] (exploiting allylic strain and other acyclic conformational effects) are used as turn mimics

and as nucleators. Nowick and co-workers have developed an elegant strategy involving utilization of a combination of two different templates (N, N-linked oligoureas and aromatic amides) for creating molecules that mimic protein β-turns.[98] Recently Sessler[99] and Vasella[85a, 84b] groups used dialkynylated anthracene or anthraquinone templates in order to understand the intermolecular interactions in nucleic acids and in cellulose derivatives.

Fig. 3 Model for *Bis*--furan system

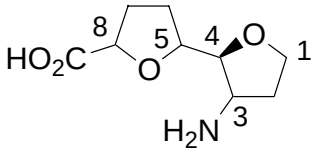

It evident from the above description that the available templates will be either rigid aromatic rings or posses certain stereochemical factors which strongly direct the orientation of attached oligomers. In this context, we are interested to synthesize flexible molecules with little directional influence and their further exploration as nucleating agents for mimicking the secondary structural elements of the biopolymers. Taken together with the importance of developing new templates and the potential of sugar amino acids in providing various oligomers with backbones of discrete and predictable folding patterns, we have designed a new class of templates (Figure 3).

Figure 4. Possible diastereomeric *bis*—furan templates

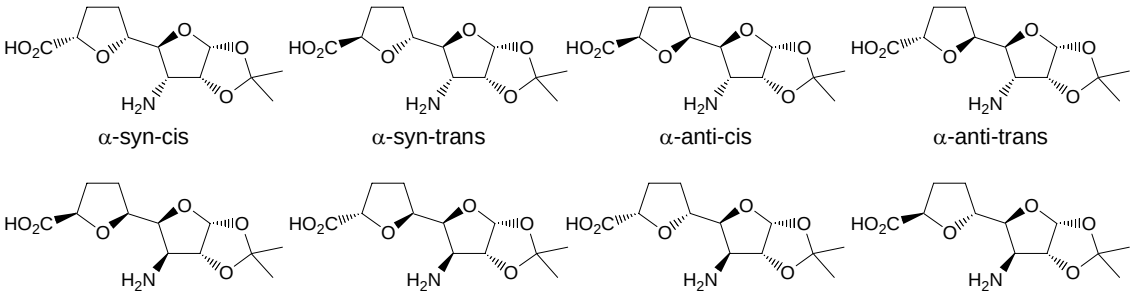

(α/β = NH_2 orientation, *syn*/*anti*, *cis*/*trans* are the relative stereochemistry between C-3, C-5, C-5-C-8 repsectively)

Our design integrates the sugar amino acids with the sub-unit of ionophore class of natural products i.e. *bis*-furan. As shown in the Figure 4, there are several possible distereomeric templates even after considering D-pentofuranose as one of the partner. Additionally, each structure can have at least three possible conformers considering the free rotation around the C-4-C-5 bond, namely *gt*, *tg* and *gg* (g = gauche, t = trans Figure 4). If one looks at the orientation of the furan rings with the three possible conformers, it is evident

that only the tg conformer should provide the requisite orientation of the two active groups with a *syn*-orientation.

Figure 5. Definition of *gt*, *tg*, and *gg* rotamers of the C-4-C-5 bond rotamers

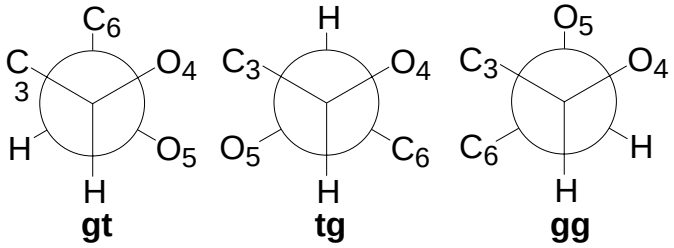

In order to prioritize the available diastereomers, we considered this as one of the criteria and accordingly, we intended to carry out modeling of templates for various physical parameters and analysis of the information available from the single crystal X-rays structural data. To highlight, the designed templates are new in the field of peptide chemistry.

Single Crystal Structural Analyses of *bis*--furan templates:

A search of the Cambridge Structural Database (CSD) was performed using a wild-entry (Figure 5) which resulted in about 40 entries with a wide structural diversity. In order to identify the requisite structural elements, we have analyzed all the available structures and selected only those structures where no metal atom is present and where the requisite *bis*-furan unit is not part of a cyclic system. This resulted in selecting about 10 structures.

Figure 6. Model for crystal study of *Bis-furan*s

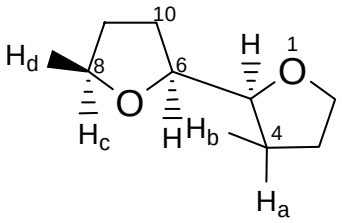

Conformational analyses of furanose rings:

The pseudorotational wheel (Figure 7) was initially developed for substituted cyclopentanes and adapted for use in furanose ring systems by Altona and Sundaralingam[100] in conjunction with their work describing the conformational preferences of ribonucleosides. The difference between pseudorotational angels for *Envelope* as well as *Twist* confrmations of THF ring is maintained to be 36^0. The presence of two such flexible conformers in our

systems complicates the prioritization of a designed template from the possible 8 diastereomers (fig. 4). However, as out lined above our main concern was the preferred orientation of C-4-O···C-5-O bond when the relative configuration of the corresponding centers is *syn* or *anti*.

Fig. 7: Pseudorotational wheel for an α-D-aldofuranose ring

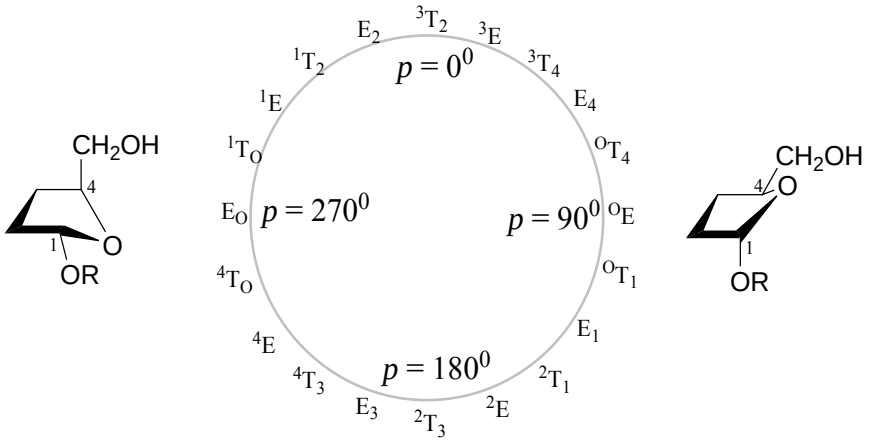

To understand the relative conformational preference, we analyzed the suitable X-ray structures using Mercury software and selected following three different molecular structures obtained from CSD where one can find the requisite *tg* conformation between the two furan rings. All these structures have one common structural feature that they have the two THF rings attached to each other in *anti* fashion. This examination indicated that the requisite *tg* conformation should be obtained by selecting *anti*-configured *bis*-furans.

Table 1. Torsion angle and distances between various functionalities at 4 and 8 position

Name	**Torsion Angel**	**Distances between various points**			
		H_a H_c	**H_b H_d**	**H_a H_d**	**H_b H_c**
HINGUG	65.29	5.085	5.89	4.819	5.519
HONPOP	-69.86	5.453	6.708	5.271	6.708
RUVXAH	73.26	4.031	3.063	3.071	4.707

Figure 8. Molecular Structure of **HINGUG** and the wire frame representation of the key *bis*-furan unit

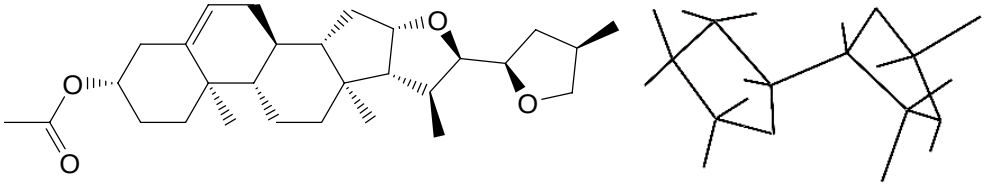

HINGUG: The space group is P_{212121}. The structure of this compound is shown above. In this case atom Hd is a methylene carbon. The *bis*-furan portion of this molecule is shown in fig. 8 above.

Figure 9. Molecular Structure of **HONPOP** and the wire frame representation of the key *bis*-furan unit

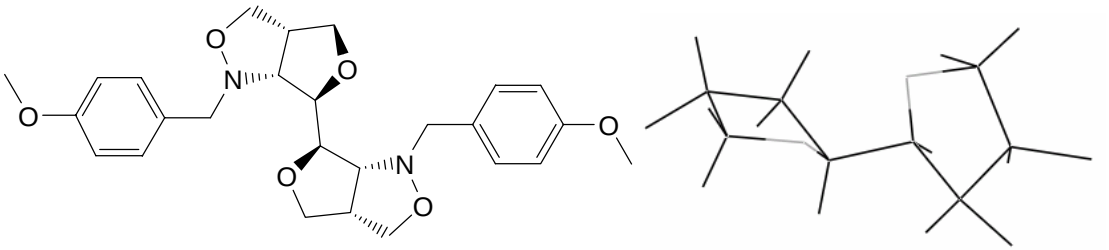

HONPOP: The space group is I_2. The structure of this compound is shown above. In this case atom Hc is a methylene. The *bis*-furan portion of this molecule is shown in fig. 9 above.

Figure 10. Molecular Structure of **RUVXAH** and the wire frame representation of the key *bis*-furan unit

RUVXAH: The space group is $P_{21/n}$. The structure of this compound is shown above. In this case atom atom Hc is a carbon attached to oxygen. The *bis*-furan portion of this molecule is shown in fig. 10 above.

After establishing the stereochemical requirements for the requisite *tg*-conformation, we next proceeded further to find out the relative orientation of acid and amino functional groups by measuring the torsion angles between two rings and various distances between functionalities present at 4 and 8 position and the results are shown in Table 1.

Table 2 Various computational values of designed UAA templates

Structure	**Config. at C_3, C_5, C_8**	**Torsion angle**	**Distances between various points**			
			H_a H_c	**H_b H_d**	**H_a H_d**	**H_b H_c**
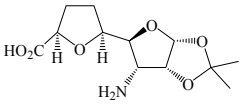 **α-anti-cis**	R, S, S	**-69.2**	**5.194**	**5.245**	**4.658**	**5.538**
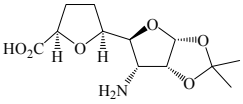 **α-anti-trans**	R, S, R	-60.6	4.916	5.545	5.195	4.919
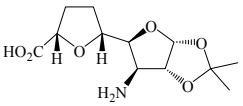 **β-anti-cis**	S, R, S	-51.1	4.885	4.371	4.735	5.411
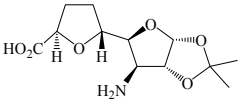 **β-anti-cis**	S, R, R	-54.9	4.6	4.931	5.08	5.22

From these results it is evident that for an anti fusion of bis-furan system the magnitude of the torsion angel between the two rings is expected to be in the range of 600±30. The sign of the angel is determined by the rotation of the plane. For the Gaussian interaction various bonds between functionalities at 4 and 8 position are expected to be in the range as follows Ha-Hc 4.2±0.2Å, Hb-Hd 5.2±0.2Å, Ha-Hd 4.9±0.5Å, Hb-Hc 4.9±0.5Å. As shown in Figure 3, for the flexibility of three stereo-centers in all eight possible distereoisomers can be considered. However, prioritizing an anti fusion of the bis-furan ring, the rest of the four syn conformers are eliminated. Various computational values (torsion angles and distances between various functionalities present at C-3 and C-8, for the

remaining four isomers are shown in Table 2 below. These values are obtained from the computer-generated models using Chem-3D version Ultra 9.0.

Fig. 11 Computational model for distereoisomer **α-anti-cis**

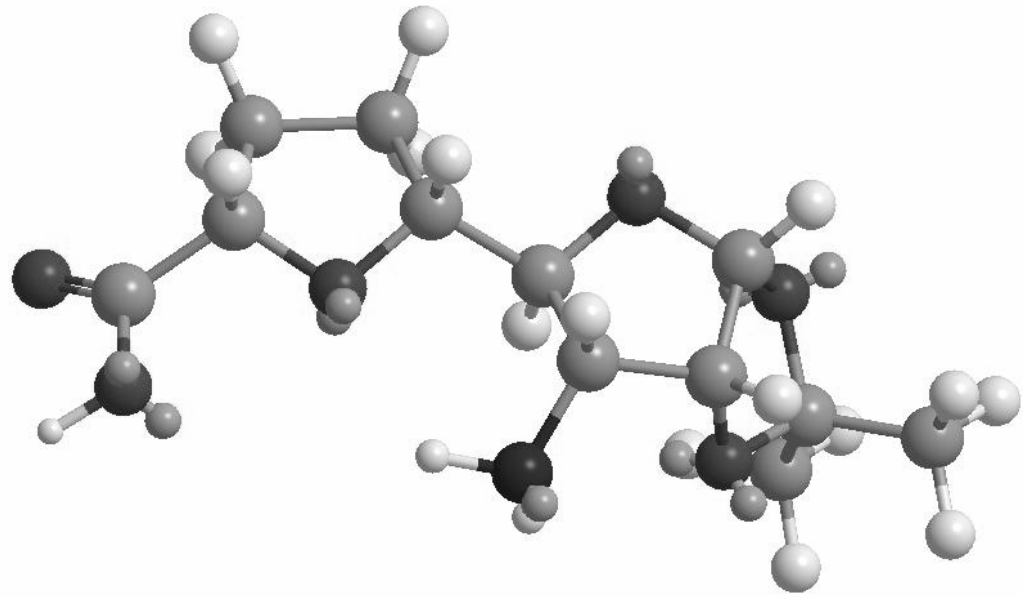

From these results it is quiet clear that for the orientation of amine β- to furanoside ring the torsion angles does not match with the requisite *anti*-conformation. The magnitude of the torsion angels for both these isomers is found to be too less for availing such activity. Thus these two conformers are eliminated which leaves only two structures with amine functionality as α- to furanoside ring. Between the two remaining conformers the torsion angel of α-anti-cis conformer is -69.2^0 and for α-anti-trans -60.6^0. It is quiet evident from the Table 1 that the magnitude of the torsion angle for the two rings to be in *tg* conformation is expected to be in the range of $69^0 \pm 3^0$, and only one structure satisfies all these values and i.e. **α-anti-cis** with the value of 69.2^0.

After being designed, the BFAA (Bis Furan Amino Acid) **1** became our main concern. The following effect of peptide formation, the mimics and various conformations the peptide takes, when C=O of acid and NH of amine are at distant position in a molecule, and to investigate the secondary structure obtained by folding we selected this particular structure (Figure 9) and a retrosynthetic analysis for the synthesis of the same is depicted.

Figure 12. Identified BFAA **1** and the intended strategy for its synthesis

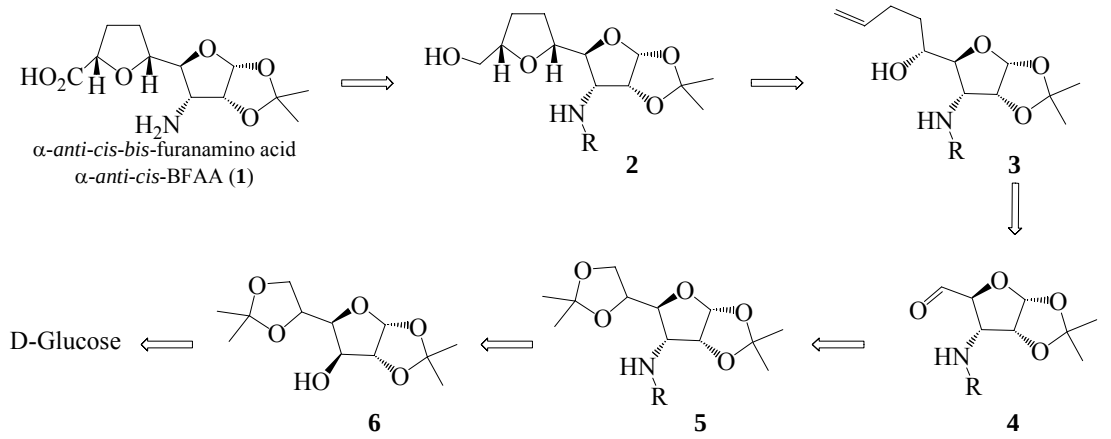

Retrosynthetic analyses:

Our intended synthesis of **1**, is based upon a stereoselective construction of the second furan unit using electrophlilic cycloetherification reaction of the substrate **3**. Gurjar et. al. have reported a similar type of cyclization,[101c] however, keeping a benzyloxy substituent at C-3 position. The key intermediate **3** can be prepared from the suitably protected aminofuran aldehyde **4** by using Grignard chemistry. The synthesis of **4** is a straightforward proposition from the glucose diacetonide **6**.

Scheme 1

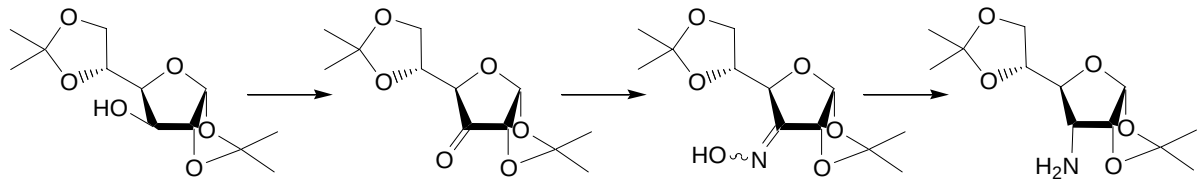

As intended the synthesis of **1** started with the preparation of glucose diacetonide by known literature procedure. Oxidation of the diacetonide **6** (1,2,5,6-di-*O*-isopropylidine-α̃-D-glucofuranoside) using pyridinium dichromate (PDC) gave the ketone **7** in good yield, which was used for the next transformation without any further purification. The ketone **7** thus obtained was converted to its oxime **8** by treating with hydroxyl ammonium chloride and the

oxime derivative thus obtained was then reduced with LAH to afford the amine **9** (Scheme 1) exclusively in 70% overall yield for three steps.

Scheme 2

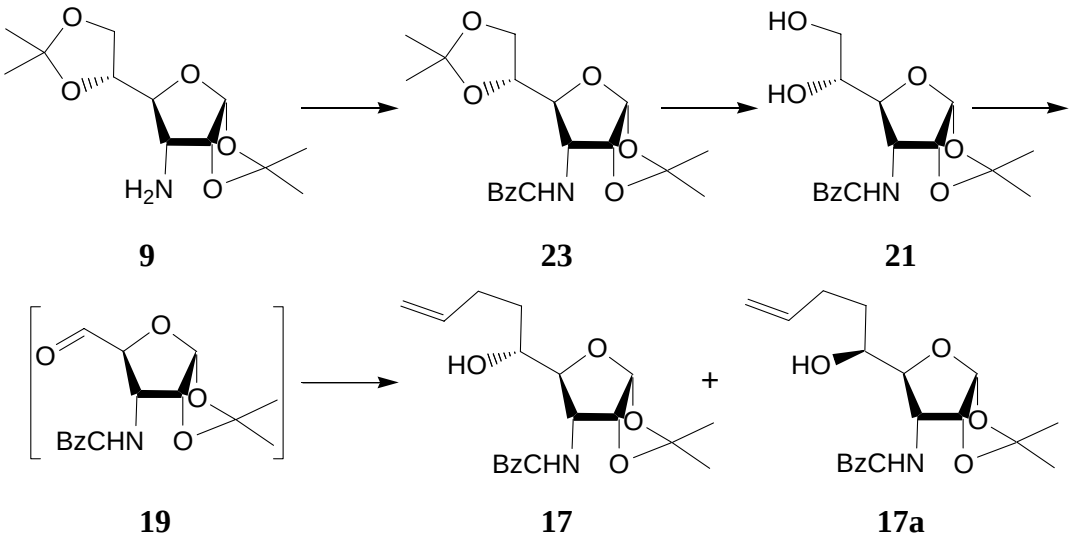

The newly generated stereocenter is confirmed by the presence of vicinal coupling of H-2 and H-3 (J = 4.7 Hz), which is not observed in case of **6**. The exclusive formation of **9** can be explained by invoking the nucleophile (hydride) approach from the less hindered *Si*-face as the isopropylidine group blocks the *Re*-face.

Scheme 3

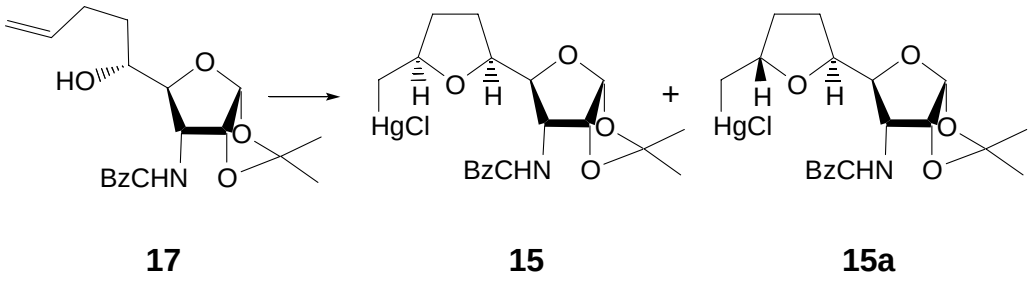

Protection of the resulting amine **9** as its benzyloxy amide **23** followed by partial hydrolysis of 5,6-*O*-isopropylidine gave the diol **21**. The absence of two singlets (at δ= 1.45, 1.36) observed in case of **23** confirms the partial hydrolysis product **21**. Treated with sodium

metaperiodate gave aldehyde **19**. Addition of butenyl magnesium bromide on aldehyde **19** gave diastereomeric mixture (1 : 1) of alcohols **17** and **17a**.

Figure 13. Compound **16** and its Molecular Structutre [102]

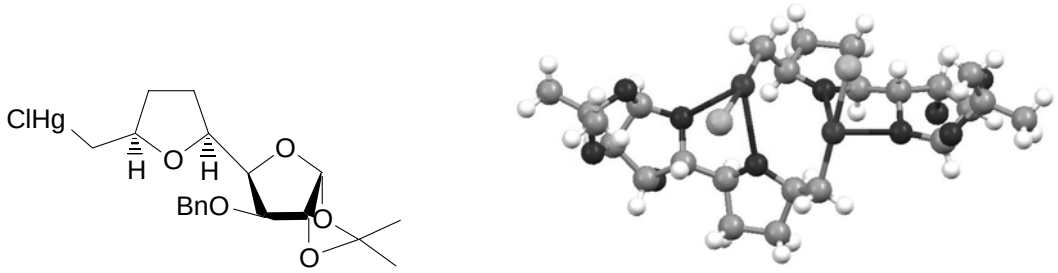

After unsuccessful attempts of selective crystallization of distereoisomers, column chromatography was used to separate the diastereomers. The mercuration of **17** gave mixture of mercury derivatives **15** and **15a** at C-8 (Scheme 3). The diastereomeric mercury derivatives were separated by column chromatography. A detailed structural investigation of **15** and **15a** was carried out by extensive NMR analysis in order to fix the newly introduced stereocenter. The investigation started with the comparison of coupling constants and chemical shifts of H-2, H-3, and H-5 and the chemical shifts of the ring junction carbons (Table 3).

Table 3. δ/*J* Comparison of various H and C signals of compounds **15**, **15a**, **16**

15a			**15**			**16**			
δ		*J*	δ		*J*	δ		*J*	
2.21	dd	12.12, 2.52	2.29	dd	11.88, 5.43	2.12	dd	11.92, 4.37	**H_9**
2.49	dd	12.0, 5.44							
4.15	m		4.15	dd	7.4, 5.11, 3.66	4.17	q	7.15	**H_5**
4.21	m		4.24	d	5.05	4.03	dd	6.76, 3.18	**H_4**
4.21	m		4.38	dd	5.68, 5.39	4.33	m		**H_8**
4.58	dd	4.97, 4.11	4.58	dd	4.73, 3.71	3.87	d	3.18	**H_3**
5.15	m		5.15	m		4.58	d	3.97	**H_2**

Its quiet evident from these diagrams that the '*W*' arrangement observed for H-3 (*J* = 3.71 Hz) and H-5 (J = 3.66 Hz) confirms the relative stereochemistry at C-5 for compound **15**. In case of **16** the absolute stereochemistry at H-3 is '*S*' being a *gluco* conformer and in case of **15** it is '*R*' being an *allo* conformer. The '*W*' arrangement in case of **16** is difficult to be observed, because the proton at H-3 being below the plane of furanose ring can not result into this arrangement and in case of **15** the same proton is above the plane of the ring and thus it results this arrangement (confirmed by PMR spectrum).

Fig. 14 The relative configuration of compounds **15** and **16**.

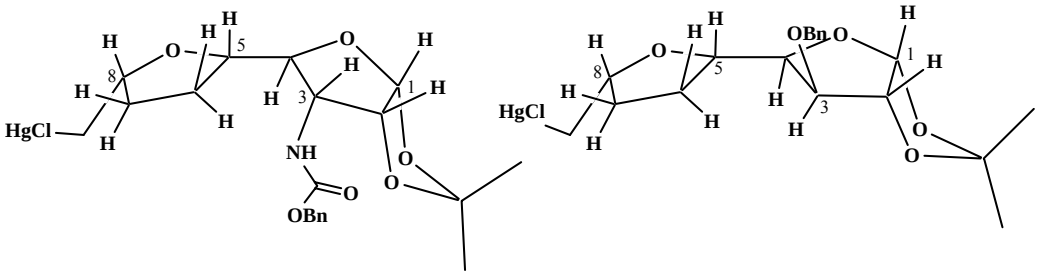

15 **16**

Thus, compound **15**, since the absolute configuration at C-3 is *'R'*, the relative configuration at C-5 is *'S'*. In case of compound **15a** similar coupling pattern for H-3 is observed. Here except for benzylic methylene group all the protons are observed little downfield compared to **15**. Since the relative configuration of **15** is fixed earlier, the relative configuration at C-8 for **15a** is *'S'*. Moreover in case of **16** H-2 splits into doublet (J = 3.97 Hz), since it has only one adjacent proton to couple with i.e. H-1. The dihedral angel with H-3 is almost 120^0, thus it shows no coupling with H-3. But in case of **15** the proton at H-3 being above the plain of the ring it couples with H-2, thus H-2 instead of showing a doublet in prior case it shows a multiplet. The proton at H-9 in both the cases shows *dd* pattern due to geminal coupling observed between two prochiral protons.

Our initial attempts to bring the oxydemercuration of **17** under established conditions using sodium borohydride in presence of molecular oxygen at room temperature were found to be problematic[101] and resulted in exclusive formation of the deoxygenated product **19**. The structure of compound **19** is evident from its PMR spectrum, where a doublet at 0.8 δ integrating for 3H is observed. The absence of signal above 3300 cm^{-1} in the IR spectrum of

compound **19** further evidenced the assigned structure. In order to over come this problem we have carried out the reaction at different temperatures and a comparative profile of the all the experiments are compiled in the Table 4.

Figure 15 Structure of deoxygenated and demercurated product **19**

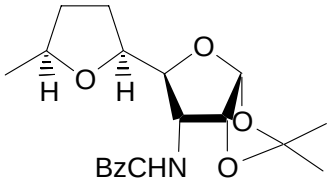

Table 4. Comparison of various observations for demercuriation reaction

Sr. No.	Temperature (^{0}C)	Isolated yield (%)	Selectivity (%)	
			Primary Alcohol	Deoxy. compound
1	25	75	2	98
2	40	69	10	90
3	55	71	30	69
4	70	79	68	29
5	85	65[a]	60	35

[a] the starting mercury complex happens to disintegrate and starting material is observed

Scheme 9

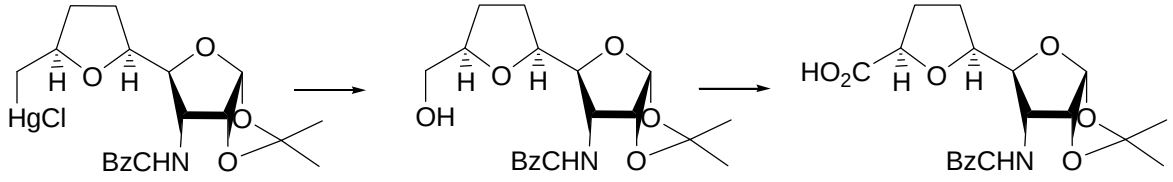

We observe that when the temperature is increased above 90 °C the starting mercury complex starts disintegrating. Thus this reaction was not investigated thereafter. With the help of these experiments we concluded that, conducting the oxy-demurcuration at 70 °C provides a better ratio and also a better yield. Although, we have not carried any kinetic experiments to explain the influence of temperature on the product ratio resulting from the oxy- and reductive-demercurations, however a tentative hypothesis will be at higher

temperatures, any intramolecular complexation of mercury either with oxygen or nitrogen might have broken and thus exposing the mercury better for the complexation with the incoming oxygen.

Scheme 10

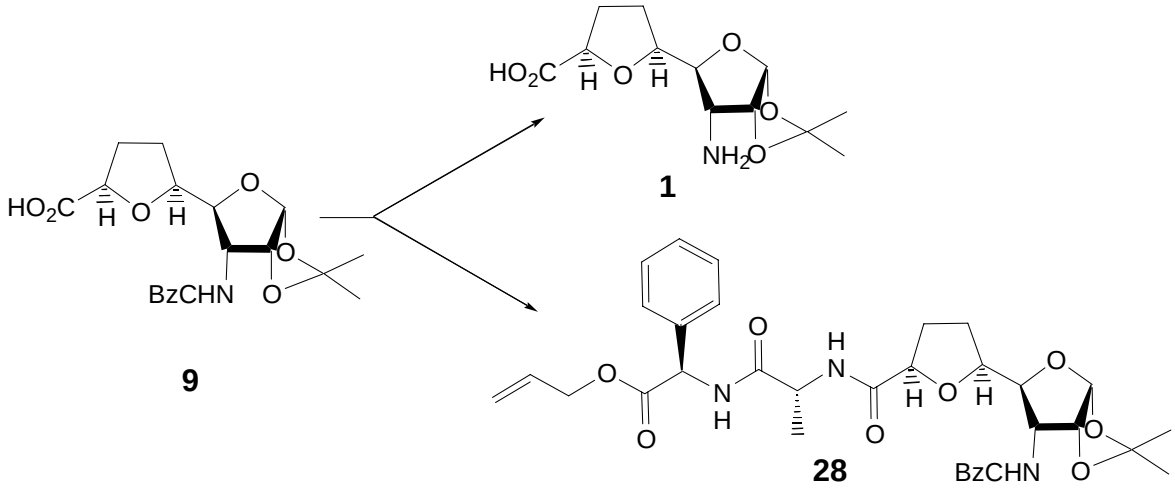

The reaction worked well and the primary alcohol **13** was obtained in 20% overall yield. Oxidation of alcohol **13** to acid **9** was achieved using RuO_4 generated insitu from $RuCl_3$ and $NaIO_4$ in 50% yield. The acid was characterized by NMR analysis as a single isomer without any epimerization. Further this acid was coupled with dipeptide (obtained from alanine and phenyl glycine) using EDCI and HOBt as coupling agents gave the tripeptide **28** in 69% yield. The tripeptide **28** was characterized by various spectroscopic methods. The activity testing and further modifications of this tripeptide **28** are under progress.

Experimental Work

3-Deoxy-3-amino-1,2:5,6-di-*O*-isopropylidine-α-D-allofuranoside (9)

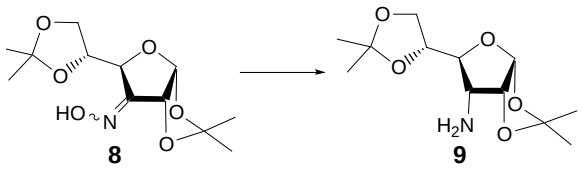

To a vigorously stirred suspension of LAH (12.25 g, 322 mmol) in THF (400 ml) at 0 °C a solution of oxime **8** (40 g, 147 mmol) in THF (400 ml) was added drop wise maintaining the internal temperature below 5 °C. The reaction mixture was heated to reflux for 5 h and stirred at room temperature overnight. Excess LAH was quenched with the addition of saturated Na_2SO_4 solution and ether (500 ml) was added and the stirring was continued for another 5 h. The layers were separated, aqueous layer was extracted with ether and the combined organic extract was dried (Na_2SO_4) and concentrated. The crude was purified by silica gel column chromatography (30% EtOAc in petether containing 1% TEA) to afford **9** (36.5 g, 96%) as white solid.

M.p.:	76°
$[\alpha]_D^{25}$	+ 2.72 (*c* = 0.95, $CHCl_3$)
IR ($CHCl_3$):	υ: 3437 cm^{-1}
^{1}H NMR	δ: 1.34 (s, 3H), 1.36 (s, 3H), 1.45 (s, 3H), 1.54 (s, 3H), 1.68 (bs, 2H), 3.13 (dd, *J* = 4.7, 9.0 Hz, 1H), 3.60 (dd, *J* = 6.3, 9.0 Hz, 1H), 3.99 – 4.11 (m, 3H), 4.55 (dd, *J* = 3.9, 4.7 Hz, 1H), 5.75 (d, *J* = 3.5 Hz, 1H)
^{13}C NMR	4.78, 25.97, 26.12, 26.25, 57.62, 66.62, 76.66, 80.51, 80.91, 103.77, 109.11, 111.73 ppm
Elemental Anal. $C_{12}H_{21}NO_5$	Calcd: C, 55.58; H, 8.16; N, 5.40 Found: C, 55.08; H, 8.72; N, 5.58

3-Deoxy-3-*N*-benzyloxycarbonyl-1,2:5,6-di-*O*-isopropylidine-α-D-allofuranoside (23)

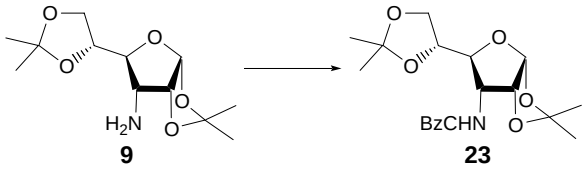

At 0 °C, a vigorously stirred solution of **9** (36.5 g, 141 mmol) in 1,4-dioxane (300 ml) was treated with a solution of sodium bicarbonate (23.68 g, 282 mmol) in water (300 ml). To this benzyl chloro formate (36.1 g, 30 ml, 212 mmol) was added drop wise maintaining the internal temperature below 5 °C and the stirring was continued for additional 8 h at the same temperature. After completion, the reaction mixture was concentrated under reduced pressure and extracted with EtOAc. The combined organic extract was washed with water, brine, dried (Na_2SO_4) and evaporated under reduced pressure. The crude product was purified by chromatography on silica gel (15% EtOAc in pet ether) to obtain **23** (52.62 g, 95%) as pale yellow solid.

M.p.:	79°
IR ($CHCl_3$):	υ 1690 cm^{-1}
^{1}H NMR	δ: 1.33 (s, 6H), 1.40 (s, 3H), 1.53 (s, 3H), 3.84 (dd, *J* = 4.7, 9.4 Hz, 1H), 3.94 (d, *J* = 6.3 Hz, 1H), 4.07 (m, 1H), 4.24 (dd, *J* = 4.7, 5.5 Hz, 1H), 4.61 (t, *J* = 4.0 Hz, 1H), 5.11 (d, *J* = 4.3 Hz, 2H), 5.19 (m, 1H), 5.8 (d, *J* = 3.9 Hz, 1H), 7.35 (s, 5H)
^{13}C NMR	25.12, 26.09, 26.34, 55.18, 65.19, 66.75, 75.54, 78.50, 78.86, 103.8, 109.32, 112.19, 127.91, 128.21, 136.12, 155.37 ppm.
CHN Anal.	Calcd: C, 61.06; H, 6.92; N, 3.56
$C_{20}H_{27}NO_7$	Found: C, 61.23; H, 6.60; N, 3.47

3-*N*-Benzyloxycarbonyl-3-deoxy-1,2-*O*-isopropylidine-α-D-allofuranoside (**21)**

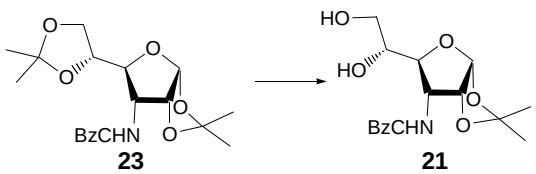

A solution of the compound **23** (35 g, 105 mmol) in methanol (500 ml) and aq. H_2SO_4 (0.8%, 500 ml) was stirred with frequent TLC monitoring at room temperature. On completion, the reaction was quenched with solid sodium carbonate and methanol was removed under reduced pressure and extracted repeatedly with EtOAc. The combined organic extracts were washed with water, brine, dried (Na_2SO_4) and evaporated under reduced pressure. The crude product thus obtained was purified by chromatography on silica gel (50% EtOAc in pet ether) to afford **21** (25.15 g, 80%) as yellow syrup.

$[\alpha]_D^{25}$	+ 12.23 (c = 0.95, $CHCl_3$)
IR ($CHCl_3$):	υ 3425, 1690 cm^{-1}
^{1}H NMR	δ: 1.32 (s, 3H), 1.52 (s, 3H), 3.61 (dd, *J* = 5.5, 11.4 Hz, 1H), 3.72 (m, 1H), 3.78 (m, 2H), 3.95 – 4.08 (m, 2H), 4.60 (t, *J* = 4.7 Hz, 1H), 5.11 (s, 2H), 5.57 (d, *J* = 8.6 Hz, 1H), 5.79 (d, *J* = 3.5 Hz, 1H), 7.35 (s, 5H).
^{13}C NMR	26.46, 26.59, 55.51, 63.58, 67.57, 72.47, 79.29, 80.1, 103.79, 112.64, 128.38, 128.48, 128.57, 135.81, 156.92 ppm.
Elemental Anal.	Calcd: C, 56.63; H, 6.24; N, 4.13.
$C_{17}H_{23}NO_7$	Found: C, 50.89; H, 6.09; N, 3.23.

3-*N*-Benzyloxycarbonyl-3,6-dideoxy-1,2-*O*-isopropylidine-α-L-*talo*-non-8-enofuranoside (17)

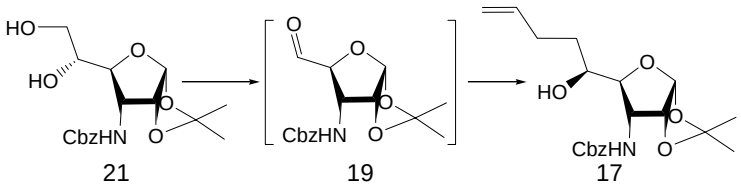

At 0 °C, a suspension of diol **21** (5 g, 28.3 mmol) and sodium bicarbonate (3 g) were dissolved in methanol-water (1:1, 70ml). Solid sodium meta periodate (12.125 g, 56.7 mmol) was added slowly over 30 min maintaining the reaction temperature at 5 °C. after completing the addition stirring was continued for additional 30 min at rt. The solids were filtered off, filtrate was concentrated and extracted with DCM. The combined organic extracts were washed with water, dried (Na_2SO_4) and evaporated under reduced pressure. The crude aldehyde thus obtained was dissolved in THF (50 ml) and butenyl magnesium bromide obtained from butenyl bromide (7.649 g, 5.8 ml, 56.7 mmol) and magnesium (1.36 g, 56.7 mmol) in THF (70 ml), was slowly added at 0 °C. The reaction mixture was stirred for 20 min. at 0 °C and on completion, reaction was quenched with saturated ammonium chloride solution. Then it was washed with four portions of EtOAc and the organic extracts were washed with water and brine, dried (Na_2SO_4) and evaporated under reduced pressure to obtain the distereomeric mixture of alcohols **17** and **17a**. This mixture was separated by chromatography using silica gel 230-400 mesh (17% EtOAc in pet ether). The major product was achieved (2.67 g, 50%) as a white solid.

M.p.:	82°C
$[\alpha]_D^{25}$	+ 36.97 (c = 1.4, $CHCl_3$)
^{1}H NMR	1.33 (s, 3H), 1.51 (s, 3H), 1.59 (m, 2H), 2.17 (m, 2H), 3.65 (m, 2H), 4.16 (dt, *J* = 4.6, 9.4 Hz, 1H), 4.6 (dd, *J* = 3.9, 4.8 Hz, 1H), 4.95 (m, 2H), 5.08 (m, 1H), 5.12 (s, 2H), 5.28 (d, *J* = 9.6 Hz, 1H), 5.83 (d, *J* = 3.6 Hz, 1H), 5.78 – 5.95 (m, 1H), 7.36 (s, 5H).

^{13}C NMR	26.03, 26.25, 29.82, 32.26, 52.86, 66.87, 67.78, 78.62, 81.52, 103.74, 111.91, 114.39, 127.88, 128.15, 135.78, 137.95, 156.08 ppm.
Elemental Anal.	Calcd: C, 63.64; H, 7.21; N, 3.71.
$C_{20}H_{27}NO_6$	Found: C, 60.84; H, 6.91; N, 3.45.

5-[(2S, 5R) 2-(3-*N*-Benzyloxycarbonyl-3-deoxy-1,2-*O*-isopropylidine-α-D-ribofuranoside) tetrahydrofuryl methyl] mercuric (II) chloride (15)

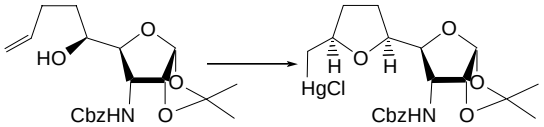

The alcohol **17** (3.5 g, 9.4 mmol) in DCM (30 ml) was stirred vigorously for 24 h with freshly crystallized mercuric acetate (4.5 g, 14.2 mmol). The reaction mixture was cooled and saturated sodium chloride solution (15 ml) was added to this. The reaction mixture was stirred vigorously for further 2 h. Then it was diluted with water (100 ml) and extracted with DCM (50 ml). The combined extracts were dried (Na_2SO_4), evaporated under reduced pressure to obtain the crude mixture of distereoisomers. This mixture was separated by chromatography on silica gel 230-400 mesh (25% EtOAc in pet ether). The major product was obtained as a white gel (2.6 g, 45%) and characterized as a single distereoisomer.

$[\alpha]_D^{25}$	+ 27.71 (c = 1.45, $CHCl_3$)
^{1}H NMR	1.25 - 1.32 (m, 1H), 1.32 (s, 3H), 1.51 (s, 3H), 1.80 – 2.23 (m, 4H), 2.29 (dd, *J* = 11.9, 5.4 Hz, 1H), 3.68 (dd, *J* = 3.4, 9.2 Hz, 1H), 4.15 (ddd, *J*= 7.7, 5.1, 3.7 Hz, 1H), 4.24 (d, *J* = 5.1 Hz, 1H), 4.38 (dd, *J* = 5.7, 5.4 Hz, 1H), 4.58 (dd, *J* = 4.7, 3.7 Hz, 1H), 5.12 (s, 2H), 5.15 – 5.20 (m, 1H), 5.81 (d, *J* = 3.5 Hz, 1H), 7.36 (s, 5H)
^{13}C NMR	19.58, 26.36, 29.17, 35.38, 38.25, 53.24, 67.22, 78.47, 81.27, 104.0, 111.98, 128.25, 128.25, 128.36, 128.53, 136.22, 155.79 ppm
Elemental Anal.	Calcd: C, 39.22; H, 4.28; N, 2.29
$C_{20}H_{26}ClHgNO_6$	Found: C, 39.28; H, 4.98; N, 2.1

Analysis for compound 15a

$[\alpha]_D^{25}$	+ 33.64 (c = 1.1, $CHCl_3$)
^{1}H NMR	1.33 (s, 3H), 1.50 (s, 3H), 1.53 (m, 2H), 2.00 - 2.21 (m, 4H), 3.63 (d, *J* = 9.62 Hz, 1H), 4.22 (m, 2H), 4.50 (m, 1H), 4.62 (t, *J* = 4.12 Hz, 1H), 5.11 - 5.22 (m, 3H), 6.18 (m, 1H), 7.36 (m, 6H)
^{13}C NMR	19.58, 26.36, 29.17, 35.38, 38.25, 53.24, 67.22, 75.92, 78.47, 78.85, 81.27, 102.31, 104.00, 111.98, 128.25, 128.36, 128.53, 136.22, 155.79 ppm
Elemental Anal.	Calcd: C, 39.22; H, 4.28; N, 2.29
$C_{20}H_{26}ClHgNO_6$	Found: C, 38.93; H, 4.20; N, 2.65

5-(2S, 5R) 2-(3-*N*-Benzyloxycarbonyl-3-deoxy-1,2-*O*-isopropylidine-α-D-ribofuranoside) tetrahydrofuryl methanol (13)

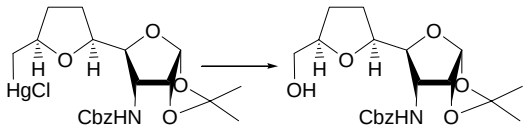

15 **13**

A solution of compound **15** (2.5 g, 3.9 mmol) in DMF (20 ml) was bubbled with oxygen gas for 18 h at 70 °C. Then the reaction mixture was cooled to room temperature and added dropwise to a suspension of sodium borohydride (156 mg, 4.7 mmol) in DMF (30 ml) at 0 °C with continuous bubbling of oxygen gas. The addition was continued over a period of 3 h maintaining the reaction temperature below 5 °C. After the complete addition, the reaction was monitored by TLC and on completion the reaction was quenched by methanol. The reaction mixture was diluted with water and extracted with four portions of diethyl ether. The combined organic layers were washed thoroughly with water and brine, dried (Na_2SO_4), evaporated under reduced pressure and purified by chromatography on silica gel (45% EtOAc in pet ether) to obtain pure alcohol (1.27 g, 79%) as thick syrup.

$[\alpha]_D^{25}$ + 27.21 (c = 1.1, $CHCl_3$)

^{1}H NMR	1.19 (s, 3H), 1.26 (s, 3H), 1.55 – 1.77 (m, 2H), 2.01 – 2.26 (m, 2H), 2.82 (bs, 1H), 3.57 (dd, *J* = 2.3, 9.2 Hz, 2H), 4.09 (dt, *J* = 5.2, 9.4 Hz, 1H), 4.53 (dd, *J* = 3.9, 4.8 Hz, 1H), 4.91 (m, 1H), 5.01 (dd, *J* = 3.46, 1.64 Hz, 1H), 5.05 (s, 2H), 5.21 (d, *J* = 8 Hz, 1H), 5.76 (d, *J* = 3.6 Hz, 1H), 7.29 (s, 5H)
^{13}C NMR	26.36, 26.62, 27.43, 27.96, 53.86, 55.52, 64.47, 65.13, 67.20, 78.97, 79.63, 80.11, 80.94, 104.02, 112.26, 128.28, 128.35, 128.51, 136.07, 155.79 ppm
Elemental Anal.	Calcd: C, 61.06; H, 6.92; N, 3.56
$C_{20}H_{27}NO_7$	Found: C, 62.84; H, 7.74; N, 3.66

5-(2S, 5R) 2-(3-*N*-Benzyloxycarbonyl-3-deoxy-1,2,-*O*-isopropylidine-α-D-ribofuranoside) tetrahydrofuran carboxylic acid (9)

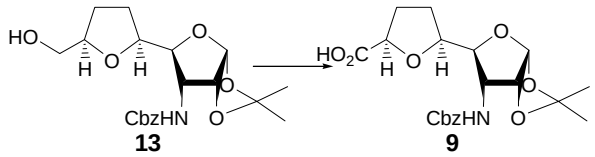

13 **9**

Acetonitrile (1 ml), CCl_4 (1 ml) and water (2 ml) was stirred vigorously with sodium meta periodate (218 mg, 1.15 mmol), $RuCl_3$ (10 mg, 20 mole %) at 0 °C for half hour. Primary alcohol **13** (200 mg, 0.51 mmol) was dissolved in same solvent system and added at once with sodium meta periodate (218 mg, 1.15 mmol). The reaction mixture was maintained at 0 °C for further half hour. The excess RuO_4 was quenched by solid sodium sulfite (2 g) at 5 °C and reaction mixture was diluted with water. The organic phase was concentrated under reduced pressure and the crude product was isolated in DCM. The organic layer was washed thoroughly with sodium sulfite solution and water, dried (Na_2SO_4) and evaporated under reduced pressure. The crude product was purified by chromatography on silica gel 100-200 mesh (35% EtOAc and 2% acetic acid in pet ether) to produce **9** as white thick syrup (104 mg, 50%).

$[\alpha]_D^{25}$	+ 8.26 (c = 0.6, $CHCl_3$)

^{1}H NMR	1.33 (s, 3H), 1.52 (s, 3H), 2.17 – 2.76 (m, 4H), 3.8 (d, *J* = 9.3 Hz, 1H), 4.41 – 4.3 (m, 1H), 4.6 (t, *J* = 4.2 Hz, 1H), 4.74 (m, 1H), 5.11 (s, 2H), 5.25 (d, *J* = 8.2 Hz, 1H), 5.8 (d, *J* = 3.4 Hz, 1H), 7.36 (s, 5H)
^{13}C NMR	24.23, 26.27, 26.65, 27.78, 53.19, 67.13, 78.91, 82.0, 96.04, 104.27, 112.62, 128.44, 135.94, 155.56, 176.84 ppm
Elemental Anal.	Calcd: C, 58.96; H, 6.18; N, 3.44
$C_{20}H_{25}NO_8$	Found: C, 54.40; H, 6.03; N, 3.74

F-MOC NH. Ala Phe .OAll (29)

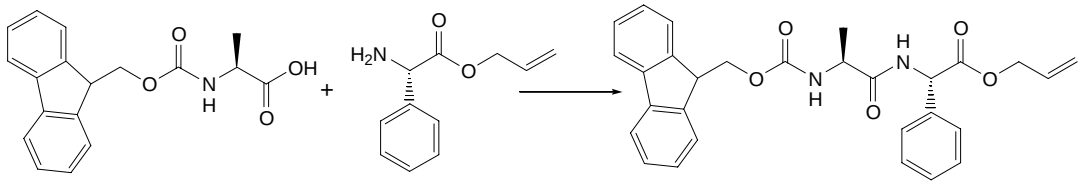

29

The allyl protected phenylglycine (5 g, 26 mmol), HOBt (4.35 g, 52 mmol) and F-moc protected alanine (8.141 g, 26 mmol) were dissolved in DCM-DMF (3:1, 40 ml). The reaction mixture was cooled to 0 °C. EDCI (9.968 g, 52 mmol) was added to the reaction mixture in portions to maintain the internal temperature below 5 °C. The reaction mixture was stirred for 8 h at rt. On completion, the reaction mixture was quenched (ice) and diluted with water, extracted in DCM (3X50 ml). The combined organic extracts were washed with 2% acetic acid in water followed by water and 10 % sodium bicarbonate, dried (Na_2SO_4) and evaporated under reduced pressure. The crude product thus obtained was purified by chromatography on silica gel (25% EtOAc in pet ether). The dipeptide (11.42 g, 90%) was analyzed as a white solid compound.

M.p.:	85°
^{1}H NMR	1.33 (d, *J* = 6.9 Hz, 3H), 4.17 (dd, *J* = 14.1, 7 Hz, 1H), 4.29 (m, 2H), 4.37 (dd, *J* = 10.2, 7.3 Hz, 1H), 4.55 (d, *J* = 5.7 Hz, 2H), 4.84 (dt, *J* = 8, 5.9 Hz, 1H), 5.25 (m, 2H), 5.39 (d, *J* = 7.6 Hz, 1H), 5.82 (m, 1H), 7.25 (m, 11H), 7.55 (d, *J* = 7.2 Hz, 2H), 7.72 (d, *J*= 7.2 Hz, 2H)

^{13}C NMR	17.89, 24.20, 25.00, 33.19, 36.87, 39.19, 46.37, 47.48, 49.69, 52.73, 64.87, 65.83, 117.86, 119.14, 124.48, 126.03, 126.32, 126.91, 127.58, 128.59, 130.85, 135.61, 140.40, 143.14, 155.15, 170.26, 171.89 ppm
Elemental Anal.	Calcd: C, 69.09; H, 6.85; N, 7.32
$C_{29}H_{28}N_2O_5$	Found: C, 68.94; H, 6.93; N, 7.21

5-(2S, 5R) 2-(3-*N*-Benzyloxycarbonyl-3-deoxy-1,2,-*O*-isopropylidine-α-D-ribofuranoside) tetrahydrofuran carboxy. ala.phe. OAll (28)

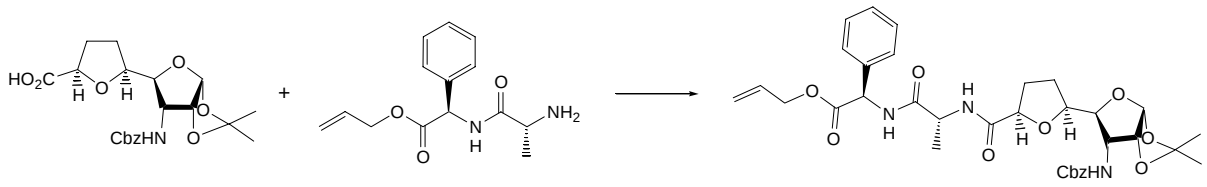

9 **29** **28**

At 0 °C, to a solution of acid **9** (200 mg, 0.51 mmol), HOBt (138 mg, 1 mmol), free amine of dipeptide **29** (155 mg, 0.59 mmol) in DCM (5 ml) was added EDCI (195 mg, 1 mmol) in portions to maintain the internal temperature below 5 °C. The reaction mixture was stirred for 8 h at RT and on completion, quenched by ice. The reaction mixture was diluted with water and product was extracted in DCM (3X25 ml). The combined organic extracts were washed with 0.1% acetic acid in water followed by water and 10 % sodium bicarbonate, dried (Na_2SO_4), evaporated reduced pressure and the crude product thus obtained was purified by chromatographic method on silica gel (45% EtOAc in pet ether). The tripeptide **28** (199 mg, 60%) was analyzed as thick syrup.

$[\alpha]_D^{25}$	+36.97(c = 1.4, $CHCl_3$)
^{1}H NMR	1.32 (s, 3H), 1.50 (s, 3H), 1.62 (d, *J* = 5.1 Hz, 3H), 1.94 - 2.14 (m, 4H), 3.43 (m, 2H), 3.51 (dt, *J* = 10.4, 5.7 Hz, 2H), 3.62 (m, 1H), 3.74 (dt, *J*= 9.8, 5.7 Hz, 1H), 3.98 (m, 1H), 4.16 (t, *J* = 9.4, 4.9 Hz, 1H), 4.25 (dt, *J*= 6.6, 2.7 Hz, 1H), 4.57 (m, 2H), 4.69 (t, *J* = 6.6 Hz, 1H), 5.10 (m, 2H), 5.23 – 5.33 (m, 2H), 5.70 (d, *J* = 3.7 Hz, 1H), 5.84 (m, 1H), 7.34 (m, 10H), 7.71 (d, *J* = 8 Hz, 1H), 7.82 (d, *J* = 8.2 Hz, 1H)

^{13}C NMR	24.45, 25.10, 25.44, 25.57, 26.26, 26.33, 26.56, 26.89, 27.35, 28.45, 28.74, 28.97, 43.11, 43.25, 46.35, 53.68, 54.25, 67.06, 76.07, 77.20, 78.92, 79.14, 80.03, 81.32, 103.97, 110.76, 112.28, 117.77, 125.27, 126.21, 128.08, 128.43, 129.19, 129.32, 136.08, 155.63, 169.11, 169.62, 169.95 ppm
Elemental Anal.	Calcd: C, 62.66; H, 6.34; N, 6.45
$C_{34}H_{41}N_3O_{10}$	Found: C, 62.39; H, 6.19; N, 6.67

References

1. (a)Fischer, E. ; Fourneau, E. *Ber. Dtsch. Chem. Ges.* **1901**, *34*, 2868. (b)Fischer, E. *Ber. Dtsch. Chem. Ges.* **1905**, *38*, 605.
2. (a) Curtius, T. *J. Prakt. Chem.* **1882**, *26*, 145. (b) Curtius, T. *J. Prakt. Chem.* **1904**, *70*, 57.
3. (a)Carpino, L.A. *J. Am. Chem. Soc.* **1957**, *79*, 4427. (b)McKay, F.C.; Albertson, N.F. *J. Am. Chem. Soc.* **1957**, *79*, 4686.
4. Schwyzer, R.; Sieber, P. *Nature* **1963**, **199**, 172.
5. (a)Sheehan, J.C.; Hess, G.P. *J. Am. Chem. Soc.* **1955**, *77*, 1067. (b)Khorana, H.G. *Chem. Ind. (London)* **1955**, *33*, 1087.
6. Goodman, M.; McGahren, W.J. *Tetrahedron* **1967**, *23*, 2031.
7. Merrifield, R.B. *J. Am. Chem. Soc.* **1963**, *85*, 2149.
8. Tam, J.P.; Heath, W.; Merrifield, R.B. *J. Am. Chem. Soc.* **1983**, *105*, 6442.
9. Carpino, L.A.; Han, G.Y. *J. Am. Chem. Soc.* **1970**, *92*, 5748.
10. Aguilar, M.-I. HPLC of Peptides and Proteins: Methods and Protocols. Monash University, Clayton, Victoria, Australia **2004**.
11. Chapman, J.R. Mass Spectrometry of Proteins and Peptides. Sale, Manchester, UK **2000**.
12. Koglin, N.; Zorn, C.; Beumer, R.; Cabrele, C.; Bubert, C.; Sewald, N.; Reiser, O.; Beck-Sickinger, A. G.; *Angew. Chem. Int. Ed.* **2003**, *42*, 202.
13. Bolin, A. K.; Millhauser, G. L. *Acc. Chem. Res.* **1999**, *32*, 1027,
14. Hayen, A.; Schmitt, M. A.; Ngassa, F. N.; Thomasson, K. A.; Gellman S. H. *Angew. Chem. Int. Ed.* **2004**, *43*, 505 –510
15. (a) Seebach, D.; Overhand, M.; Kühnle, F. N. M.; Martinoni, B.; Oberer, L.; Hommel, U.; Widmer, H. *Helv. Chim. Acta* **1996**, *79*, 913. (b) Seebach, D.; Ciceri, P. E.; Overhand, M.; Jaun, B.; Rigo, D.; Oberer, L.; Hommel, U.; Amstutz, R.; Widmer, H. *Helv. Chim. Acta* **1996**, *79*, 2043. (c) Seebach, D.; Gademann, K.; Schreiber, J. V.; Matthews, J. L.; Hintermann, T.; Jaun, B.; Oberer, L.; Hommel, U.; Widmer, H. *Helv. Chim. Acta*, **1997**, *80*, 2033. (d) Seebach, D.; Abele, S.; Gademann, K.; Guichard, G.; Hintermann, T.; Jaun, B.; Matthews, J. L.; Schreiber,

J. V.; Oberer, L.; Hommel, U.; Widmer, H. *Helv. Chim. Acta* **1998**, *81*, 932. (e) Hintermann, T.; Seebach, D.; *Chimia* **1997**, *50*, 244. (f) Daura, X.; van Gunsteren, W. F.; Rigo, D.; Jaun, B.; Seebach, D. *Chem. Eur. J.* **1997**, *3*, 1410. (g) Appella, D. H.; Christianson, L. A.; Karle, I. L.; Powell, D. R.; Gellman, S. H. *J. Am. Chem. Soc.* **1996**, *118*, 13071. (h) Appella, D. H.; Christianson, L. A.; Klein, D. A.; Powell, D. R.; Huang, X.; Barchi, J. J. Jr.; Gellman, S. H. *Nature* **1997**, *387*, 381. (i) Krauthäuser, S.; Christianson, L. A.; Powell, D. R.; Gellman, S. H. *J. Am. Chem. Soc.* **1997**, *119*, 11719. (j) Gellman, S. H. *Acc. Chem. Res.* **1998**, *31*, 173. (k) Borman, S. *Chem. Eng. News* **1997**, *75*, 32. (l) Koert, U. *Angew. Chem.Int. Ed.* **1997**, *36*, 1836. (m) Iverson, B. L. *Nature* **1997**, *385*, 113.

16. Daura, X.; Gademann, K.; Jaun, B.; Seebach, D.; van Gunsteren, W. F.; Mark A. E. *Angew. Chem. Int. Ed.* **1999**, *38*, 236.
17. Sharma, G. V. M.; Nagendar, P.; Jayaprakash, P.; Krishna, P. R.; Ramakrishna, K. V. S.; Kunwar A. C. *Angew. Chem. Int. Ed.* **2005**, *44*, 5878.
18. Cambridge Crystallographic Data Centre publication no. **CCDC-113798**.
19. Seebach, D.; Abele, S.; Gademann, K.; Jaun B. *Angew. Chem. Int. Ed.* **1999**, *38*, 1595.
20. Fisk, J. D.; Gellman S. H. *J. Am. Chem. Soc.* **2001,** *123*, 343.
21. (a)Haque, T. S.; Little, J. C.; Gellman, S. H. *J. Am. Chem. Soc.* **1994**, *116*, 4105. (b)Haque, T. S.; Little, J. C.; Gellman, S. H. *J. Am. Chem. Soc.* **1996**, *118*, 6975. (c)Karle, I. L.; Awasthi, S. K.; Balaram, P. *Proc. Natl. Acad. Sci. U.S.A.* **1996**, *93*, 8189. (d)Haque, T. S.; Gellman, S. H. *J. Am. Chem. Soc.***1997**, *119*, 2303. (e)Raghothama, S. R.; Awasthi, S. K.; Balaram, P. *J. Chem. Soc.; Perkin Trans. 2* **1998**, 137. (f)Stanger, H. E.; Gellman, S. H. *J. Am. Chem. Soc.* **1998**, *120*, 4236.
22. . (a)Morita, H.; Kondo, K.; Hitotsuyanagi, Y.; Takeya, K.; Itokawa, H.; Tomioka, N.; Itai, A.; Iitaka, Y. *Tetrahedron* **1991**, *47*, 2757. (b)Itokawa, H.; Takeya, K.; Hitotsuyanagi, Y.; Morita, H. *The Alkaloides*; Cordell, G. A.; Ed.; Academic Press: 1997; Vol. 49, pp 301.
23. Kessler, H. *Angew. Chem.; Int. Ed.* **1982**, *21*, 512.
24. Boger, D. L.; Zhou, J.; Borzilleri, R. M.; Nukui, S.; Castle, S. L. *J. Org. Chem.* **1997**, *62*, 2054.

25. (a)Feng, Y.; Pattarawarapan, M.; Wang, Z.; Burgess, K. *J. Org. Chem.* **1999**, *64*, 9175. (b)Wipf, P.; Henninger, T. C.; Geib, S. J. *J. Org. Chem.* **1998**, *63*, 6088. (c)Haque, T. S.; Gellman, S. H. *J. Am. Chem. Soc.* **1997**, *119*, 2303. (d)Cristau, P.; Marie-The´re`se M.; Marie-Elise T. H. D.; Vors, J. P.; Zhu J. Org. Lett **2004**, *6*, 3183.

26. (a) Grafv. Roedern, E.; Lohof, E.; Hessler, G.; Hoffmann, M.; Kessler, H. *J. Am. Chem. Soc.* **1996**, *118*, 10156. (b) Szabo, L.; Smith, B. L.; McReynolds, K. D.; Parrill, A. L.; Morris, E. R.; Gervay, J. *J. Org. Chem.* **1998**, *63*, 1074.

27. (a) Nagai, U.; Sato, K. *Tetrahedron Lett.* **1985**, *26*, 647. (b) Nagai, U.; Sato, K.; Nakamura, R.; Kato, R. *Tetrahedron* **1993**, *49*, 3577. (c) Haubner, R.; Sehmitt, W.; Hölzemann, G.; Goodman, S. L.; Jonczyk, A.; Kessler, H. *J. Am. Chem. Soc.* **1996**, *118*, 7881.

28. Cambridge Crystallographic Data Centre publication no. **CCDC-102538**.

29. Geycr, A.; Bockelmann, D.; Weisscnbach, K.; Fischer H. *Tetrahedron Lett.* **1999**, *40*, 477.

30. Viles, J. H.; Patel, S. U.; Mitchell, J. B. O.; Moody, C. M.; Justice, D. E.; Uppenbrink, J.; Doyle, P. M.; Harris, C. J.; Sadler, P. J.; Thornton, J. M. *J. Mol. Biol.* **1998**, *279*, 973.

31. Wipf, P.; Henninger, T. C.; Geib, S. J. *J. Org. Chem.* **1998,** *63*, 6088.

32. Nowick, J. S.; Smith, E. M.; Pairish, , M. *Chem. Soc. Rev.* **1996**, *25*, 401.

33. (a) Wilmot, C. M.; Thornton, J. M. *Protein Engineering* **1990**, *3*, 497. (b) Wilmot, C. M.; Thornton, J. M. *J.Mol. Biol.* **1988**, *203*, 221.

34. (a) Blanco, A. G.; Sola, M.; Gornis-Rüth, F. X.; Coll, M. *Structure* **2002**, *10*, 701. (b) Somers, W. S.; Phillips, S. E. V. *Nature* **1992**, *359*, 387.

35. (a) Puglishi, J. D.; Chen, L.; Blanchard, S.; Frankel, A.D. *Science*, **1995**, *270*, 1200. (b) Variani, G. *Acc. Chem. Res.* **1997**, *30*, 189.

36. Strynadka, N. C. J.; Jensen, S. E.; Alzari, P. M.; James, M. N. G. *Nat. Struct. Biol.* **1996**, *3*, 290.

37. (a) Jaroniec, C. P.; MacPhee, C. E.; Bajaj, V. S.; McMahon, M. T.; Dobson, C. M.; Griffin, R. G. *PNAS* **2004**, *101*, 711. (b) Serpell, L. C.; Blake, C. C. F.; Fraser, P.E. *Biochemistry* **2000**, *39*, 13269.

38. Collinge, J. *Annu. Rev. Neurosci.* **2001**, *24*, 519.

39. McDonnell, J. M.; Fushman, D.; Cahill, S. M.; Sutton, B. J.; Cowburn, D. *J. Am. Chem. Soc.* **1997**, *119*, 5321.

40. (a) Derrick, J. P.; Davis, G. J.; Dauter, Z.; Wilson, K. S.; Wigley, D. B. *J. Mol. Biol.* **1992**, *227*, 1253. (b) Derrick, J. P.; Wigley, D. B. *Nature* **1992**, *359*, 752. (c) Derrick, J. P.; Wigley, D. B. *J. Mol. Biol.* **1994**, *243*, 906. (d) Boutillon, R.; Wintjens, G.; Lippens, H.; Drobecq, A.; Tartar, A. *Eur. J. Biochem.* **1995**, *231*, 166.

41. Kwong, P. D.; Wyatt, R.; Robinson, J.; Sweet, R. W.; Sodroski, J.; Hendrickson, W. A. *Nature* **1998**, *393*, 648.

42. (a) Ball, J. B.; Alewood, P. F. *J. Mol. Recogn.* **1990**, *3*, 55. (b) Marshall, G. R. *Curr. Opin. Struct. Biol.* **1992**, *2*, 904.

43. Butterfield, S. M.; Waters, M. L. *J. Am. Chem. Soc.* **2003**, *125*, 9580.

44. (a) Robinson, J. A. *Synlett*. **1999**, 429. (b) Nowick, J. S. *Acc. Chem. Res.* **1999**, *32*, 287.

45. (a) Armitage, B. A. *Annu. Rep. Prog. Chem. Sect. B* **2000**, *96*, 187. (b) Lai, J. R.; Huck, B. R.; Weisblum, B.; Gellman, S. H. *Biochemistry* **2002**, *41*, 12835.

46. (a) Ramírez-Alvarado, M.; Blanco, F. J.; and Serrano, L. *Protein Sci.* **2001** *10*, 1381. (b) Sibanda, B. L.; Blundell, T. L.; and Thornton, J. M. *J. Mol. Biol.* **1989**, *229*, 759. (c) Williamson, M. P. *Biopolymers* **1990**, *29*, 1423. (d) Karplus, M. *J. Phys. Chem.* **1959**, *30*, 11. (e) Serrano, L.; Horovitz, A.; Avron, B.; Bycroft, M.; Fersht, A. *Biochemistry* **1990**, *29*, 9343. (f) Ramírez-Alvarado, M.; Blanco, F. J.; Niemann, H.; Serrano, L. *J. Mol. Biol.* **1997**, *273*, 898. (g) de Alba, E.; Jiménez, M. A.; Rico, M., Nieto, J. L. *Folding & Design* **1996**, *1*, 122.

47. *Carey: Organic Chemistry*, Fifth edition, The McGraw Hill Companies, **2004**, 1145.

48. *Carey: Organic Chemistry*, Fifth edition, The McGraw Hill Companies, **2004**, 1148.

49. (a) Wessel, H. P.; Mitchell, C.; Lobato, C. M.; Schmid, G. *Angew. Chem.* **1995**, *107*, 2920. (b) Nicolaou, K. C.; Flörke, H.; Egan, M. G.; Barth, T. V.; Estevez, A. *Tetrahedron Lett.* **1995**, *36*, 1775. (c) Suhara, Y.; Hildreth, J. E. K.; Ichikawa, Y. *Tetrahedron Lett.* **1996**, *37*, 1575. (d) Graf von Roedern, E.; Kessler, H. *Angew.*

Chem. Int. Ed. **1994**, *33*, 667. (e) Graf von Roedern, E.; Lohof, E.; Hessler, G.; Hoffmann, M.; Kessler, H.; *J. Am. Chem. Soc.* **1996**, *118*, 10156. (f) Suhara, Y.; Ichikawa, M.; Hildreth, J. E. K.; Ichikawa, Y. *Tetrahedron Lett.* **1996**, *37*, 2549. (g) Szabo, L.; Smith, B. L.; McReynolds, K. D.; Parrill, A. L.; Morris, E. R.; Gervay, J.; *J. Org. Chem.* **1998**, *63*, 1074. (h) Lohof, E.; Burkhart, F.; Born, M. A.; Planker, E.; Kessler, H. in *Advances in Amino Acid Mimetics and Peptidomimetics, Vol. 2. (*Ed.: A. Abell), JAI Press Inc.; Stanford, Connecticut, **1999**, pp. 263-292. (i) Brittain, D. E. A.; Watterson, M. P.; Claridge, T. D. W.; Smith, M. D.; Fleet, G. W. J. *J. Chem. Soc. Perkin Trans. 1* **2000**, 3655. (j) Hungerford, N. L.; Claridge, T. D. W.; Watterson, M. P.; Aplin, R. T.; Moreno, A, Fleet, G. W. J. *J. Chem. Soc. Perkin Trans. 1* **2000**, 3666.

50. Williamson, A. R.; Zamenhof, S. *J. Biol. Chem.* **1963**, *238*, 2255.
51. Heyns, K.; Kiessling, G.; Lindenberg, W.; Paulsen, H.; Webster, M. E. *Chem. Ber.* **1959**, *92*, 2435.
52. Knapp, S. *Chem. Rev.* **1995**, *95*, 1859.
53. Knapp, S.; Jaramillo, C.; Freeman, B. *J. Org. Chem.* **1994**, *59*, 4800.
54. (a) Coutsogeorgopoulos, C.; Bloch, A.; Watanabe, K. A.; Fox, J. J. *J. Med. Chem.* **1975**, *18*, 771. (b) Fox, J. J.; Kuwada, Y.; Watanabe, K. A. *Tetrahedorn Lett.* **1968**, *57*, 6029. (c) Kotick, M. P.; Klein, R. S.; Watanabe, K. A.; Fox, J. J. *Carbohydr. Res.* **1969**, *11*, 369. (d) Lichtenthaler, F. W.; Morino, T.; Mezel, H. M. *Tetrahedron Lett.* **1975**, *16*, 665. (e) Watanabe, K. A.; Falco, E. A.; Fox, J. J. *J. Am. Chem. Soc.* **1972**, *94*, 3272.
55. (a) Haruyama, H.; Takayama, T.; Kinoshita, T.; Kondo, M.; Nakajima, M.; Haneishi, T. *J. Chem. Soc.; Perkin Trans. 1* **1991**, *7*, 1637. (b) Nakajima, M.; Itoi, K.; Takamatsu, Y.; Kinoshita, T.; Okazaki, T.; Kawakubo, K.; Shindo, M.; Honma, T.; Tohjigamori, M.; Haneishi, T. *J. Antibiot.* **1991**, *44*, 293. (c) Siehl, D. L.; Subramanian, M. V.; Walters, E. W.; Lee, S. F.; Anderson, R. J.; Toschi, A. G. *Plant Physiol.* **1996**, *110*, 753.
56. Umezawa, H.; Aoyagi, T.; Komiyama, T.; Morishima, H.; Hamada, M.; Takeuchi, T. *J. Antibiot.* **1974**, *27*, 963.

57. (a)Wester, H. J.; Schottelius, M.; Scheidhauer, K.; Meisetschlager,G.; Herz, M.; Rau, F. C.; Reubi, J. C.; Schwaiger, M. *Eur. J. Nucl. Med. Mol. Imaging* **2003**, *30*, 117. (b)Leisner, M.; Kessler, H.; Schwaiger, M.; Wester, H. J. *J. Labelled Compd. Radiopharm.* **1999**, *42. (Suppl.)*, S549. (c)Schottelius, M.; Wester, H. J.; Reubi, J. C.; Senekowitsch-Schmidtke, R.; Schwaiger, M. *Bioconjugate Chem.;* **2002**, 13, 2004. (d) Wester, H. J.; Schottelius, M.; Scheidhauer, K.; Reubi, J.C.; Wolf, I.; Schwaiger, M. *Eur. J. Nucl. Med. Mol. Imag.* **2002**, *29*, 28. (e) Haubner, R.; Kuhnast, B.; Mang, C.; Weber, W. A.; Kessler, H.; Wester, H. J.; Schwaiger, M. *Bioconjugate Chem.;* **2004**, 15, 61.

58. Brandstetter, T. W.; de la Fuente, C.; Kim, Y. H.; Cooper, R. I.; Watkin, D. J.; Oikonomakos, N. G.; Johnson, L. N.; Fleet, G. W. J. *Tetrahedron* **1996**, *52*, 10711.

59. Estevez, J. C.; Smith, M. D.; Lane, A. L.; Crook, S.; Watkin, D. J.; Besra, G. S.; Brennan, P. J.; Nash, R. J.; Fleet, G. W. J. *Tetrahedron Asymm.* **1996**, *7*, 387.

60. Brandstetter, T. W.; Wormland, M. R.; Dwek, R. A.; Butters, T. D.; Platt, F. M.; Tsitsanou, K. E.; Zographos, S. E.; Oikonomakos, N. G.; Fleet, G. W. J. *Tetrahedron Asymm.* **1996**, *7*, 157.

61. Estevez, J. C.; Burton, J. W.; Estevez, R. J.; Ardron, H.; Wormald, M. R.; Dwek, R. A.; Brown, D.; Fleet, G. W. J. *Tetrahedron Asymmetry* **1998**, *9*, 2137.

62. Dondoni, A.; Marra, A. *Chem. Rev.* **2000**, *100*, 4395.

63. (a) Estevez, J. C.; Smith, M. D.; Lane, A. L.; Crook, S.; Watkin, D. J.; Besra, G. S.; Brennan, P. J.; Nash, R. J.; Fleet, G. W. J. *Tetrahedron Asymm.* **1996**, *7*, 387. (b) Brandstetter, T. W.; Wormland, M. R.; Dwek, R. A.; Butters, T. D.; Platt, F. M.; Tsitsanou, K. E.; Zographos, S. E.; Oikonomakos, N. G.; Fleet, G. W. J. *Tetrahedron Asymm.* **1996**, *7*, 157-. (c) Estevez, J. C.; Smith, M. D.; Wormland, M. R.; Besra, G. S.; Brennan, P. J.; Nash, R. J.; Fleet, G. W. J. *Tetrahedron Asymm.* **1996**, *7*, 391.

64. (a) Watterson, M. P.; Pickering, L.; Smith, M. D.; Hudson, S. J.; Marsh, P. R.; Mordaunt, J. E.; Watkin, D. J.; Newman, C. J.; Fleet, G. W. J. *Tetrahedron Asymmetry* **1999**, *10*, 1855. (b) Hungerford, N. L.; Fleet, G. W. J. *J. Chem. Soc. Perkin Trans. 1* **2000**, 3680.

65. (a) Bichard, C. J. F.; Brandstetter, T. W.; Estevez, J. C.; Fleet, G. W. J.; Hughes, D. J.; Wheatley, J. R.; Dyson, J. E. *J. Chem. Soc. Perkin Trans. 1* **1996**, *17*, 2151. (b) Brimacombe, J. S.; Tucker, L. C. N. *Carbohydrate Res.* **1966**, *2*, 341. (c) Brimacombe, J. S.; Tucker, L. C. N. *Carbohydrate Res.* **1965**, *1*, 332. (d) Wheatley, J. R.; Bichard, C. J. F.; Mantell, S. J.; Son, J. C.; Hughes, D. J.; Fleet, G. W. J.; Brown, D. *J. Chem. Soc., Chem. Commun.* **1993**, *13*, 1065.

66. Poitout, L.; Merrer, Y. L.; Depezay, J. C. *Tetrahedron Lett.* **1995**, *36*, 6887.

67. (a) Chakraborty, T. K.; Jayaprakash, S.; Diwan, P. V.; Nagaraj, R.; Jampani, S. R. B.; Kunwar, A. C. *J. Am. Chem. Soc.* **1998**, *120*, 12962. (b) Chakraborty, T. K.; Ghosh, S.; Jayaprakash, S.; Sharma, J. A. R. P.; Ravikanth, V.; Diwan, P. V.; Nagaraj, R.; Kunwar, A. C. *J. Org. Chem.* **2000**, *65*, 6441. (c) Smith, M. D.; Long, D. D.; Marquess, D. G.; Claridge, T. D. W.; Fleet, G. W. J.; *Chem. Commun.* **1998**, 2039. (d) Smith, M. D.; Fleet, G. W. J. *J. Peptide Sci.* **1999**, *5*, 425.

68. (a) Brittain, D. E. A.; Watterson, M. P.; Claridge, T. D. W.; Smith, M. D.; Fleet, G. W. J. *J. Chem. Soc. Perkin Trans. 1* **2000**, 3655. (b) Hungerford, N. L.; Claridge, T. D. W.; Watterson, M. P.; Aplin, R. T.; Moreno, A.; Fleet, G. W. J. *J. Chem. Soc. Perkin Trans. 1* **2000**, 3666.

69. (a) Kirshenbaum, K.; Zuckermann, R. N.; Dill, K. A. *Curr. Opin. Struct. Biol.* **1999**, *9*, 530. (b) Soth, M. J.; Nowick, J. S. *Curr. Opin. Chem. Biol.* **1997**, *1*, 120.

70. Seeberger, P. H. *Solid Support Oligosaccharide Synthesis and Combinatorial Carbohydrate Libraries*, Wiley, New York, **2001**. (b) Seeberger, P. H.; Haase, W. C. *Chem. Rev.* **2000**, *100*, 4349.

71. (a) Fuchs, E. F.; Lehmann, J. *Chem. Ber.* **1975**, *108*, 2254. (b) Fuchs, E. F.; Lehmann, J. *Chem. Ber* **1975**, *45*, 135. (c) Fuchs, E. F.; Lehmann, J. *Carbohydr. Res.* **1976**, *49*, 267. (d) Fuchs, E. F.; Lehmann, J. *Chem. Ber.* **1976**, *109*, 267.

72. Yoshimura, J.; Ando, H.; Sato, T.; Tsuchida, S. *Bull. Chem. Soc. Jpn.* **1976**, *49*, 2511.

73. Suhara, Y.; Ichikawa, M.; Hildreth, J. E. K.; Ichikawa, Y. *Tetrahedron Lett.* **1996**, *37*, 2549.

74. (a) Szabo, L.; Smith, B. L.; McReynolds, K. D.; Parrill, A. L.; Morris, E. R.; Gervay, J. *J. Org. Chem.* **1998**, *63*, 1074. (b) Müller, C.; Kitas, E.; Wessel, H. P. *J. Chem. Soc. Chem. Commun.* **1995**, 2425.

75. (a) Goodnow, R. A. J.; Richou, A. R.; Tam, S. *Tetrahedron Lett.* **1997**, *38*, 3195. (b) Goodnow, R. A. J.; Tam, S.; Pruess, D. L.; McComas, W. W. *Tetrahedron Lett.* **1997**, *38*, 3199.

76. (a) Fügedi, P.; Peto, C. in *8th European Carbohydrate Symposium*, Sevilla, Spain, **1995**, p. Abstract A75. (b) Fügedi, P.; Peto, C.; Wang, L. in *9th European Carbohydrate Symposium*, Mailland, Italy, **1996**, p. Abstract B0013. (c) Peto, C.; Fügedi, P.; Wlasichuk, K. in *8th European Carbohydrate Symposium*, Sevilla, Spain, **1995**, p. Abstract A 74. (d) Fügedi, P.; Petö, C. J.; Wang, L.; in *9th European Carbohydrate Symposium*, Uetrecht, Netherlands, **1997**, pp. A113-A114.

77. van Well, R. M.; Overkleeft, H. S.; Overhand, M.; Vang Carstensen, E.; van der Marel, G. A.; van Boom, J. H. *Tetrahedron Lett.* **2000**, *41*, 9331.

78. (a) Stöckle, M.; Kessler, H. in *11th European Carbohydrate Symposium*, Lisbon, **2001**, p. P157. (b) Stöckle, M.; Locardi, E.; Gruner, S.; Kessler, H. in *20th International Carbohydrate Symposium* (Ed.: J. Thiem), LCI Publisher GmbH, Hamburg, **2000**, p. 124.

79. Locardi, E.; Stöckle, M.; Gruner, S.; Kessler, H. *J. Am. Chem. Soc.* **2001**, *123*, 8189.

80. (a) Rhodes, D.; Schwabe, J. W. R.; Chapman, L.; Fairall, L. *Phil. Trans. R. Soc. Lond. B* **1996**, *351*, 501. (b) Herzner, H.; Reipen, T.; Schultz, M.; Kunz, H. *Chem. Rev.* **2000**, *100*, 4495. (c) Lindhorst, T. K. *Top. Curr. Chem.* **2002**, *218*, 201.

81. (a) Sharon, N. *Chem. Rev.* **1998**, *98*, 637. (b) Balaram, P. *Pure and App. Chem.* **1992**, *64*, 1061. (c) Schneider, J. P.; Kelly, J. W. *Chem. Rev.* **1995**, *95*, 2169. (d) Balaram, P. *J. Peptide Res.* **1999**, *54*, 195.

82. (a) Venkatraman, J.; Shankaramma, S. C.; Balaram, P. *Chem. Rev.* ***2001***, *101*, 3131. (b) Smith, J. A.; Pease, L. G. *CRC Crit. Rev. Biochem.* **1980**, *8*, 314.

83. (a) Prabhakaran, E. N.; Rajesh, V.; Dubey, S.; Iqbal, J. *Tetrahedron lett.* **2001**, *42*, 339 (b) Lilley, D. M. J. *Biopolymers* **1998**, *48*, 101. (c) Blackburn, G. M.; Gait, M. J. *Nucleic Acids in Chemistry and Biology*, Oxford, **1996**. (d) Lilley, D. M. J. *The*

Formation of Alternative Structures in DNA, ed. S. M. Hecht, Oxford University Press, Oxford, **1996**

84. (a) Sinden, R. R.; Pearosn, C. E.; Potaman, V. N.; Ussery, W. D. *Adv. Genome Biol.* **1998**, *5A*, 1. (b) Alzeer, J.; Cai, C. Z.; Vasella, A. *Helv. Chim. Acta* **1995**, *78*, 242.
85. (a) Murty, K. V. S. N.; Vasella, A. *Helv. Chim. Acta* **2001**, *84*, 939. (b) Vijayakumar, E. K. S.; Balaram, P. *Biopolymers* **1983**, *22*, 2133.
86. Sudha, T. S.; Balaram, P. *Int. J. Peptide and Protein Res.* **1983**, *21*, 381.
87. (a) Karle, I. L.; Kaul, R.; Rao, R. B.; Raghothama, S.; Balaram, P. *J. Am. Chem. Soc.* **1997**, *119*, 12048. (b) Cheng, R. P.; Gellman, S. H.; de Grado, W. F. *Chem. Rev.* **2001**, *101*, 3219.
88. (a) Gellman, S. H. *Acc. Chem. Res.* **1998**, *31*, 173. (b) Seebach, D.; Matthews, J. L. *Chem. Commun.* **1997**, 2015. (c) Seebach, D.; Abele, S.; Gademann, K.; Jaun, B. *Angew. Chem. Int. Ed.* **1999**, *38*, 1595.
89. Hanessian, S.; Luo, X.; Schaum, R.; Michnick, S. *J. Am. Chem. Soc.* **1998**, *120*, 8569.
90. Daura, X.; Gademann, K.; Jaun, B.; Seebach, D.; van Gunsteren, W. F.; Mark, A. E. *Angew. Chem. Int. Ed.* **1999**, *38*, 236
91. Hintermann, T.; Gademann, K.; Jaun, B.; Seebach, D. *Helv. Chim. Acta* **1998**, *81*, 983.
92. Karle, I. L.; Pramanik, A.; Banerjee, A.; Bhattacharjya, S.; Balaram, P. *J. Am. Chem. Soc.* **1997**, *119*, 9087.
93. Belvis, L.; Gennari, C.; Mielgo, A.; Potenza, D.; Scolastic, C. *Eur. J. Org. Chem.* **1999,** 389.
94. (a) Jungheim, L. N.; Boyd, D. B.; Indelicato, J. M.; Pasini, C. E.; Preston, D. A.; Alborn, W. E. J. *J. Med. Chem.* **1991**, *34*, 1732. (b) Tsang, K. Y.; Diaz, H.; Graciani, N.; Kelly, J. W. *J. Am. Chem. Soc.* **1994**, *116*, 3988.
95. Chitnumsub, P.; Fiori, W. R.; Lashuel, H. A.; Kelly, J. W. *Bioorg. Med. Chem. lett.* **1999**, *7*, 39.
96. (a) Winningham, M. J.; Sogah, D. Y. *Macromolecules* **1997**, *30*, 862. (b) Jones, I. G.; Jones, W.; North, M. *J. Org. Chem.* **1998**, *63*, 1505.

97. (a) Ranganathan, D.; Haridas, V.; Kurur, S.; Thomas, A.; Madhusudhan, K. P.; Nagaraj, R.; Kunwar, A. C.; Sarma, A. V. S.; Karle, I. L. *J. Am. Chem. Soc.* **1998**, *120*, 8448. (b) Wipf, P.; Henniger, T. C.; Geib, S. J. *J. Org. Chem.* **1998**, *63*, 6088.

98. (a) Gardner, R. R.; Liang, G. B.; Gellaman, S. H. *J. Am. Chem. Soc.* **1999**, *121*, 1806. (b) Nowick, J. S. *Acc. Chem. Res.* **1999**, *32*, 287.

99. (a) Wilson, M. E.; Nowick, J. S. *Tetrahedron lett.* **1998**, *39*, 6613. (b) Sessler, J. L.; Wang, R. *J. Am. Chem. Soc.* **1996**, *118*, 980.

100. Altona, C.; Sundaralingam, M. *J. Am. Chem. Soc.* **1972**, *94*, 8205.

101. (a) Speziale, V.; Roussel, J.; Lattes, A. *J. Heterocycl. Chem.* **1974**, *11*, 771. (b) Vincens, M.; Dumont, C.; Vidal, M. *Can. J. Chem.* **1979**, *57*, 2314. (c) Gurjar, M. K.; Mohapatra, S.; Phalgune, U. D.; Puranik, V. G.; Mohapatra, D. K. *Tetrahedron Lett.* **2004**, *45*, 7899. (d) Sih, J. C.; Graber, D. R. *J. Org. Chem.* **1982**, *47*, 4919.

102. Cambridge Crystallographic Data Center reference no. **CCDC 244671**.

Spectral Data

Proton magnetic resonance spectra were recorded on AC-200 MHz, MSL-300 MHz and Bruker-500 MHz spectrometer using tetra methyl silane (TMS) as an internal standard. Chemical shifts have been expressed in ppm units downfield from TMS.

^{13}C Nuclear magnetic spectra were recorded on AC-50 MHz, MSL-75 MHz and Bruker-125 MHz spectrometer.

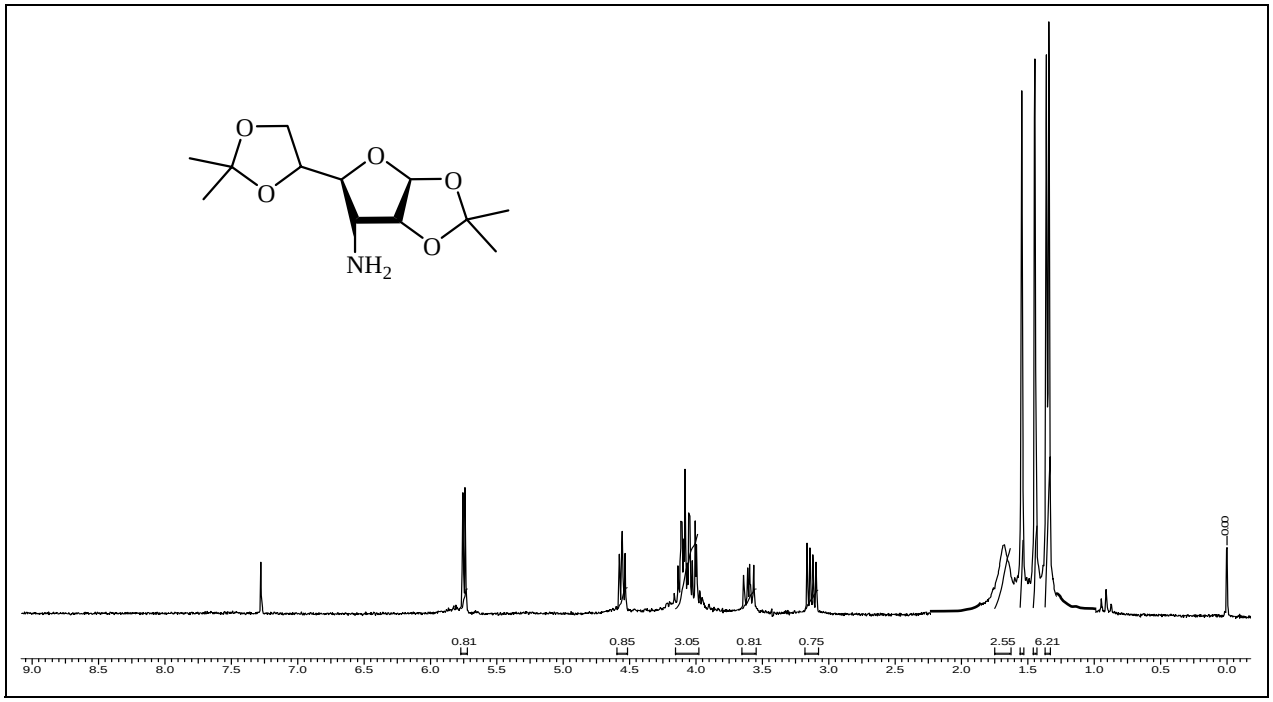

Spectral data for Compound no. 25

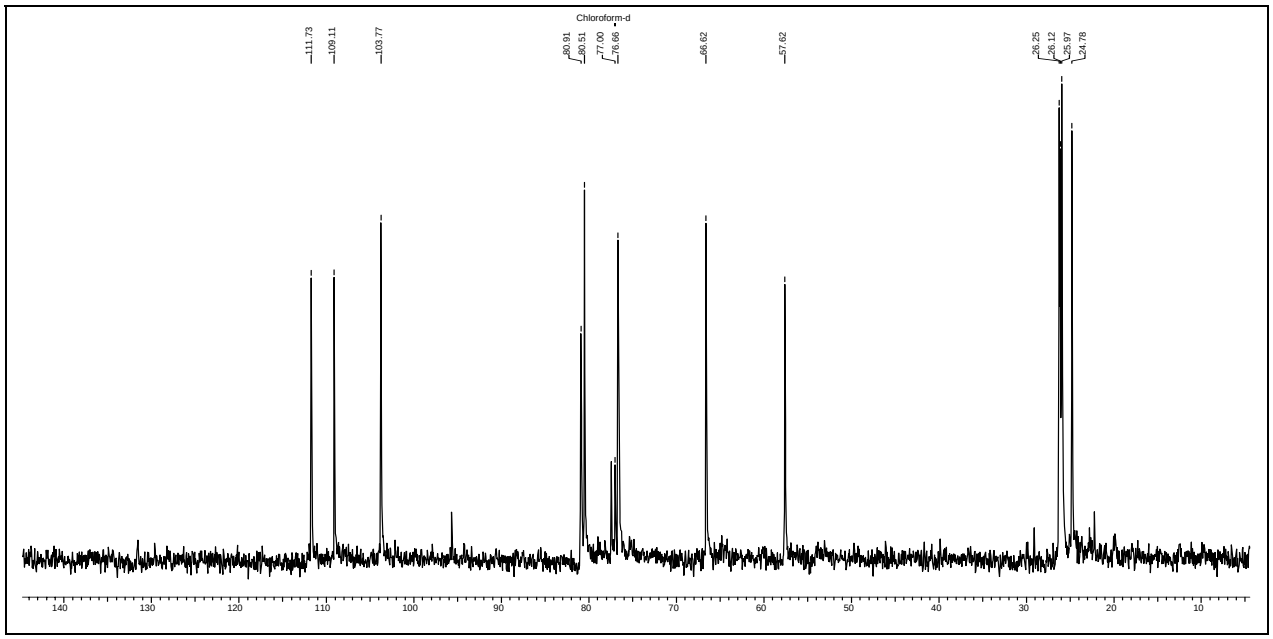

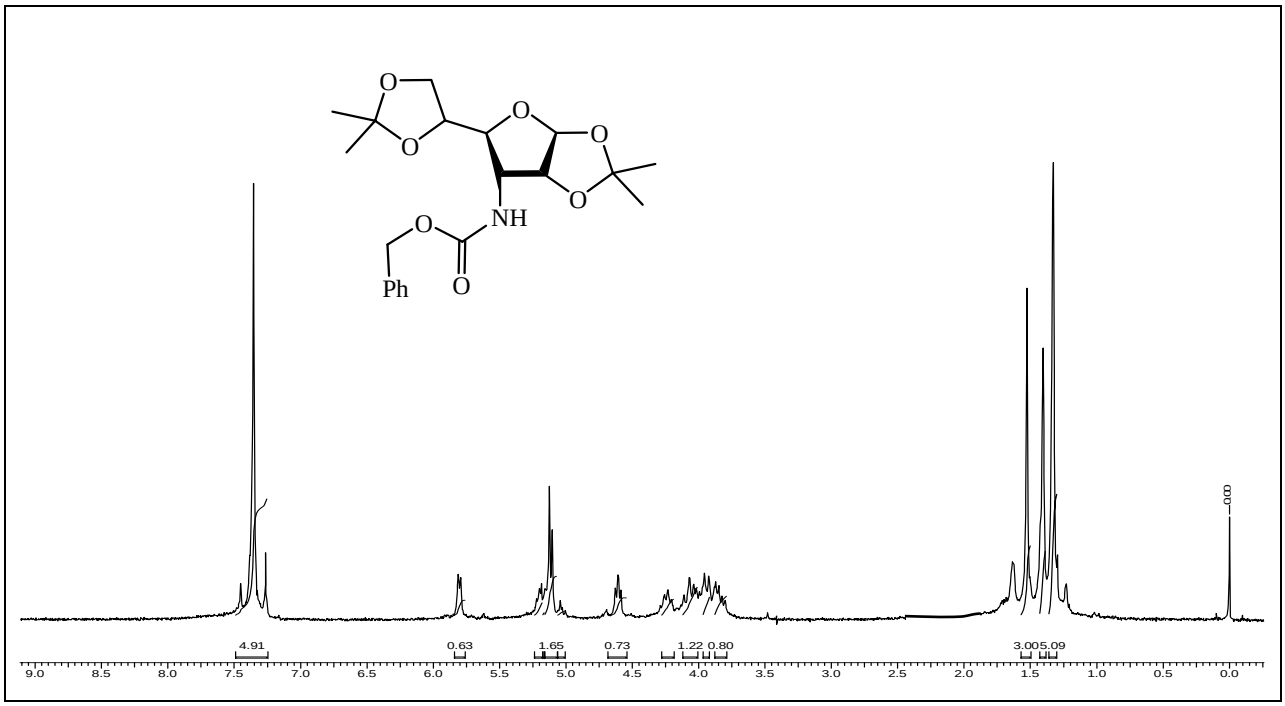

Spectral data for Compound no. 23

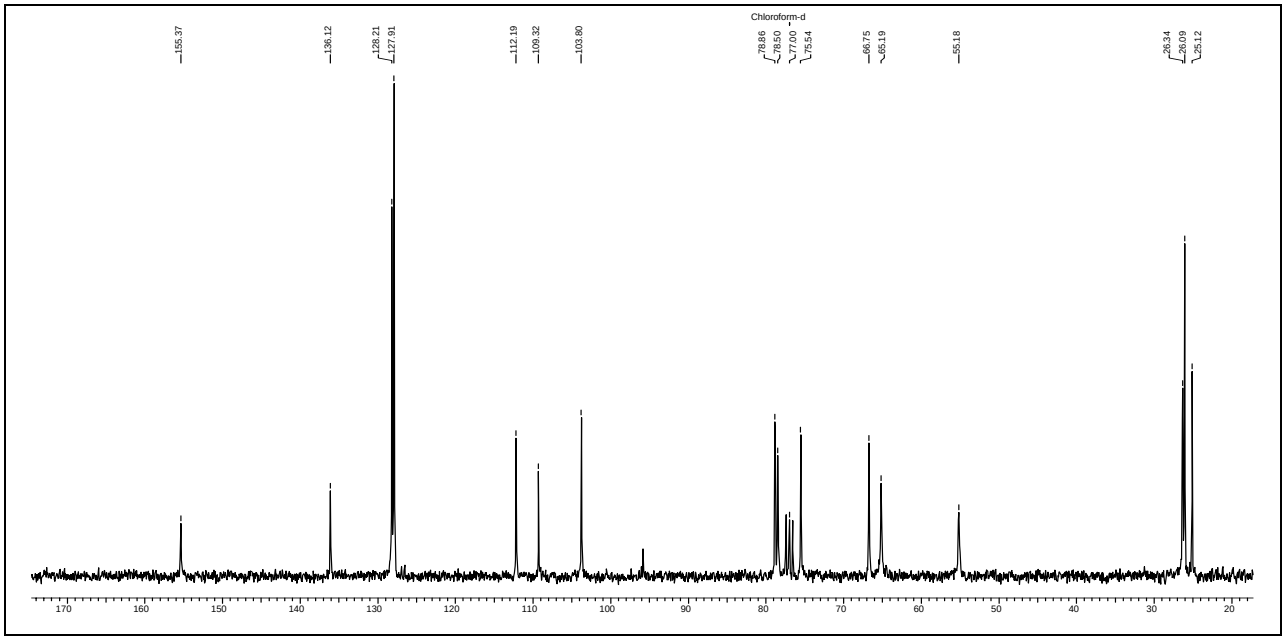

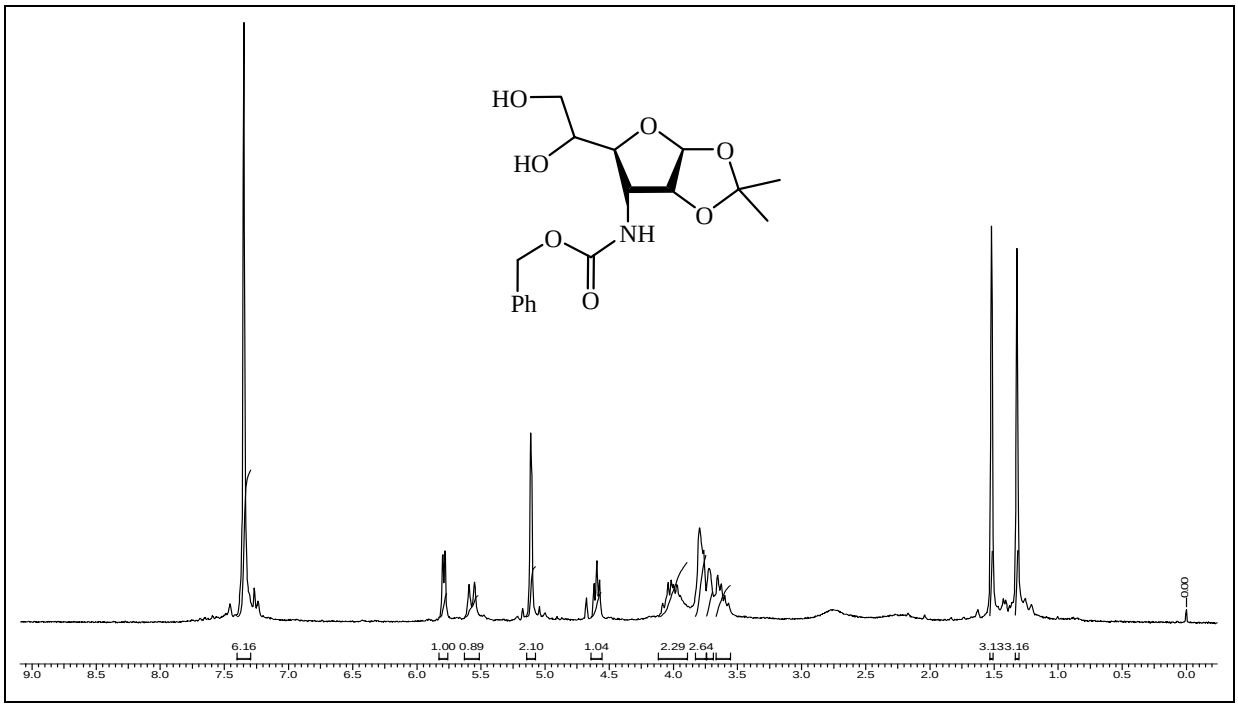

Spectral data for Compound no. 21

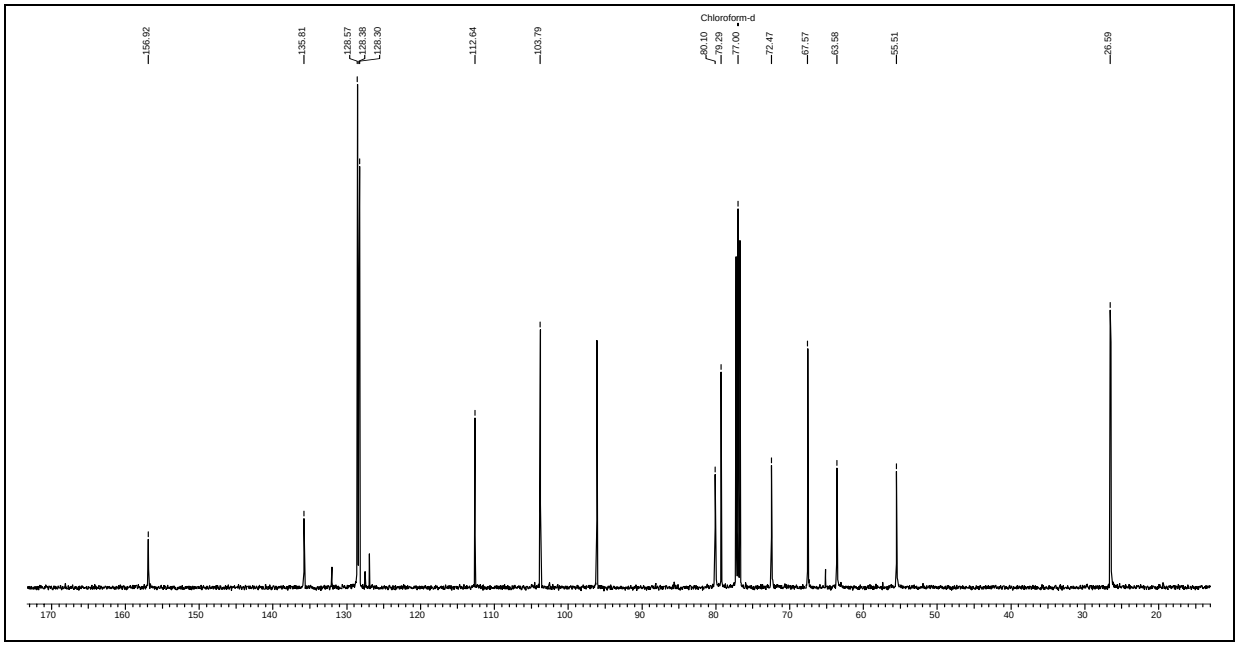

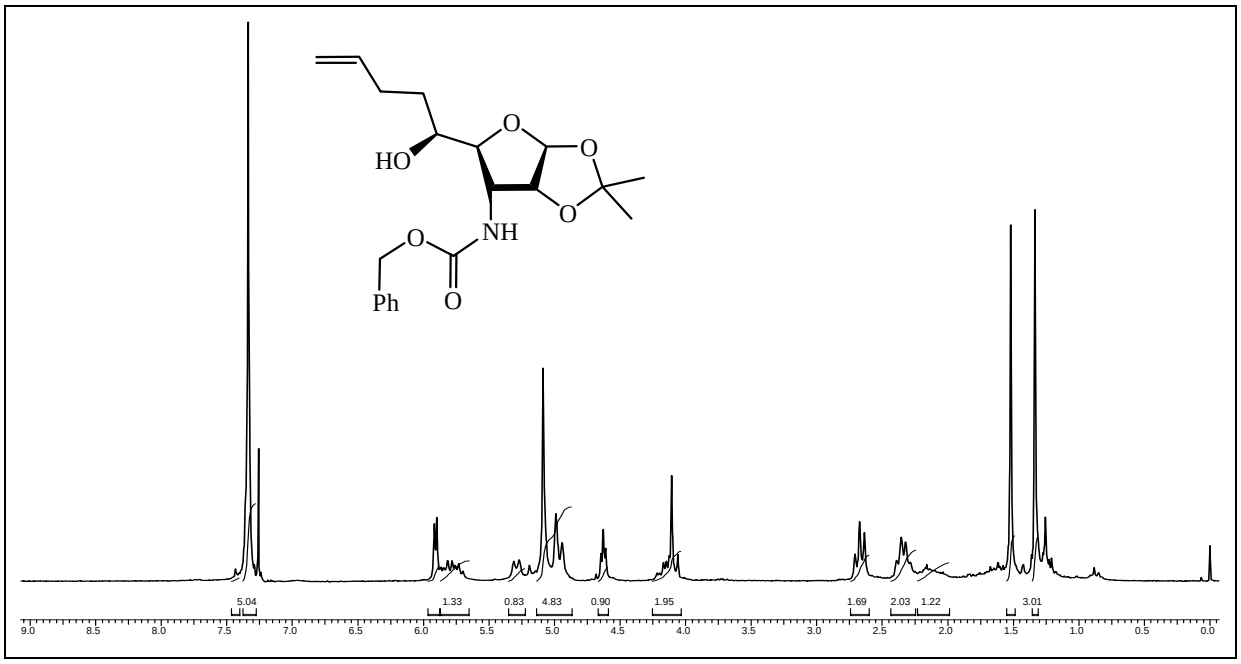

Spectral data for Compound no. 17

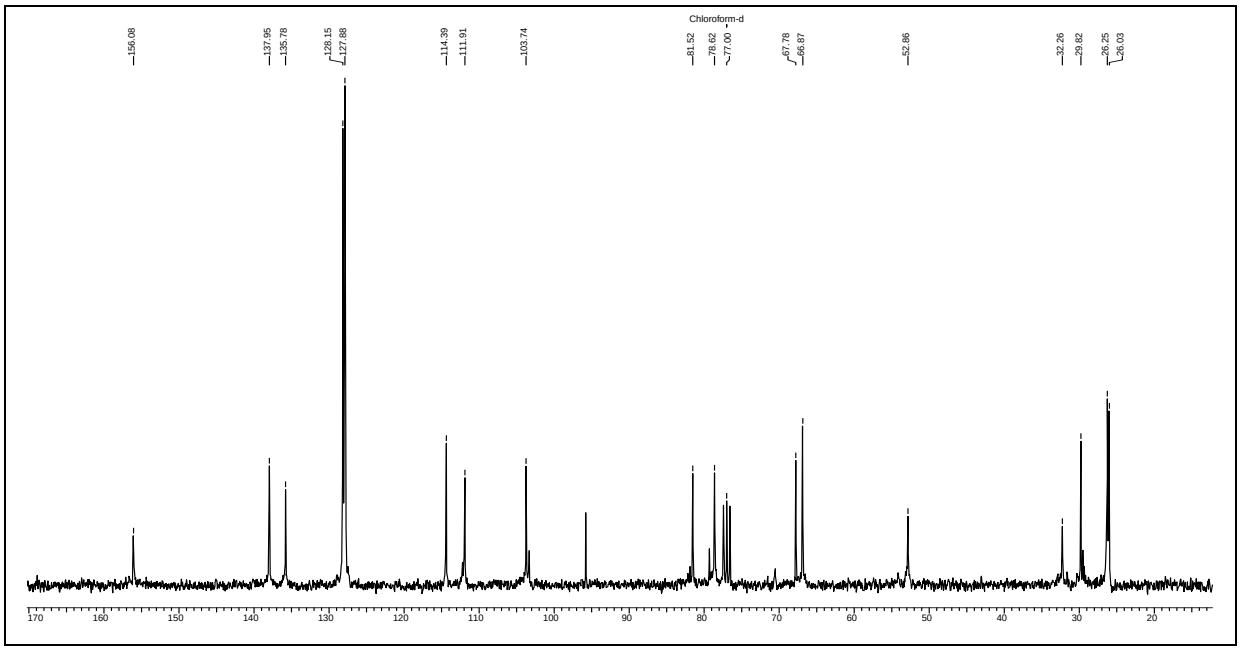

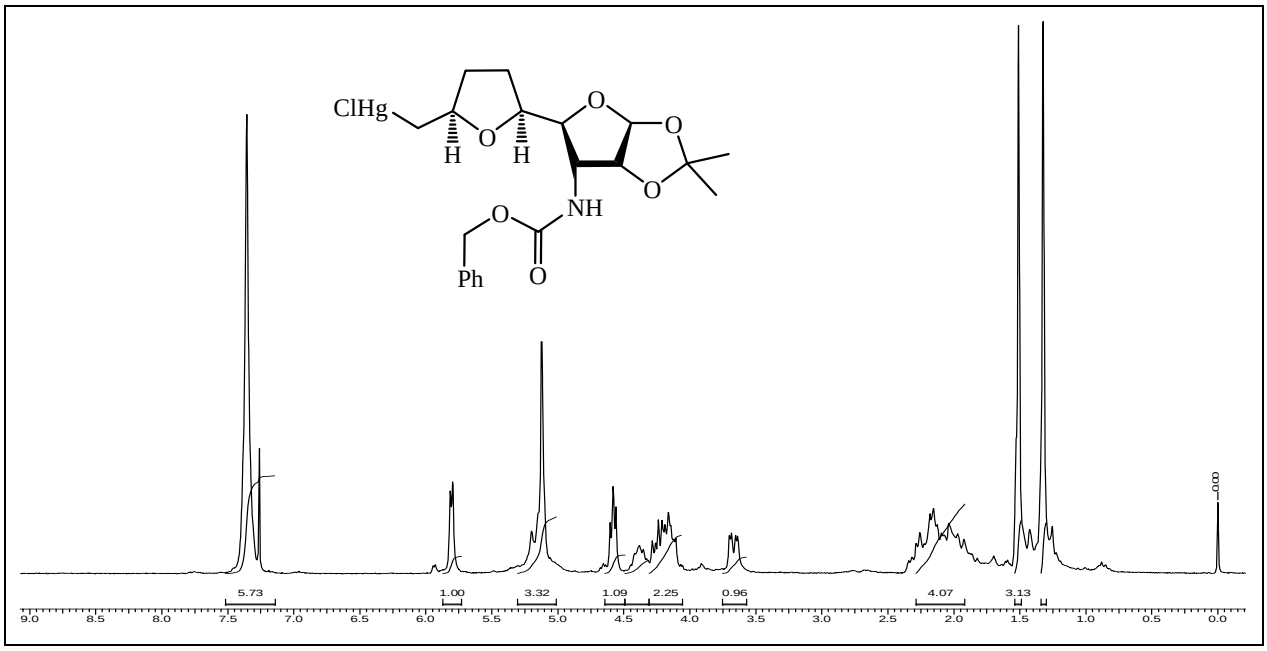

Spectral data for Compound no. 15

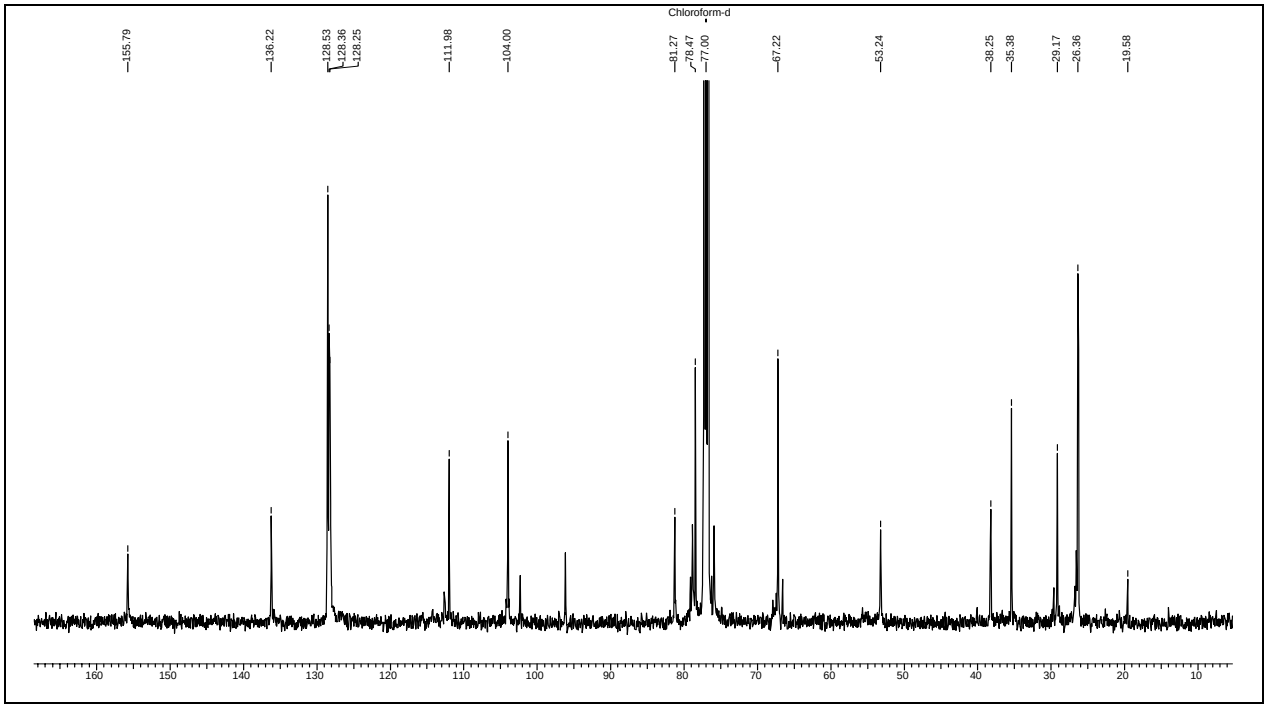

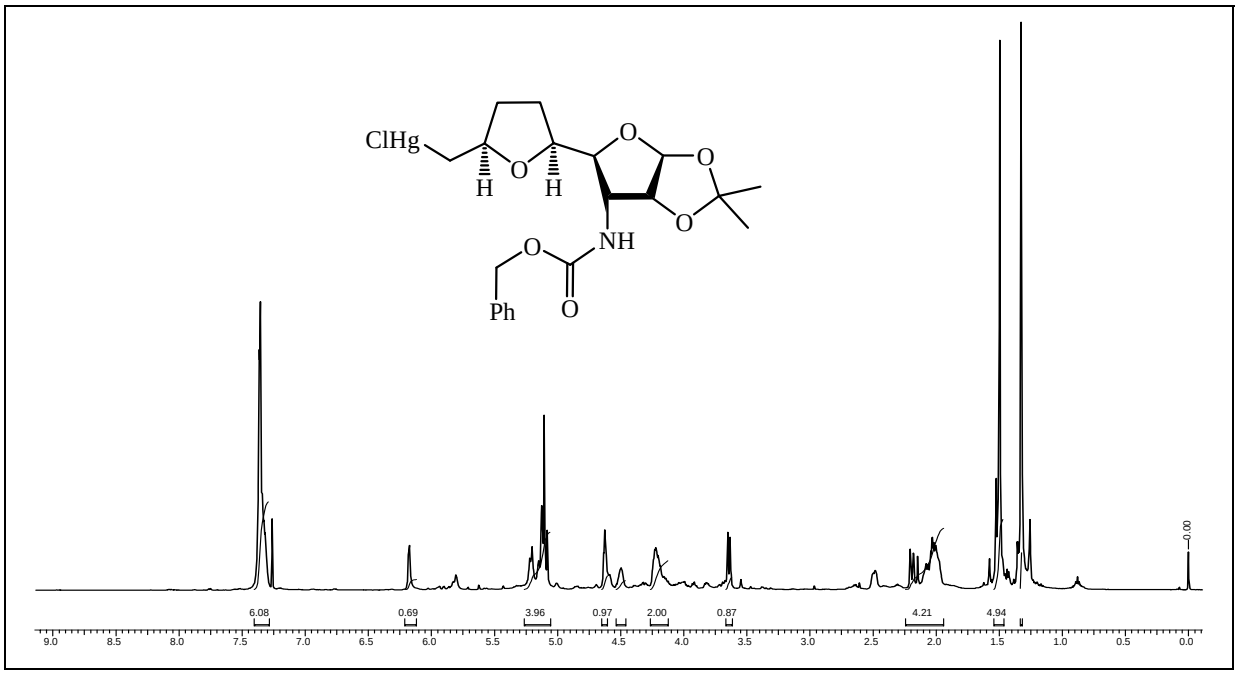

Spectral data for Compound no. 15a

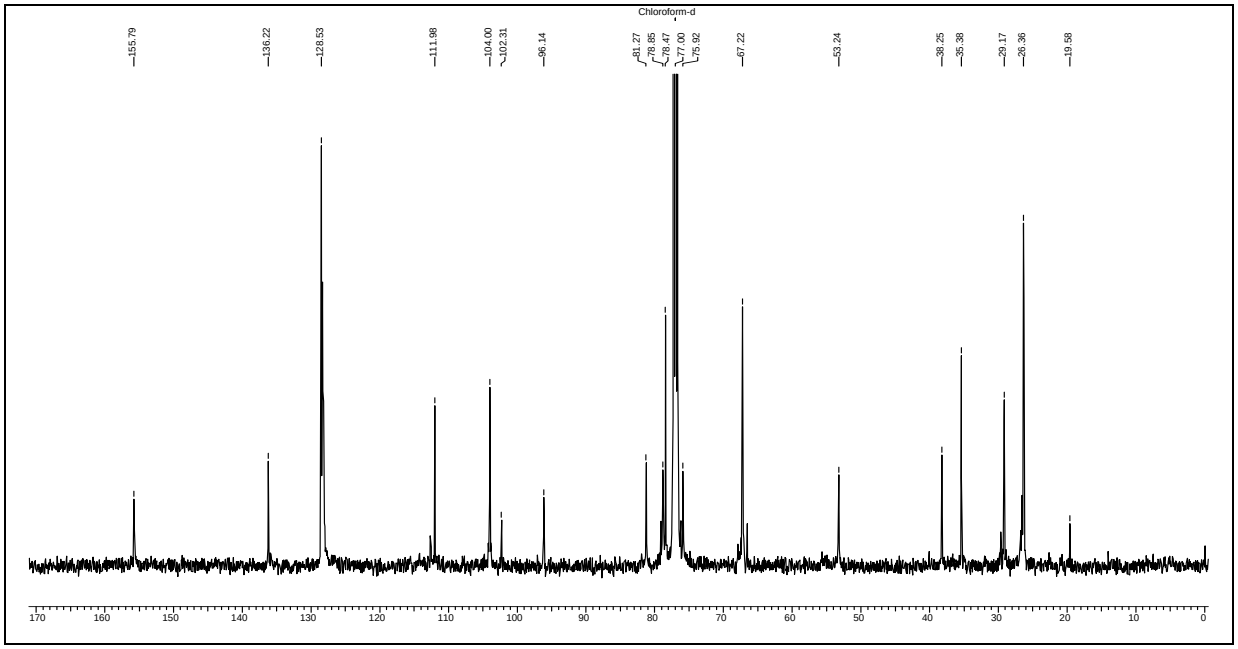

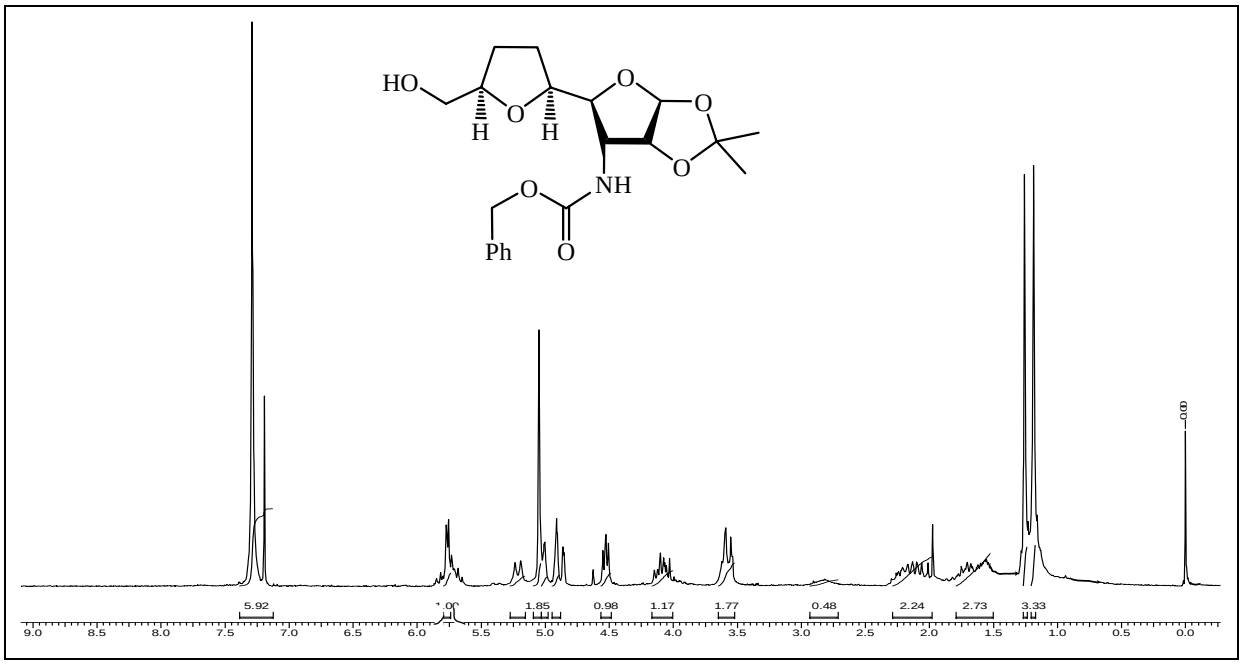

Spectral data for Compound no. 13

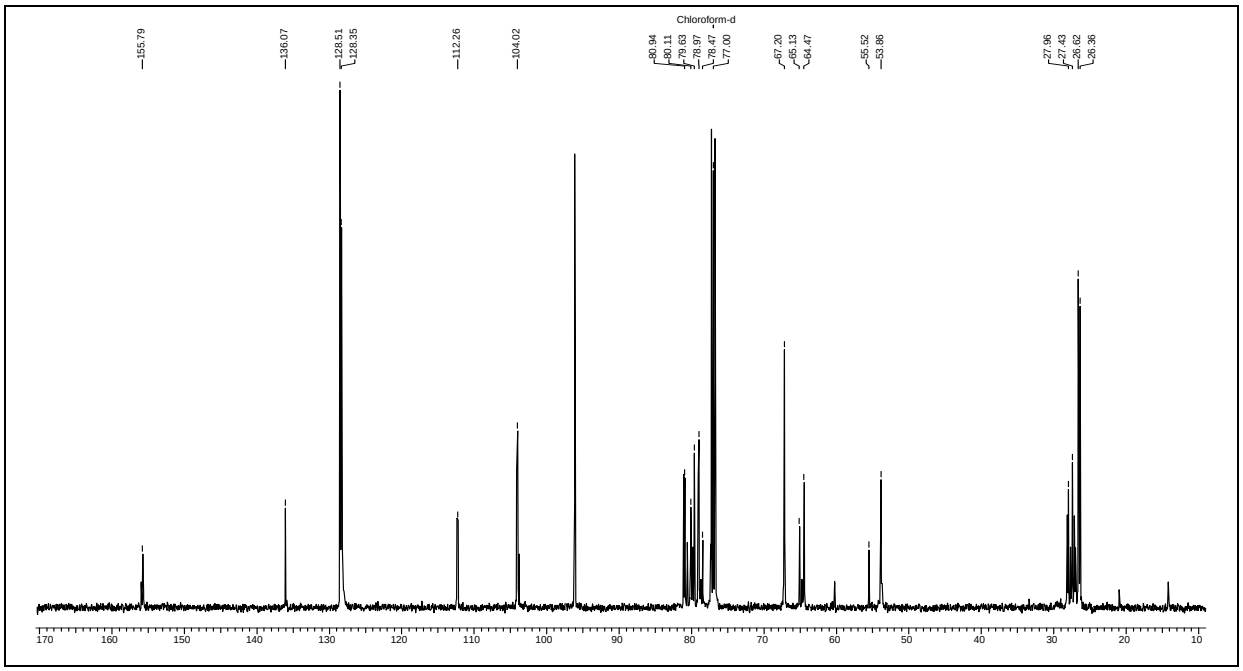

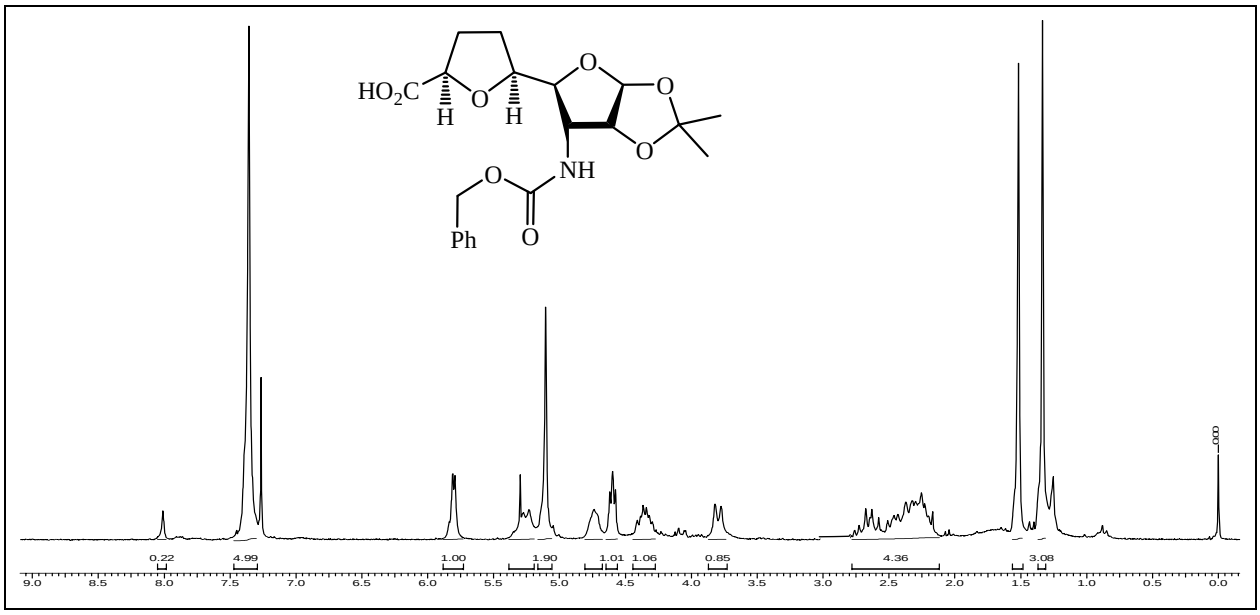

Spectral data for Compound no. 9

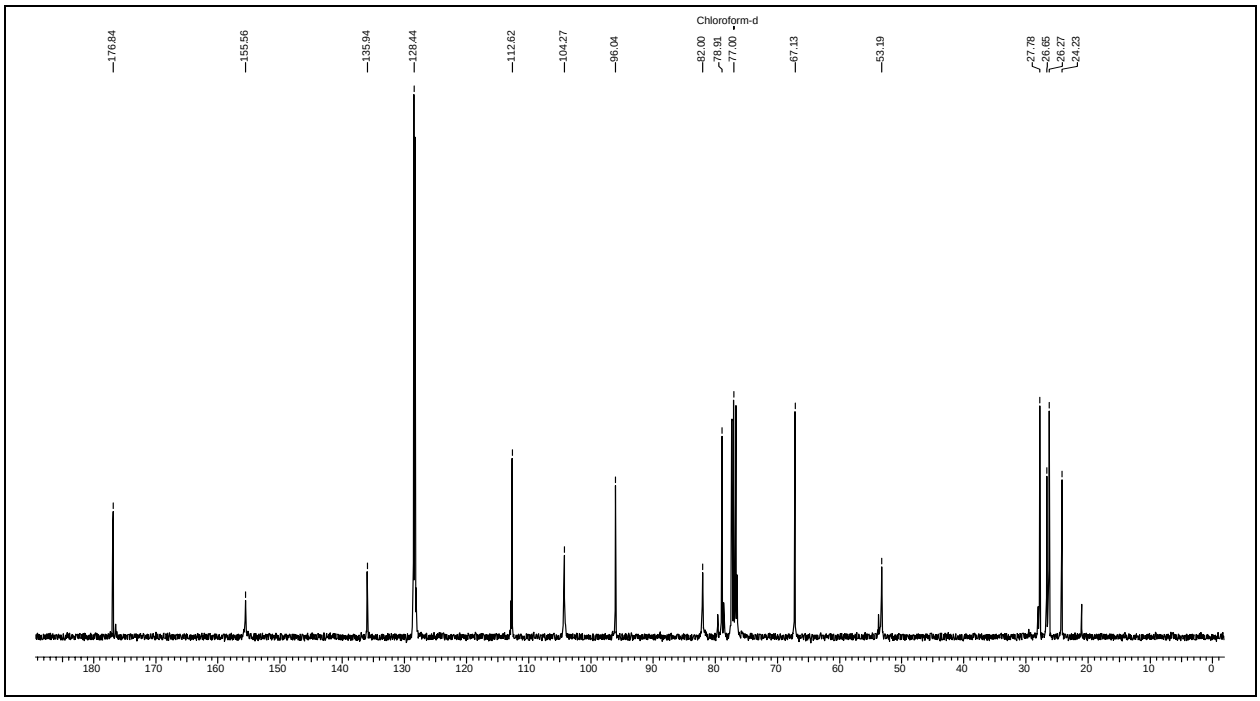

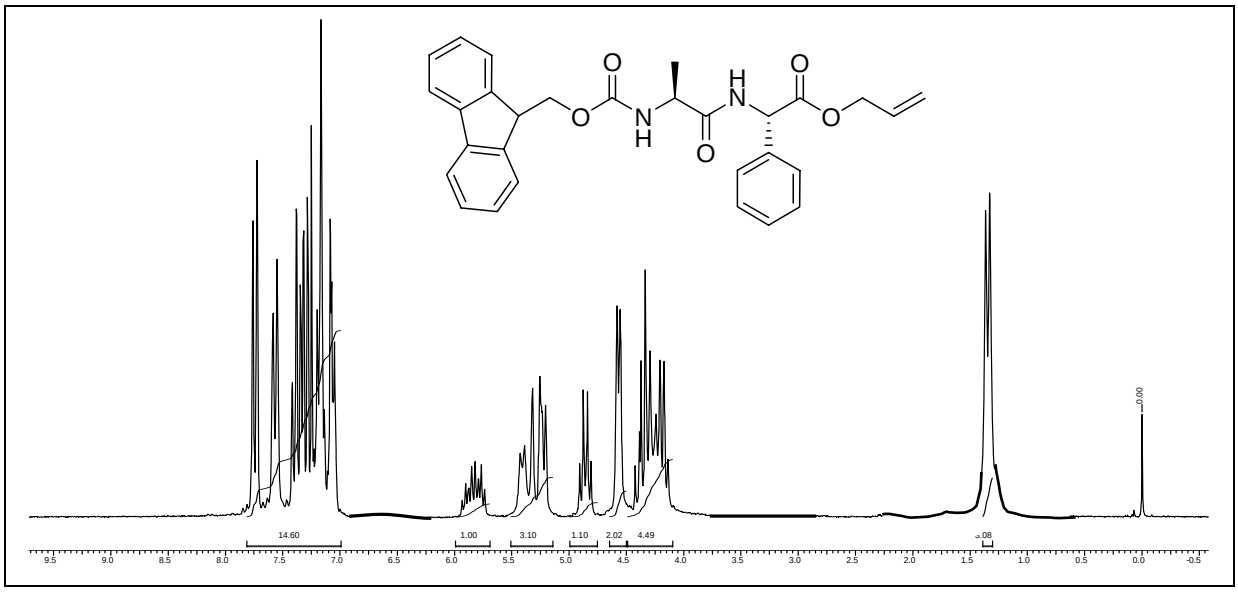

Spectral data for Compound no. 29

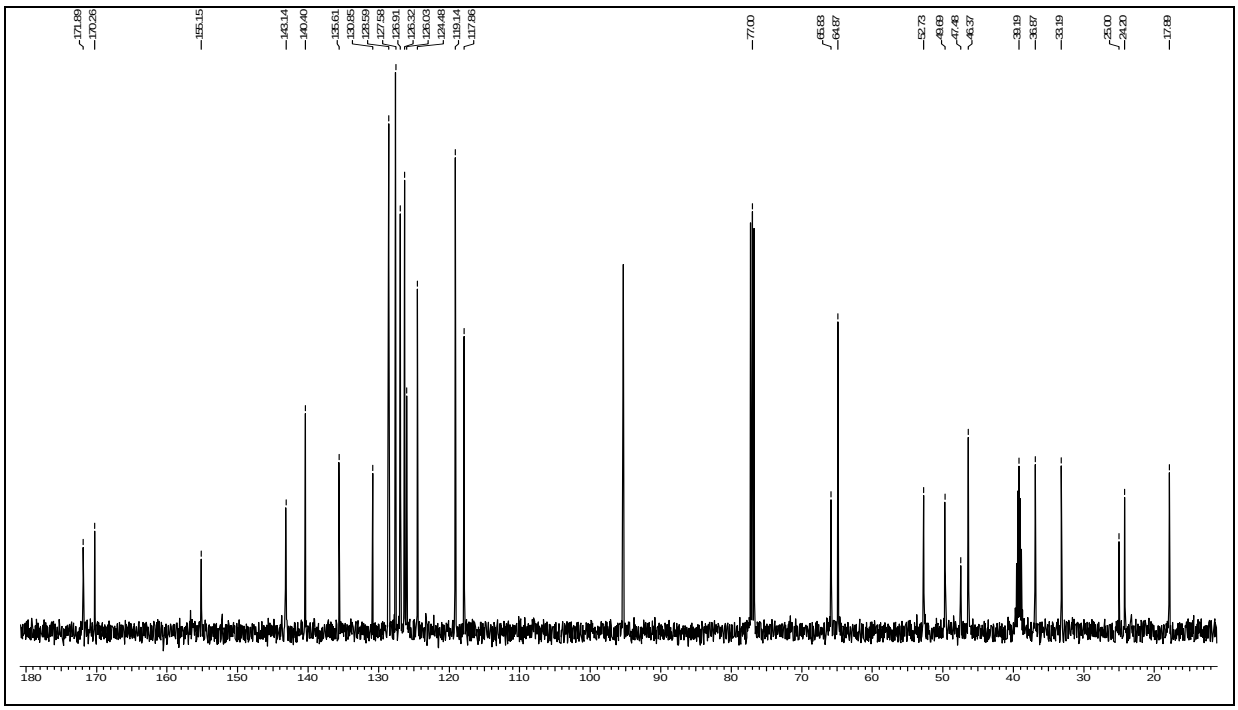

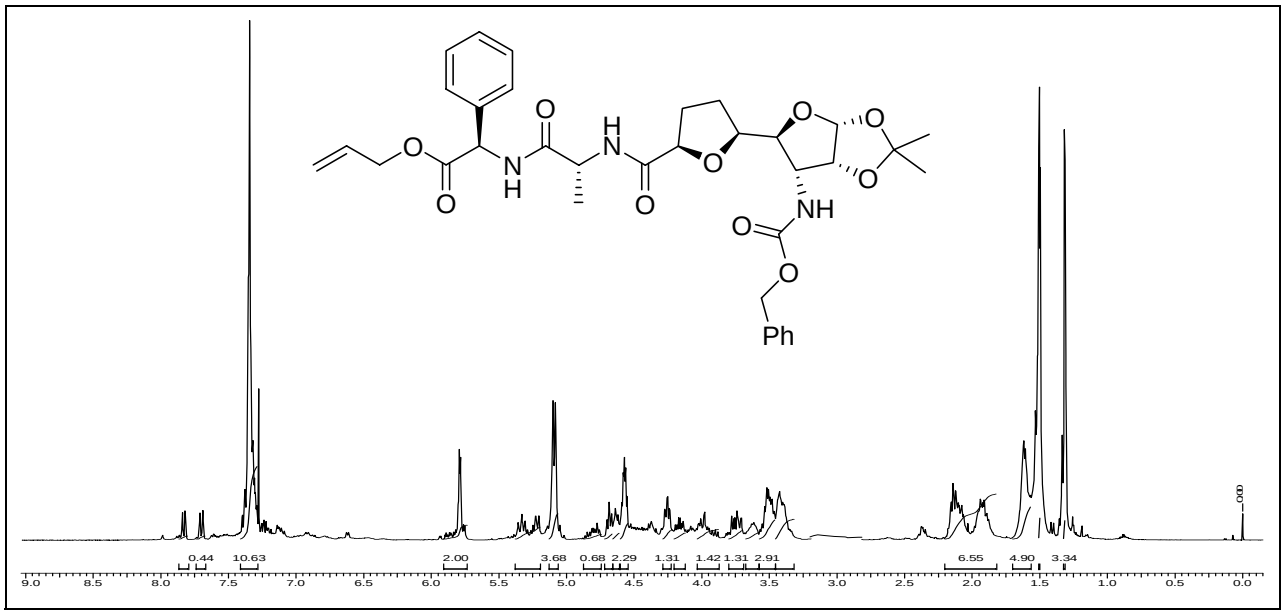

Spectral data for Compound no. 28

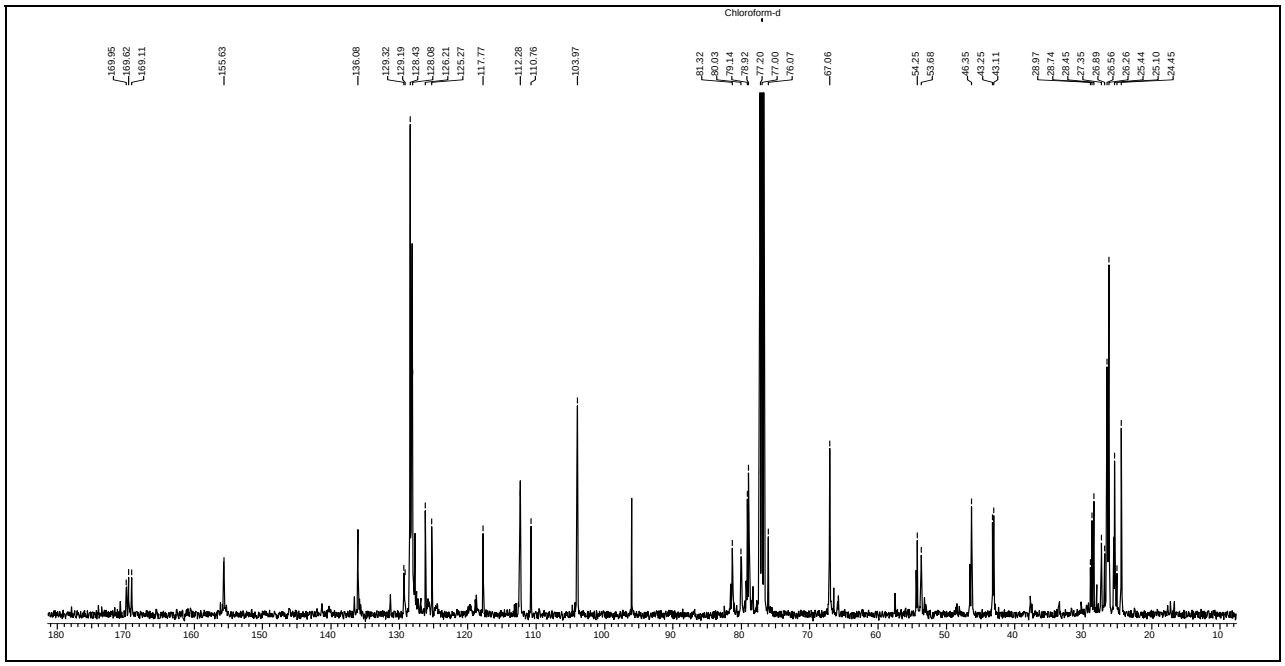

CHAPTER III:

HYDROGEN BONDING IN VARIOUS HEXOSE SUGAR 3-C ALKYNOLS

Introduction

The hydrogen bond is a unique phenomenon in structural chemistry and biology. Its fundamental importance lies in its role in molecular association its functional importance stems from both thermodynamics and kinetic reasons.[1] The "hydrogen bond" or "hydrogen bridge" concept has proved to be one of the most useful structural concepts in modern science. The properties of substances containing hydrogen bonds depend on the strength, symmetry, and polarity of these bonds. These characteristics, in turn, are related to the effective electro-negativities of the bridgehead atoms, the distance between these atoms, and the degree of coupling with other hydrogen bonds. Symmetrical hydrogen bonds exist in the FHF^- and $H_50_2^+$ ions and in some acidic compounds. Coupled hydrogen bond systems exist, for example, in ice, liquid water, hydroquinone clathrates, starch, cellulose, polypeptides, nucleic acids and silicate hydrates.

Fig. 1 Hydrogen bonding observed in various simple compounds

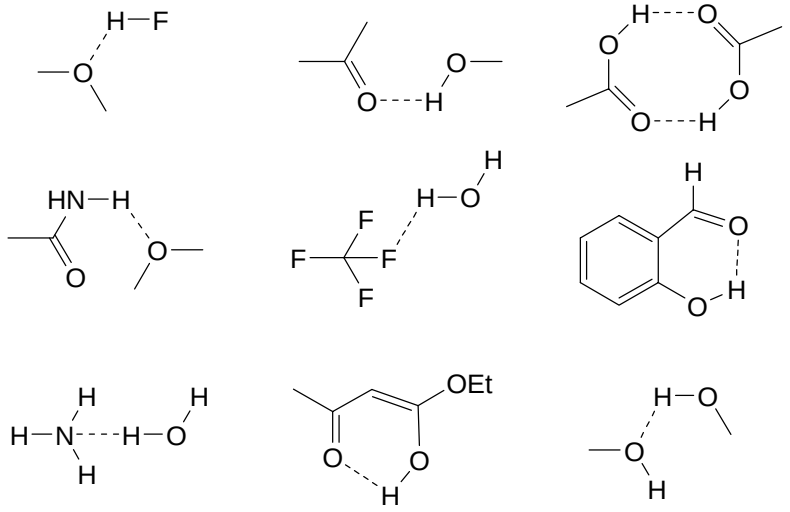

A hydrogen bond is a bond between a functional group A-H and an atom or group of atoms B in the same or a different molecule[1k]. Hydrogen bonds are formed when A is carbon, phosphorous, sulfur, selenium, oxygen, nitrogen, or halogens and when B is oxygen, nitrogen, or fluorine etc. The oxygen may be singly or doubly bonded and the nitrogen

singly, doubly, or triply bonded. The bonds are usually represented by dotted lines, as shown in fig. 1.

The criteria for the existence of H bonds are somewhat more clear cut than for any other intermolecular interactions[2]. No single criterion or single physical manifestations, however, can establish the presence of H bonding in a given system beyond any reasonable doubt. Some convenient operational criteria for the existence of H bonding are listed below

1. Hydrogen bonding occurs between a proton donor group A – H and a proton acceptor group B, where A as well as B are electronegative atom., O, N, S, halogens or C. Generally, an H bond can be characterized as a proton shared by two lone electron pairs.
2. Hydrogen bonding is a distinctly directional and specific interaction. It is more localized than any other type of weak intermolecular interaction, where the acceptor group is a π-electron orbital, H bonding is probably no more directed than a typical charge-transfer complex such as that between iodine and benzene. Hydrogen bonds are linear but appreciable variation in the angel can occur.
3. The total H bond length is equal to or less than the sum of the van der Waals radii of atoms A and B, i.e. the total bond length construction caused by H bond formation is equal to or is greater than twice the van der Waals radius of the hydrogen atom. In molecular crystals, where specific directional interactions between molecules are absent, the molecules are packed together so that the distance of closest approach for a given pair of atoms are nearly constant in going from one crystal/compound to another.
4. The enthalpy of H bonds generally falls in the range of 1 to 10 kcal/mol. Intermolecular interactions other than H bonding also fall within this range.
5. Hydrogen bonding is an association phenomenon. It causes a decrease in the total number of free molecules and an increase in the average molecular weight (except in the case of intramolecular H bonding)

In H bonding a specific covalent A – H group interacts with a specific acceptor site. The A – H bond is hereby weakened but not broken, and the properties of the acceptor group are also affected. When the covalent A – H bond is broken to form the anion A^- and the

protonated base $H - B^+$ we no longer have H bonding but an acid base reaction with proton transfer.

Hydrogen bonds can exist in the solid and liquid phases and in solution[3]. Many organic reactions that can be done in aqueous media, is due, in part, to the hydrogen-bonding nature of aqueous media[4]. Even in the gas phase, compounds that form particularly strong hydrogen bonds may still be associated[5]. Acetic acid, for example, exists in the gas phase as a dimer, as shown above, except at very low pressures[6]. In solution and in the liquid phase, hydrogen bonds rapidly form and break. The mean lifetime of the $NH_3 \cdots H_2O$ bond is $2X10^{-12}$ s[7]. Except for a few very strong hydrogen bonds[8], such as the $FH \cdots F^-$ bond, which has energy of ~50kcal mol^{-1} (210kJmol^{-1}), the strongest hydrogen bonds are the $FH \cdots F$ bond and the bonds connecting one carboxylic acid with another. The energies of these bonds are in the range of 6 – 8 kcal mol^{-1} (25-30 kJ mol^{-1}) (for carboxylic acids, this refers to the energy of each bond). In general, short contact hydrogen bonds between fluorine and HO or NH are rare[9]. Other OH-O and NH-N bonds have energies of 3 - 6 kcal mol^{-1} (12-25 kJ mol^{-1}). The intramolecular $O\text{-}H \cdots N$ hydrogen bond in hydroxyl amines is also rather strong[10]. To a first approximation, the strength of hydrogen bonds increases with increasing acidity of A-H and basicity of B, but the parallel is far from exact[11].

A quantitative measure of the strengths of hydrogen bonds has been established, involving the use of an α scale to represent hydrogen-bond donor acidities and a β scale for hydrogen-bond acceptor basicities.[12] The use of the β scale, along with another parameter, ξ, allows hydrogen-bond basicities to be related to proton-transfer basicities (pK values).[13] A database has been developed to locate all possible occurrences of bimolecular cyclic hydrogen bond motifs in the Cambridge Structural Database[14], and donor-acceptor as well as polarity parameters have been calculated for hydrogen-bonding solvents[15]. When two compounds whose molecules form hydrogen bonds with each other are both dissolved in water, the hydrogen bond between the two molecules is usually greatly weakened or completely removed[16], because the molecules generally form hydrogen bonds with the water molecules rather than with each other, especially since the water molecules are present in such great numbers. In amides, the oxygen atom is the preferred site of protonation or complexation with water.[17]

Many studies have been made of the geometry of hydrogen bonds[18], and the evidence shows that in most (though not all) cases the hydrogen is on or near the straight line formed by A and B[19]. This is true both in the solid state (where X-ray crystallography and neutron diffraction have been used to determine structures),[20] and in solution.[21] It is significant that the vast majority of intramolecular hydrogen bonding occurs where six-membered rings (counting the hydrogen as one of the six) can be formed, in which linearity of the hydrogen bond is geometrically favorable, while five-membered rings, where linearity is usually not favored (though it is known), are much rarer. Except for the special case of FH—F^- bonds, the hydrogen is not equidistant between A and B. For example, in ice the O-H distance is 0.97 Å, while the H···O distance is 1.79 Å.[22] The hydrogen bond in the enol of malonaldehdye, in organic solvents, is asymmetric with the hydrogen atom closer to the basic oxygen atom.[23]

Fig. 2 Various examples showing three center two electron hydrogen bonding

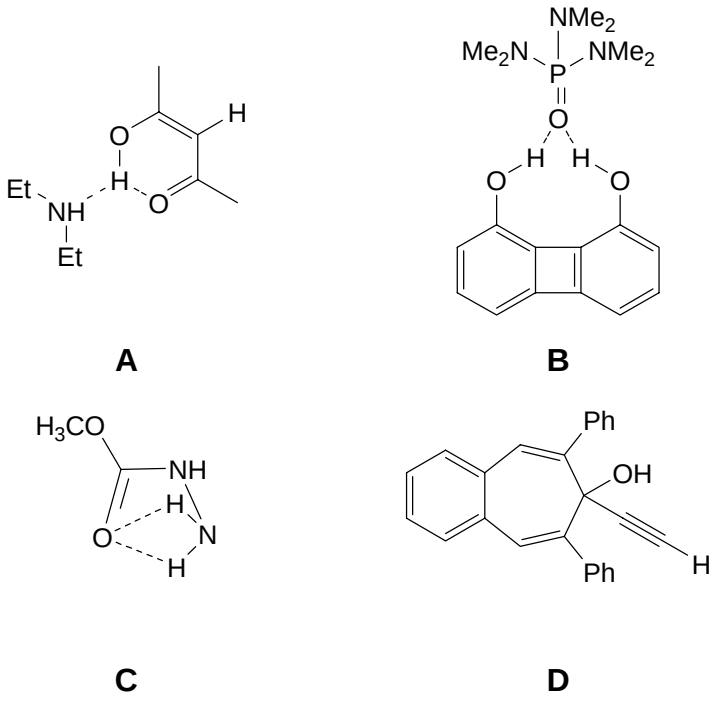

In certain cases, X-ray crystallography has shown that a single *H-A* can form simultaneous hydrogen bonds[24] with two *B* atoms (bifurcated or three-center hydrogen bonds). As example an adduct **A** is formed from pentane-2,4-dione (in its enol form) and

diethylamine, in which the O-H hydrogen simultaneously bonds to O and N (the N-H hydrogen forms a hydrogen bond with the O of another pentane-2,4-dione molecule).[25] On the other hand, in adduct **B** formed from 1,8-biphenylenediol and hexamethyl phosphoramide (HMPA), the *B* atom (in this case oxygen) forms simultaneous hydrogen bonds with two *A-H* hydrogens.[26] Another such case is found in methyl hydrazine carboxylate **C**.[27] There is recent evidence, however, that symmetrical hydrogen bonds to carboxylates should be regarded as two-center rather than three-center hydrogen bonds since the criteria traditionally used to infer three-center hydrogen bonding are inadequate for carboxylates.[28] There is also an example of cooperative hydrogen bonding in crystalline 2-ethynyl-6,8-diphenyl-7H-benzocyclohepten-7-ol **D**.[29]

The first attempts to understand the hydrogen bond used an electrostatic model. Pauling[30] argued that hydrogen can participate in only one covalent bond, and that a second "hydrogen bond" must be due to an ionic interaction between the partially positive hydrogen and lone pair of the neighboring molecule. Simple electrostatic calculations of the hydrogen-bond energies were carried out by a number of workers[31]. Among them Lennard-Jones and Pople[32], Using a four-electron point charge model and placing the charges to fit the experimental dipole moment of water, these workers found an H-bond energy of 6 kcal/mol. It should be noted that, in disagreement with the view expressed by Pimentel[31a] and Bratoz[31b], the lack of correlation of H-bond energy with dipole moment of the proton acceptor is not a conclusive argument against electrostatic theories of the H bond. At the distances where H bonding occurs, the dipole moment approximation is a poor one and higher multipoles must be considered. 1,4-Dioxane forms strong hydrogen bonds because each oxygen is a good source of electron density (despite an average dipole moment of 0.4 D). The fact that amines are better proton acceptors than nitriles can be rationallzed by arguing that the electrons in the amine (sp^3) lone pair extend further toward the proton donor than those in the nitrile (sp). Arguments against an exclusively electrostatic model of the hydrogen bond have been given by many authors, but the strongest arguments against the electrostatic model are as follows.

- There is certainly charge redistribution upon H-bond formation, as evidenced by the infrared spectral intensity changes upon bond formation.

- At the H-bonded distance between the two fragments, there must be considerable closed-shell (exclusion principle) repulsion between the two fragments.

Inclusion of this repulsion energy nullifies the good agreement between the H-bond experimental energy and that calculated by the simple electrostatic models. This is not to say that electrostatic calculations cannot be useful in discussing certain aspects of H bonding; for example, Bader[33] was able to rationalize X-H force constant shifts in H-bonded systems with an electrostatic model.

Fig. 3 Different types of hydrogen bonding patterns observed in diacetamide crystals

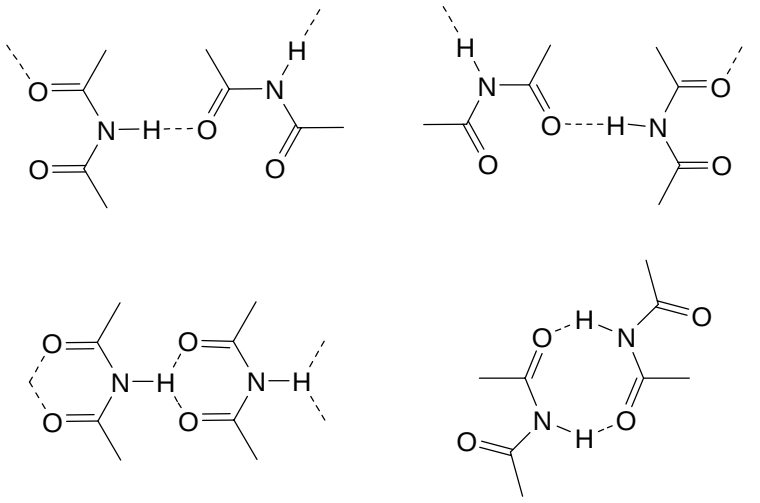

Various efforts to characterize hydrogen bonding have proliferated[34] since its discovery. Wells was one of the first to recognize the importance of hydrogen bond patterns, independent of the geometry or of spectroscopic or thermal properties of the bonds[35]. This perspective provided new insights into the role of hydrogen bonds in controlling the structures of ensembles of molecules. This topological point of view allowed one to characterize subsets of crystal structures or arrays, namely, the hydrogen-bonded subset.

To attempt to estimate all the Contributions to the H-bond energy, Coulson and Danielson[36] and Tsubomura[37] developed an empirical valence bond approach to determine the various contributions. A similar model, emphasizing the charge-transfer aspects of H bonding, was developed by Puranik and Kumar[38] and Bratoz[31b]. The conclusion of the valence bond theories was that 'At long A···B distances the H-bond energy is mainly

electrostatic, but at shorter distances repulsion and delocalization (intra- and intermolecular) come into play'.

Benzoic acids form cyclic dimers. Salicylic acid has an intramolecular hydrogen bond[39]. These hydrogen-bond patterns seem obvious because they satisfy the chemical criteria of pairing a somewhat acidic hydrogen with an electronegative atom, and because spectroscopic and crystallographic studies have confirmed our chemical intuition about how and when hydrogen bonds should form in these and in similar frequently studied structures, Etter[40] expanded on Donohue's rule that in the solid state all available acidic protons participate in the hydrogen bonding. He studied diacetamide crystals. He pointed out that in hydrogen bonding acceptors are utilized to the extent that hydrogen bond donors and that in a crystal containing multiple donors and acceptors a bond is preferably formed between the best donor (acid) and the best acceptor (base) as the energy of hydrogen bond is far greater than van der Waal's interactions. Hydrogen bonds in molecular crystals are structure determining.

The dominance of the distribution for organic crystals by a few space groups was clear from the beginning groups accounted for 44% of the organic structures[41]. The only symmetry elements present in these dominant space groups were inversion centers, two fold skew axes (a rotation about an axis, followed by a translation along the direction of the axis) and glide planes (a reflection in a plane, followed by a translation parallel with that plane). The space group of a crystal is a mathematical description of the symmetry inherent in the structure. The word 'group' in the name comes from the mathematical notion of a group, which is used to build the set of space groups. Nowacki considered the zigzag chains of molecules produced by the screw and glide operations. Macky[42] observed that if M_t was the number of different space groups that occurred at least t times, then $1/M_t$ varied almost linearly with t. he used this observation to estimate the number of unobserved space groups and hence the total number of possible space groups and he concluded that as the number of unobserved space groups agreed with the statistical estimate their absence is due to chance and not to the intrinsic impossibility for physical reasons of the occurrence of certain space groups. The hydrogen bonding motifs displayed by mono alcohols in many systems excluding carbohydrates were described briefly by Bernstein *et.al*[43] and more comprehensively in terms of graph set theory by Brock and Duncan[44].

These qualitative, valence bond based theories, put forth at a time when more precise, non empirical calculations could not be carried out, constituted a very important step forward toward rationalization of many of the phenomena associated with H bonding. They did not, however, lend themselves easily to more quantitative calculations or to an understanding of why certain H bonds are stronger than others.

Significance of various notations used in X-Ray Crystallography[44d]

The set of molecules to be analyzed is called an array. Some or all of the molecules in the array are associated through hydrogen bonds. This array need not be in a crystal structure, but regularly repeating sets such as those found in crystal structures are particularly suitable for graph-set assignments. The geometry of a hydrogen bond is not critical in these analyses, so even a hand-drawn picture of a hypothetical set of molecules is sufficient for making graph-set assignments.

A network is a subset of an array in which each molecule in the network is connected to every other molecule by at least one hydrogen-bonded pathway. A network contains any number of different kinds of hydrogen bonds. Our challenge is to define the morphology of this network.

A motif is a special type of network. It is a hydrogen-bonded set in which only one type of hydrogen bond is present. A hydrogen-bond type is defined by the chemical nature of the proton donor and acceptor used in the hydrogen bond. Thus, a hydrogen bond between a phenol and a nitro group would be a different type from a hydrogen bond between a phenol and a ketone. A motif is constructed by identifying all occurrences of one of these types of hydrogen bonds throughout the network. The subset of molecules that becomes hydrogen-bonded together by this operation is called a motif. The ability to single out one type of hydrogen-bond pattern at a time is one of the most useful features of this graph-set method. Graph sets are assigned first to motifs, and then to networks. Frequently only one or a few motifs need to be assigned to answer questions about preferred aggregate patterns. This level of analysis is easy to learn, and to remember. The process of making the assignments is what is important here. It allows one to see clearly how multiple hydrogen-bond patterns are interrelated and to focus on the chemistry of particular sets of molecules.

A graph set is specified using the pattern designator (G), its degree (r), and the number of donors (d) and acceptors (a), as shown $\boldsymbol{G_d^a(r)}$**.** *G is a descriptor referring to the pattern of hydrogen bonding. It has four different assignments based on whether hydrogen bonds are inter- or intramolecular: S, C, R and D. S (standing for self) denotes an intramolecular hydrogen bond. Different patterns of intramolecular hydrogen bonds are not specified with this notation. A method for specifying particular intramolecular hydrogen bonds in cyclic peptide structures has been developed and may be useful for other types of molecules as well. For intermolecular bonds, C refers to hydrogen-bonded chains that are infinite, R refers to rings. A typical ring pattern is a cyclic carboxylic acid dimer. D refers to non-cyclic dimers and other finite hydrogen bonded sets, such as a phenol hydrogen-bonded to acetone. The parameter r refers to the degree, being either the number of atoms in a ring or the repeat length of a chain. For a ring, in an S or R set, the degree is defined as the number of atoms in the ring, counted by traversing the ring in one direction along the shortest chain of covalent and hydrogen bonds until all the atoms in the ring have been counted once. For a chain, C, the degree is the repeat length of the monomer unit in the chain, i.e., the number of atoms encountered by traversing the shortest pathway from the hydrogen atom of one hydrogen bond to the acceptor atom of the next. For D motifs the degree is the number of atoms in the entire length of the hydrogen-bonded set starting with the proton of the first hydrogen bond, proceeding along the shortest pathway, and ending with the acceptor atom in the last hydrogen bond of the set. If there is only one hydrogen bond in the motif, then the degree of the D pattern is 2. Since this pattern occurs so frequently, r = 2 is considered the default degree value for a D pattern and it is not specified. The parameters d and a refer to the number of different kinds of donors (d) and acceptors (a) used in the hydrogen-bond pattern. When all the molecules in a set are the same, d and a will be the number of participating donors and acceptors per molecule. When the set is composed of different kinds of molecules, d and a will be the sum of the participating donors and acceptors from all the different molecules. The default value for d and a is 1.*

Assigning graph sets to motifs

1. *Identify the different types of hydrogen bonds in the array of interest. One motif will be generated for each type of hydrogen bond.*

2. *Rank the hydrogen bonds by chemical priority. This step is necessary so hydrogen-bond patterns can be reconstructed from graph sets [prioritization can be performed consistently by using the Cahn-lngold-Prelog rules which have been extended here to include hydrogen bonds. If hydrogen bonds are encountered that are not covered by application of these rules, they should be enumerated arbitrarily before proceeding further.*
3. *Generate a motif, selecting the highest priority hydrogen bond, H(I), and finding all occurrences of this bond in the array. To identify a motif choose one molecule as the starting point and identify all molecules that are attached to it by H(I). Then proceed from each of these molecules to all others bonded to them by H(I), etc. until a molecule is encountered which has no additional attached molecules, or until it is obvious that the set is infinite. The process is like gluing certain molecules in an array together [with H(1) glue], then pulling one molecule out of the array to see which additional molecules come with it, and whether they form an infinite (C) or a finite (S, R or D) set. This step is the essential decoding step in the procedure.*
4. *Assign a graph set to the motif. A straightforward example is given as example (I) in Table 1, with graph set D. Example (II) is an infinite (II) chain, with degree 7. Its complete graph set is C(7) (A stands for proton acceptor and DH for proton donor). In some cases H(I) occurs in a ring as well as (III) in a chain. In these cases, the ring may be indicated as a subset, given in brackets. For (III), the complete graph set is $C_1^2(8)$ $[R_1^2(4)]$. If the hydrogen atom of a (IV) single hydrogen bond occurs in two of the same rings at the same time, then the graph set assigned to one of the patterns is doubled. For (IV) (Table 1) the graph set is 2 $R_1^2(4)$.*
5. *Repeat steps three and four until graph sets (v) have been assigned to all hydrogen-bond types.*

In geometry and crystallography a Bravais Lattice is an infinite set of points generated by a set of discrete translation operations. A Bravais lattice looks exactly the same no matter for which point one views it the position vectors of a Bravais lattice.

A crystallographic point group or crystal class is a set of symmetry operations that leave a point fixed, like rotations or reflections, which leave the crystal unchanged. It is a symmetry group. It can be shown that there exist only 32 unique crystallographic point

groups. The point group of a crystal, among other things, determines the symmetry of the crystal's optical properties For instance; one knows whether it is birefringent, or whether it shows the Pockels effect, simply by knowing its point group.

The point groups are denoted by their component symmetries. There are a few standard notations used by crystallographers, mineralogists, and physicists. There are two main forms of notation, Schoenflies and Paterson notation.

Schoenflies notation: In Schoenflies notation, point groups are denoted by a letter symbol with a subscript. The symbols mean the following:

- *The letter O (for octahedron) indicates that the group has the symmetry of an octahedron (or cube), with (O_h) or without (O) improper operations (those that change handedness).*
- *The letter T (for tetrahedron) indicates that the group has the symmetry of a tetrahedron. T_d includes improper operations, T excludes improper operations, and T_h is T with the addition of an inversion.*
- *C_n (for cyclic) indicates that the group has an n-fold rotation axis. C_{nh} is C_n with the addition of a mirror (reflection) plane perpendicular to the axis of rotation. C_{nv} is C_n with the addition of a mirror plane parallel to the axis of rotation.*
- *S_n (for Spiegel, German for mirror) denotes a group that contains only an n-fold rotation-reflection axis.*
- *D_n (for dihedral or two-sided) indicates that the group has an n-fold rotation axis plus a two-fold axis perpendicular to that axis. D_{nh} has, in addition, a mirror plane perpendicular to the n-fold axis. D_{nv} has, in addition to the elements of D_n, mirror planes parallel to the n-fold axis.*

Paterson notation consists of a set of four symbols. The first describes the centering of the Bravais lattice (P, C, I or F). The next three describe the most prominent symmetry operation visible when projected from a, b and c faces respectively. These symbols are the same as used in point groups, with the addition of glide planes and screw axis, described above. By way of example, the space group for quartz is $P3_121$, showing that it exhibits primitive centering of the motif (i.e. once per unit cell), with a threefold screw axis projecting on one face, and two fold rotation axis another. Note that it does not explicitly contain the crystal system.

The space group of a crystal is a mathematical description of the symmetry inherent in the structure. The word 'group' in the name comes from the mathematical notion of a group, which is used to build the set of space groups. The set of all 230 space groups is made from the combination of the 32 crystallographic point groups with the 14 Bravais lattices which belong to one of 7 crystal systems. This results in a space group being a combination of a unit cell with some form of motif centering, along with the point operations of reflection, rotation and improper-rotation. In addition, there are the translational symmetry elements. The basic translation is covered by the lattice type, leaving combinations of reflections and rotations with translation:

Screw axis: A rotation about an axis, followed by a translation along the direction of the axis. These are noted by a number, n, to describe the degree of rotation, where the number is how many operations must be applied to compete a full rotation (e.g., 3 would mean a rotation one third of the way around the axis each time). The degree of translation is then added as a subscript showing how far along the axis the translation is, as a portion of the parallel lattice vector. So, 2_1 is a two-fold rotation followed by a translation of 1/2 of the lattice vector.

Glide plane: A reflection in a plane, followed by a translation parallel with that plane. This is noted by a, b or c, depending on which axis the glide is along. There is also the n glide, which is a glide along a face, and the d glide, which is along the body diagonal of the unit cell.

*It is easily noted that not all of the possible combinations of the Bravais lattices, crystal systems and point groups are apparent in the space groups (32 * 14 = 448 < 230). This is because a number of different combinations are isomorphic with each other (that is, they turn out to be the same thing). This was proved using group theory, and is the source of the word 'group' in the title.*

There are a number of methods of identifying space groups. The International Union of Crystallography publishes a table (more correctly, a hefty tome of tables) of all space groups, and assigns each a unique number.

The use of graph sets as a tool for analyzing hydrogen-bond patterns of large numbers of structures allows one to determine graph set distributions corresponding to a class of

molecules containing one particular functional group, and conversely functional group distributions corresponding to all structures with a particular graph set. Hydrogen-bond rules reflect these relationships and provide useful information about preferred connectivity patterns, hydrogen-bond selectivity, and stereoelectronic properties of hydrogen bonds for a particular functional group or for sets of functional group.

General Rules for hydrogen bonding[40a]

1. All good proton donors and acceptors are used in hydrogen bonding
2. If six-membered ring intramolecular hydrogen bonds can form, they will usually do so in preference to forming intermolecular hydrogen bonds
3. the best proton donors and acceptors remaining after intramolecular hydrogen-bond formation form intermolecular hydrogen bonds to one another

Additional Rules for Nitro anilines

4. Amino protons will hydrogen bond to nitro groups, if no better proton acceptors are present
5. One or more intermolecular amino-nitro hydrogen bonds will form
6. The aggregate patterns formed from intermolecular hydrogen bonds between substituents in *meta* and *para* positions will be acentric
7. The amino-nitro interaction is usually a three-center hydrogen bond, $R_1^2(4)$
8. Proton acceptors are present *ortho*-substituted primary nitro anilines usually form two-center intermolecular hydrogen bonds with graph set $R_2^2(6)$ rather than three center in a variety of different packing patterns and space groups.

The first rule was developed by Donohue during the early days of crystallography when there were only a handful of organic crystal structures known. This is still the most useful of all the hydrogen-bond rules.[40b] A second rule, complementary to the first one, is that all good acceptors will be used in hydrogen bonding when there are available hydrogen-bond donors.[40c] This rule is not followed as rigorously as the first one, but it is a useful corollary nonetheless. The third rule, frequently observed in our work on co-crystal design, is that the best hydrogen-bond donor and the best hydrogen-bond acceptor will preferentially

form hydrogen bonds to one another.[40d] These rules reflect energetically favorable kinds of intermolecular association. What is not intuitively obvious is that crystal packing patterns also reflect these simple rules so frequently.

A lovely example of this effect is seen in the *urylene* and substituted *urylene* structures studied by Fowler et al.[45] The urea portions of the molecules have a bidentate chain pattern whether or not the carboxylic acid substituents are present. Conversely, the typical carboxylic acid dimer pairs which are found in most acid structures are preserved in the acid-substituted *urylenes*. In this example, each functional group retains its preferred hydrogen-bond pattern in the presence of the other functional group.

Fig. 4 Hydrogen-bond pattern of a disubstituted urea (Urylene derivatives)

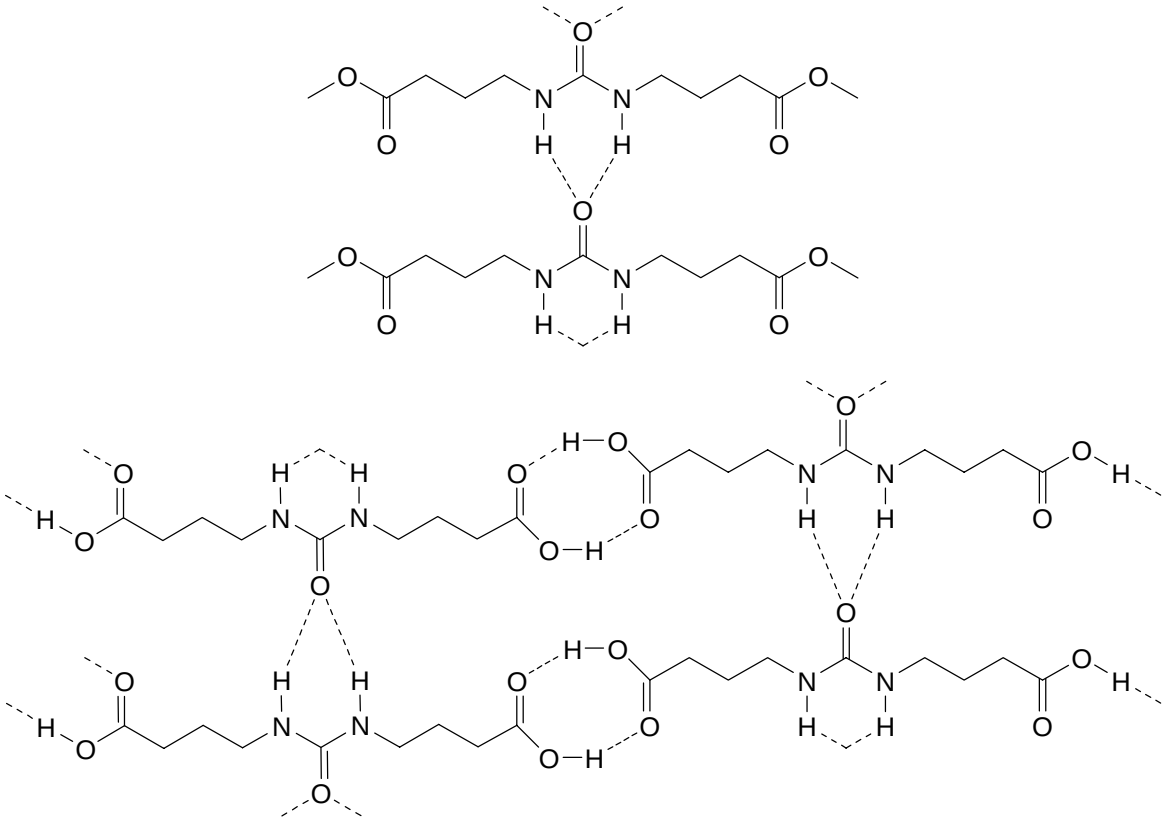

The IR frequencies of groups such as O-H or C=O are shifted when the group is hydrogen bonded. Hydrogen bonding always moves the peak toward lower frequencies, for both the *A-H* and the *B* groups, though the shift is greater for the former. For example, a free OH group of an alcohol or phenol absorbs at ~3590- 3650cm^{-1}, while a hydrogen-bonded

OH group is found ~50-100 cm^{-1} lower.[46] In many cases, in dilute solution, there is partial hydrogen bonding, that is, some OH groups are free and some are hydrogen bonded. In such cases two peaks appear. Infrared spectroscopy can also distinguish between inter- and intramolecular hydrogen bonding, since intermolecular peaks are intensified by an increase in concentration while intramolecular peaks are unaffected. Other types of spectra that have been used for the detection of hydrogen bonding include Raman, electronic[47], and NMR.[48] Since hydrogen bonding involves a rapid movement of protons from one atom to another, NMR records an average value. Hydrogen bonding can be detected because it usually produces a chemical shift to a lower field. Hydrogen bonding changes with temperature and concentration, and comparison of spectra taken under different conditions also serves to detect and measure it. As with IR spectra, intramolecular hydrogen bonding can be distinguished from intermolecular by its constancy when the concentration is varied.

Fig. 5 Polar hydrogen-bonded co-crystal composed of carboxylic acid heterodimers linked into a polar array by nitro aniline hydrogen bonds

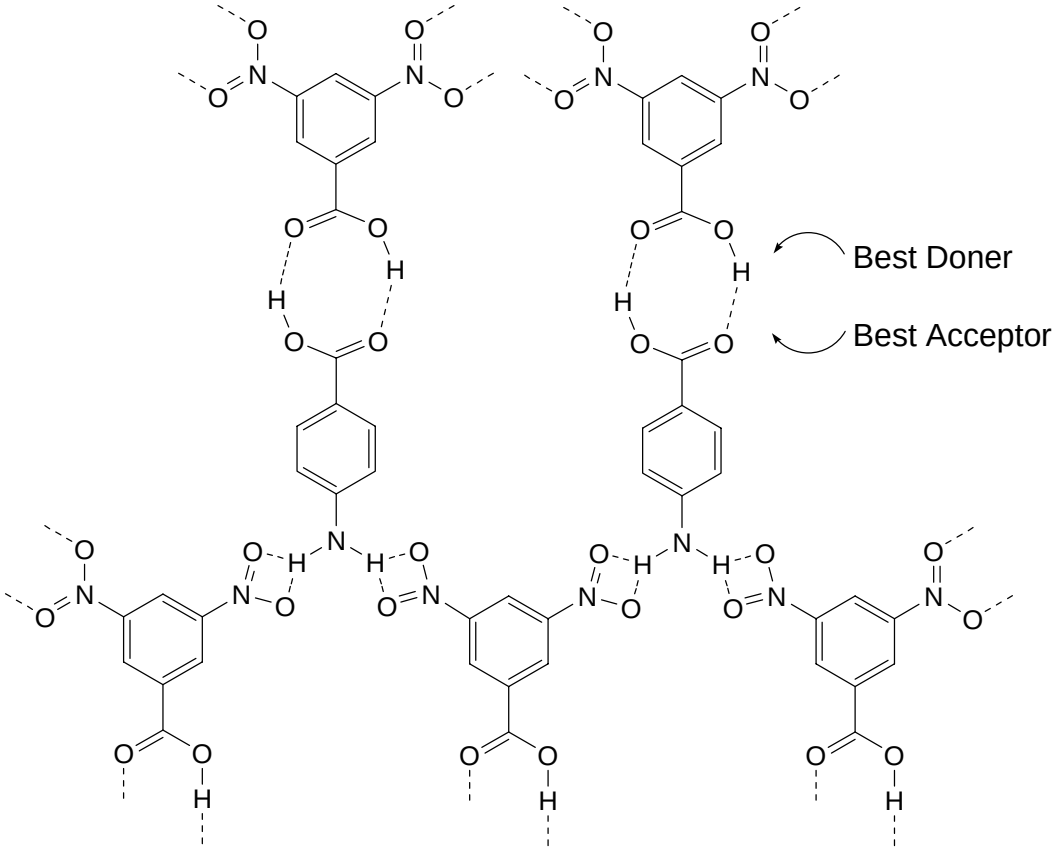

Expected or typical hydrogen-bond patterns may not occur for a variety of reasons, including the presence of multiple competitive hydrogen-bond sites, steric overcrowding, or competing dipolar and ionic forces. Hydrogen-bond rules for homomeric nitro anilines were determined from data obtained using the Cambridge Data Base. Molecules that are better acceptors than the nitro group, such as triphenylphosphine oxide, were introduced as guest molecules during crystallization of p-nitroaniline to specifically perturb the $-NH_2\cdots O_2N-$ interaction. A co-crystal with the aniline hydrogens bonding to the phosphine oxide oxygen atom was obtained.[49] An alternative co-crystal system could be prepared by using hydrogen bonds instead of σ bonds to link the nitro and aniline groups together. For example, a nitro-substituted benzoic acid and an amino-substituted benzoic acid form co-crystals of heteromeric dimers. The acids bond to one another to provide the σ-bond like link, while the nitro and aniline -NH groups remain to link these dimers into polymer chains according to the nitroaniline hydrogen-bond rules.

Fig. 6 Bicyclic compound with three center two electronic configuration

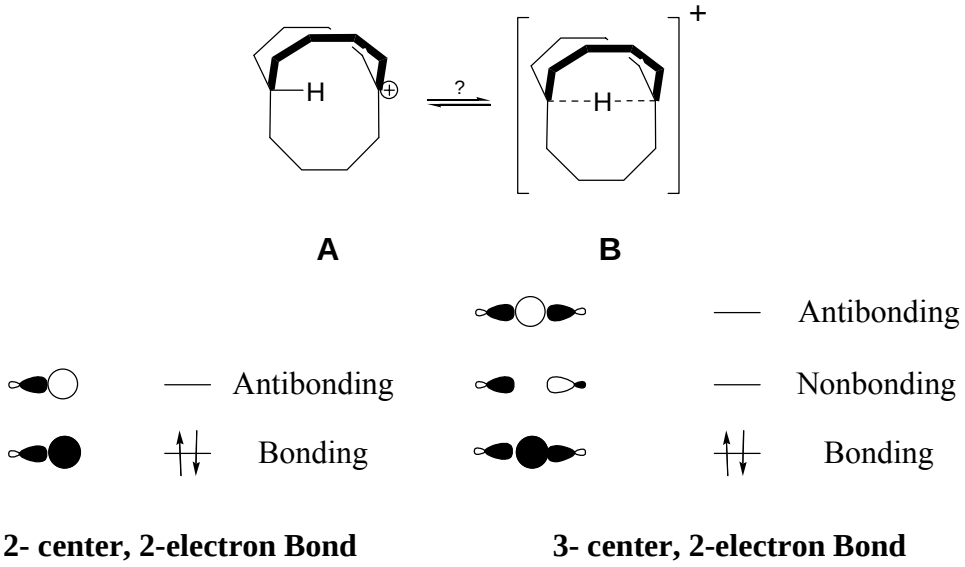

There are three types of C-H bonds found that are acidic enough to form weak hydrogen bonds.[50] These are found in terminal alkynes (RC=CH),[51] chloroform and some other halogenated alkanes, and HCN. Sterically unhindered C-H groups ($CHCl_3$, CH_2Cl_2,

terminal alkyne) form short contact hydrogen bonds with carbonyl acceptors, where there is a significant preference for coordination with the conventional carbonyl lone-pair direction.[52] There is evidence that double and triple bonds, aromatic rings,[53] and even cyclopropane rings[54] may be the *B* component of hydrogen bonds, but these bonds are very weak. An interesting case is that of the in bicyclo[4.4.4]-l-tetradecyl cation **A**. NMR and IR spectra show that the actual structure of this ion is **B**, in which both the *A* and the *B* component of the hydrogen bond is a carbon.[55] These are sometimes called 3-center, 2-electron C-H···C bonds.[56]

Fig. 7 Hydrogen bonding with π electron cloud.

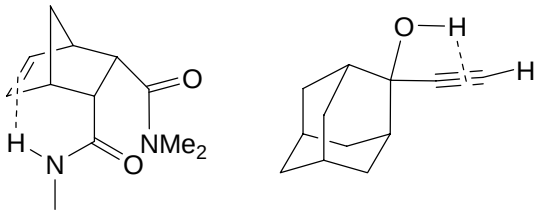

A **B**

Weak hydrogen bonds can be formed between appropriate hydrogen and a π-bond, both with alkenes and with aromatic compounds. For example, IR data in dilute dichloromethane suggests that the predominant conformation for the bis-amide **A** (fig. 7) contains an N—H···π hydrogen bond involving the C=C unit.[57] The strength of an intramolecular π-facial hydrogen bond between an NH group and an aromatic ring in chloroform has been estimated to have a lower limit of -4.5 ± 0.5kcalmol^{-1}.[58] A neutron diffraction study of crystalline 2-ethynyladamantan-2- ol **B** shows the presence of an unusual O—H···π hydrogen bond, which is short and linear, as well as the more common O-H···O and C-H···O hydrogen bonds.[59]

In supramolecular chemistry the hydrogen bond is able to control and direct the structures of molecular assemblies because it is sufficiently strong and sufficiently directional this control is both reliable and reproducible and extends to the most delicate of architectures. The interplay between the orientation of donor/acceptors and the stability arising due to hydrogen bonding have been fascinating and studied in detail on simple naturally available bicycles.

A comparison of the 2,3-anhydropyranose moieties in fig. 8 reveals a difference in their conformations, in that the pyranose ring in **B** has a distorted sofa conformation ($^5E \rightarrow {}^5H_0$).[60] This difference may be due to the configuration of the oxirane ring and the different substituents at C-6'. The nature of the 6'-substituent plays an important role in establishing the ring conformation. Thus, in **A**, HO-6' forms a strong intermolecular hydrogen-bond to O-6 of the neighboring molecule. Since **B** is acetylated at position 6', the intermolecular packing forces in 1 and 2 are completely different in nature. Those in **B** being predominantly van der Waals or dipole-dipole forces. The most important factor which influences the conformational differences is the value of the torsion angle ϕ, which is affected by the steric relation of the oxirane ring and glycosidic bond (trans in **A**, cis in **B**). Different intermolecular interactions also influence the conformations of the rings.

Fig. 8 Conformation of 3-*O*-(2,3-anhydro-4-deoxy-α-L-lyxo-hexopyranosyl)-1,2:5,6-di-*O*-isopropylidine-α-D-glucofuranose.

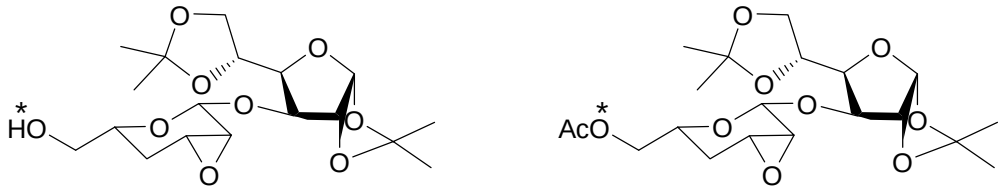

A **B**

The molecular structure shown in fig. 9 shows clearly that the molecule has a dimeric cyclic acetal- hemiacetal structure, formed by self aldol condensation of two monomers; each consists of a furanose ring in the D-xylo configuration, sharing C-l and C-2 with a 1,4-dioxolane ring.[61] The two monomeric partners are interconnected through ether bridges formed by the addition of the OH-3 function of one monomer to the keto group of the second monomer, thus forming a central 1,3-dioxane ring. These results confirm that the previously assigned chemical structure **B** of **A** is correct. Although the absolute configuration at the asymmetric centers produced as a result of dimerization at C-5 and C-5' was not directly determined, it can be assigned as *5R* and 5'S, respectively, based on the known configurations of the other chiral centers. The orientation of O-5' about the C-5'-C-4' bond is trans-gauche to O-4' and C-3', with the torsion angles 0-5'-C-5'-C-4'-O-4' and O-5-C-5'-C-

4'-C-3' being 170.0(2)^0 and 46.4(2)^0, respectively. Similarly, the orientation of O-5 about O-5-C-5 bond is trans-gauche to C-3 and O-4 with the torsion angles 0-5-C-5-C-4-C-3 and 0-5-C-5-C-4-0-4 being 179.0(2)^0 and 62.0(2)^0, respectively. In contrast to the crystalline state, compound was found to exist in solution, mainly, in the monomeric form **A**. This was evident from the presence of a signal attributable to an aldehydic proton in its ^{1}H NMR spectrum measured at 400 MHz (δ = 9.57 ppm in acetonitrile-d_4). This was further supported by the fact that the monomeric form **A** could be readily isolated as its crystalline 1,3-diphenylimidazolidine derivative in an overall yield of 74% from 1,2-O-isopropylidene-α-D-glucofuranose by treatment of the oxidation product **A** with N,N'-diphenyl ethylidenediamine in methanol containing acetic acid.

Fig. 8 Structure of 1,2-*O*-isopropylidine-a-D-xylo-pentodialdo-1,4-furanose

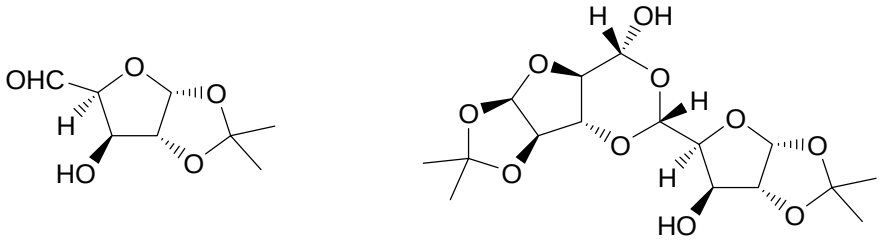

A **B**

The molecular structure and atomic numbering of 2,3:4,5-di-*O*-isopropylidene-1-*O*-methyl-β-D-fructopyranose (A) are illustrated in Fig. 9. The D form of this compound was assumed, based on the configuration of the starting material.[62] The crystal structure determination confirmed that the molecule has the *arabino* configuration and that the anomeric carbon atom has the β configuration. It should be noted that this anomeric configuration is dictated by the orientation of O-3 and by the presence of the five-membered ring defined by C-2-C-3-O-3-C-8-O-2 in the thermodynamically more stable cis-fusion to the six-membered ring defined by C-2-C-3-C-4-C-5-C-6-O-6. Compound **A** should have a six-membered ring conformation similar to that of its unmethylated parent compound **C**. This is in view of the fact that the predominant force determining the conformation of the central ring is the two fused side-rings and not the functionality on the exocyclic group. In contrast, **A** should be different from compound **B** which has the anomeric ring spiro, i.e., not fused to

the central ring. Because the solution structure of a similar compound (**D**) has been reported,[63] those results will be utilized for comparison. In **D**, the ring conformation is indicated by the magnitude of the proton-proton coupling-constants. These values indicate a torsion angle between H-3 and H-4 of ~60^0 and between H-4 and H-5 of ~20^0. These values fit the skew conformation $^3S_0$. Compound **C** was reported[64] to exist in two crystallographically independent molecules (A and B), and this was confirmed in our study. Our torsion-angle values for crystalline **C** are 69^0 and 10^0 (for molecule A), and 65^0 and 16^0 (for molecule B). These values are in marked contrast to the values of 164^0 and 26^0 in **B**, the conformation of which is a chair ($^2C_5$) but are somewhat distorted toward a half-chair ($^2H_0$). These same angles in **A** are 78^0 and 9^0 and are, as expected, similar to the values for **C**, which indicates that **A** is also in the $^3S_0$ conformation. Because this compound is in a skew conformation, a bond-length inter-comparison of **A** to data for **C** to the literature data for **C** was of interest.[64] The C-O bond lengths of the pyranose ring for all the data sets show the usual shortening of the bond to the anomeric carbon atom, even though the compound is in a skew, not a chair, conformation. The C-O bond lengths in the 2,3-*O*-isopropylidene ring do not show a significant pattern between the compounds, even though C-2 and C-3 differ in degree of substitution. The C-O bond lengths in the 4,5-*O*-isopropylidene ring do not show significant differences, even though C-4 and C-5 have the same degree of substitution.

Fig. 9 Structures of various fructose derivatives

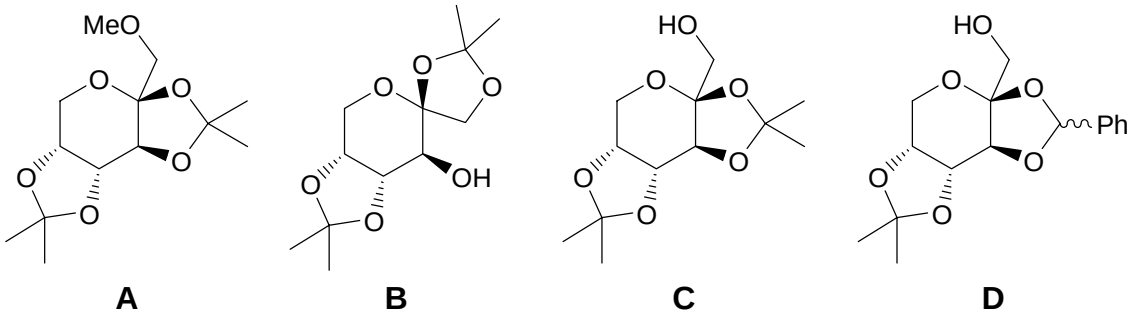

The exocyclic side-chain of **A** would be expected to have a different orientation from that found in **C**, due to the lack of a hydrogen atom on O-l and the resulting loss of hydrogen-bond donor ability. The torsion angle about the C-1-C-2 bond has similar values in **A** and **C**. The torsion angle C-7-O-l-C-l-C-2 in **A** is -102^0, in contrast to **C**, where this angle is -75^0 in

molecule A and -69^0 in molecule B. Thus, the presence of hydrogen bonds in **C** decreases this value by -30^0. Another factor to consider is the steric interaction between the methyl group protons on C-7 and C-9, which would cause an increase in this value towards the expected 180^0. Crystal packing forces are the probable cause of the difference between the expected and observed values for this torsion angle.

Fig. 10 Structure of methyl 6-deoxy-2,3-0-isopropylidene-α-D-manno-heptofuranoside

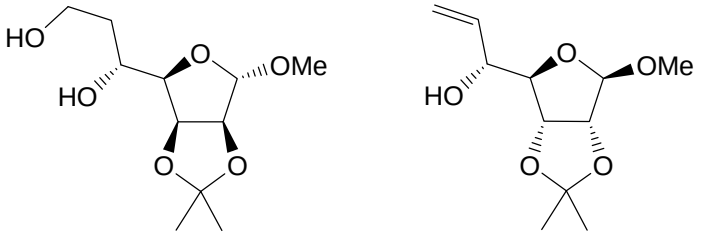

A **B**

The presence of the 2,3-*O*-isopropylidene grouping and the α-glycosidic methyl group imposes some conformational rigidity on **A**.[65] The torsion angles O-4-C-l-O-l-CH_3 and C-2-C-1-O-l-CH_3 are 62.3^0 and 177.4^0, respectively, corresponding rather favorably to the glycosidic system exhibiting the anomeric effect. The furanoside and 2,3-*O*-isopropylidene rings are in envelope forms, ^sE and E_3, respectively. In the furanose ring, atoms C-l-C-2-C-3-C-4 and, in the 1,3-dioxolane ring, atoms O-2-C-2-C-3-O-3 lie in single planes. This shape resembles strongly the X-ray structure determined for methyl 6,6,7,7-tetradehydro-6,7-dideoxy- 2,3-O-isopropylidene-β-D-allo-heptofuranoside **B**. The side chain C-5-C-6-C-7 is in an extended zigzag conformation. The torsion angle C-4 ···C-7 corresponds to ca. 170^0. The calculated structure fits rather well to the experimentally determined shape. Compound **A** forms two kinds of intermolecular hydrogen bonds involving both hydroxyl groups occurring in the side chain of the molecule. Considering the O-H···acceptor distances, the bonds are relatively strong in nature. They form a system of planes. Probably, the existence of these hydrogen bonds in the crystal lattice is responsible for some discrepancies, involving torsion angles in the side chain, between the MM and X-ray model. The X-ray structural determination of **A** definitely confirms its manno configuration.

Hydrogen bonds are important because of the effects they have on the properties of compounds, among them.

1. Intermolecular hydrogen bonding raises boiling points and frequently melting points.
2. If hydrogen bonding is possible between solute and solvent, this greatly increases solubility and often results in large or even infinite solubility where none would otherwise be expected.
3. Hydrogen bonding causes lack of ideality in gas and solution laws.
4. As previously mentioned, hydrogen bonding changes spectral absorption positions.
5. Hydrogen bonding, especially the intramolecular variety, changes many chemical properties. For example, it is responsible for the large amount of enol present in certain tautomeric equilibria. Also, by influencing the conformation of molecules, it often plays a significant role in determining reaction rates.[66] Hydrogen bonding is also important in maintaining the three-dimensional structures of protein and nucleic acid molecules.

Present Work

Extensive investigations in crystallography in determination and analysis of building blocks beyond the molecule have led to major advances in the prediction and design of crystal structures of organic materials with specific properties. The crystal sub-structural units occurring repeatedly in many known crystal structures can be relied upon to be influential in steering molecules into desired packing arrangements in new materials. Lehn first pointed out that 'just as there is a field of molecular chemistry based on the covalent bond, there is a field of supramolecular chemistry, the chemistry of molecular assemblies and the intermolecular bond.[67]

Figure 1 Various single bond synthons

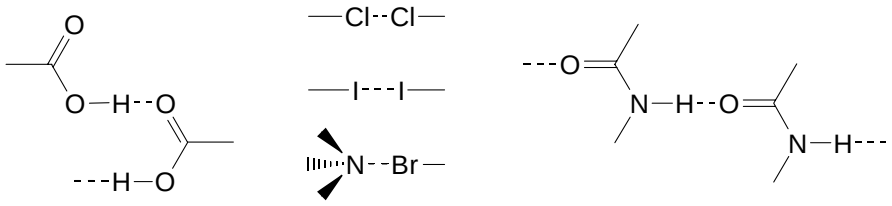

In both molecular and supramolecular chemistry retrosynthetic methods, using a 'disconnection' approach to dissect a complex molecule or crystal structure into smaller subunits connected by available synthons, are in principle possible. These synthons can be used to derive various supramolecular architecture.[68]

Figure 2 Multiple bond Synthons

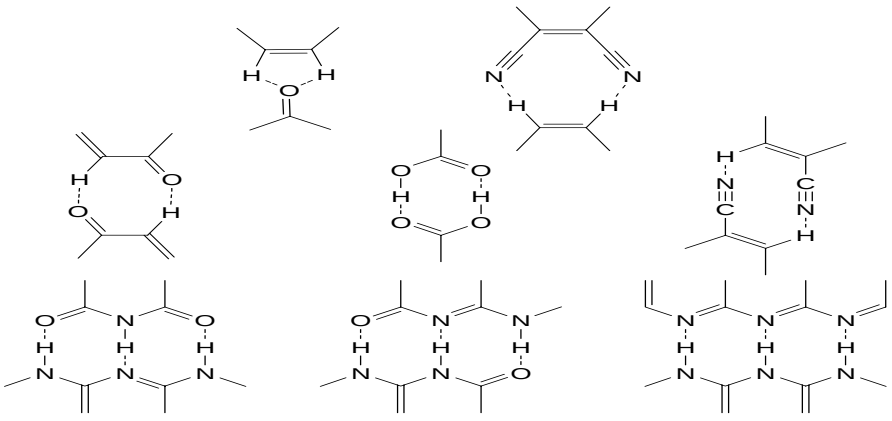

Chiral propargylic alcohols are very useful synthetic precursors to many organic compounds.[69] Supramolecular structures formed by propargylic alcohols are recently been topic of interest. Various interesting intermolecular interactions in these compounds because of the hydroxy groups and the π electrons of the C≡C bonds are noticed.[2b, 70] It has been shown recently, that diaryl-substituted (an aryl and a perfluoroaryl moiety) chiral propargylic alcohols can form cyclic hexameric supramolecular assemblies as a result of the cooperation between three major intermolecular forces: O–H···O hydrogen bonding, C–H···F–C hydrogen bonding involving organic fluorine atoms, and π–π stacking interactions between the pentafluorophenyl and phenyl rings.[71]

Figure 3 Supramolecular assemblies of chiral propargyl alcohols

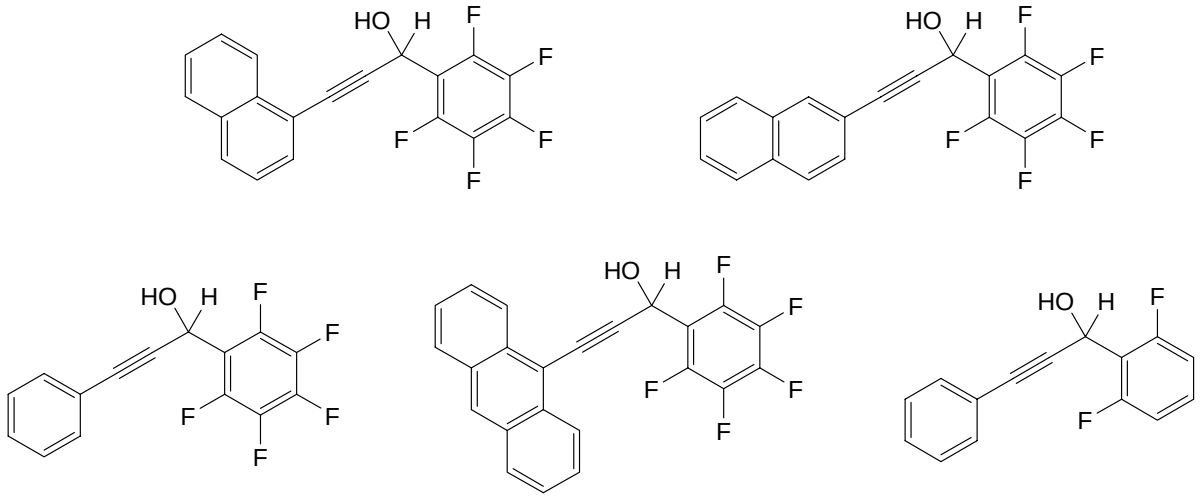

The structural analysis in carbohydrate systems is a topic that has been dealt with the help of several analytical tools. Because understanding the intramolecular interactions especially of hydrogen bonding is a puzzle even with the simple sugars like D-glucose in solution and needs a more sophisticated calculations and extensive solution and solid state NMR analyses in case of oligosaccharides beyond 2 units. However, investigations to understand the intramolecular interaction with various functionalized monosaccharides have been led to some predictable conformational preferences and possible intramolecular hydrogen bonding. Carbohydrate ring systems are in general electron deficient when compared to simple pyran or cyclohexane. The free hydroxyl groups in carbohydrate

derivatives are unique in being appended on an electron deficient cyclic ether framework, and closely located near to good hydrogen-bond donors as well hydrogen-bond acceptors.

Every carbon atom of the ring is attached to at least one oxygen atom (–I effect). Thus for a free hydroxyl group, the O-H bond is more polarized and the shift of electron density is more towards oxygen. Best proton donors and the best proton acceptors are very closely located in carbohydrate systems. Thus according to the very first rule for hydrogen bonding, they happen to form sufficiently strong hydrogen bonded network. The hydrogens (commonly called as proton) look for stability by means of hydrogen bonding with various nearby oxygen atoms or any electron rich element present with in the van der Wall radi.

Scheme 1

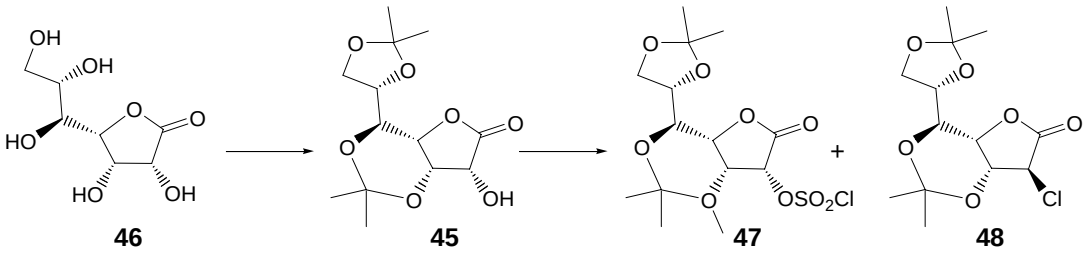

Our foray in this area was intrigued by one of the compound that has been synthesized in our lab in the context of a total synthesis. As part of our research focused on the radical allylation of sugar derived α-halolactones and exploration of the resulting α-*C*-allylated lactones as potential chiral pool materials to derive biologically active natural products, we have attempted the chlorination of 3,5:6,7-di-*O*-isopropylidene-D-*glycero*-D-*gulo*-heptonolactone **45** which can be prepared starting from inexpensive D-*glycero*-D-*gulo*-heptonolactone **46**. However, attempted chlorination of **45** was sluggish and resulted with an inseparable mixture of the desired chlorinated product **48** and the C(2)-*O*-sulphonolychloride **47**.

It has been already reported that lactone **46** can be easily brominated at C(2) and C(7).[3] Lundt and co-workers have already shown that di-*O*-tosylation of aldonolactones and the di-*O*-mesylation of hexonolactones show good selectivity when the hydroxy groups at C(2) and C(3) are *cis*-oriented.[4] Furthermore, the selectivity is highest for the lactones which have the side chain also *cis* to the two hydroxyl groups mentioned.[4] In this context, it will be

of interest to learn whether the possible (?) intramolecular hydrogen bonding between C(2)-OH and O-C(3) or the stability of the intermediate C(2)-O-sulphonyl chloride or the non-cooperative electronic factors for the intramolecular SN^2 can be the one of rationale for the observed difficulties in chlorination. Indeed the observed large $J_{HO\text{-}H\text{-}C(2)}$ = 10.0 Hz in the ^{1}H-NMR of **45** indicated the presence of an intramolecular hydrogen bond[5] and is further supported by IR–spectra measured at different concentrations. In order to see the connection between intramolecular hydrogen bond and the difficulties in chlorination found, the present structure investigation was carried out. The crystal structure of parent lactone **46** has been already examined, however weak intramolecular hydrogen bonds are observed between the hydroxyl groups other than HO-C(2).

Figure 4 Packing diagram of compound **45** down c axis

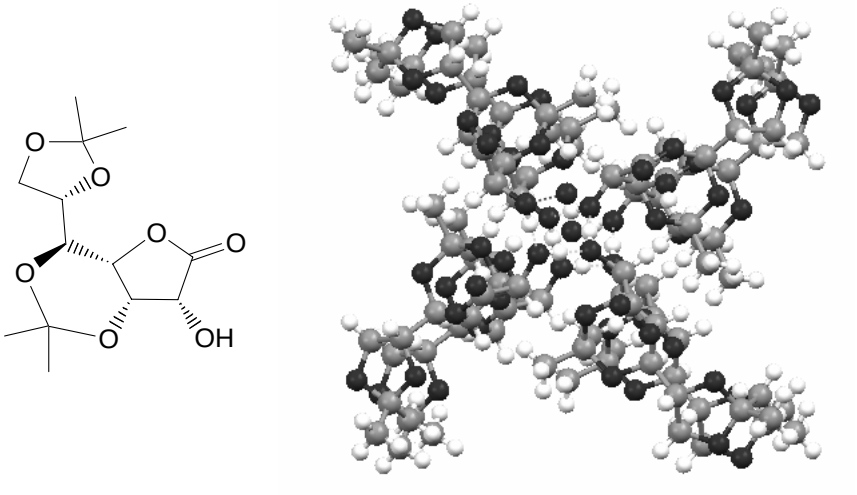

Crystals of **45** suitable for single crystal X-ray diffraction analysis were grown in a mixture of ethyl acetate/hexane by slow evaporation at room temperature. The 3,5,6,7 di-*O*-isopropylidine-D-*glycero*,D-*gulo*-heptono-1,4-lactone (**45**), contains three different structural units: namely, 5-, and 6-membered isopropylidenes and a furano-lactone with an unprotected hydroxy group adjacent to the lactone carbonyl. Very interesting pattern of hydrogen bonding was observed in the molecular structure of compound **45**. The compound crystallizes in tetragonal spacegroup, P4(3). The furanolactone portion of the **45** adopts an E_3 conformation in the solid state. Molecules of the lactone **45** are linked intermolecularly

into infinite chains by O2–H···O2 hydrogen bonds into a left handed helical chain which runs parallel to the *c*-axis and involves successive rotations about the *a*-axis by 126.9˚ followed in each case by a translation of ca. a/3 (Figure 4). An intermolecular weak C–H···O hydrogen bonding between C–H2···O7 (143.66˚ and 2.665Å) connecting the two adjacent anti-parallel repeating units was observed. Various crystallographic parameters and various bond tables are included in Appendix A in this chapter.

Figure 5 Structure of 1,2:5,6 di-*O*-isopropylidine-α-D-glucofuranoside **27** and **27a**

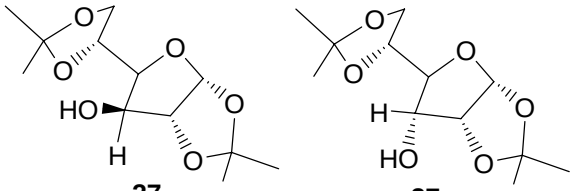

Intrigued by the structural analysis of compounds **45**, we were interested to closely analyze the rigid carbohydrate frame works (preferably acetonide protected) with one free hydroxyl group and their inter- and/or intramolecular associations. In this process we come across with two simple compounds **27** and **27a**, which are epimeric at free hydroxyl positions. These are commonly called as '*Glucose Diacetonide*' and '*Allose Diacetonide*'. These two compounds can be considered as textbook compounds now, as they form the starting material for a variety of natural products or drug candidates. However, it was surprising to notice that crystal structure for these two compounds is not yet documented. As far as **27** is concerned, this compound has a free hydroxyl group at C-3 position and being the *gluco* configured, this hydroxyl group orients above the plane of the furanose ring. The hydrogen attached to the oxygen has no electronic effect due to the adjacent isopropylidines or nearby oxygen. The other compound shown is its C-3 epimer i.e. *allo* compound **27a**. This compound has the free hydroxyl in the vicinity of the nearby oxygens of the fused isopropylidine ring. We have searched for CCDC for some related molecules baring the acetonide groups and investigated for hydrogen bonding parameters the results of which are listed in table 1.

Table 1. Hydrogen bonding parameters observed in various reported crystal structures baring similar subunits

	D-H···A	d(D-H)	d(H···A)	d(D···A)	<(DHA)	Configuration at C2,C3,C4,C5
AWOMUU	O3-H···O6	0.85	2.063	2.831	150.04	L-Talo
GAFPEI	O3-H···N1	1.056	1.779	2.805	162.78	D-Gluco
NUCGAT	O3-H···O4	0.899	1.994	2.855	159.88	
GAFPIM	O3-H···O8	0.718	2.144	2.825	158.73	D-Allo
XAFMEX	O3-H···O4	0.782	2.24	2.878	139.23	

It is quiet evident from these results that all these compounds show similarity in spatial distance between donor and acceptor atoms [d(D···A) in the range of 2.855 ±0.05Å]. In case of both *gluco* isomers, the O-H bond length is almost 0.2 Å more compared to both *allo* isomers. Similar trend is observed in case of d(H···A), in case of both *allo* isomers this distance is almost 0.3 Å more compared to both *gluco* isormers. This is quite surprising as one anticipates the orientation of both the donor and acceptor in the same place should lead to a positive hydrogen bond which in turn result in the lengthening of the O-H distance. An explanation for this might be because of the lone pair electron repulsion in other words rabbit ear effect.

In continuation of our curiosity taken together with the supramolecular structures formed by propargylic alcohols which are recently been topic of interest, we designed two classes of compounds which are epimeric propargyl alcohol to learn about the inter- and intramolecular interactions in these compounds because of the hydroxy groups and the π electrons of the C≡C bonds and stereoelectronic factors due to the adjacent isopropylidene group. Before we proceed for the synthesis and the structural analyses of these compounds its pertinent to mention here a brief account of the possible stereoelectronic effects which might influence structural factors by extending the analyses of such compounds.

These compound have a free hydroxyl group at C3 position orienting above or below the sugar plane. However, now the C3-H is replaced by alkyne functional groups and is anticipated create some interaction with the adjacent oxygens of the 1,2-isopropylidene. In

case of *allo* series (α at C-3) we may not anticipate any interaction, as the newly orientating alkyne group will adopt the unhindered position in the space. The electronic repulsive forces would be minimum and the conformation may not have any distortion in it and one can anticipate a substantially similar structure like what we noticed in the simple allo analogues. In case of *gluco* series, now the alkyne is oriented syn to the isopropylidene group (β at C-3) and effects on hydroxyl group will be minimum but now in this case since the bulk at the *Re* face of the furanoside ring is increased compared to **27a**, the electronic factors arising due to this will be interesting to study. As this functionality carries free electrons in its π-sub shell, the non-bonding electrons of adjacent isopropylidine oxygens may interact with the bonding π orbitals of incoming functionality and can cause inter-electronic repulsions. If these orbitals interact with the anti-bonding orbitals then they might result into entropy change thus resulting into conformational changes. In any case there might result distortion of the parent ring structure.

Figure 6 Designed 1,2:5,6 di-*O*-isopropylidine-3*C*-alkynyl-α-D-*gluco*/*allo*furanosides

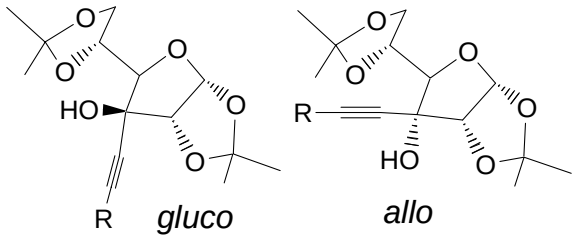

R = H, Ph, *p*-NO_2Ph, *p*-MeOPh

Additionally, we planned to keep different functional groups on alkyne for example free alkyne, phenyl derivative, the *p*-nitro phenyl derivative and *p*-methoxy phenyl derivative. These four substrates are selected because when the alkyne is attached to C-3 position in two possible orientations (α or β), the +I effect partially stabilize the system. The phenyl ring further attached to this alkyne happens to supply extra electrons available with it in its π-clowd. Further when this phenyl ring is functionalized with an appropriate group either to stabilize the π-clowd by +M effect (-OMe group) or destabilize by means of –M effect (-NO_2 group), the resulting structural information will provide some clues about the influence of stereoelectronic factors over the hydrogen bonding.

Figure 7 Planned straegy for alkynol exploiting the highselectivity observed with *gluco*-derivatives and the intended double elimination reaction

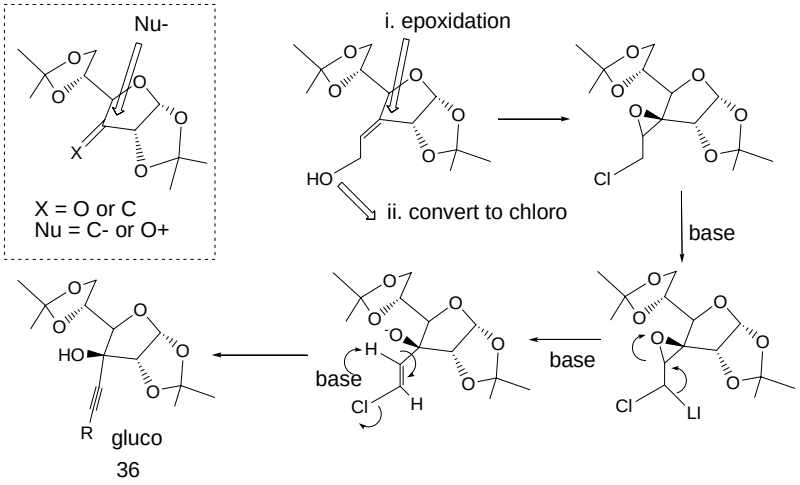

Synthesis of mode substrates 36 – 37

The synthesis of allo analogues is already documented in the literature. One can make x, y, and z from the parent alkyne by using Sonogashira coupling. The synthesis of parent alkyne is by simple addition of an alkynylanion to the 3-ulose derivative. In general it is well documented in the literature with glucose diacetonide system, the nucleophilic additions takes mainly from the β-face because of the concave like structure and due to the hinderance from the *Re* face of the isopropylidene, pushing the thus generated hydroxyl functionality α - to the tetrahydrofuran ring resulting into exclusively *allo*-configured compound. However, the adjacent isopropylidine ring prohibits such a nucleophilic attack with retention of HO-configuration. Nonetheless, for making the *gluco*-configured compound an appropriate approach will be the introduction of oxygen at a later stage like epoxidation of an *exo*-methylene compound, which indeed results exclusively from the β-face. Keeping this in mind we have devised a strategy funded upon the double elimination of a halomethylene oxirane to provide the key *gluco* fingered alkynol.

The synthesis of the other three substrates of this series will be a simple proposition by considering the established Sonogashira coupling. A brief retrosynthetic strategy for gluco congifured alkynol **36** is given in figure 7.

Scheme 2

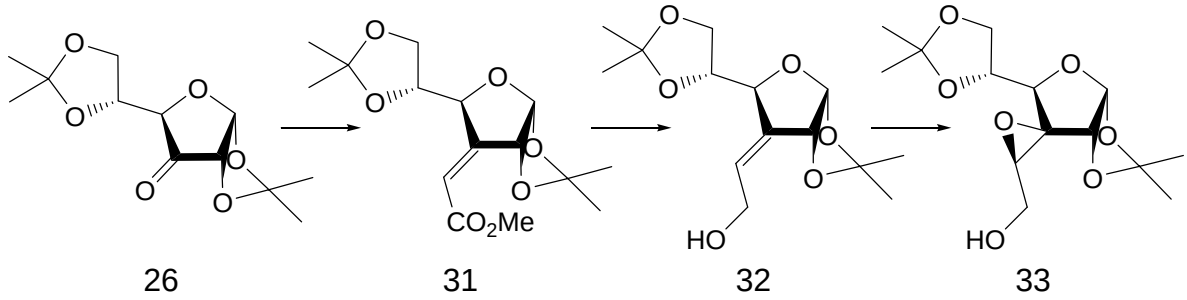

26 31 32 33

For the synthesis of the epoxide **33** the known ketone **26** is subjected to wittig olefination using the wittig yilide obtained form methyl bromo acetate and triphenyl phosphene. This α,β unsaturated olefin compound **31** is partly reduced using DIBAl-H. The compound **32** carries an olefin functionality which is conformed by the NMR analysis of compound **32**. In the NMR spectrum of **32** we observe a triplet of triplet pattern at 6.1δ value with coupling constants 6.3 and 1.8 Hz.

Figure 8 Compound **32**

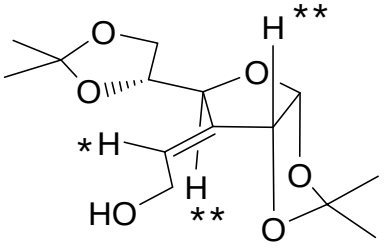

The olefinic proton couples with adjacent methylene protons and the protons at C-2 and C-4 these protons acquire 'W' arrangement when oriented in space. This confirms the availability of olefin at C-3 position. The C-3 carbon is in SP_2 hybridization state and thus when we treat this carbon with peracid the incoming oxygen prefers the β-face in comparison to α-face. The reaction works well and we achieve the exclusive epoxide formation with desired absolute configuration. The disappearance of the signal at 6.1δ value and a signal at 3.53 δ value in PMR spectrum of **33** clearly indicates the formation of epoxide. The β-epoxide is confirmed by the loss of 'W' coupling previously seen and the proton being α it no more gets into such arrangement.

Figure 9 Splitting pattern of olefinic proton in **32**

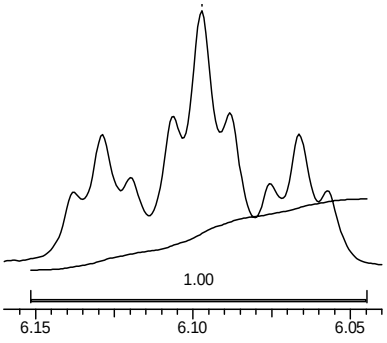

Having the desired epoxide with a free primary alcohol (confirmed by IR), our next task was to convert the compound **33** into desired alkyne isomer **36**. To achieve we need a

good leaving group at the methylene carbon instead of primary alcohol. Thus we plan to convert this alcohol to iodo derivative. When we subjected this alcohol to iodination conditions in presence of triphenyl phosphene, imidazole and elemental iodine in refluxing toluene we got a compound (**35**), which shows a pattern in the PMR spectrum shown in Figure 10.

Figure 10 Portion of the PMR spectrum of compound **35**

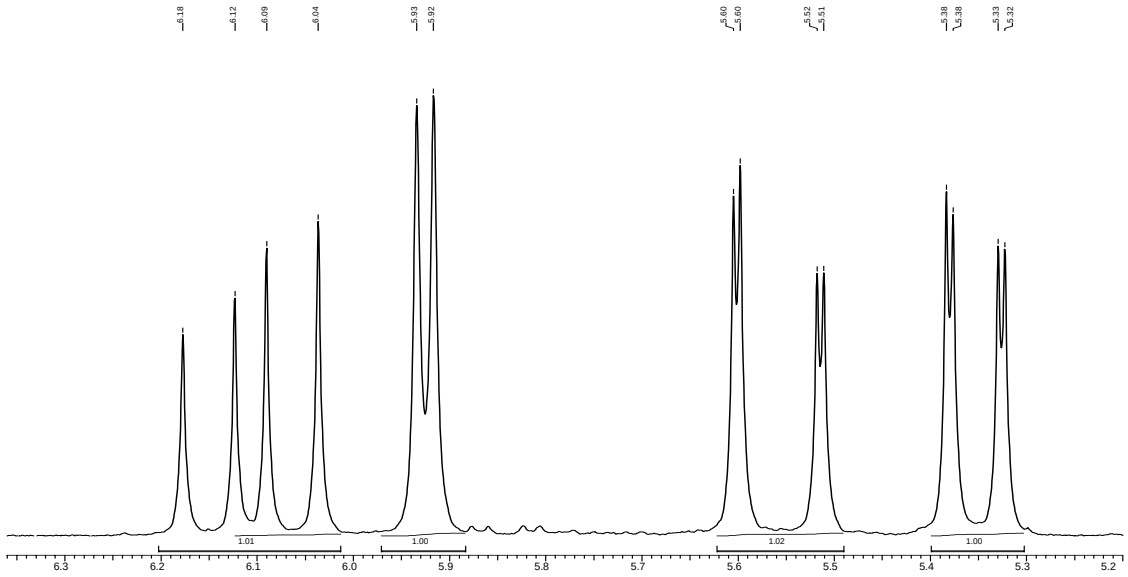

Scheme 3

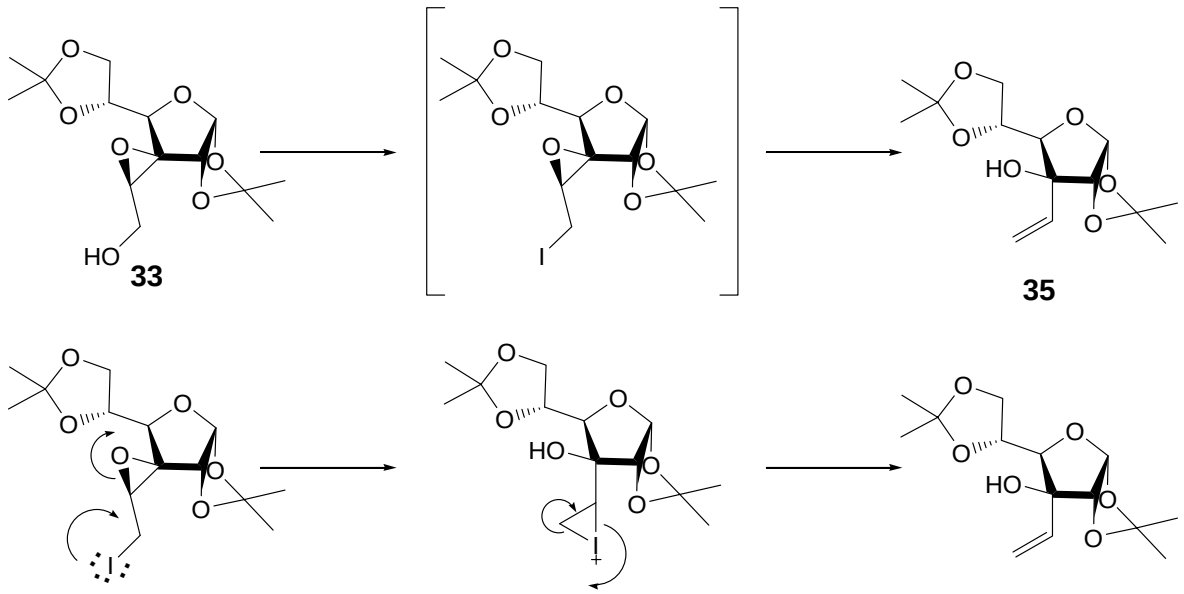

The doublet at 5.92 δ is accounted for the proton at C-1 position that couples with proton at C-2 position giving rise to a doublet (J = 3.5 Hz). The three doublet of doublets observed at 5.38 (J = 10.7 Hz, 1.4 Hz), 5.60 (J = 17.4 Hz, 1.4 Hz), 6.12 (J = 17.4 Hz, 10.7 Hz) δ value should be accounted for the availability of olefinic system. This shows that the epoxide **33** is so fragile that a base like imidazole also can open the oxirane ring, giving rise to terminal olefin with loss of iodo functionality. The plausible mechanism for the formation of **35** is shown in scheme 3. Our aim to synthesize alkyne was unsuccessful by this method so we planned to convert this alcohol into chloro derivative.

Scheme 4

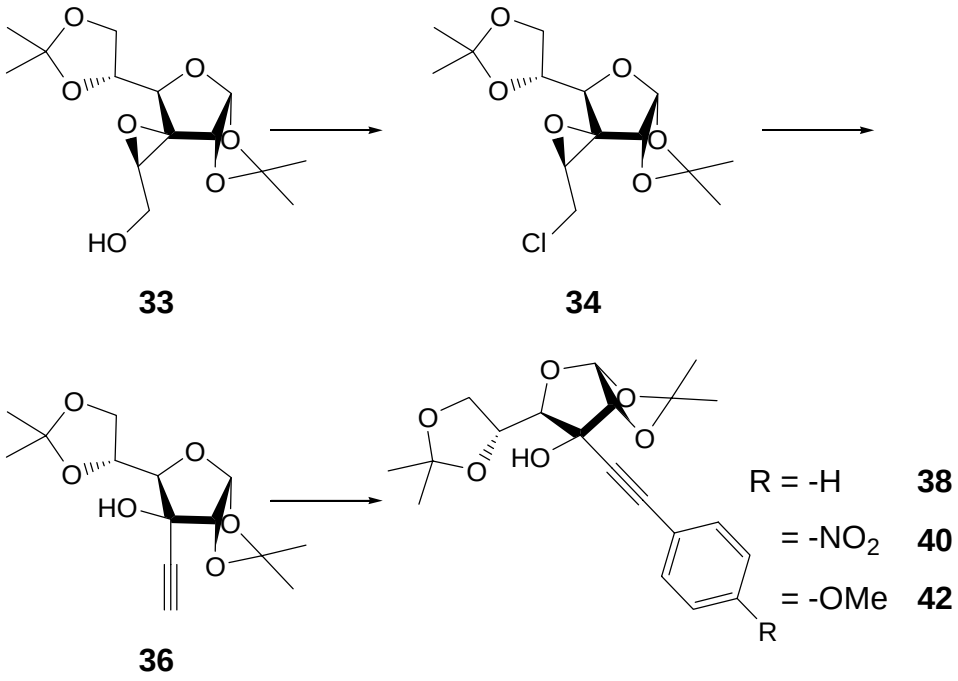

33 **34** **36**

38 **40** **42**

When the epoxide **33** is subjected to chlorination conditions in presence of triphenyl phosphene and carbon tetra chloride we got a compound which had lost the free hydroxyl group (the previously seen signal for hydroxyl group in IR was lost) more over it didn't show any olefinic splitting pattern in PMR. Instead in the elemental analysis it confirmed the presence of chlorine group. Thus we confirm the formation chloro derivative **34** with the epoxide intact. When this chloro derivative is treated with a stronger base (n-BuLi in comparison to imidazol in prior case) it resulted into a compound that showed a singlet at

2.68 δ value which can be accounted for the alkyne proton. Thus finally we synthesized the targeted compound **36** in approximately 15% overall yield.

Scheme 5

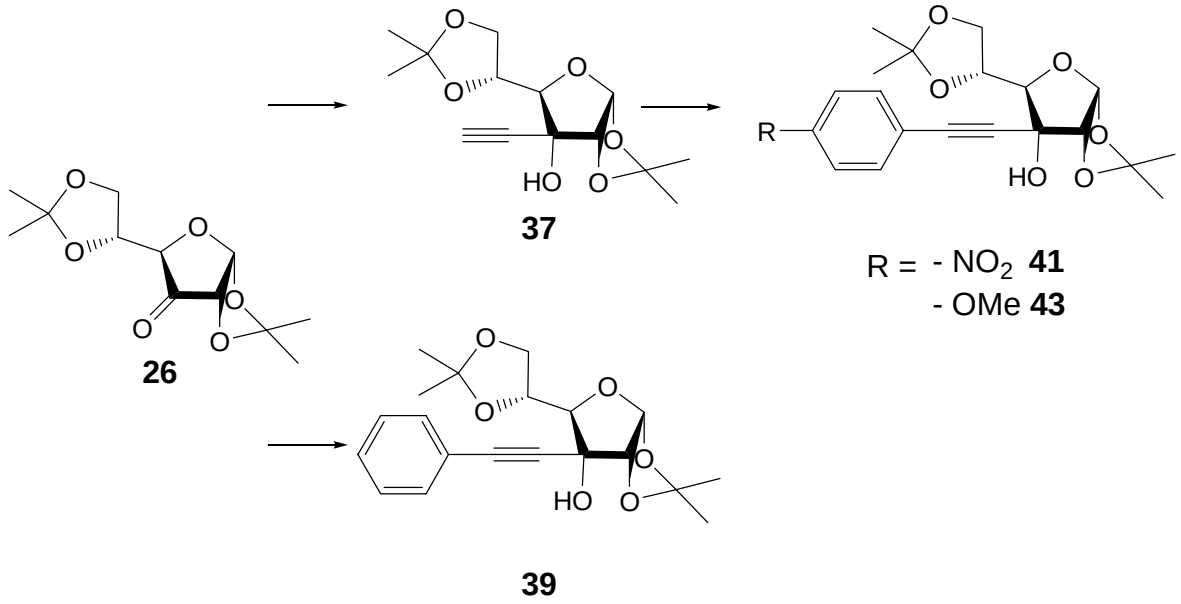

Now that we had the free alkynol our next objective was to synthesize the aromatic analogues of this alkyne this task was comparatively simpler. For this we subjected this alkyne to Sonogashira cross coupling reaction with different aromatic iodides in presence of tetrakis triphenyl phosphene Palladium complex ($Pd(PPh_3)_4$). The coupling reaction works well and we synthesize the aromatic analogues in fairly good yields up to 70%. The schematic plan for this is shown in scheme 4.

In this way starting from **27** (gluco conformer) we achieve all the alkyne analogues in gluco conformation in fairly good to moderate yield without facing any critical problem with stereochemistry. Then having the gluco conformers of all the alkynes we next switched to the synthesis of the allo conformers of these analogues (C-3 epimers). The synthesis of C-3 epimers was not a diffcult task at all since as discussed earlier when the nucleophylic attack was achieved with the ketone **26**, it preferentially comes from the Si face, thus pushing the resulting hydroxyl group down. Thus when the alkyne nucleophyle is treated with **26** we got the desired compounds **37** and aromatic derivatives **39**, **41**, **43** in good yields. The schematic plan for this is given in scheme 5. The synthesis of all these compounds was achieved on

moderate scale. The reactions worked well and the products are confirmed by spectroscopic methods.

On careful investigation of PMR of all these eight isomers we find a repeating pattern of chemical shift for the free hydroxyl proton the interesting feature is that when this hydroxyl group is flanked by the adjacent isopropylidines (allo conformer), then the proton attached to oxygen should form intramolecular hydrogen bonding with the oxygen at C-2 position resulting into deshielding effect compared to its gluco conformer but on the contrary we find that the same proton being in the vicinity of adjacent isopropylidines is shielded by almost 0.5 δ value. In case of aromatic protons we find the same trend of shielding. All the allo conformers show shielding of aromatic protons by almost 0.5 δ value.

Table 2 van der Waal distances between some of the atoms

Compound	**Atom 1**	**Atom 2**	**Distance in Å**
36	Proton of free hydroxyl at C-3	Oxygen at C-5	3.316
		Furanose ring oxygen at C-4	4.228
	Alkyne C-H	Ring oxygen at C-2	4.056
37	Proton of free hydroxyl at C-3	Ring oxygen at C-2	2.047
		Isopropylidine Methyl proton	2.0

As far as the aromatic protons are concerned it is quiet obvious since the π-cloud of the aromatic ring is repelled by the side chain isopropylidines, causing interelectronic repulsion and due to this the protons are shielded. But as far as the hydroxyl is concerned the proton being the better donor of hydrogen bonding and the adjacent oxygen being better acceptor the hydrogen bonding should occur. But such results were not observed. The van der Waal distances between various atoms of compounds **36** and **37** are shown in table 2.

From both these models it is very clear that in case of compound **36** the free hydroxyl is unhindered and the effect of adjacent isopropylidines is negligible. In case of compound **37** the free hydroxyl group is in the viscinity of the nearby isopropylidines and thus these isopropylidines create hindrance to this hydroxyl proton and thus shilding effect is observed

in case of all the allo conformers. The comparison of various signals observed in PMR spectrum of all these compounds are shown in table no. 3

Table 3 Comparison of chemical shift of different protons

	C-1	C-2	C-4	C-5	-OH
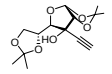 **Gluco (36)**	5.89 (3.5)	4.44	4.14	4.44	3.69
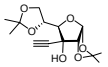 **Allo (37)**	5.80 (3.5)	4.60 (3.1)	3.82 (8.2)	4.42	3.11
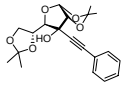 **Gluco (38)**	5.96 (3.7)	4.50 (3.5)	4.28 (3.4)	4.53 (6.3, 4.8)	3.74
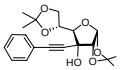 **Allo (39)**	5.85 (3.5)	4.67 (3.5)	3.96 (7.4)	4.46 (7.4, 5.9, 5.1)	3.12
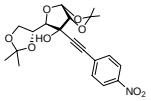 **Gluco (40)**	5.94 (3.5)	4.49 (3.5)	4.23 (5.8)	4.44 (6.1)	3.68
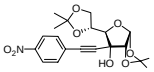 **Allo (41)**	5.87 (3.5)	4.70 (3.5)	3.96 (8.1)	4.44 (8.1, 4.9, 3.2)	3.24
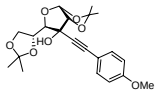 **Gluco (42)**	5.91 (3.5)	4.46 (3.4)	4.21	4.21	3.59
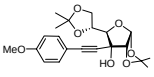 **Allo (43)**	5.87 (3.3)	4.68 (3.3)	3.99 (7.4)	4.53	3.15

Now that we had all the eight isomers in hand our next objective was to compare the hydrogen bonding patterns observed and study the distortion to be observed in the structure. To do so we crystallized all these isomers in the solvent mixture of ethyl acetate in pet ether with varying the ratio of polarity. Out of eight isomers both phenyl derivatives and the nitro aromatic derivative of gluco conformer failed to crystallize out. Remaining five compounds developed into fine crystals, which were subjected to crystallographic study.

For compound **36** the ORTEP diagram is shown in Figure 11. The graph set for this is $C_1^1(5)$ $C_1^1(6)$. The compound is crystallized in 25% ethyl acetate in petroleum ether. The compound crystallizes into fine needle crystals. A very strong hydrogen bonding pattern is observed between the free hydroxyl and the furanose ring oxygen and it forms a long chain when viewed down the skew axis *a*. Molecules of this alkyne derivative are linked into infinite chains along *c* by O-H···O hydrogen bonds of free hydroxyl group with furanoside oxygen.

Figure 11 ORTEP diagram for **36**

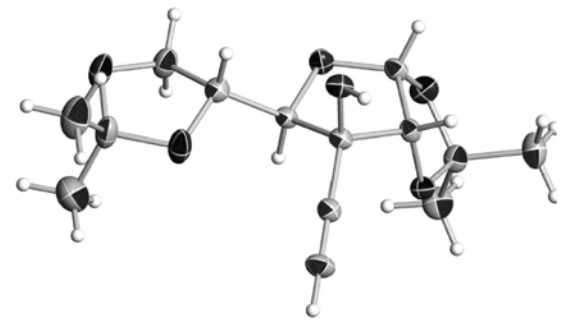

Table.4 Hydrogen bonds for **36**

D-H···A	d(D-H)	d(H···A)	d(D···A)	<(DHA)
O3-H···O4	0.820	2.049	2.855	167.69

In this case OH group acts as donor. The crystal point group is $P2_12_12_1$. As expected, the approach of hydrogen is dictated by the direction of lone pairs of donating oxygen present as the member of furanoside ring. Successive molecules in each hydrogen-bonded chain are related by the operations of a crystallographic 2_1 screw axis which runs parallel to *b*. When the structure is viewed along c axis it happens to look like a sheet. Various crystallographic parameters and various bond tables are included in Appendix A in this chapter.

Figure 12 Hydrogen bonding pattern observed in **36**

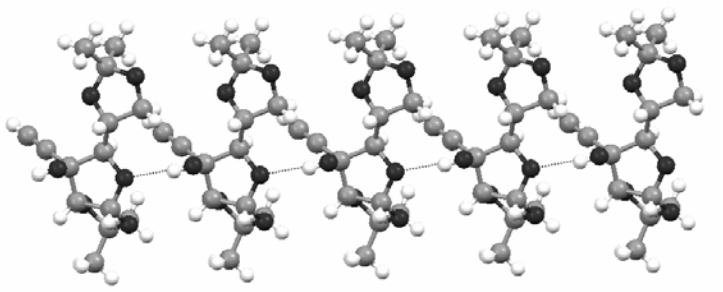

For compound **37** the ORTEP diagram is shown in Figure 13. The graph set for this is $C_1^1(5)$. The compound is crystallized in 25% ethyl acetate in petroleum ether. The compound crystallizes into fine flakes type crystals. A very strong hydrogen bonding pattern is observed between the free hydroxyl and the isopropylidine ring oxygen(C-1) and it forms a long chain when viewed down the skew axis *b*. Molecules of this alkyne derivative are linked into infinite chains along a by O-H···O hydrogen bonds of free hydroxyl group with isopropylidine ring oxygen(C1).

Figure 13 ORTEP diagram for **37**

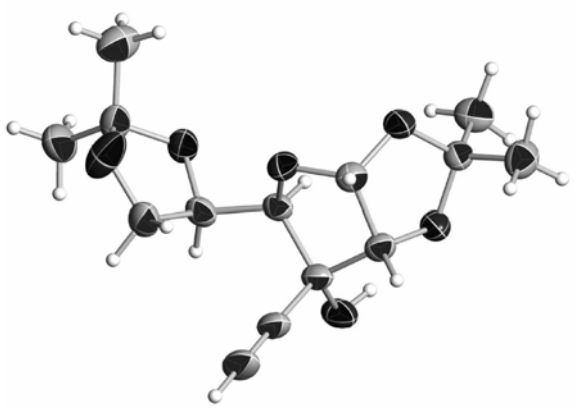

Table 5 Hydrogen bonds for **37**

D-H···A	d(D-H)	d(H···A)	d(D···A)	<(DHA)
O3-H···O1	0.820	2.578	3.224	136.72

In this case OH group acts as donor. The crystal point group is $P_{2_12_12_1}$. As expected, the approach of hydrogen is dictated by the direction of lone pairs of donating oxygen present as the member of isopropylidine ring. Successive molecules in each hydrogen-bonded chain are related by the operation of a crystallographic 2_1 screw axis which runs parallel to *a*. When the structure is viewed along c axis it happens to look like a helix wound anticlockwise

running downwords. Various crystallographic parameters and various bond tables are included in Appendix A in this chapter.

Figure 14 Hydrogen bonding pattern observed in **37**

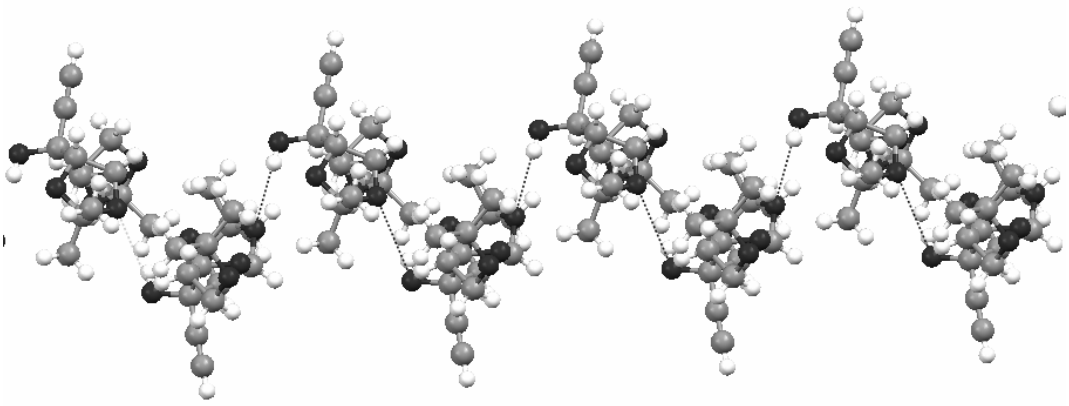

For compound **41** the ORTEP diagram is shown in Figure 15. The graph set for this is $C_1^1(6)$. The compound is crystallized in 20% ethyl acetate in petroleum ether. The compound crystallizes into diamond type crystals. A very strong hydrogen bonding pattern is observed between the free hydroxyl and the side chain oxygen (C-5) and it forms a long chain when viewed down the skew axis *a*. Molecules of this alkyne derivative are linked into infinite chains along *b* by O-H···O hydrogen bonds of free hydroxyl group with side chain oxygen (C-5). In this case OH group acts as donor. The crystal point group is $P2_12_12_1$. As expected, the approach of hydrogen is dictated by the direction of lone pairs of donating oxygen present as the member of furanoside ring. Successive molecules in each hydrogen-bonded chain are related by the operations of a crystallographic 2_1 screw axis which runs parallel to *b*. When the structure is viewed along *a* axis it happens to look like a helix wound anticlockwise running downwards. Various

Figure 15 ORTEP diagram for **41**

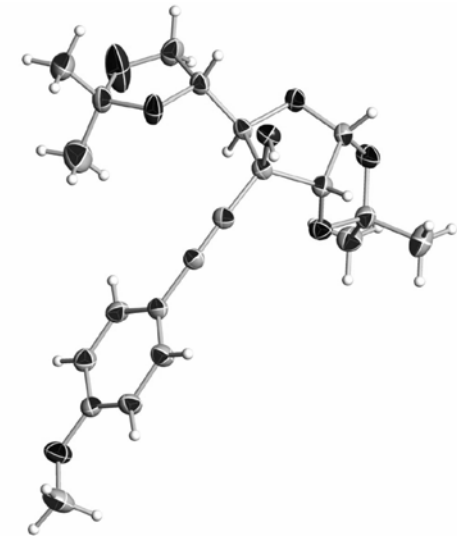

crystallographic parameters and various bond tables are included in Appendix A in this chapter.

Table.6 Hydrogen bonds for **41**

D-H···A	d(D-H)	d(H···A)	d(D···A)	<(DHA)
O3-H···O4	0.820	2.001	2.806	166.94

Figure 16 Hydrogen bonding pattern observed in **41**

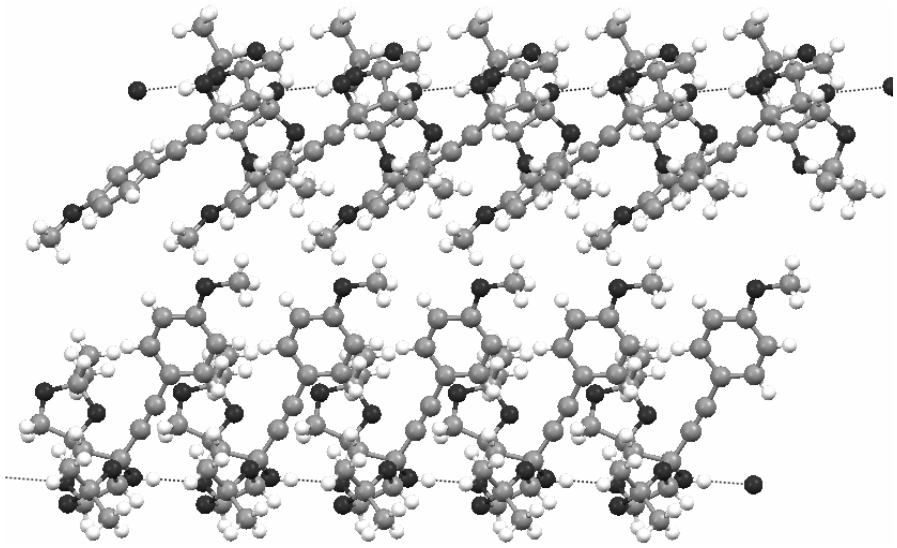

Figure 17 ORTEP diagram for **42**

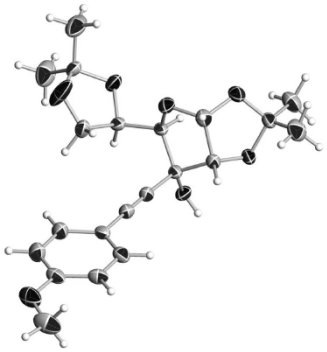

For compound **42** the ORTEP diagram is shown in Figure 16. The graph set for this is $C_1^1(5)$ $C_1^1(6)$. The compound is crystallized in 30% ethyl acetate in petroleum ether. The compound crystallizes into needle crystals. A very strong hydrogen bonding pattern is observed between the free hydroxyl and the furanose ring oxygen and it forms a long sheet when viewed down the skew axis *a*. Molecules of this alkyne derivative are linked into infinite chains along *b* by O-H···O hydrogen bonds of free hydroxyl group with furanose ring oxygen.

Table.7 Hydrogen bonds for **42**

D-H···A	d(D-H)	d(H···A)	d(D···A)	<(DHA)
O3-H···O2	0.820	2.003	2.816	171.39

In this case OH group acts as donor. The crystal point group is $P2_1$. As expected, the approach of hydrogen is dictated by the direction of lone pairs of donating oxygen present as the member of furanoside ring. Successive molecules in each hydrogen-bonded chain are related by the operations of a crystallographic 2_1 screw axis which runs parallel to *c*. When the structure is viewed along *a* axis it happens to look like a sheet. Various crystallographic parameters and various bond tables are included in Appendix A in this chapter.

Figure 18 Hydrogen bonding pattern observed in **42**

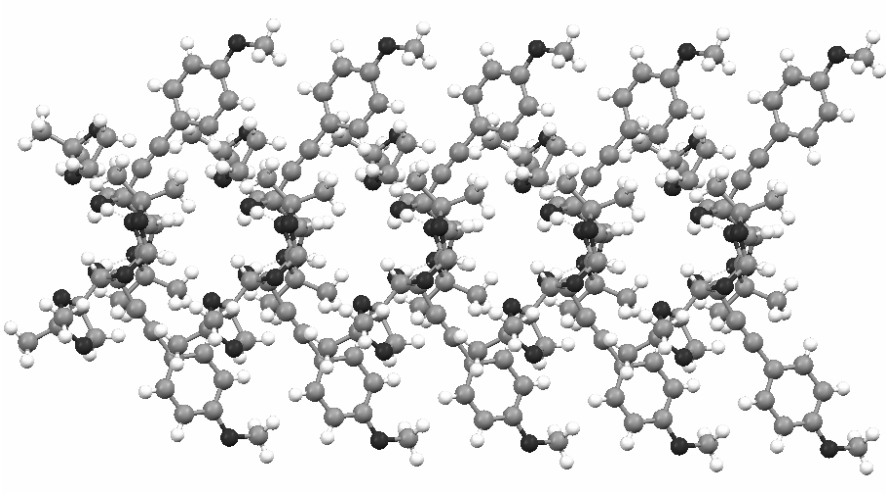

For compound **43** the ORTEP diagram is shown in Figure 18. The graph set for this is $D_1^1(4)$. The compound is crystallized in 30% ethyl acetate in petroleum ether. The compound crystallizes into needle crystals. A very strong hydrogen-bonding pattern is observed between the free hydroxyl and

Figure 19 ORTEP diagram for **43**

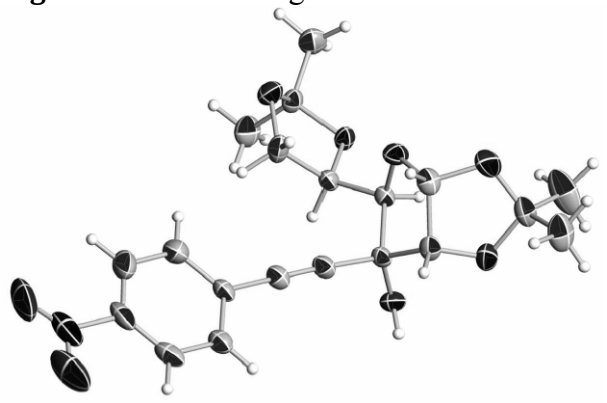

the isopropylidine ring oxygen (C-2) and it forms a dimer. Molecules of this alkyne derivative are linked into dimeric form by O-H···O hydrogen bonds of free hydroxyl group with isopropylidine ring oxygen (C-2). In this case OH group acts as donor. The crystal point group is $P2_12_12$. As expected, the approach of hydrogen is dictated by the direction of lone pairs of donating oxygen present as the member of isopropylidine ring (C-2). Various crystallographic parameters and various bond tables are included in Appendix A in this chapter.

Table 8 Hydrogen bonds for **43**

D-H···A	d(D-H)	d(H···A)	d(D···A)	<(DHA)
O3-H···O5	0.820	2.007	2.825	175.31

Figure 20 Hydrogen bonding pattern observed in **43**

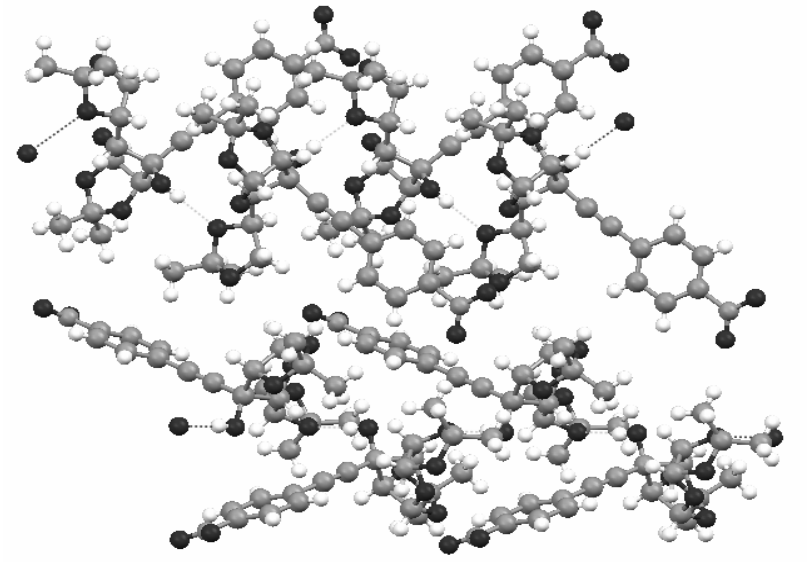

To conclude, our present investigation necessitates a study to understand the relationship between the hydrogen bonding motifs displayed by monoalchols and the properties of the solids that contain these motifs in carbohydrate systems. The free hydroxyl groups in carbohydrate derivatives are unique in being appended on an electron deficient cyclic ether framework, and closely located near to good hydrogen-bond donors as well hydrogen-bond acceptors. In all the crystal structures studied no hydrogen bonding is

observed between the O-H and the π-electron cloud of the alkyne functionality. This shows that in all the cases the alkyne and the hydroxyl proton prefer not to reside in a single plane. In any case no intramolecular hydrogen bonding is observed. The helical conformation observed in the starting precursors (**45**, **27**, **27a**) is not observed in any case. Except for **43**, rest all four crystal structures show chain formation with the help of hydrogen bonding and in case of **43** it tends to dimerize. Except for **37**, all the compounds show hydrogen bonding in the range of 2.8 Å (in case of **37** d(D···A) is 3.225Å). Interestingly in all the cases the O-H bond length is 0.82Å, which confirms that what ever may be the absolute stereochemistry of the alcohol the intramolecular hydrogen bonding do not occure between O3H···O2 in case of allo. These parameters probably act in the solid state but in liquid state probably some different do act resulting into shielding of hydroxyl proton (confirmed from the NMR).

One of the interesting feature is observed during the synthesis of these compounds is that the elimination reaction that takes place in presence of imidazole as base resulting into olefin formation. The process of analyzing the relationship between the hydrogen bonding and crystal structure properties in carbohydrate systems is under progress.

Experimental Work

3-deoxy-1,2,5,6-di-*O*-isopropylidine-3,3-C-[(methoxycarbonyl)methyllene]-α-D-ribofuranoside (31)

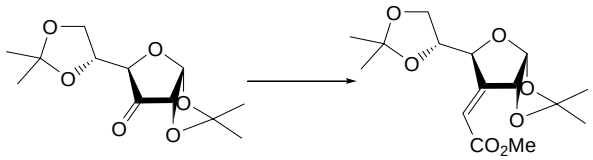

26 **31**

To the wittig yilide (14.33 g, 43 mmol), synthesized from methyl bromo acetate and triphenyl phosphene, in toluene (500 ml) ketone **26** (10 g, 39 mmol) was added and refluxed for 2h. Then the reaction mixture was filtered through celite, concentrated under reduced pressure and the crude product was purified by chromatography on silica gel (15% EtOAc in pet ether) to afford pure product **31** (7.18 g, 59%) as thick yellow syrup.

$[\alpha]_D^{25}$	+ 101.58 (c = 1.3, $CHCl_3$)
IR ($CHCl_3$):	υ: 1739 cm^{-1}
^{1}H NMR	δ: 1.36 (S, 3H), 1.41 (s, 3H), 1.44 (s, 3H), 1.50 (s, 3H), 3.79 (s, 3H), 3.95 – 4.10 (m, 3H), 4.64 (ddd, *J* = 7.5 Hz, 2.1 Hz, 1.3 Hz, 1H), 5.73 (dt, *J* = 4 Hz, 1.4 Hz, 1H), 5.82 (d, *J* = 4.1 Hz, 1H), 6.35 (dd, *J* = 2.2 Hz, 1.5 Hz, 1H)
^{13}C NMR	24.14, 25.45, 25.88, 26.08, 50.21, 65.98, 103.65, 108.71, 111.29, 116.0, 154.94, 163.93 ppm
Elemental Anal. $C_{15}H_{22}O_7$	Calcd: C: 56.63, H: 7.04 Found: C: 56.11, H: 7.08

3-deoxy-1,2,5,6-di-*O*-isopropylidine-3,3-C-[(hydroxymethyl)methyllene]-α-D-ribofuranoside (32)

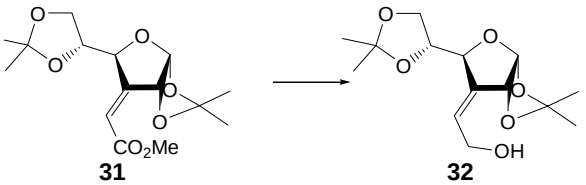

Ester **31**(3 g, 9.5 mmol) in DCM (30 ml) was cooled to -78 °C for 10 mins. DIBAl-H (16 ml, 23.8 mmol) was added slowly maintaining the internal temp. at -78 °C. The reaction was stirred for half hour. Methanol (0.8 ml) was added to this dropwise at -78 °C followed by saturated solution of sodium potassium tartarate dropwise till effervescence at 0 °C over a period of 2h. The reaction mixture was extracted in DCM and the aqueous layer was washed with three portions of DCM (25 ml). The combined organic extracts were dried (Na_2SO_4), evaporated under reduced pressure and the crude product was purified by chromatography on silica gel (25% EtOAc in pet ether) that afforded pure product **32** (2.38 g, 87%) as a colorless thick syrup.

$[\alpha]_D^{25}$	+ 130.65 (c = 1.3, $CHCl_3$)
IR ($CHCl_3$):	υ: 3345 cm^{-1}
^{1}H NMR	δ: 1.34 (S, 3H), 1.38 (s, 3H), 1.42 (s, 3H), 1.48 (s, 3H), 2.88 (bs, 1H), 3.88 – 4.06 (m, 3H), 4.32 (d, *J* = 6.5 Hz, 2H), 4.61 (d, *J* = 5.6 Hz, 1H), 5.21 (d, *J* = 4.4 Hz, 1H), 5.82 (d, *J* = 4.3 Hz, 1H), 6.1 (tt, *J* = 1.8 Hz, 6.2 Hz, 1H)
^{13}C NMR	25.17, 26.35, 27.09, 27.12, 59.58, 66.42, 77.28, 78.25, 79.7, 104.65, 109.52, 112.03, 127.8, 139.48 ppm
Elemental Anal.	Calcd: C: 58.73, H: 7.74
$C_{14}H_{22}O_6$	Found: C: 58.85, H: 6.80

3,1'-anhydro-(R-2-hydroxyethyl) 1,2,5,6-di-*O*-isopropylidine-α-D-glucofuranoside (33)

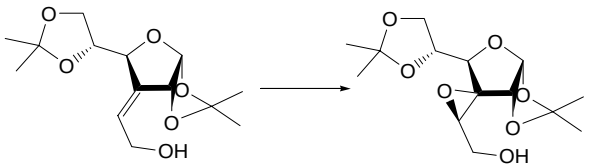

32 **33**

To alcohol **32** (1 g, 3.84 mmol) in DCM (10 ml) was added sodium carbonate (0.97 g, 11.52 mmol) in water (10 ml) at 0 °C. m-Chloro perbenzoic acid (1.81 g, 10.5 mmol) was added slowly in portions at 0 °C to avoid the effervescence. The reaction mixture was slowly warmed to room temperature and stirred for 2h. On completion the reaction mixture was filtered through celite, the filtrate was washed with water and the aqueous layer was extracted with fresh DCM. The combined organic extracts were dried (Na_2SO_4), evaporated under reduced pressure and the crude product thus obtained was purified by chromatography on silica gel (28% EtOAc in pet ether) to achieve pure product **33** (970 mg, 91%) as colorless thick syrup.

$[\alpha]_D^{25}$	+ 60.98 (c =1.3, $CHCl_3$)
^{1}H NMR	δ: 1.31 (s, 3H), 1.34 (s, 3H), 1.41 (s, 3H), 2.31 (bs, 1H), 3.53 (t, *J* = 5.6 Hz, 1H), 3.77 (dd, *J* = 5.7 Hz, 12.5 Hz, 1H), 3.91 (d, *J* = 5.4 Hz, 1H), 3.97 – 4.07 (m, 3H), 4.32 (dd, *J* = 5.7 Hz, 1.5 Hz, 1H), 4.54, (d, *J* = 4.2 Hz, 1H), 5.95 (d, *J* = 4.2 Hz, 1H)
^{13}C NMR	25.29, 26.50, 26.80, 26.91, 57.12, 62.03, 66.97, 68.72, 72.79, 77.00, 82.64, 104.33, 109.64, 112.51 ppm
Elemental Anal.	Calcd: C: 55.62, H: 7.33
$C_{14}H_{22}O_7$	Found: C: 55.45, H: 6.93

3-ethenyl-1,2,5,6-di-*O*-isopropylidine-α-D-glucofuranoside (35)

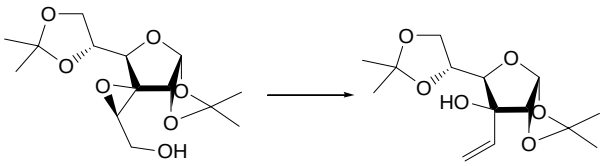

33 **35**

The epoxy alcohol **33** (1 g, 3.31 mmol) was mixed with triphenyl phosphene (0.868 g, 3.31 mmol), imidazole (0.424 g, 6.62 mmol) in toluene (10 ml). Freshly sublimed iodine (0.841 g, 3.31 mmol) was added at 100 °C and the reaction mixture was refluxed for 2h. On completion, the reaction mixture was filtered through celite, washed with EtOAc, the organic extracts were washed with 2% sodium thiosulfate solution and water, dried (Na_2SO_4), evaporated under reduced pressure and the crude product thus obtained was purified by chromatography on silica gel (25% EtOAc in pet ether) to obtain pure product **35** (930 mg, 98%) as a white solid.

M.p.:	75°
$[\alpha]_D^{25}$	+ 89.11 (c = 1.2, $CHCl_3$)
^{1}H NMR	δ: 1.31 (s, 3H), 1.33 (s, 3H), 1.41 (s, 3H), 1.53 (s, 3H), 3.20 (bs, 1H), 3.93 - 4.09 (m, 3H), 4.22 (d, *J* = 3.5 Hz, 1H), 4.39 (dt, *J* = 6.7 Hz, 4.7 Hz, 1H), 5.38 (dd, *J* = 10.7 Hz, 1.4 Hz, 1H), 5.60 (d, *J* = 17.4 Hz, 1.4 Hz, 1H), 5.93 (d, *J* = 3.5 Hz, 1H), 6.09 (dd, *J* = 17.4 Hz, 10.7 Hz, 1H)
^{13}C NMR	25.18, 26.32, 26.53, 27.07, 66.33, 74.37, 81.16, 81.90, 88.40, 104.64, 109.48, 112.34, 116.05, 136.07 ppm
Elemental Anal.	Calcd: C: 58.73, H: 7.74
$C_{14}H_{22}O_6$	Found: C: 55.86, H: 7.39

3,1'-anhydro-(R-2-chloroethyl)-1,2,5,6-di-*O*-isopropylidine-α-D-glucofuranoside (34)

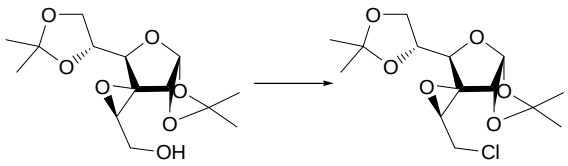

33 **34**

To the epoxy alcohol **33** (4.3 g, 14.2 mmol) in CCl_4 (50 ml) freshly crystallized triphenyl phosphene (7.5 g, 28.5 mmol) was added and the reaction mixture was refluxed for 10h. Then reaction mixture was allowed to cool to room temperature and quenched by addition of water. The reaction mixture was extracted in DCM, the organic layer was washed with water, dried (Na_2SO_4), evaporated under reduced pressure and the crude product thus obtained was purified by chromatography on silica gel (15% EtOAc in pet ether) to achieve pure product (4.29 g, 94%) as a thick colorless syrup.

$[\alpha]_D^{25}$	+105.41 (c = 1, $CHCl_3$)
^{1}H NMR	δ: 1.31 (s, 6H), 1.41 (s, 3H), 1.54 (s, 3H), 3.44 - 3.64 (m, 2H), 3.88 - 4.07 (m, 4H), 4.29 (dd, *J* = 6.19 Hz, 1.39Hz, 1H), 4.41 (d, *J* = 4.04 Hz, 1H), 5.92 (d, *J* = 4.04 Hz, 1H)
^{13}C NMR	25.18, 26.46, 26.73, 26.85, 43.26, 57.22, 66.87, 70.16, 72.54, 76.68, 82.44, 104.23, 109.63, 112.70 ppm
Elemental Anal.	Calcd: C: 52.42, H: 6.60
$C_{14}H_{21}ClO_6$	Found: C: 54.39, H: 6.57

3-ethynyl 1,2,5,6-di-*O*-isopropylidine-α-D-glucofuranoside 36

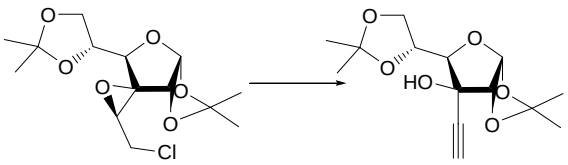

34 **36**

Epoxy chloride **34** (1 g, 3.12 mmol) was dissolved in THF (15 ml). n-BuLi (5ml, 9.36 mmol) was added dropwise to this at -78 °C. The reaction mixture is monitored by TLC and on completion saturated ammonium chloride solution was added dropwise to quench excess base. The reaction mixture was extracted in EtOAc, the organic layer was washed with brine, dried over Na_2SO_4, evaporated under reduced pressure and crude product was purified by chromatography on silica gel (25% EtOAc in pet ether) to obtain pure product as white crystalline solid in 72% yield.

M.p.:	75°
IR ($CHCl_3$):	υ: 3390, 3306, 3019, 2990, 2937, 2234, 1455, 1384, 1375, 1216, 1073, 998, 759 cm^{-1}.
$\mathbf{[\alpha]_D^{25}}$	+96.61 (c = 1, $CHCl_3$)
^{1}H NMR	δ: 1.36 (s, 3H), 1.38 (s, 3H), 1.50 (s, 3H), 1.56 (s, 3H), 2.68 (s, 1H), 3.69 (bs, 1H), 4.08 - 4.22 (m, 3H), 4.39 - 4.48 (m, 2H), 5.89 (d, J = 3.53 Hz, 1H)
^{13}C NMR	25.36, 26.57, 27.04, 66.57, 74.26, 75.39, 76.29, 80.50, 82.37, 86.88, 104.73, 109.95, 112.83 ppm
Elemental Anal.	Calcd: C: 59.14, H: 7.09
$\mathbf{C_{14}H_{20}O_6}$	Found: C: 62.08, H: 7.08

3-ethynyl 1,2,5,6-di-*O*-isopropylidine-α-D-allofuranoside 37

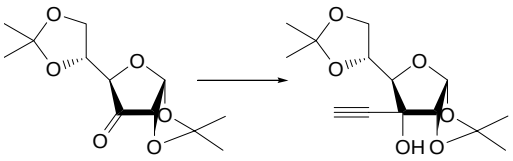

26 **37**

In a two neck RBF fitted with reflux condenser and gas bubbler magnesium was flame dried. Iodine followed by dry THF was added on cooling. The reaction mixture was refluxed for 15 mins. (half of the total qtt.) n-Chlorobutene was added in portions. When the reaction becomes vigorous it was cooled by ice water bath and rest of the chloro butane was added

dropwise. After complete generation of grignard (grey color appear and most of the magnesium consumed) acetylene gas was passed (through a setup of an empty trap, trap containing sulfuric acid and a separating funnel of NaOH) till a thick blackwash slurry was formed. Vigorous stirring was done at 0 °C and ketone was added slowly dropwise. After completion of the reaction (monitored by TLC) it was quenched with saturated ammonium chloride solution at 0 °C and stirred overnight. The reaction mixture was extracted in EtOAc, dried over sodium sulfate and the solvent was removed under reduced pressure. The crude product was purified by chromatographic technique using 20% EtOAc in pet ether. The final product was obtained as yellow crystalline solid, which was recrystallized from EtOAc pet ether in 75% yield.

M.P.	74 °C
IR ($CHCl_3$):	υ: 3390, 3306, 3019, 2990, 2937, 2234, 1455, 1384, 1375, 1216, 1073, 998, 759 cm^{-1}.
^{1}H NMR	δ: 1.37 (s, 6H), 1.46 (s, 3H), 1.60 (s, 3H), 2.66 (s, 1H), 3.11 (s, 1H), 3.82 (d, J = 8.22Hz, 1H), 4.02 (dd, J = 8.61, 4.70 Hz, 1H), 4.13 (dd, J = 8.6, 6.27 Hz, 1H), 4.37 - 4.47 (m, 1H), 4.60 (d, J = 3.13 Hz, 1H), 5.80 (d, J = 3.52 Hz, 1H)
^{13}C NMR	25.06, 26.61, 66.81, 74.65, 75.66, 76.85, 80.94, 84.08, 103.95, 109.44, 113.53 ppm
Elemental Anal. $C_{14}H_{20}O_6$	Calcd: C: 59.14, H: 7.09 Found:

General procedure for Sonogashira coupling

A solution of alkyne 1 (1.61 mmol), iodobenzene der. (1.34 mmol), Et_3N (6 ml), CuI (0.067 mmol), and Pd $(PPh_3)_2Cl_2$ (0.134 mmol) in DMF (3 ml) was flushed with Argon for 30 min and stirred at rt for 4 h. The reaction mixture was taken in EtOAc, washed with water, brine, dried over sodium sulfate, concentrated and purified by column chromatography (30% EtOAc in petroleum ether) to obtain coupling product.

3-phenylethynyl 1,2,5,6-di-*O*-isopropylidine-α-D-glucofuranoside 38

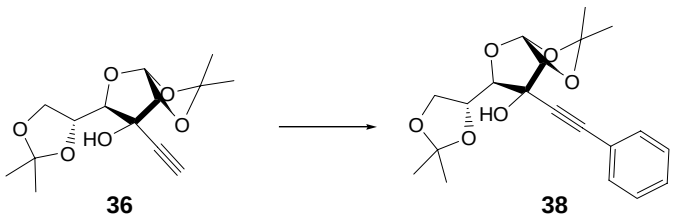

36 **38**

M.p.:	80 °C
$[\alpha]_D^{25}$	+161.3 (*c* 1, $CHCl_3$)
IR ($CHCl_3$):	υ: 3382, 3019, 2988, 2966, 2232, 1599, 1574, 1491, 1455, 1375, 1264, 1216, 1162, 1069, 872, 757 cm^{-1}.
^{1}H NMR	δ: 1.37 (s, 3H), 1.39 (s, 3H), 1.52 (s, 3H), 1.57 (s, 3H), 3.74 (bs, 1H), 4.17 (dd, J= 8.72, 6.57 Hz, 1H), 4.26 (dd, J= 8.59, 6.19 Hz, 1H), 4.28 (d, J= 3.54 Hz, 1H), 4.50 (d, J= 3.54 Hz, 1H), 4.53 (dd, J= 6.32, 4.80 Hz, 1H), 5.96 (d, J= 3.67 Hz, 1H), 7.34 (m, 5H)
^{13}C NMR	25.42, 26.73, 27.17, 66.85, 74.64, 82.53, 87.11, 96.19, 104.89, 109.95, 112.76, 128.27, 128.69, 131.82 ppm
Elemental Anal.	Calcd: 66.65, H: 6.71
$C_{20}H_{24}O_6$	Found: C: 65.98, H: 6.12

3-phenylethynyl 1,2,5,6-di-*O*-isopropylidine-α-D-allofuranoside 39

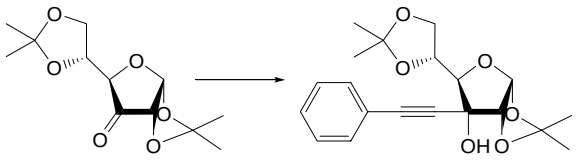

26 **39**

A two neck RBF fitted with septum and balloon adaptor was charged with phenyl acetylene 593 mg (5.8 mmol.) dwassolved in dry reagent grade THF. The solution was cooled to –78 °C and stirred under argon atmosphere. 2.9ml n-BuLi (4.6 mmol., 1.6 M in hexane) was added dropwise at -78 °C and the reaction mixture was stirred to generate lithium salt of

alkyne. Starting ketone 1gm (3.9 mmol.) was dwassolved in dry reagent grade THF and added to this lithium salt dropwise at -78 °C and the reaction mixture was stirred further for 1hr. The reaction was monitored by TLC and on completion it was quenched by sat. ammonium chloride. The reaction mixture was washed with water and extracted in EtOAc. The combined organic layers were washed with brine and dried over sodium sulfate. The solvent was removed under reduced pressure and the crude product was purified by chromatographic techniques to obtain pure product as a thick syrup in 75 % yield.

M.p.:	82 °C
IR ($CHCl_3$):	υ: 3382, 3019, 2988, 2966, 2232, 1599, 1574, 1491, 1455, 1375, 1264, 1216, 1162, 1069, 872, 757 cm^{-1}.
^{1}H NMR	δ: 1.38 (s, 3H), 1.39 (s, 3H), 1.47 (s, 3H), 1.62 (s, 3H), 3.12 (s, 1H), 3.96 (d, J= 7.43 hz, 1H), 4.08 (dd, J= 8.61, 5.08 Hz, 1H), 4.13 (dd, J= 8.61, 5.87 Hz, 1H), 4.46 (ddd, J= 7.43, 5.87, 5.08 Hz, 1H), 4.67 (d, J= 3.53 Hz, 1H), 5.85 (d, J= 3.53 Hz, 1H), 7.34 (m, 5H)
^{13}C NMR	26.55, 66.65, 74.80, 76.05, 81.52, 84.14, 85.73, 88.44, 104.07, 109.29, 113.47, 121.59, 128.18, 128.82, 131.66 ppm
Elemental Anal.	Calcd: 66.65, H: 6.71
$C_{20}H_{24}O_6$	Found: 66.25, H: 6.43

3-(4-nitrophenyl)ethynyl 1,2,5,6-di-*O*-isopropylidine-α-D-glucofuranoside 40

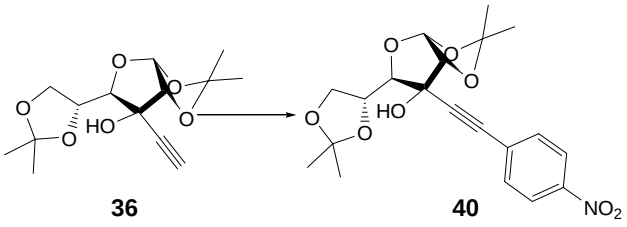

36 **40**

M.p.:	75 °C
$[\alpha]_D^{25}$	+89.0 (*c* 1, $CHCl_3$)

IR ($CHCl_3$): υ: 3398, 3020, 2991, 2938, 2349, 1595, 1520, 1493, 1455, 1375, 1216, 1164, 1070, 998, 755 cm^{-1}.

^{1}H NMR δ: 1.38 (s, 6H), 1.49 (s, 3H), 1.57 (s, 3H), 3.68 (bs, 1H), 4.19 (d, J= 5.94 Hz, 2H), 4.23 (d, J= 5.81 Hz, 1H), 4.44 (t, J= 6.07 Hz, 1H), 4.49 (d, J= 3.53 Hz, 1H), 5.94 (d, J= 3.53 Hz, 1H), 7.63 (d, J= 8.97 Hz, 1H), 8.22 (d, J= 8.97 Hz, 1H)

^{13}C NMR 26.64, 26.72, 27.11, 66.99, 74.31, 82.74, 85.80, 87.02, 91.14, 96.16, 104.94, 110.07, 112.94, 123.57, 129.05, 132.51, 147.47 ppm

Elemental Anal. Calcd: C: 59.25, H: 5.72, N: 3.46

$C_{20}H_{23}NO_8$ Found: C: 58.89, H: 5.42; N:3.50

3-(4-nitrophenyl)ethynyl 1,2,5,6-di-*O*-isopropylidine-α-D-allofuranoside 41

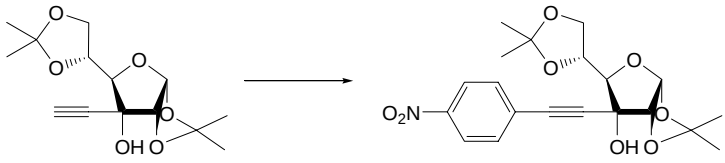

37 **41**

M.p.: 72 °C

$[\alpha]_D^{25}$ -20.52(c =1.5, $CHCl_3$)

IR ($CHCl_3$): υ: 3398, 3020, 2991, 2938, 2349, 1595, 1520, 1493, 1455, 1375, 1216, 1164, 1070, 998, 755 cm^{-1}.

^{1}H NMR δ: 1.38 (s, 3H), 1.40 (s, 3H), 1.49 (s, 3H), 1.64 (s, 3H), 3.24 (bs, 1H), 3.96 (d, J= 8.08 Hz, 1H), 4.10 (dd, J= 8.72, 4.8 Hz, 1H), 4.16 (dd, J= 8.72, 6.06 Hz, 1H), 4.44 (ddd, J= 8.08, 4.93, 3.15 Hz, 1H), 4.70 (d, J= 3.54 Hz, 1H), 5.87 (d, J= 3.54 Hz, 1H), 7.64 (dd, J= 6.95, 2.03 Hz, 2H), 8.19 (dd, J= 6.95, 1.90 Hz, 2H)

^{13}C NMR 25.08, 26.59, 26.69, 66.97, 74.82, 76.37, 81.03, 83.85, 86.39, 90.81, 104.04, 109.72, 113.80, 123.53, 128.24, 132.58, 147.50 ppm

Elemental Anal. Calcd: C: 59.25, H: 5.72, N: 3.46

$C_{20}H_{23}NO_8$ Found: C: 59.55, H: 5.69 N: 3.48

3-(4-methoxyphenyl)ethynyl 1,2,5,6-di-*O*-isopropylidine-α-D-glucofuranoside 42

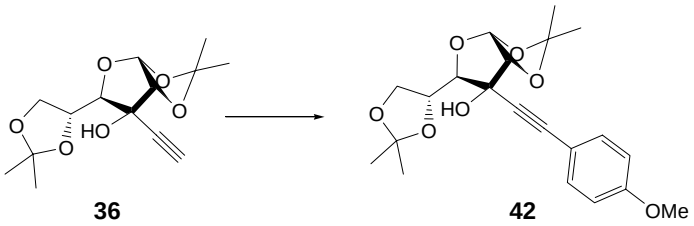

36 **42**

M.p.:	76 °C
$[\alpha]_D^{25}$	+70.5 (*c* 1, $CHCl_3$)
IR ($CHCl_3$):	υ: 3424, 2988, 2936, 2231, 1606, 1571, 1510, 1456, 1442, 1374, 1292, 1162, 998, 756 cm^{-1}
^{1}H NMR	δ: 1.36 (s, 3H), 1.38 (s, 3H), 1.50 (s, 3H), 1.56 (s, 3H), 3.59 (bs, 1H), 3.81 (s, 3H), 4.18 (dd, J= 8.47, 2.2 Hz, 2H), 4.21 (m, 2H), 4.46 (d, J= 3.41 Hz, 1H), 5.91 (d, J= 3.54 Hz, 1H), 6.80 (dd, J= 6.95, 2.2 Hz, 2H), 7.36 (dd, J= 6.95, 2.2 Hz, 2H)
^{13}C NMR	25.42, 26.67, 26.72, 27.15, 55.18, 66.76, 74.57, 76.11, 82.57, 84.24, 87.09, 87.97, 96.16, 104.86, 109.82, 112.70, 113.90, 114.38, 133.26, 159.93 ppm
Elemental Anal.	Calcd: C: 64.60, H: 6.71
$C_{21}H_{26}O_7$	Found: C: 53.78, H: 6.21

3-(4-methoxyphenyl)ethynyl 1,2,5,6-di-*O*-isopropylidine-α-D-allofuranoside 43

37 **43**

M.p.:	79 °C
$[\alpha]_D^{25}$	-7.11(c =1, $CHCl_3$)

IR ($CHCl_3$):	υ: 3424, 2988, 2936, 2231, 1606, 1571, 1510, 1456, 1442, 1374, 1292, 1162, 998, 756 cm^{-1}
^{1}H NMR	δ: 1.39 (s, 6H), 1.48 (s, 3H), 1.62 (s, 3H), 3.15 (bs, 1H), 3.82 (s, 3H), 3.99 (d, J= 7.45 Hz, 1H), 4.09 (dd, J= 5.18, 8.59 Hz, 1H), 4.17 (dd, J= 8.58, 6.32 Hz, 1H), 4.53 (m, 1H), 4.68 (d, J= 3.29 Hz, 1H), 5.87 (d, J= 3.29 Hz, 1H), 6.87 (d, J= 8.33 Hz, 2H), 7.41 (d, J= 8.34 Hz, 2H)
^{13}C NMR	26.59, 26.71, 29.65, 55.28, 66.88, 74.92, 76.24, 77.00, 81.36, 84.07, 84.15, 88.76, 104.21, 109.52, 113.58, 113.67, 113.95, 133.34, 160.10 ppm
Elemental Anal.	Calcd: C: 64.60, H: 6.71
$C_{21}H_{26}O_7$	Found: C: 65.93, H: 6.9

3,5:6,7-di-*O*-isopropylidene-D-*glycero*-D-*gulo*-heptonolactone 45

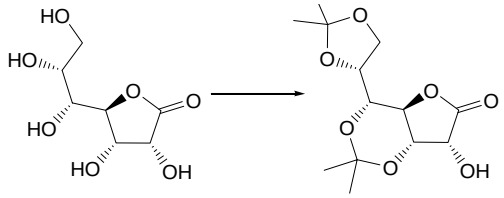

44 **45**

To a stirred slurry of **44** (260.0 g, 1.25 mol) in acetone (1870 ml) at 25 °C was added 2,2-dimethoxypropane (390 g, 461 ml, 3.75 mol). Sulfuric acid (28.2 g, 15.5 mL, 0.287 mol) was added at 0 °C, and the mixture was stirred for 8 h. The solution was quenched with 8% sodium bicarbonate (1157 ml, gas evolution). The mixture was stirred for 30 min at 10-15 °C (pH = 8-8.5) and then stored in a refrigerator for 8 h. The acetone and methanol were distilled under reduced pressure, ethyl acetate was added (2000 ml), and the mixture was stirred at 25 °C for 15 min. The organic layer was washed with dilute aqueous sodium chloride solution (966 ml), concentrated at ambient pressure to a residual volume of 500 ml. Heptane (1500 ml) was added at 65 °C. The slurry was cooled to 25 °C, held for 30 min, cooled to 0 °C, and held for 1 h. The solids were filtered and washed with heptane/ethyl acetate (3:1) containing 30 ppm of the antistatic agent Stadis 450 (2 X 100 ml). The product was dried at 45 °C to give **45** as a white crystalline solid (.7%).

M.p.:	89 °C
^{1}H NMR	δ: 1.35 (s,3H), 1.41 (s, 3H), 1.42 (s, 3H), 1.50 (s, 3H), 1.81 (bs, 1H), 3.07 (d, *J* = 9.93 Hz, 1H), 3.84 (dd, *J* = 1.99, 8.34 Hz, 1H), 3.90 (dd, *J* = 3.98, 8.74 Hz, 1H), 4.09 (dd, *J* = 6.36, 8.74 Hz, 1H), 4.30-4.32 (m, 2H), 4.48 (dd, *J* = 3.98, 9.14 Hz, 1H), 4.60 (dd, *J* = 1.98, 3.98 Hz, 1H)
^{13}C NMR	19.52, 24.88, 26.89, 28.86, 66.82, 68.19, 68.64, 69.44, 71.51, 73.02, 98.67, 109.54, 174.81 ppm
Elemental Anal.	Calcd: C: 54.16, H: 6.99
$C_{13}H_{20}O_7$	Found: C: 54.39, H: 7.21

References

1. (a) Schuster, P.; Zundel, G.; Sandorfy, C *The Hydrogen Bond*; *3 vols.;* North-Holland, Amsterdam, 1976. (b) Joesten, M.D.; Schaad, L.J. *Hydrogen Bonding*; Marcel Dekker, NY, 1974. (c) Meot-Ner, M. *Mol. Struct. Energ.;* **1987**, *4*, 71. (d) Deakyne, C.A. *Mol. Struct. Energ.;* **1987**, *4*, 105. (e) Joesten, M.D. *J. Chem. Educ.;* **1982**, *59*, 362. (f) Gur'yanova, E.N.; Gol'dshtein, I.P.; Perepelkova, T.I. *Russ. Chem. Rev.;* **1976**, *45*, 792. (g) Pimentel, G.C.; McClellan, A.L. *Annu. Rev. Phys. Chem.;* **1971**, *22*, 347. (h) Kollman, P.A.; Allen, L.C. *Chem. Rev.;* **1972**, *72*, 283. (i) Huggins, M.L. Angew. Chem. Int. Ed. Engl, 1971, 10, 147. (j) Rochester, C.H. in *Patai The Chemistry of the Hydroxyl Group*, pt. 1; Wiley: NY, **1971**, *327,* 328-369. (k) Hamilton, W.C.; Ibers, J.A. *Hydrogen Bonding in Solids*; W.A. Benjamin: NY, **1968**. (l) Chen, J.; McAllister, M.A.; Lee, J.K.; Houk, K.N. *J. Org. Chem.;* **1998**, *63*,4611
2. (a) Vinogradov, S.N.; Linnell, R.H. *Hydrogen bonding* van Nostrand Reinhold Company, NY, **1970**. (b) Desiraju, G. R.; Steiner, T. *The weak hydrogen bond in structural chemistry and Biology*, Oxford Univ. Press, **1998**.
3. Nakahara, M.; Wakai, C. *Chem. Lett*.; **1992**, 809
4. (a) Li, C. J.; Chen, T. H. *Organic Reactions in Aqueous Media*, Wiley, NY, **1997. (**b) Li, C. J. *Chem. Rev.;* **1993**, *93*, 2023.
5. Curtiss, L.A.; Blander, M. *Chem. Rev.;* **1988**, *88*, 827.
6. Hadzi, D.; Detoni, S. *Patai The Chemistry of Acid Derivatives*, pt. 1; Wiley: NY, **1979**, 213.
7. Emerson, M.T.; Grunwald, E.; Kaplan, M.L.; Kromhout, R.A. *J. Am. Chem. Soc*, **1960**, *82*, 6307.
8. Emsley, J. *Chem. Soc. Rev.* **1980**, *9*, 91.
9. Howard, J. A. K.; Hoy, V. J.; O'Hagan, D.; Smith, G. T. *Tetrahedron*, **1996**, *52*, 12613.
10. (a) Grech, E.; Nowicka-Scheibe, J.; Olejnik, Z.; Lis, T.; Pawelka, Z.; Malarski, Z.; Sobczyk, L. *J. Chem. Soc, Perkin Trans. 2*, **1996**, 343. (b) Steiner, T. *J. Chem. Soc, Perkin Trans. 2*, **1995**, 1315

11. (a) Pogorelyi, V.K.; Vishnyakova, T.B. *Russ. Chem. Rev.;* **1984**, *53*, 1154. (b) Epshtein, L.M. *Russ. Chem. Rev.;* **1979**, *48*, 854.
12. (a) Abraham, M. H.; Doherty, R. M.; Kamlet, M. J.; Taft, R. W. *Chem. Ber*, **1986**, 551. (b) Kamlet, M. J.; Abboud, J. M.; Taft, R. W. *Prog. Phys. Org. Chem.;* **1981**, *13*, 485. (c) Kamlet, M.J.; Abboud, J.M.; Abraham, M.H.; Taft, R.W. *J. Org. Chem.;* **1983**, *48*, 2877. (d) Laurence, C, Nicolet, P.; Helbert, M. *J. Chem. Soc, Perkin Trans. 2*, **1986**, 1081(e) Nicolet, P.; Laurence, C, Lucon, M. *J. Chem. Soc, Perkin Trans. 2*,**1987**, 483. (f) Abboud, J.M.; Roussel, C, Gentric, E.; Sraidi, K.; Lauransan, J.; Guiheneuf, G.; Kamlet, M.J.; Taft, R.W. *J. Org. Chem.;* **1988**, *53*, 1545. (g) Abraham, M. H.; Grellier, P. L.; Prior, D. V.; Morris, J. J.; Taylor, P.J. *J. Chem. Soc, Perkin Trans. 2*, **1990**, 521.
13. Kamlet, M. J.; Gal, J.; Maria, P.; Taft, R. W. *J. Chem. Soc, Perkin Trans. 2*, **1985**, 1583.
14. Allen, F. H.; Raithby, P. R.; Shields, G. P.; Taylor, R. *Chem. Commun.;* **1998**, 1043.
15. Joerg, S.; Drago, R. S.; Adams, J. *J. Chem. Soc, Perkin Trans. 2*, **1997**, 2431.
16. Stahl, N.; Jencks, W. P *J. Am. Chem. Soc*, **1986**, *108*, 4196.
17. Scheiner, S.; Wang, L. *J. Am. Chem. Soc*, **1993**, *115*, 1958.
18. (a) Etter, M.C. *Acc. Chem. Res.;* **1990**, *23*, 120. (b) Taylor, R.; Kennard, O. *Acc. Chem. Res.;* **1984**, *17*, 320.
19. Stewart, R. *The Proton: Applications to Organic Chemistry*; Academic Press: NY, **1985**, 148.
20. (a) Kroon, J.; Kanters, J. A.; van Duijneveldt-van de Rijdt, J. G. C. M.; van Duijneveldt, F. B.; Vliegenthart, J. A. *J. Mol. Struct*, **1975**, *24*, 109. (b) Ceccarelli, C, Jeffrey, G.A.; Taylor, R. *J. Mol. Struct.;* **1981**, *70*, 255. (c) Taylor, R.; Kennard, O.; Versichel, W. *J. Am. Chem. Soc*, **1983**, *105*, 5761; **1984**, *106*, 244.
21. Legon, A. C.; Millen, D. J. *Chem. Soc. Rev.;* **1987**, *16*, 467, *Acc. Chem. Res.;* **1987**, *20*, 39.
22. Pimentel, G. C.; McClellan, A. L. *The Hydrogen Bond*; W.H. Freeman: San Francisco, **1960**, 260.
23. Perrin, C.L.; Kim, Y. J. *J. Am. Chem. Soc*, **1998**, *120*, 12641.

24. Emsley, J.; Freeman, N. J.; Parker, R. J.; Dawes, H. M.; Hursthouse, M. B. *J. Chem. Soc, Perkin Trans. 1*, **1986**, 471.
25. (a) Taylor, R.; Kennard, O.; Versichel, W. *J. Am. Chem. Soc.;* **1984**, *106*, 244. (b) Jeffrey, G. A.; Mitra, J. *J. Am. Chem. Soc*.; **1984**, *106,* 5546. (c) Staab, H. A.; Elbl, K.; Krieger, C *Tetrahedron Lett.;* **1986**, *27*, 5719.
26. Hine, J.; Hahn, S.; Miles, D. E. *J. Org. Chem.;* **1986**, *51*, 577.
27. Caminati, W.; Fantoni, A. C.; Schafer, L.; Siam, K.; Van Alsenoy, C. *J. Am. Chem. Soc*.; **1986**, *108*, 4364.
28. Görbitz, C. H.; Etter, M. C. *J. Chem. Soc, Perkin Trans. 2*, **1992**, 131.
29. Steiner, T.; Tamm, M.; Lutz, B.; van der Maas, *J. Chem. Commun.;* **1996**, 1127.
30. Pauling, L. *Proc. Nat. Acad. Sci.;* 1928, *14***,** 359.
31. (a) Pimentel, G. C.; McClellan, A. L. *The Hydrogen Bond*, W. H Freeman, San Francisco, Calif.; **1960**.. (b) Bartoz, S. *Advan. Quantum Chem,* **1967***, 3*, 209.
32. (a) Lennard-Jones, J.; Pope, J. A. *Proc. Roy. Soc. Ser. A*, **1951**, *205*, 155. (b) Pople, J. A. *ibid.;* **1951**, *205*, 163.
33. Bader, R. F. W. *Can. J. Chem.;* **1964**, *42*, 1822.
34. (a) Latimer, W. M.; Rodeaush, W. H. *J. Am. Chem. Soc.* **1920**, *42*, 1419-1433.. (b) Schuster, P.; Zundel, G.; Sandorfv, C. *The Hydrogen Bond,* Vols. I-Ill. Amsterdam: North-Holland. **1976. (**c) Joesteiq, M. D.; Schaad, L. J. *Hydrogen Bonding.* New York: Marcel Dekker. **1974**
35. Wells, A. F. *Structural Inorganic Chemistry,* pp. 294-315. Oxford: Clarendon Press. **1962**
36. Coulson, C. A.; Danielson, U. *Ark. Fys.;* **1955**, *8*, 205, 239.
37. Tsubomura, H. *Bull. Chem. Jap.;* 1954, 27,445.
38. Puranik, P. G.; Kumar, V. *Proc. Indian Acad. Sci.;* **1963**, *58***,** 29, 327.
39. (a) Ducharme, Y.; Wuest, J. D. *J. Org. Chem.* **1988**, *53*, 5789-5791.. (b) Chang, S. K.; Hamilton, A. D. *J. Am. Chem. SOC.* **1988**, *110*, 1318-1319.. (c) Askew, B.; Ballester, P.; Buhr, C.; Jeong, K. S.; Jones, S.; Parris, K.; Williams, K.; Rebek, J.; Jr. *J. Am. Chem. SOC.* **1989**, *111*, 1082-1090,. (d) Stadler, R. Prog. Colloid *Polym. Sci.* **1987**, *75*, 140-145.

40. (a) Etter, M. C. *J. Phys. Chem.* **1991**, *95*, 4601-4618.. (b) Donohue J. *J. Phys. Chem.* **1952**, *56*, 502-510.. (c) Etter, M. C. *J. Am. Chem. SOC.* **1982**, *104*, 1095-1096.. (d) Etter, M. C. *Acc. Chem. Res.* **1990**, *23*, 120-126.
41. (a) Nowacki, W. *Helv. Chim. Acta* **1942**, *25*, 863-878.. (b) Nowacki, W. *Helv. Chim. Acta* **1943**, *26*, 459-462.. (c) Nowacki, W. *Helv. Chim. Acta* **1951**, *34*, 1957-1962.. (d) Nowacki, W. In Crystal Data; Donnay,J. D. H.; Nowacki, W.; Eds.; Geological Society of America: Boulder, CO, 1954; pp 85-104.. (e) Buergi, H.-B.; Dunitz, J. D. *Helv. Chim. Acta* **1993**, *76*, 1115-1166
42. Mackay, A. L. *Acta Crystallogr*. **1967**, *22*, 329-330.
43. a) Bernstein, J.; Etter, M. C.; Leiserowitz, L. *Structure Correlatio*n, Eds Bürgi H. -B.; Dunitz, J. D. vol. 2, pp. 432 – 507, VCH, Weinheim, Germany, **1994**; b) Brock, C. P.; Dunitz, J. D. *Chem. Mater*. **1994**, *6*, 1118 – 1127.
44. a) Bernstein, J.; Davis, R. E.; Shimoni, L.; Chang, N. L. *Angew. Chem.; Int. Ed. Engl*. **1995**, ***34***, 1555–1573; b) Etter, M. C. *Acc. Chem. Res*.; **1990**, *23*, 120–126; c) Etter, M. C. *J. Phys. Chem*. *1991*, *95*, 4601 – 4610; d) Etter, M. C.; MacDonald, J. C.; Bernstein, J. *Acta Crystallogr. Sect. B: Struct. Sci*. **1990**, *46*, 256 – 262.
45. Zhao, X.; Chang, Y. L.; Fowler, F. W.; Lauher, J. W. *J. Am. Chem. Soc.;* **1990**, *112*, 6627.
46. Tichy, M. *Adv. Org. Chem.;* **1965**, *5*, 115
47. Lees, W. A.; Burawoy, A. *Tetrahedron*, **1963**, *19*, 419.
48. (a) Davis Jr.; J. C.; Deb, K. K. *Adv. Magn. Reson.;* **1970**, *4*, 201. (b) Kumar, G.A.; McAllister, M.A. *J. Org. Chem.;* **1998**, *63*, 6968.
49. Etter, M. C.; Huang, K . S . *New Materials for Nonlinear Optics*; ACS Symposium Series, in press.
50. (a) Green, R. D. *Hydrogen Bonding by C—H Groups*; Wiley: NY, **1974**. See also, Taylor, R.; Kennard, O. J. Am. Chem. Soc, 1982, 104, 5063(b) Harlow, R. L.; Li, C.; Sammes, M. P. *J. Chem Soc, Perkin Trans. 1*, **1984**, 547. (c) Nakai, Y.; Inoue, K.; Yamamoto, G.; Oki, M. *Bull. Chem. Soc. Jap.;* **1989**, *62*, 2923. (d) Seiler, P.; Dunitz, J. D. *Helv. Chim. Acta*.; **1989**, *72*, 1125.

51. (a) Hopkinson, A. C.; *Patai The Chemistry of the Carbon-Carbon Triple Bond*, pt. 1, Wiley: NY, **1978**, 75. (b) DeLaat, A. M.; Ault, B. S. *J. Am. Chem. Soc*.; **1987**, *109*, 4232.
52. Streiner, T.; Ranters, J. A.; Kroon, J. *Chem. Comm.;* **1996**, 1277.
53. (a) Bakke, J. M.; Chadwick, D. J. *Acta Chem. Scand.; Ser. B*, **1988**, *42*, 223. (b) Atwood, J. L.; Hamada, F.; Robinson, K. D.; Orr, G. W.; Vincent, R. L. *Nature. (London*), **1991**, *349*, 683.
54. (a) Joris, L.; Schleyer, P. V. R.; Gleiter, R. *J. Am. Chem. Soc.;* **1968**, *90*, 327. (b) Yoshida, Z.; Ishibe, N.; Kusumoto, H. *J. Am. Chem. Soc.;* **1969**, *91*, 2279.
55. (a) McMurry, J. E.; Lectka, T.; Hodge, C. N. *J. Am. Chem. Soc*.; **1989**, *111*, 8867. (b) Sorensen, T. S.; Whitworth, S. M. *J. Am. Chem. Soc.;* **1990**, *112*, 8135.
56. McMurry, J. E.; Lectka, T. *Acc. Chem. Res.;* **1992**, *25*, 47.
57. Gallo, E. A.; Gelman, S. H. *Tetrahedron Lett.;* **1992**, *33*, 7485.
58. (a) Adams, H.; Harris, K. D. M.; Hembury, G. A.; Hunter, C. A.; Livingstone, D.; McCabe, J. F. *Chem. Comm.;* **1996**, 2531. (b) Steiner, T.; Starikov, E. B.; Tamm, M. *J. Chem. Soc, Perkin Trans. 2*, **1996**, 67.
59. Allen, F. H.; Howard, J. A. K.; Hoy, V. J.; Desiraju, G. R.; Reddy, D. S.; Wilson, C. C. *J. Am. Chem. Soc.;* **1996**, *118*, 4081.
60. Krajewski, J. W.; Gluzinski, P.; Banaszek, A.; Argay, G.; Kalman, A. *Carbohydr. Res.;* **1987**, *166*, 19.
61. Shalaby, M. A.; Fronczek, F. R.; Younathan, E. S. *Carbohydr. Res.;* **1994**, *261*, 203.
62. Watkins, S. F.; Kim, S. J.; Fronczek, F. R.; Voll, R. J.; Younathan, E. S. *Carbohydr. Res.;* **1990**, *197*, 33.
63. Koerner, Jr.; T. A. W.; Younathan, E. S.; Wander, J. D. *Carbohydr. Res.;* **1972**, *21*, 455.
64. Lis, T.; Weichsel, A. *Acra Crystallogr.; Sect. C*, **1987**, *43*, 1954.
65. Krajewski, J. W.; Gluzinski, P.; Pakulski, Z.; Zamojski, A.; Mishnev, A.; Kemme, A. *Carbohydr. Res.;* **1994**, *252*, 97.
66. (a) Hibbert, F.; Emsley, J. *Adv. Phys. Org. Chem.;* **1990**, *26*, 255. (b) Sadekov, I. D.; Minkin, V. I.; Lutskii, A. E. *Russ. Chem. Rev.;* **1970**, *39*, 179.

67. (a) Lehn, J.-M. *Angew. Chem. Int. Ed. Engl.* **1990**, *29*, 1304, (b) Fouquey, C.; Lehn, J.-M.; Levelut, A.-M. *Adv. Matter.* **1990**, *2*, 254, (c) Lehn, J.-M. *Pure & App. Chem.*, **1994**, *66*, 1961.

68. Desiraju, G. R. *Angew. Chem. Int. Ed. Engl.* **1995**, *34*, 2311.

69. Selected examples: (a) Modern Acetylene Chemistry (Eds.: P. J. Stang, F. Diederich), VCH, Weinheim, **1995**, (b) Marshall, J. A.; Wang, X. J. *J. Org. Chem.* **1992**, *57*, 1242, (c) Fox, M. E.; Li, C.; Marino, J. P. Jr.; Overman, L. E. *J. Am. Chem. Soc.* **1999**, *121*, 5467, (d) Myers, A. G.; Zheng, B. *J. Am. Chem. Soc.* **1996**, *118*, 4492, (e) Trost, B. M.; Krische, M. J. *J. Am. Chem. Soc.* **1999**, *121*, 6131, (f) Roush, W. R.; Sciotti, R. J. *J. Am. Chem. Soc.* **1994**, *116*, 6457, (g) Corey, E. J.; Cimprich, K. A. *J. Am. Chem. Soc.* **1994**, *116*, 3151, (h) Anand, N. K.; Carreira, E. M. *J. Am. Chem. Soc.* **2001**, *123*, 9687, (i) Pu, L. *Tetrahedron* **2003**, *59*, 9873.

70. (a) Steed, J.W.; Atwood, J. L. Supramolecular Chemistry, Wiley, Chichester, **2000**, (b) Madhavi, N. N. L.; Bilton, C.; Howard, J. A. K.; Allen, F. H.; Nangia, A.; Desiraju, G. R. *New J. Chem.* **2000**, *24*, 1, (c) Bilton, C.; Howard, J. A. K.; Manhavi, N. N. L.; Nangia, A.; Desiraju, G. R.; Allen, F. H.; Wilson, C. C. *Acta Crystallogr. Sect. B* **2000**, *56*, 1071, (d) Garcia, J. G.; Ramos, B.; Rodriguez, A. *Acta Crystallogr. Sect. C* **1995**, *51*, 2674, (e) Braga, D.; Grepioni, F.; Walther, D.; Heubach, K.; Schmidt, A.; Imhof, W.; Jrls, H. G.; Klettke, T. *Organometallics* **1997**, *16*, 4910, (f) Allen, F. H.; Howard, J. A. K.; Hoy, V. J.; Desiraju, G. R.; Reddy, D. S.; Wilson, C. C. *J. Am. Chem. Soc.* **1996**, *118*, 4081, (g) Madhavi, N. N. L.; Desiraju, G. R.; Bilton, C.; Howard, J. A. K.; Allen, F. H. *Acta Crystallogr. Sect. C* **2000**, *56*, 1359, (h) Banerjee, R.; Mondal, R.; Howard, J. A. K.; Desiraju, G. R. *Cryst. Growth Des.* **2006**, *6*, 999.

71. Hyacinth, M.; Chruszcz, M.; Lee, K. S.; Sabat, M.; Gao, G.; Pu, L. *Angew. Chem. Int. Ed.* **2006**, *45*, 5358.

Appendix

Table 1 Bond Lengths (Å) for different alkyne derivatives

	36	**37**	**41**	**42**	**43**
C(1) - C(2)	1.527(3)	1.521(3)	1.519(4)	1.529(3)	1.539(5)
C(1) - H(1)	0.98	0.98	0.98	0.98	0.98
C(10) - C(11)	1.506(3)	1.513(3)	1.504(4)	1.507(4)	1.494(5)
C(11) - H(11A)	0.96	0.96	0.96	0.96	0.96
C(11) - H(11B)	0.96	0.96	0.96	0.96	0.96
C(11) - H(11C)	0.96	0.96	0.96	0.96	0.96
C(12) - C(13)	1.504(4)	1.515(4)	1.496(3)	1.483(4)	1.482(5)
C(12) - H(12A)	0.96	0.96	0.96	0.96	0.96
C(12) - H(12B)	0.96	0.96	0.96	0.96	0.96
C(12) - H(12C)	0.96	0.96	0.96	0.96	0.96
C(13) - C(14)	1.511(4)	1.484(4)	1.507(4)	1.499(5)	1.473(5)
C(14) - H(14A)	0.96	0.96	0.96	0.96	0.96
C(14) - H(14B)	0.96	0.96	0.96	0.96	0.96
C(14) - H(14C)	0.96	0.96	0.96	0.96	0.96
C(2) - C(3)	1.531(3)	1.547(3)	1.533(3)	1.533(3)	1.548(4)
C(2) - H(2)	0.98	0.98	0.98	0.98	0.98
C(3) - C(4)	1.540(3)	1.538(3)	1.538(3)	1.545(3)	1.526(4)
C(3) - C(7)	1.471(3)	1.467(3)	1.471(3)	1.471(3)	1.478(4)
C(4) - C(5)	1.519(3)	1.511(3)	1.514(3)	1.512(3)	1.504(4)
C(4) - H(4)	0.98	0.98	0.98	0.98	0.98
C(5) - C(6)	1.505(3)	1.538(3)	1.524(3)	1.513(4)	1.525(4)
C(5) - H(5)	0.98	0.98	0.98	0.98	0.98
C(6) - H(6A)	0.97	0.97	0.97	0.97	0.97
C(6) - H(6B)	0.97	0.97	0.97	0.97	0.97
C(7) - C(8)	1.172(3)	1.171(3)	1.193(3)	1.188(3)	1.191(4)

C(9) - C(10)	1.513(3)	1.498(3)	1.499(4)	1.490(4)	1.493(5)
C(9) - H(9A)	0.96	0.96	0.96	0.96	0.96
C(9) - H(9B)	0.96	0.96	0.96	0.96	0.96
C(9) - H(9C)	0.96	0.96	0.96	0.96	0.96
O(1) - C(1)	1.399(2)	1.409(2)	1.390(3)	1.398(3)	1.414(4)
O(1) - C(10)	1.442(3)	1.424(3)	1.424(3)	1.434(3)	1.413(4)
O(2) - C(10)	1.430(2)	1.425(3)	1.417(3)	1.427(3)	1.436(4)
O(2) - C(2)	1.421(2)	1.412(2)	1.409(3)	1.418(3)	1.410(3)
O(3) - C(3)	1.418(2)	1.406(3)	1.403(3)	1.419(3)	1.405(3)
O(3) - H(3)	0.82	0.82	0.82	0.82	0.82
O(4) - C(1)	1.422(2)	1.406(3)	1.407(3)	1.421(3)	1.401(4)
O(4) - C(4)	1.447(2)	1.417(3)	1.423(3)	1.446(3)	1.423(4)
O(5) - C(13)	1.423(3)	1.412(3)	1.435(3)	1.410(3)	1.411(4)
O(5) - C(5)	1.418(3)	1.425(3)	1.440(3)	1.414(3)	1.425(4)
O(6) - C(13)	1.417(3)	1.406(3)	1.420(3)	1.394(4)	1.389(4)
O(6) - C(6)	1.424(3)	1.406(3)	1.427(3)	1.326(4)	1.369(4)
C(8) - H(8)	0.93	0.93			
C(8) - C(15)			1.444(3)	1.441(3)	1.436(4)
C(15) - C(16)			1.383(4)	1.384(3)	1.380(5)
C(15) - C(20)			1.382(4)	1.394(3)	1.384(5)
C(16) - C(17)			1.383(4)	1.384(4)	1.398(5)
C(16) - H(16)			0.93	0.93	0.93
C(17) - C(18)			1.354(4)	1.379(4)	1.381(5)
C(17) - H(17)			0.93	0.93	0.93
C(18) - C(19)			1.367(5)	1.379(3)	1.365(5)
C(19) - C(20)			1.389(4)	1.368(4)	1.365(5)
C(19) - H(19)			0.93	0.93	0.93
C(20) - H(20)			0.93	0.93	0.93
N(1) - C(18)			1.486(4)		
O(7) - N(1)			1.189(5)		
O(8) - N(1)			1.239(5)		

C(21) - H(21A)	0.96	0.96
C(21) - H(21B)	0.96	0.96
C(21) - H(21C)	0.96	0.96
O(7) - C(18)	1.367(3)	1.359(4)
O(7) - C(21)	1.407(4)	1.391(5)

Symmetry transformations used to generate equivalent atoms.

Table 2 Bond Angles (deg.) for different alkyne derivatives.

	36	**37**	**41**	**42**	**43**
C(1) - C(2) - C(3)	103.61(15)	104.40(16)	104.02(19)	104.27(18)	103.2(2)
C(1) - C(2) - H(2)	112.6	113	112.9	112.3	112.4
C(1) - O(1) - C(10)	108.94(15)	109.86(15)	110.3(2)	109.22(17)	109.2(3)
C(1) - O(4) - C(4)	110.13(14)	108.21(15)	109.84(18)	110.89(16)	107.0(2)
C(10) - C(11) - H(11A)	109.5	109.5	109.5	109.5	109.5
C(10) - C(11) - H(11B)	109.5	109.5	109.5	109.5	109.5
C(10) - C(11) - H(11C)	109.5	109.5	109.5	109.5	109.5
C(10) - C(9) - H(9A)	109.5	109.5	109.5	109.5	109.5
C(10) - C(9) - H(9B)	109.5	109.5	109.5	109.5	109.5
C(10) - C(9) - H(9C)	109.5	109.5	109.5	109.5	109.5
C(11) - C(10) - C(9)	113.1(2)	113.0(2)	112.7(3)	113.2(2)	113.0(3)
C(12) - C(13) - C(14)	113.4(3)	112.7(2)	113.0(2)	112.2(3)	112.5(4)
C(13) - C(12) - H(12A)	109.5	109.5	109.5	109.5	109.5
C(13) - C(12) - H(12B)	109.5	109.5	109.5	109.5	109.5
C(13) - C(12) - H(12C)	109.5	109.5	109.5	109.5	109.5
C(13) - C(14) - H(14A)	109.5	109.5	109.5	109.5	109.5
C(13) - C(14) - H(14B)	109.5	109.5	109.5	109.5	109.5
C(13) - C(14) - H(14C)	109.5	109.5	109.5	109.5	109.5
C(13) - O(6) - C(6)	106.66(16)	109.4(2)	106.67(18)	113.3(2)	111.5(3)
C(2) - C(1) - H(1)	110.9	111	110.7	111.2	111.3

C(2) - C(3) - C(4)	101.29(14)	99.84(16)	100.22(18)	101.51(17)	100.4(2)
C(2) - O(2) - C(10)	106.55(15)	108.94(16)	108.4(2)	106.60(17)	107.1(2)
C(3) - C(2) - H(2)	112.6	113	112.9	112.3	112.4
C(3) - C(4) - H(4)	109.9	108	108.9	109.8	107.8
C(3) - O(3) - H(3)	109.5	109.5	109.5	109.5	109.5
C(4) - C(5) - H(5)	109.8	109.5	108.7	109.4	108.9
C(5) - C(4) - C(3)	115.27(15)	118.05(16)	114.55(19)	115.47(19)	117.9(2)
C(5) - C(4) - H(4)	109.9	108	108.9	109.8	107.8
C(5) - C(6) - H(6A)	111.5	110.8	110.7	110.5	110.6
C(5) - C(6) - H(6B)	111.5	110.8	110.7	110.5	110.6
C(5) - O(5) - C(13)	108.20(17)	110.22(15)	106.68(17)	110.50(19)	109.0(2)
C(6) - C(5) - C(4)	117.15(17)	116.97(19)	117.3(2)	115.3(2)	118.1(3)
C(6) - C(5) - H(5)	109.8	109.5	108.7	109.4	108.9
C(7) - C(3) - C(2)	113.95(16)	110.17(19)	108.6(2)	112.82(19)	106.1(2)
C(7) - C(3) - C(4)	113.13(16)	112.62(18)	113.09(19)	112.12(19)	113.9(3)
C(7) - C(8) - H(8)	180	180			
C(8) - C(7) - C(3)	179.2(2)	178.1(3)	176.9(3)	175.2(2)	172.3(4)
H(11A) - C(11) - H(11B)	109.5	109.5	109.5	109.5	109.5
H(11A) - C(11) - H(11C)	109.5	109.5	109.5	109.5	109.5
H(11B) - C(11) - H(11C)	109.5	109.5	109.5	109.5	109.5
H(12A) - C(12) - H(12B)	109.5	109.5	109.5	109.5	109.5
H(12A) - C(12) - H(12C)	109.5	109.5	109.5	109.5	109.5
H(12B) - C(12) - H(12C)	109.5	109.5	109.5	109.5	109.5
H(14A) - C(14) - H(14B)	109.5	109.5	109.5	109.5	109.5
H(14A) - C(14) - H(14C)	109.5	109.5	109.5	109.5	109.5
H(14B) - C(14) - H(14C)	109.5	109.5	109.5	109.5	109.5
H(6A) - C(6) - H(6B)	109.3	108.9	108.8	108.7	108.8
H(9A) - C(9) - H(9B)	109.5	109.5	109.5	109.5	109.5
H(9A) - C(9) - H(9C)	109.5	109.5	109.5	109.5	109.5
H(9B) - C(9) - H(9C)	109.5	109.5	109.5	109.5	109.5
O(1) - C(1) - C(2)	105.77(15)	105.57(17)	105.3(2)	105.42(18)	103.9(3)

O(1) - C(1) - H(1)	110.9	111	110.7	111.2	111.3
O(1) - C(1) - O(4)	111.04(16)	110.70(17)	112.0(2)	110.73(18)	111.0(3)
O(1) - C(10) - C(11)	109.49(19)	109.5(2)	109.0(3)	109.7(2)	111.5(3)
O(1) - C(10) - C(9)	109.51(19)	109.36(19)	110.0(3)	109.1(2)	109.7(3)
O(2) - C(10) - C(11)	109.18(18)	110.59(19)	110.8(3)	110.7(2)	110.0(3)
O(2) - C(10) - C(9)	111.02(19)	108.68(19)	108.3(2)	109.6(2)	108.4(3)
O(2) - C(10) - O(1)	104.14(15)	105.41(15)	105.9(2)	104.21(17)	103.8(2)
O(2) - C(2) - C(1)	102.60(15)	104.62(17)	103.7(2)	102.97(17)	104.8(2)
O(2) - C(2) - C(3)	112.17(15)	108.19(17)	109.6(2)	112.07(18)	110.9(3)
O(2) - C(2) - H(2)	112.6	113	112.9	112.3	112.4
O(3) - C(3) - C(2)	107.10(15)	113.98(17)	116.0(2)	107.64(18)	116.0(2)
O(3) - C(3) - C(4)	107.52(15)	112.42(18)	107.29(19)	107.76(18)	107.4(2)
O(3) - C(3) - C(7)	112.99(16)	107.77(18)	111.33(19)	114.11(18)	112.7(3)
O(4) - C(1) - C(2)	107.04(15)	107.35(17)	107.24(19)	106.74(17)	108.0(3)
O(4) - C(1) - H(1)	110.9	111	110.7	111.2	111.3
O(4) - C(4) - C(3)	103.73(14)	104.22(16)	104.36(18)	103.96(16)	104.4(3)
O(4) - C(4) - C(5)	107.83(15)	110.08(16)	111.12(19)	107.76(18)	110.5(3)
O(4) - C(4) - H(4)	109.9	108	108.9	109.8	107.8
O(5) - C(13) - C(12)	110.3(2)	108.5(2)	109.4(2)	108.9(3)	109.4(3)
O(5) - C(13) - C(14)	108.1(2)	110.3(3)	110.9(2)	108.2(3)	111.1(3)
O(5) - C(5) - C(4)	108.01(16)	107.70(15)	109.42(18)	109.48(19)	108.1(2)
O(5) - C(5) - C(6)	101.95(18)	103.47(18)	103.6(2)	103.7(2)	103.5(3)
O(5) - C(5) - H(5)	109.8	109.5	108.7	109.4	108.9
O(6) - C(13) - C(12)	108.1(2)	107.0(3)	108.7(2)	111.9(3)	107.1(4)
O(6) - C(13) - C(14)	110.4(3)	113.3(2)	111.3(2)	110.0(3)	111.1(3)
O(6) - C(13) - O(5)	106.31(18)	104.57(17)	103.08(17)	105.3(2)	105.4(3)
O(6) - C(6) - C(5)	101.52(18)	104.64(18)	105.2(2)	106.3(2)	105.5(3)
O(6) - C(6) - H(6A)	111.5	110.8	110.7	110.5	110.6
O(6) - C(6) - H(6B)	111.5	110.8	110.7	110.5	110.6
C(7) - C(8) - C(15)			178.6(3)	174.2(3)	178.7(4)
C(15) - C(16) - H(16)			119.9	119.3	119.7

C(15) - C(20) - H(20)	120.1	119.5	119.4
C(16) - C(15) - C(20)	119.7(3)	117.6(2)	118.3(3)
C(16) - C(15) - C(8)	119.5(2)	123.1(2)	120.2(3)
C(16) - C(17) - H(17)	120.5	120.1	120.3
C(17) - C(16) - C(15)	120.2(3)	121.4(3)	120.6(3)
C(17) - C(16) - H(16)	119.9	119.3	119.7
C(17) - C(18) - C(19)	122.4(3)	119.3(2)	119.8(3)
C(18) - C(17) - C(16)	119.0(3)	119.9(2)	119.3(4)
C(18) - C(17) - H(17)	120.5	120.1	120.3
C(18) - C(19) - H(19)	120.6	119.6	119.7
C(18) - O(7) - C(21)		118.9(2)	119.1(4)
C(19) - C(20) - C(15)	119.8(3)	121.1(2)	121.1(4)
C(19) - C(20) - H(20)	120.1	119.5	119.4
C(20) - C(15) - C(8)	120.8(3)	119.3(2)	121.5(3)
C(20) - C(19) - C(18)	118.8(3)	120.7(2)	120.7(4)
C(20) - C(19) - H(19)	120.6	119.6	119.7
H(21A) - C(21) - H(21B)		109.5	109.5
H(21A) - C(21) - H(21C)		109.5	109.5
H(21B) - C(21) - H(21C)		109.5	109.5
O(7) - C(18) - C(17)		125.4(2)	124.1(4)
O(7) - C(18) - C(19)		115.4(2)	116.1(4)
O(7) - C(21) - H(21A)		109.5	109.5
O(7) - C(21) - H(21B)		109.5	109.5
O(7) - C(21) - H(21C)		109.5	109.5
C(19) - C(18) - N(1)	117.7(4)		
C(17) - C(18) - N(1)	119.8(4)		
O(7) - N(1) - C(18)	118.7(5)		
O(7) - N(1) - O(8)	125.9(4)		
O(8) - N(1) - C(18)	115.4(4)		

Symmetry transformations used to generate equivalent atoms.

Table 3 Torsion Angles (deg.) for different alkyne derivatives.

	36	**37**	**41**	**42**	**43**
C(1) - C(2) - C(3) - C(4)	33.08(18)	25.64(19)	31.0(2)	31.3(2)	25.2(3)
C(1) - C(2) - C(3) - C(7)	154.87(16)	93.0(2)	87.7(2)	151.44(18)	93.6(3)
C(1) - C(2) - C(3) - O(3)	79.41(17)	145.70(17)	146.1(2)	81.8(2)	140.5(3)
C(1) - O(1) - C(10) - C(11)	137.95(18)	100.7(2)	109.6(3)	96.0(2)	87.2(3)
C(1) - O(1) - C(10) - C(9)	97.5(2)	135.0(2)	126.4(2)	139.5(2)	146.8(3)
C(1) - O(1) - C(10) - O(2)	21.3(2)	18.3(2)	9.6(3)	22.5(2)	31.1(3)
C(1) - O(4) - C(4) - C(3)	27.58(18)	38.43(19)	30.7(2)	26.2(2)	40.1(3)
C(1) - O(4) - C(4) - C(5)	150.28(16)	165.96(15)	154.6(2)	149.20(18)	167.9(2)
C(10) - O(1) - C(1) - C(2)	1.1(2)	5.7(2)	6.1(3)	3.1(2)	16.4(4)
C(10) - O(1) - C(1) - O(4)	116.88(17)	121.53(18)	110.2(2)	118.2(2)	132.2(3)
C(10) - O(2) - C(2) - C(1)	33.08(18)	20.9(2)	25.9(2)	31.8(2)	23.8(3)
C(10) - O(2) - C(2) - C(3)	143.66(16)	131.74(17)	136.5(2)	143.31(19)	134.5(3)
C(13) - O(5) - C(5) - C(4)	151.53(19)	136.1(2)	148.76(19)	119.6(2)	142.3(3)
C(13) - O(5) - C(5) - C(6)	27.5(2)	11.6(3)	23.0(2)	3.9(3)	16.2(4)
C(13) - O(6) - C(6) - C(5)	35.5(2)	21.4(3)	23.0(3)	10.3(4)	11.2(5)
C(2) - C(3) - C(4) - C(5)	154.72(15)	161.13(17)	159.3(2)	152.74(19)	162.9(3)
C(2) - C(3) - C(4) - O(4)	37.08(17)	38.69(18)	37.6(2)	34.9(2)	39.8(3)
C(2) - C(3) - C(7) - C(8)	98(15)	33(9)	60(5)	45(3)	4(3)
C(2) - O(2) - C(10) - C(11)	151.29(17)	93.7(2)	95.2(3)	83.5(2)	85.4(3)
C(2) - O(2) - C(10) - C(9)	83.3(2)	141.8(2)	140.7(3)	150.9(2)	150.6(3)
C(2) - O(2) - C(10) - O(1)	34.42(18)	24.6(2)	22.8(3)	34.3(2)	34.0(3)
C(3) - C(4) - C(5) - C(6)	174.94(19)	81.7(2)	86.3(3)	168.3(2)	71.9(4)
C(3) - C(4) - C(5) - O(5)	70.8(2)	162.38(17)	156.15(19)	51.9(3)	171.1(3)
C(4) - C(3) - C(7) - C(8)	147(15)	143(9)	170(5)	69(3)	106(3)
C(4) - C(5) - C(6) - O(6)	155.80(18)	112.4(2)	120.7(2)	111.2(3)	122.7(4)
C(4) - O(4) - C(1) - C(2)	6.2(2)	21.0(2)	10.1(3)	6.0(2)	22.8(3)
C(4) - O(4) - C(1) - O(1)	108.83(17)	93.73(19)	104.9(2)	108.3(2)	90.4(3)
C(5) - O(5) - C(13) - C(12)	110.6(2)	138.7(2)	153.1(2)	118.4(3)	137.9(3)

C(5) - O(5) - C(13) - C(14)	124.9(3)	97.4(2)	81.7(2)	119.4(3)	97.2(4)
C(5) - O(5) - C(13) - O(6)	6.3(3)	24.7(3)	37.6(2)	1.7(3)	23.1(4)
C(6) - O(6) - C(13) - C(12)	137.7(2)	143.8(3)	153.4(2)	110.3(4)	137.8(4)
C(6) - O(6) - C(13) - C(14)	97.7(2)	91.4(3)	81.5(2)	124.3(4)	99.0(4)
C(6) - O(6) - C(13) - O(5)	19.3(3)	28.7(3)	37.4(2)	7.9(4)	21.4(5)
C(7) - C(3) - C(4) - C(5)	82.9(2)	44.3(3)	43.9(3)	86.6(2)	50.1(4)
C(7) - C(3) - C(4) - O(4)	159.44(15)	78.1(2)	77.8(2)	155.60(18)	73.1(3)
O(1) - C(1) - C(2) - C(3)	136.36(15)	122.81(17)	134.0(2)	134.71(18)	120.9(3)
O(1) - C(1) - C(2) - O(2)	19.49(19)	9.2(2)	19.4(2)	17.5(2)	4.8(3)
O(2) - C(2) - C(3) - C(4)	76.86(18)	85.37(18)	79.4(2)	79.4(2)	86.6(3)
O(2) - C(2) - C(3) - C(7)	44.9(2)	155.97(17)	161.9(2)	40.8(3)	154.7(3)
O(2) - C(2) - C(3) - O(3)	170.65(14)	34.7(2)	35.7(3)	167.56(16)	28.8(4)
O(3) - C(3) - C(4) - C(5)	42.5(2)	77.7(2)	79.2(2)	39.8(2)	75.4(3)
O(3) - C(3) - C(4) - O(4)	75.10(16)	159.88(16)	159.03(17)	78.0(2)	161.4(2)
O(3) - C(3) - C(7) - C(8)	24(15)	92(9)	69(5)	168(3)	132(3)
O(4) - C(1) - C(2) - C(3)	17.89(19)	4.7(2)	14.6(3)	16.9(2)	3.1(3)
O(4) - C(1) - C(2) - O(2)	98.98(16)	108.91(19)	100.1(2)	100.25(19)	113.1(3)
O(4) - C(4) - C(5) - C(6)	59.6(2)	37.7(2)	31.6(3)	76.0(3)	48.1(4)
O(4) - C(4) - C(5) - O(5)	173.92(16)	78.2(2)	85.9(2)	167.59(18)	68.9(3)
O(5) - C(5) - C(6) - O(6)	38.2(2)	5.8(3)	0.1(3)	8.5(3)	3.3(4)
C(15) - C(16) - C(17) - C(18)			1.6(4)	1.9(4)	0.4(5)
C(16) - C(15) - C(20) - C(19)			0.0(4)	1.4(4)	3.1(6)
C(16) - C(17) - C(18) - C(19)			1.3(5)	0.1(4)	3.4(5)
C(17) - C(18) - C(19) - C(20)			0.3(5)	1.2(4)	3.1(6)
C(18) - C(19) - C(20) - C(15)			0.4(5)	0.5(4)	0.2(6)
C(20) - C(15) - C(16) - C(17)			1.0(4)	2.6(4)	2.7(5)
C(3) - C(7) - C(8) - C(15)			42(15)	33(5)	139(17)
C(7) - C(8) - C(15) - C(16)			47(12)	146(2)	104(18)
C(7) - C(8) - C(15) - C(20)			133(12)	31(3)	77(18)
C(8) - C(15) - C(16) - C(17)			178.8(2)	174.2(2)	178.2(3)
C(8) - C(15) - C(20) - C(19)			179.7(3)	175.5(2)	177.8(4)

O(7) - C(18) - C(19) - C(20)		177.4(2)	177.4(4)
C(16) - C(17) - C(18) - O(7)		178.4(2)	177.2(3)
C(21) - O(7) - C(18) - C(17)		6.3(4)	4.1(5)
C(21) - O(7) - C(18) - C(19)		175.3(3)	176.4(4)
O(7) - N(1) - C(18) - C(17)	169.8(3)		
O(7) - N(1) - C(18) - C(19)	9.8(5)		
O(8) - N(1) - C(18) - C(17)	11.1(5)		
O(8) - N(1) - C(18) - C(19)	169.2(3)		
C(16) - C(17) - C(18) - N(1)	178.4(3)		
N(1) - C(18) - C(19) - C(20)	179.4(3)		

Symmetry transformations used to generate equivalent atoms.

Table 4 Bond angles of mirror image sheet for compound **45**

C(1') - C(2') - C(3')	103.43(17)	**H(14E) - C(14') - H(14D)**	109.5
C(1') - C(2') - H(2')	112.4	**H(14F) - C(14') - H(14D)**	109.5
C(1') - O(1') - C(10')	109.24(16)	**H(14F) - C(14') - H(14E)**	109.5
C(1') - O(4') - C(4')	110.58(15)	**H(21D) - C(21') - H(21E)**	109.5
C(10') - C(11') - H(11D)	109.5	**H(21D) - C(21') - H(21F)**	109.5
C(10') - C(11') - H(11E)	109.5	**H(21E) - C(21') - H(21F)**	109.5
C(10') - C(11') - H(11F)	109.5	**H(6'A) - C(6') - H(6'B)**	108.9
C(10') - C(9') - H(9D)	109.5	**H(9D) - C(9') - H(9F)**	109.5
C(10') - C(9') - H(9E)	109.5	**H(9E) - C(9') - H(9D)**	109.5
C(10') - C(9') - H(9F)	109.5	**H(9E) - C(9') - H(9F)**	109.5
C(12') - C(13') - C(14')	111.0(4)	**O(1') - C(1') - C(2')**	105.54(18)
C(13') - C(12') - H(12D)	109.5	**O(1') - C(1') - H(1')**	111.2
C(13') - C(12') - H(12E)	109.5	**O(1') - C(1') - O(4')**	110.46(17)
C(13') - C(12') - H(12F)	109.5	**O(1') - C(10') - C(11')**	109.2(2)
C(13') - C(14') - H(14D)	109.5	**O(1') - C(10') - C(9')**	109.23(19)
C(13') - C(14') - H(14E)	109.5	**O(2') - C(10') - C(11')**	111.0(2)

C(13') - C(14') - H(14F)	109.5	**O(2') - C(10') - C(9')**	109.58(19)
C(13') - O(5') - C(5')	108.6(2)	**O(2') - C(10') - O(1')**	104.22(17)
C(15') - C(16') - C(17')	122.9(3)	**O(2') - C(2') - C(1')**	102.74(17)
C(15') - C(16') - H(16')	118.5	**O(2') - C(2') - C(3')**	112.86(18)
C(15') - C(20') - C(19')	120.8(3)	**O(2') - C(2') - H(2')**	112.4
C(15') - C(20') - H(20')	119.6	**O(3') - C(3') - C(2')**	106.79(18)
C(16') - C(15') - C(20')	117.0(2)	**O(3') - C(3') - C(4')**	106.80(17)
C(16') - C(15') - C(8')	122.3(2)	**O(3') - C(3') - C(7')**	112.24(17)
C(16') - C(17') - H(17')	120.4	**O(4') - C(1') - C(2')**	106.88(17)
C(17') - C(16') - H(16')	118.5	**O(4') - C(1') - H(1')**	111.2
C(17') - C(18') - C(19')	119.4(2)	**O(4') - C(4') - C(3')**	103.89(16)
C(17') - C(18') - O(7')	124.9(2)	**O(4') - C(4') - C(5')**	107.17(18)
C(18') - C(17') - C(16')	119.2(3)	**O(4') - C(4') - H(4')**	109.8
C(18') - C(17') - H(17')	120.4	**O(5') - C(13') - C(12')**	110.2(3)
C(18') - C(19') - C(20')	120.7(3)	**O(5') - C(13') - C(14')**	108.2(3)
C(18') - C(19') - H(19')	119.7	**O(5') - C(5') - C(4')**	108.84(19)
C(18') - O(7') - C(21')	117.7(2)	**O(5') - C(5') - C(6')**	102.9(2)
C(19') - C(18') - O(7')	115.7(2)	**O(5') - C(5') - H(5')**	110
C(19') - C(20') - H(20')	119.6	**O(6') - C(13') - C(12')**	107.6(3)
C(2') - C(1') - H(1')	111.2	**O(6') - C(13') - C(14')**	112.9(4)
C(2') - C(3') - C(4')	101.33(16)	**O(6') - C(13') - O(5')**	106.8(2)
C(2') - O(2') - C(10')	106.87(17)	**O(6') - C(6') - C(5')**	104.5(2)
C(20') - C(15') - C(8')	120.6(2)	**O(6') - C(6') - H(6'A)**	110.8
C(20') - C(19') - H(19')	119.7	**O(6') - C(6') - H(6'B)**	110.8
C(3') - C(2') - H(2')	112.4	**O(7') - C(21') - H(21D)**	109.5
C(3') - C(4') - H(4')	109.8	**O(7') - C(21') - H(21E)**	109.5
		O(7') - C(21') - H(21F)	109.5

Symmetry transformations used to generate equivalent atoms.

Table 5 Torsion angles of mirror image sheet for compound **45**

C(1') - C(2') - C(3') - C(4')	34.1(2)	**C(3') - C(7') - C(8') - C(15')**	22(7)
C(1') - C(2') - C(3') - C(7')	157.03(19)	**C(4') - C(3') - C(7') - C(8')**	125(3)
C(1') - C(2') - C(3') - O(3')	77.56(19)	**C(4') - C(5') - C(6') - O(6')**	140.5(3)
C(1') - O(1') - C(10') - C(11')	99.6(2)	**C(4') - O(4') - C(1') - C(2')**	2.7(2)
C(1') - O(1') - C(10') - C(9')	136.09(19)	**C(4') - O(4') - C(1') - O(1')**	111.66(19)
C(1') - O(1') - C(10') - O(2')	19.0(2)	**C(5') - O(5') - C(13') - C(12')**	98.2(3)
C(1') - O(4') - C(4') - C(3')	24.7(2)	**C(5') - O(5') - C(13') - C(14')**	140.3(4)
C(1') - O(4') - C(4') - C(5')	148.10(18)	**C(5') - O(5') - C(13') - O(6')**	18.5(3)
C(10') - O(1') - C(1') - C(2')	0.9(2)	**C(6') - O(6') - C(13') - C(12')**	115.3(4)
C(10') - O(1') - C(1') - O(4')	114.23(19)	**C(6') - O(6') - C(13') - C(14')**	121.8(4)
C(10') - O(2') - C(2') - C(1')	32.9(2)	**C(6') - O(6') - C(13') - O(5')**	3.0(4)
C(10') - O(2') - C(2') - C(3')	143.65(17)	**C(7') - C(3') - C(4') - C(5')**	82.4(3)
C(13') - O(5') - C(5') - C(4')	147.3(2)	**C(7') - C(3') - C(4') - O(4')**	160.21(18)
C(13') - O(5') - C(5') - C(6')	25.0(3)	**C(7') - C(8') - C(15') - C(16')**	106(4)
C(13') - O(6') - C(6') - C(5')	12.2(4)	**C(7') - C(8') - C(15') - C(20')**	71(4)
C(15') - C(16') - C(17') - C(18')	0.1(6)	**C(8') - C(15') - C(16') - C(17')**	176.7(4)
C(16') - C(15') - C(20') - C(19')	0.7(5)	**C(8') - C(15') - C(20') - C(19')**	176.3(3)
C(16') - C(17') - C(18') - C(19')	0.4(6)	**O(1') - C(1') - C(2') - C(3')**	138.23(18)
C(16') - C(17') - C(18') - O(7')	179.8(3)	**O(1') - C(1') - C(2') - O(2')**	20.6(2)
C(17') - C(18') - C(19') - C(20')	0.9(6)	**O(2') - C(2') - C(3') - C(4')**	76.2(2)
C(18') - C(19') - C(20') - C(15')	1.0(6)	**O(2') - C(2') - C(3') - C(7')**	46.8(2)
C(2') - C(3') - C(4') - C(5')	153.40(19)	**O(2') - C(2') - C(3') - O(3')**	172.16(16)
C(2') - C(3') - C(4') - O(4')	36.0(2)	**O(3') - C(3') - C(4') - C(5')**	41.8(2)
C(2') - C(3') - C(7') - C(8')	119(3)	**O(3') - C(3') - C(4') - O(4')**	75.6(2)
C(2') - O(2') - C(10') - C(11')	84.5(2)	**O(3') - C(3') - C(7') - C(8')**	4(3)
C(2') - O(2') - C(10') - C(9')	149.75(19)	**O(4') - C(1') - C(2') - C(3')**	20.6(2)
C(2') - O(2') - C(10') - O(1')	33.0(2)	**O(4') - C(1') - C(2') - O(2')**	97.00(19)
C(20') - C(15') - C(16') - C(17')	0.2(6)	**O(4') - C(4') - C(5') - C(6')**	73.9(3)
C(21') - O(7') - C(18') - C(17')	0.1(4)	**O(4') - C(4') - C(5') - O(5')**	171.41(18)

C(21') - O(7') - C(18') - C(19')	179.5(3)	**O(5') - C(5') - C(6') - O(6')**	22.4(3)
C(3') - C(4') - C(5') - C(6')	170.6(2)	**O(7') - C(18') - C(19') - C(20')**	179.6(3)
C(3') - C(4') - C(5') - O(5')	55.9(3)		

Symmetry transformations used to generate equivalent atoms.

Spectral Data

Proton magnetic resonance spectra were recorded on AC-200 MHz, MSL-300 MHz and Bruker-500 MHz spectrometer using tetra methyl silane (TMS) as an internal standard. Chemical shifts have been expressed in ppm units downfield from TMS.

^{13}C Nuclear magnetic spectra were recorded on AC-50 MHz, MSL-75 MHz and Bruker-125 MHz spectrometer.

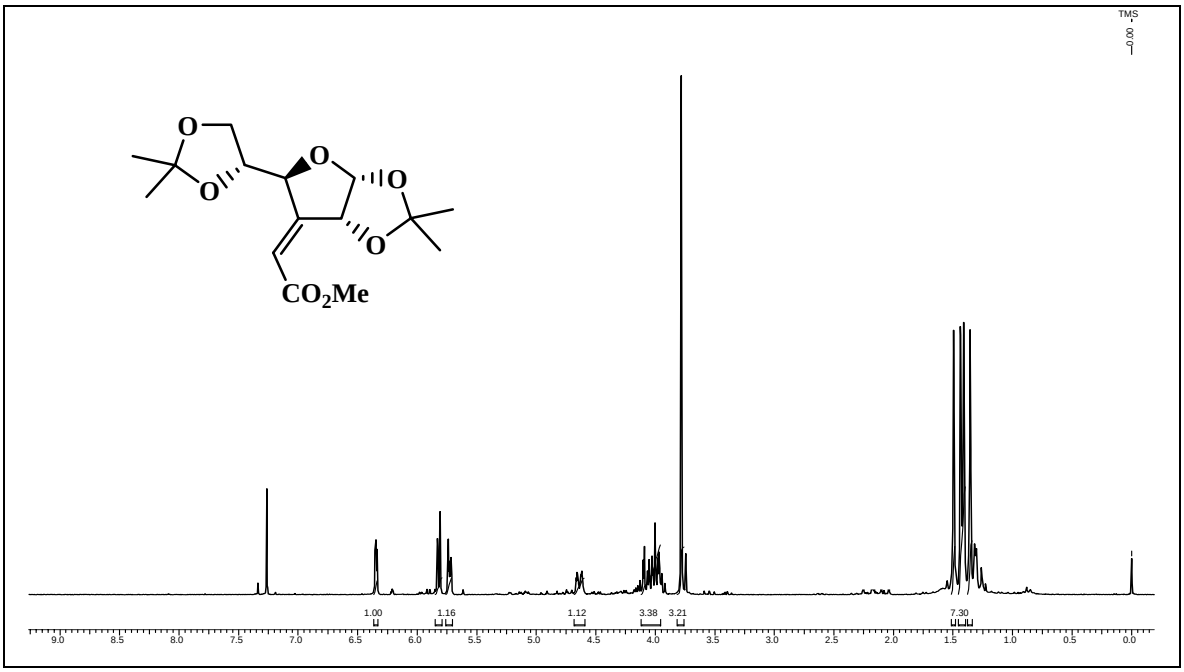

Spectral data for Compound no. 31

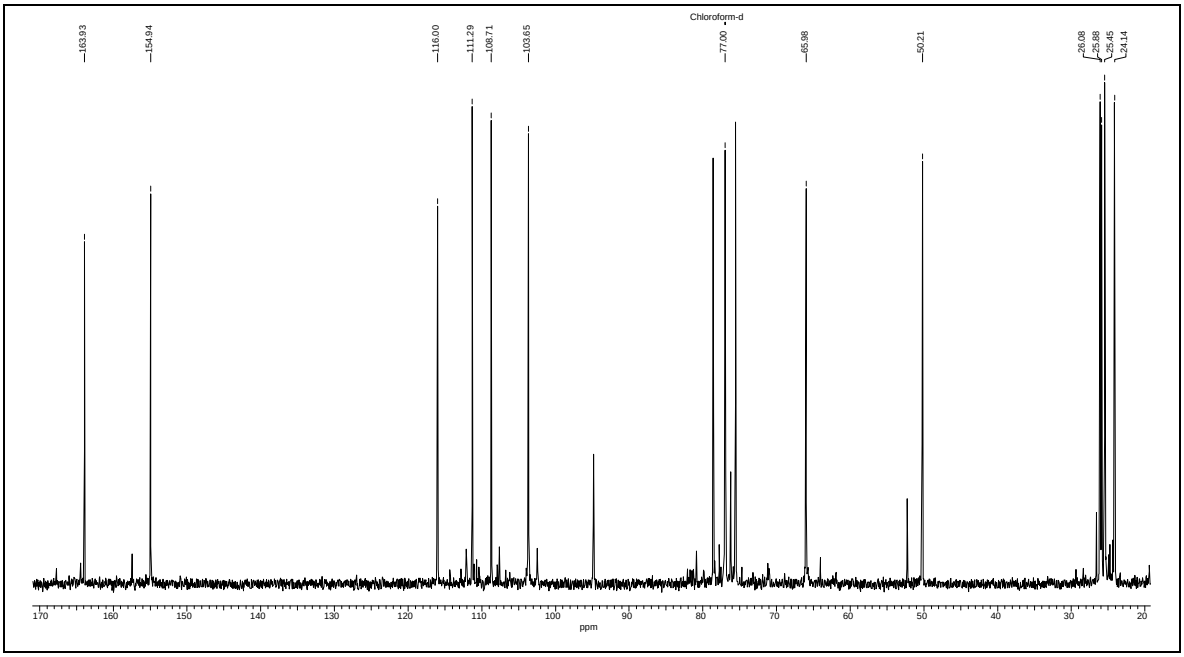

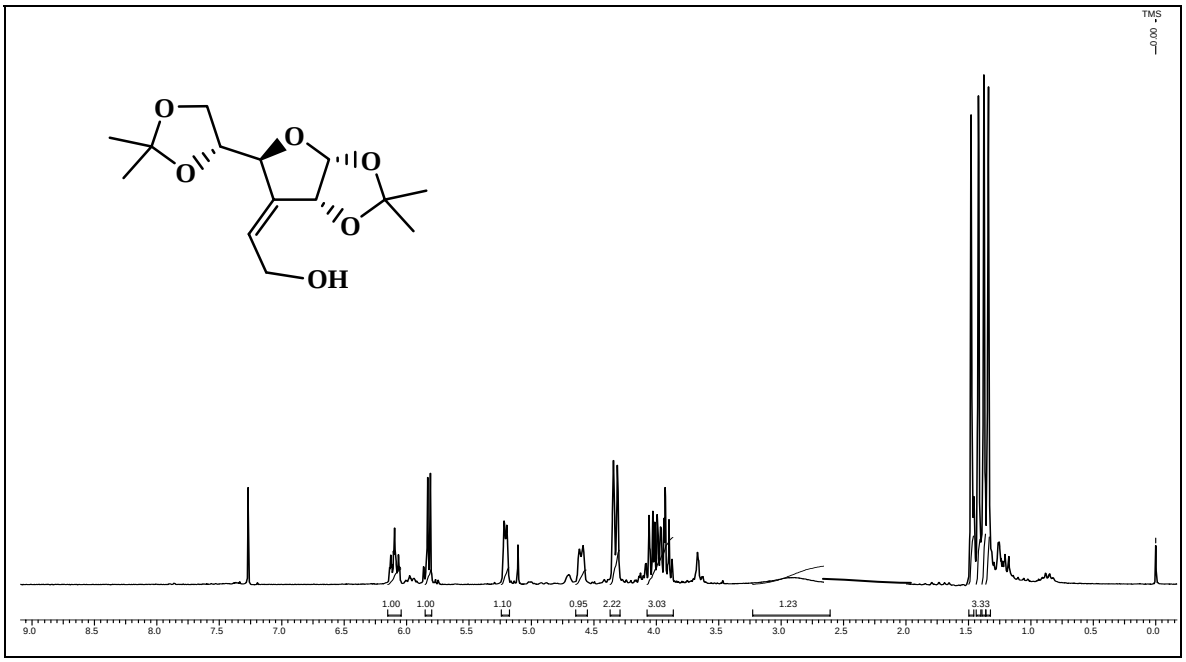

Spectral data for Compound no. 32

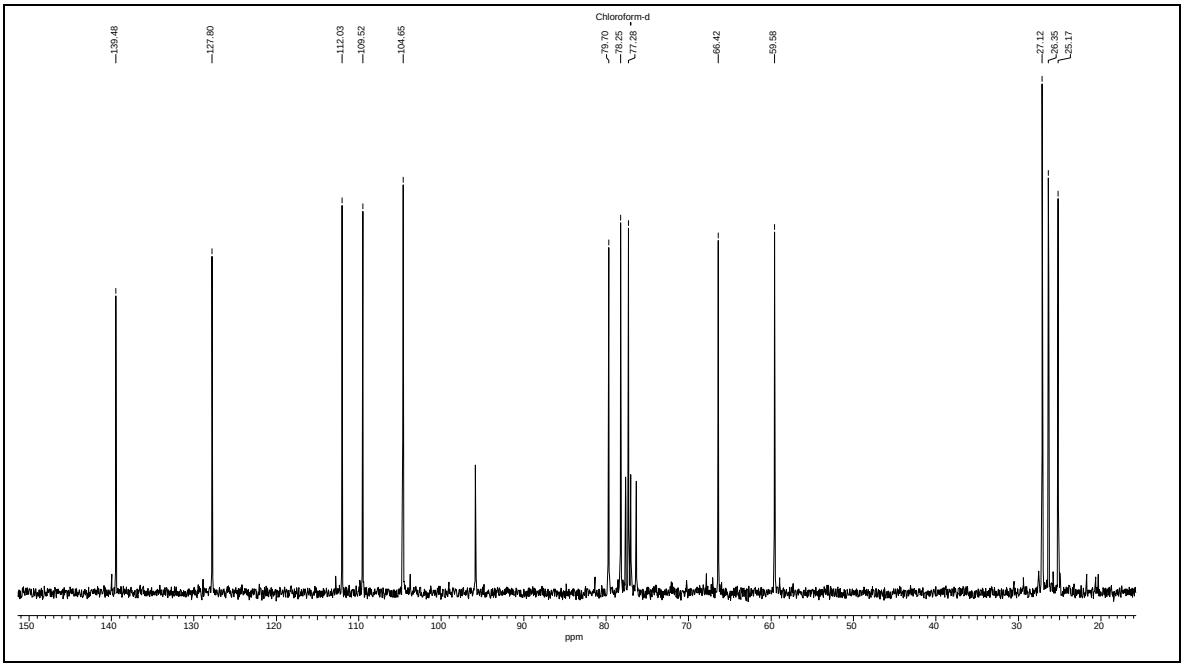

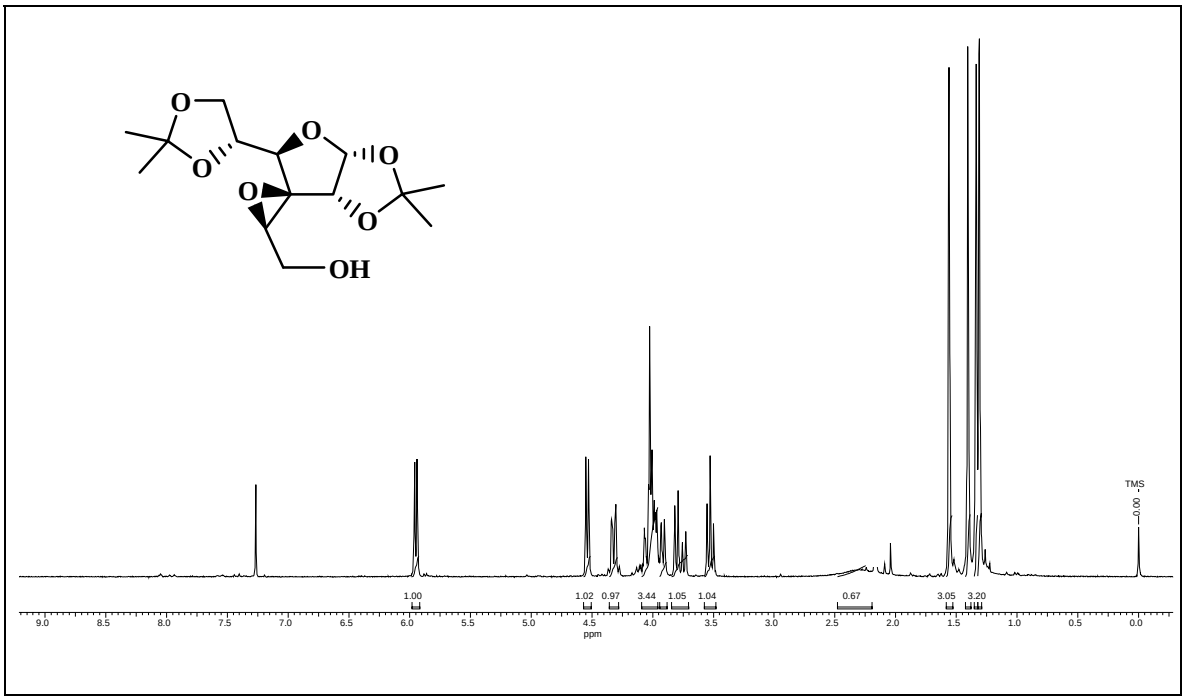

Spectral data for Compound no. 33

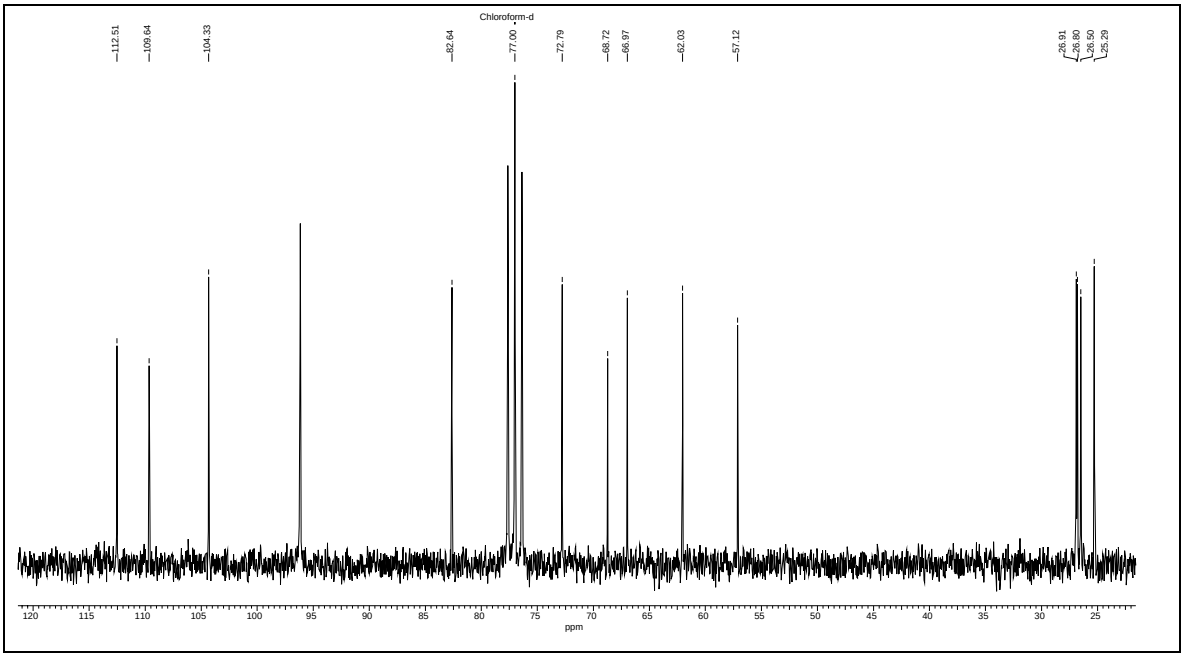

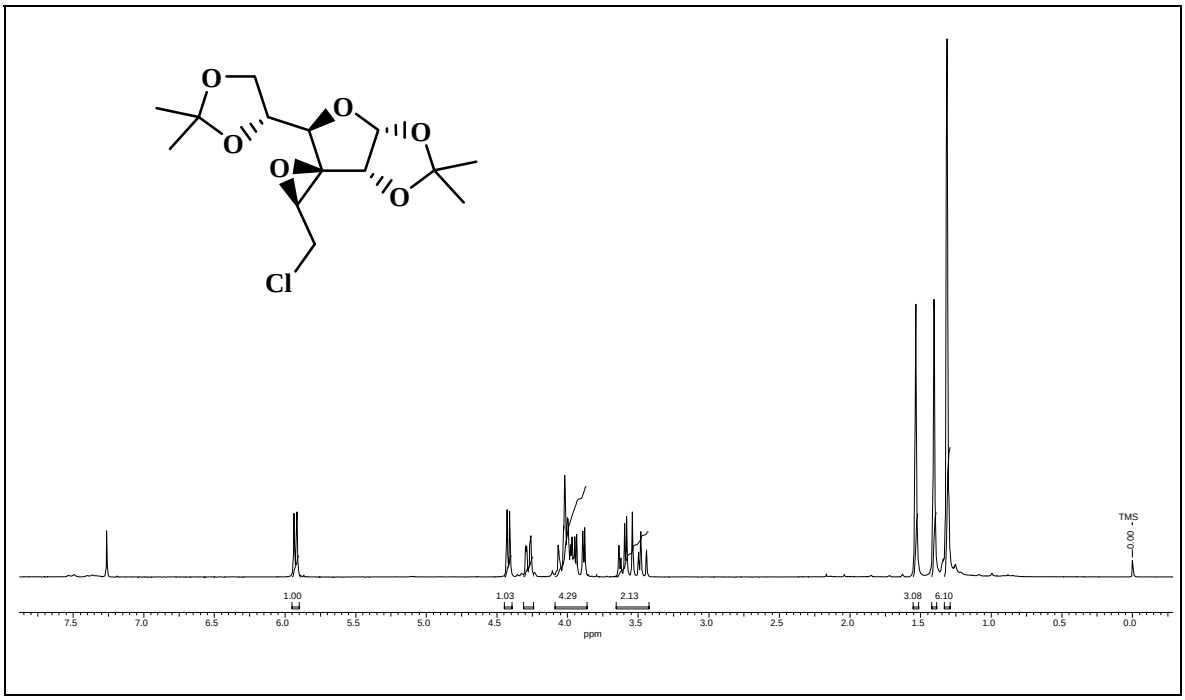

Spectral data for Compound no. 34

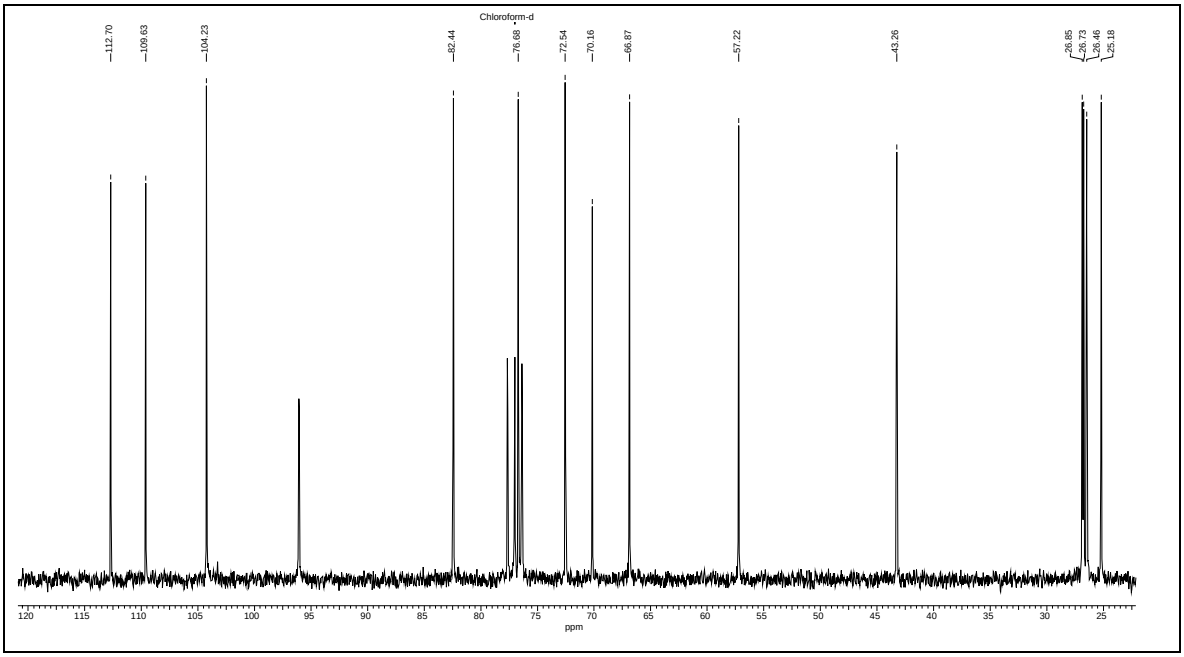

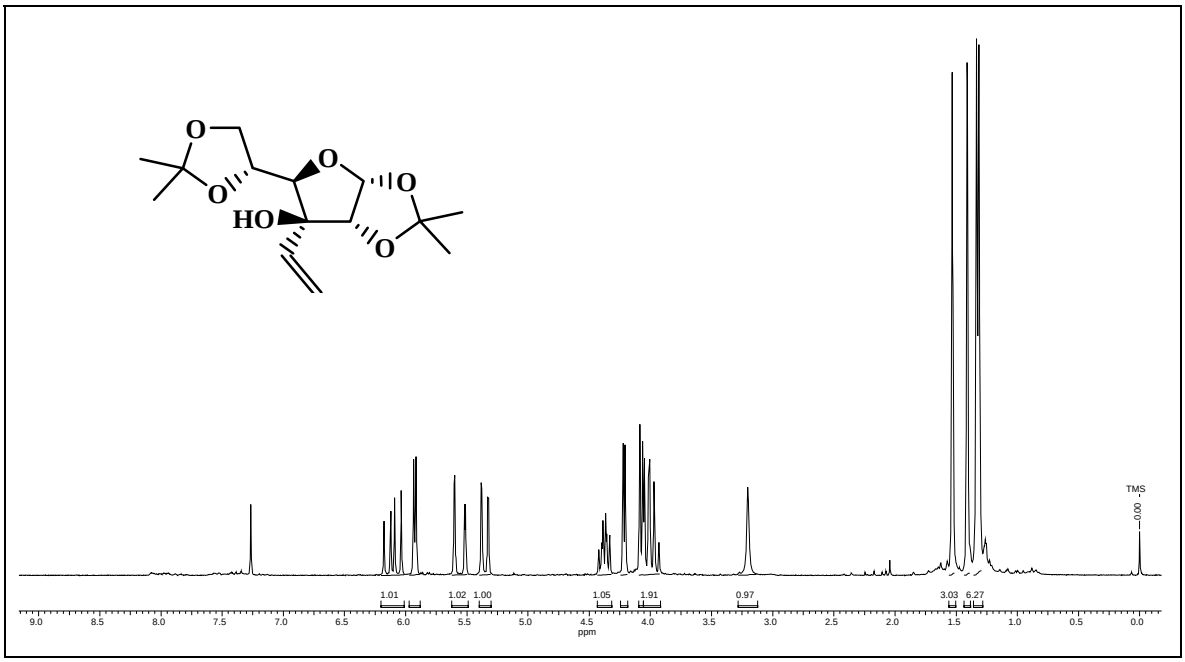

Spectral data for Compound no. 35

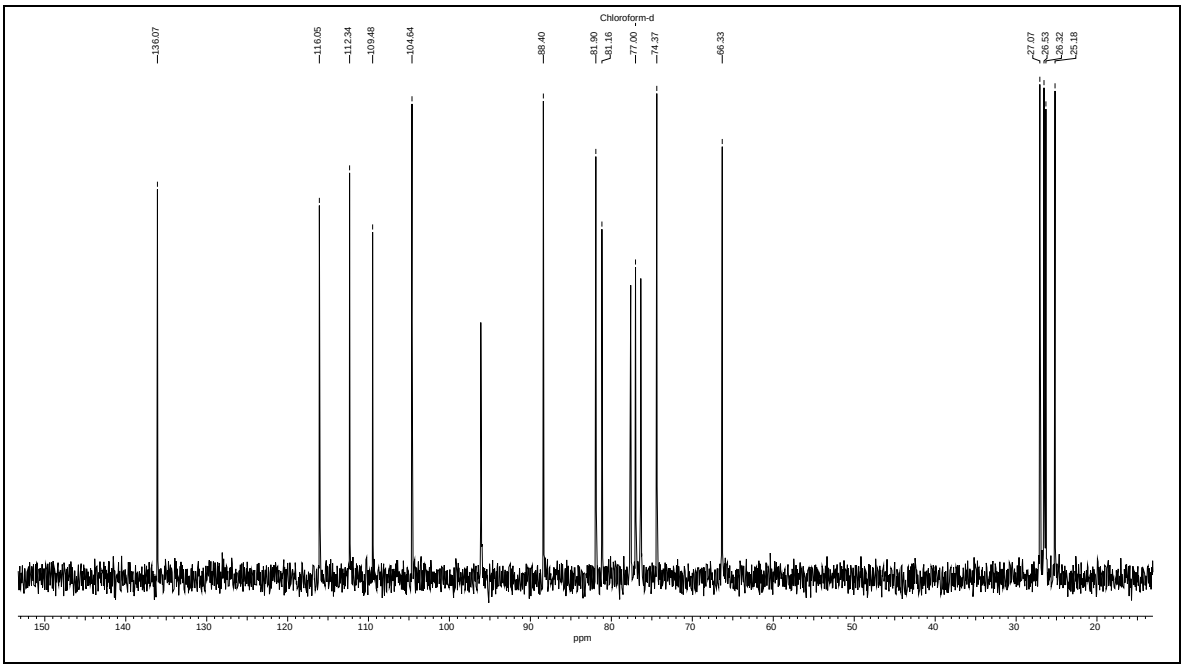

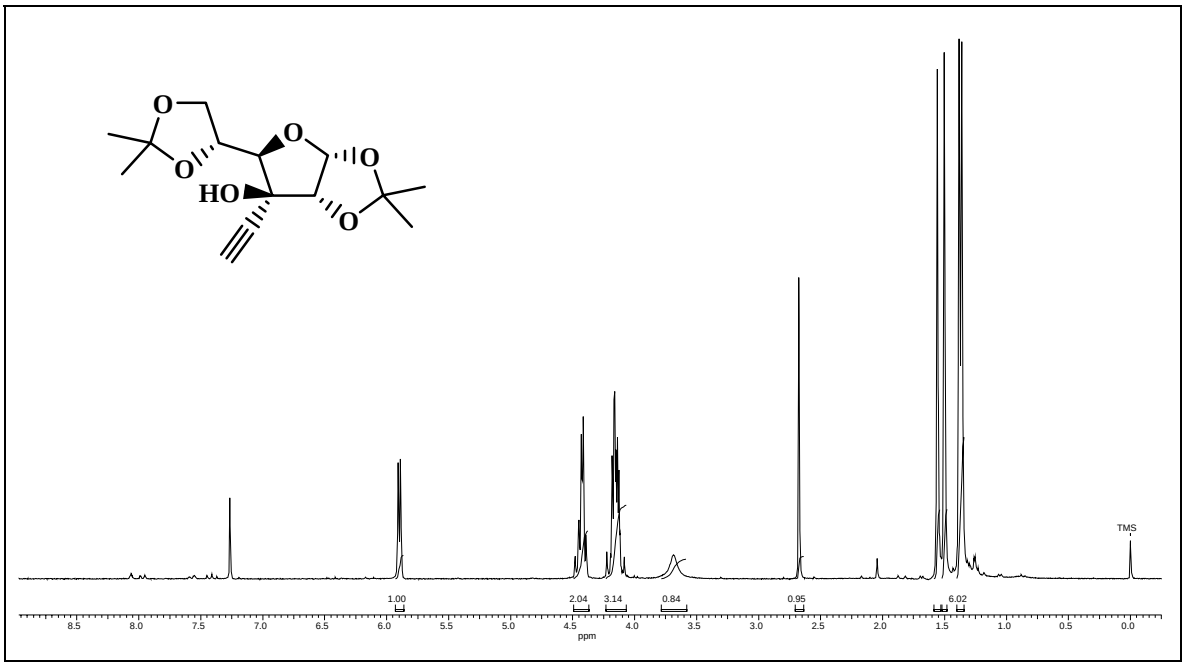

Spectral data for Compound no. 36

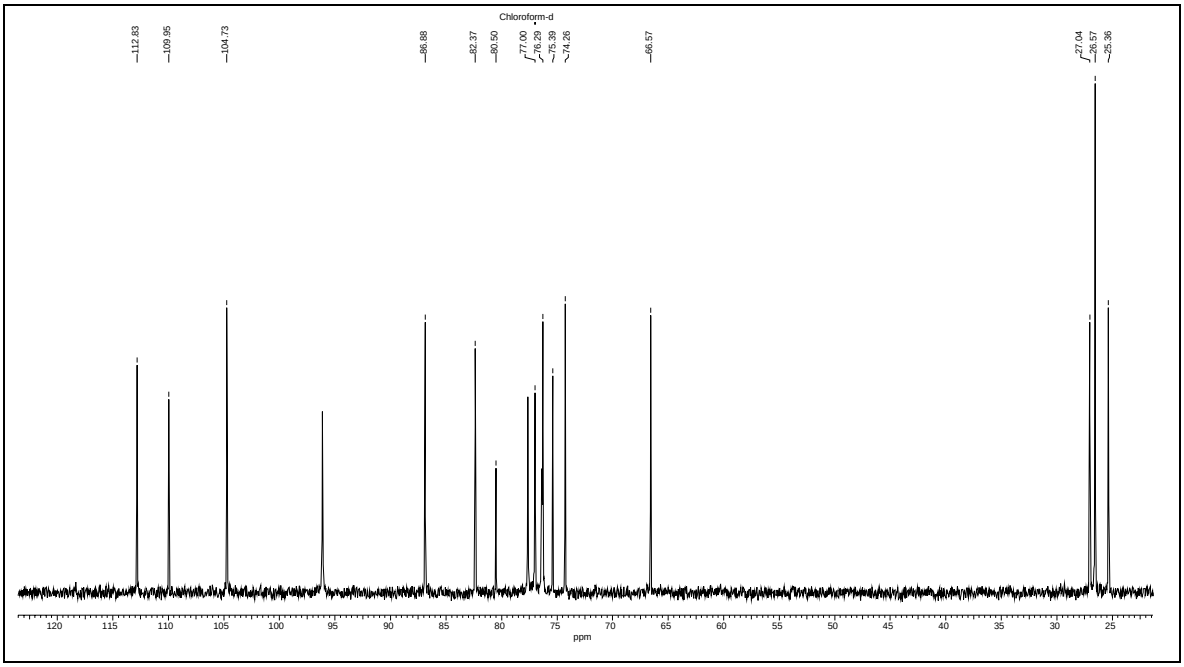

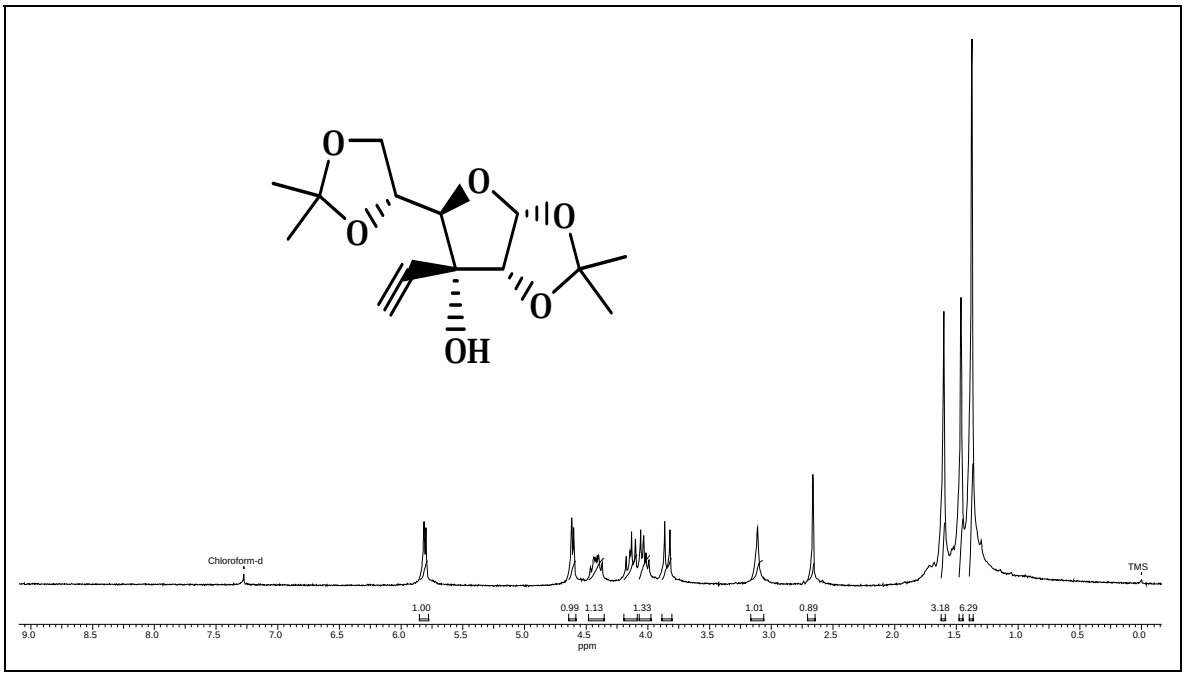

Spectral data for Compound no. 37

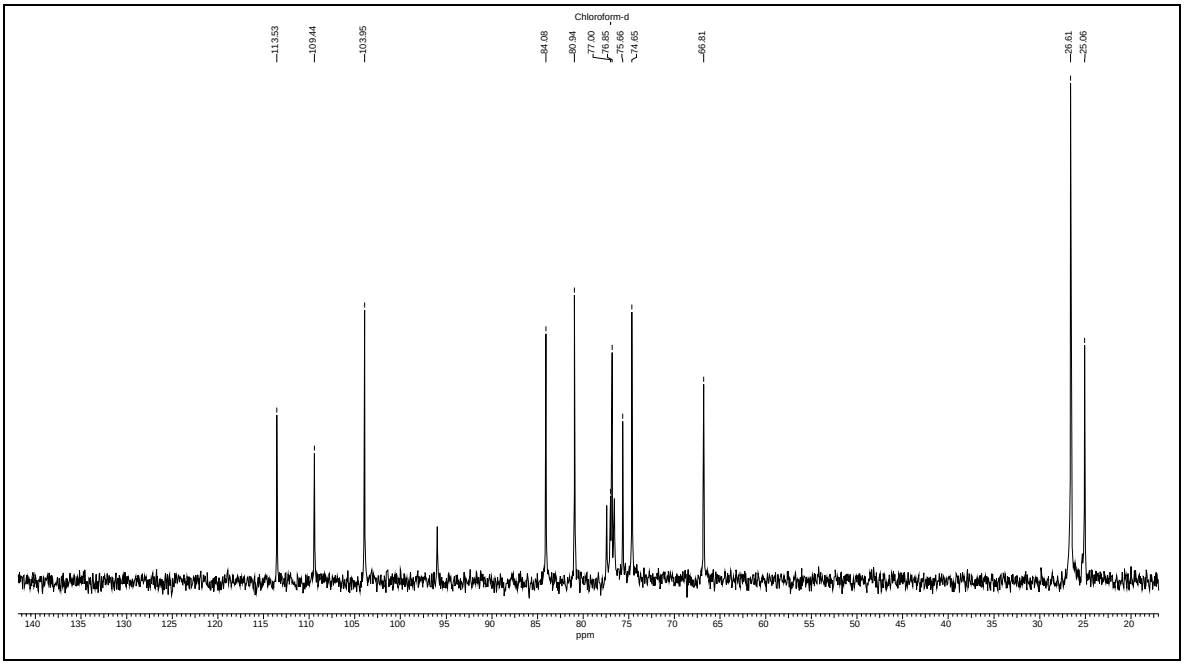

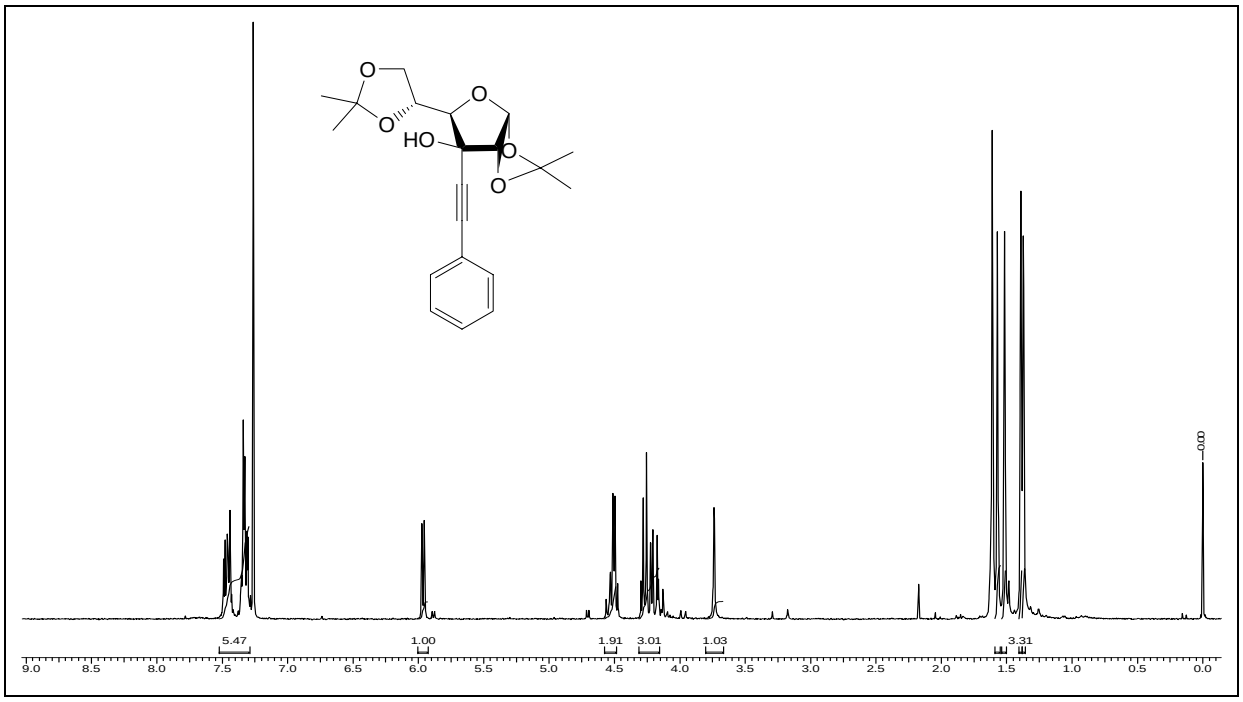

Spectral data for Compound no. 38

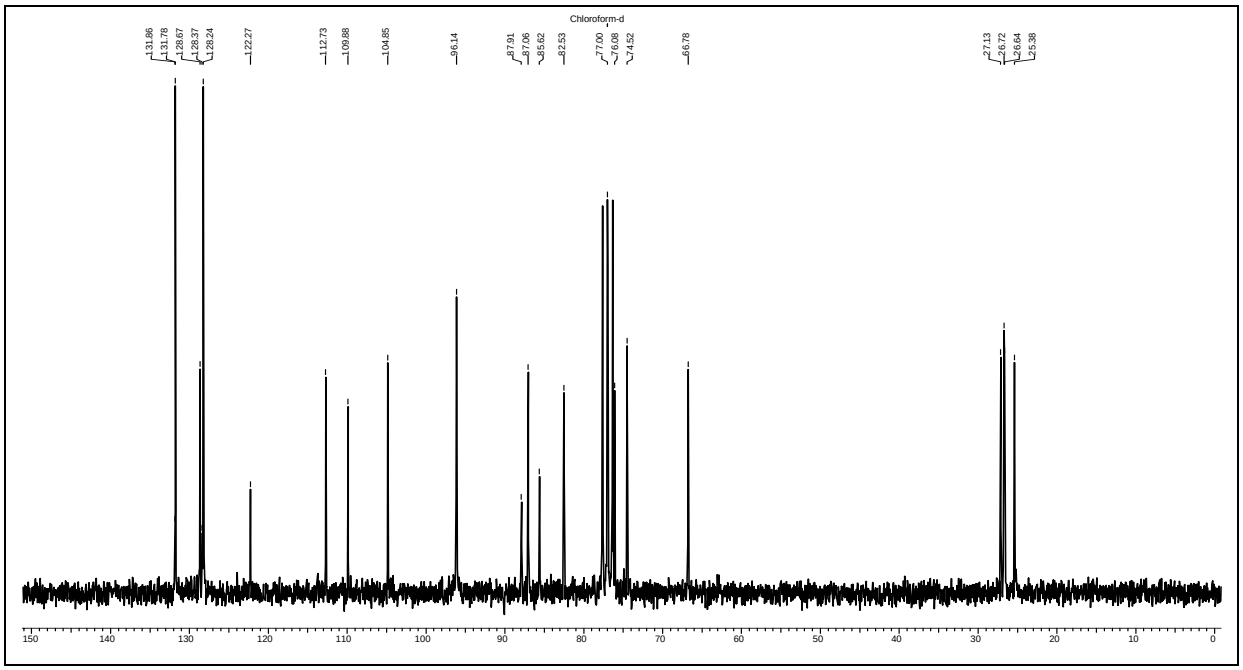

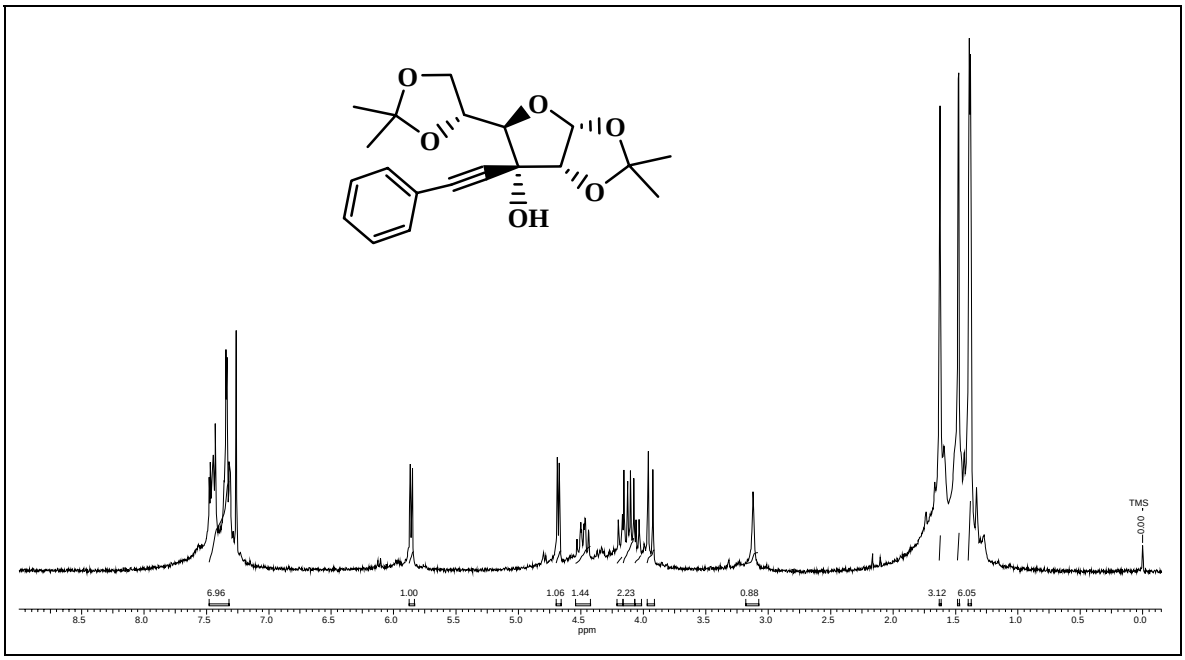

Spectral data for Compound no. 39

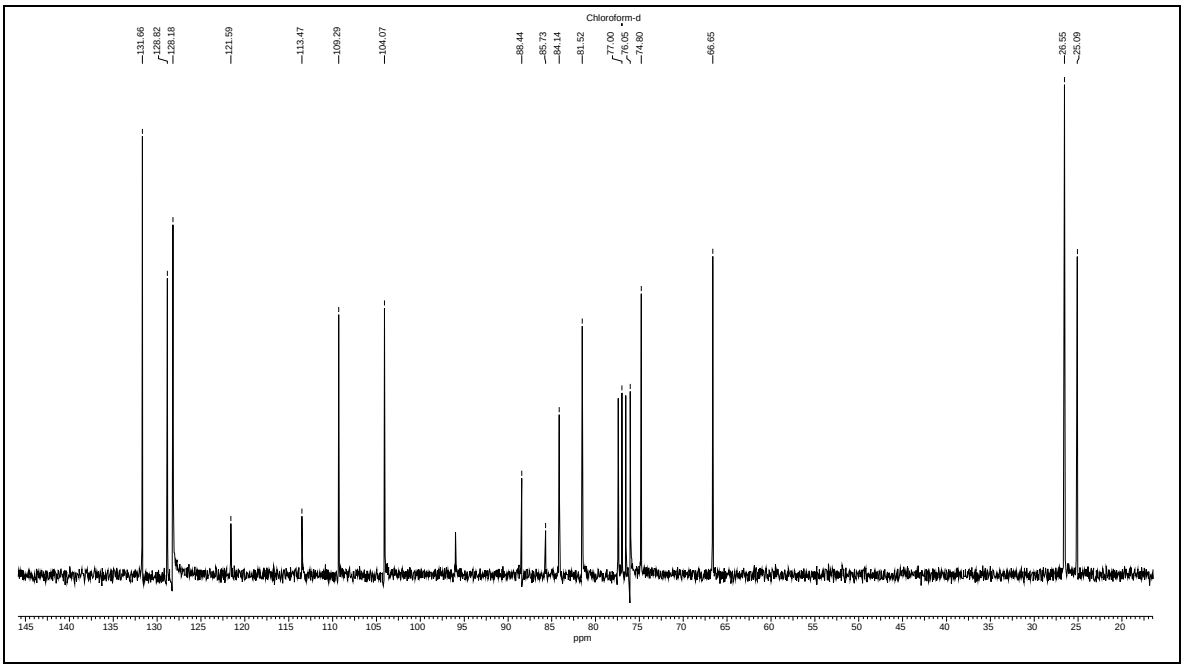

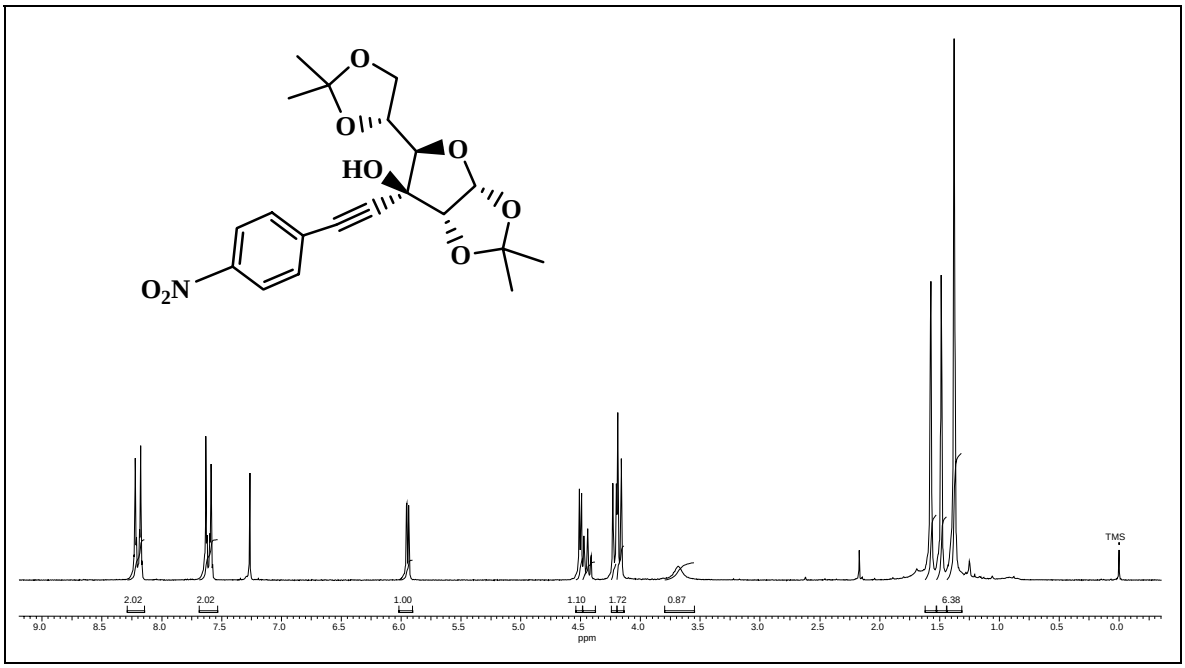

Spectral data for Compound no. 40

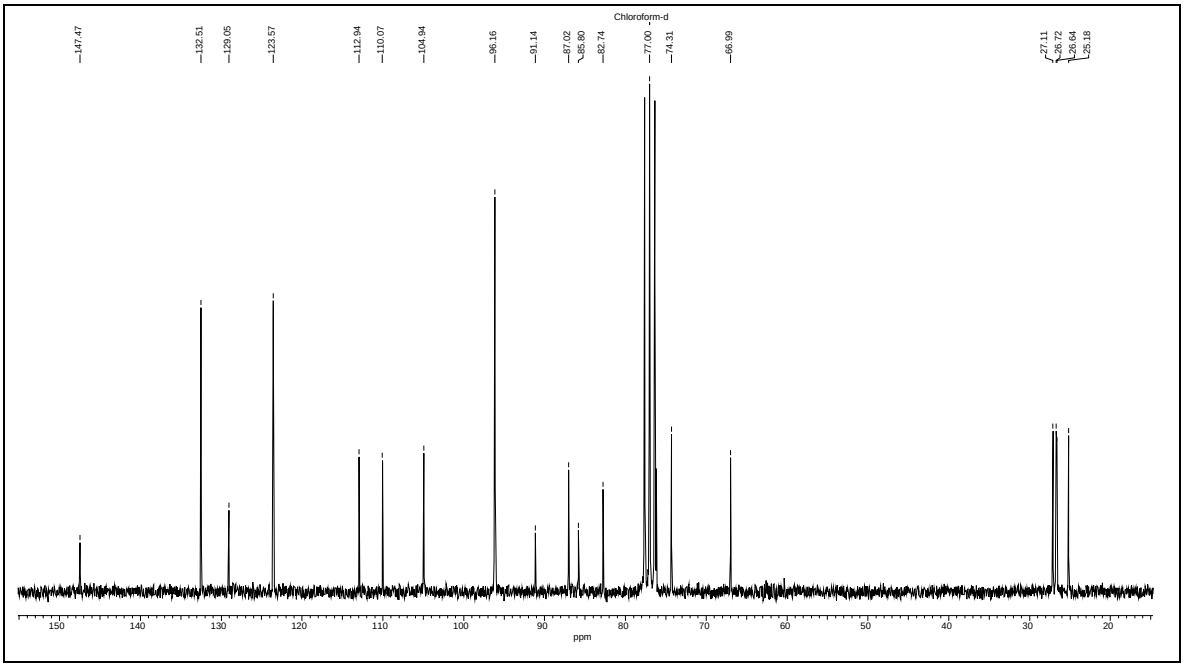

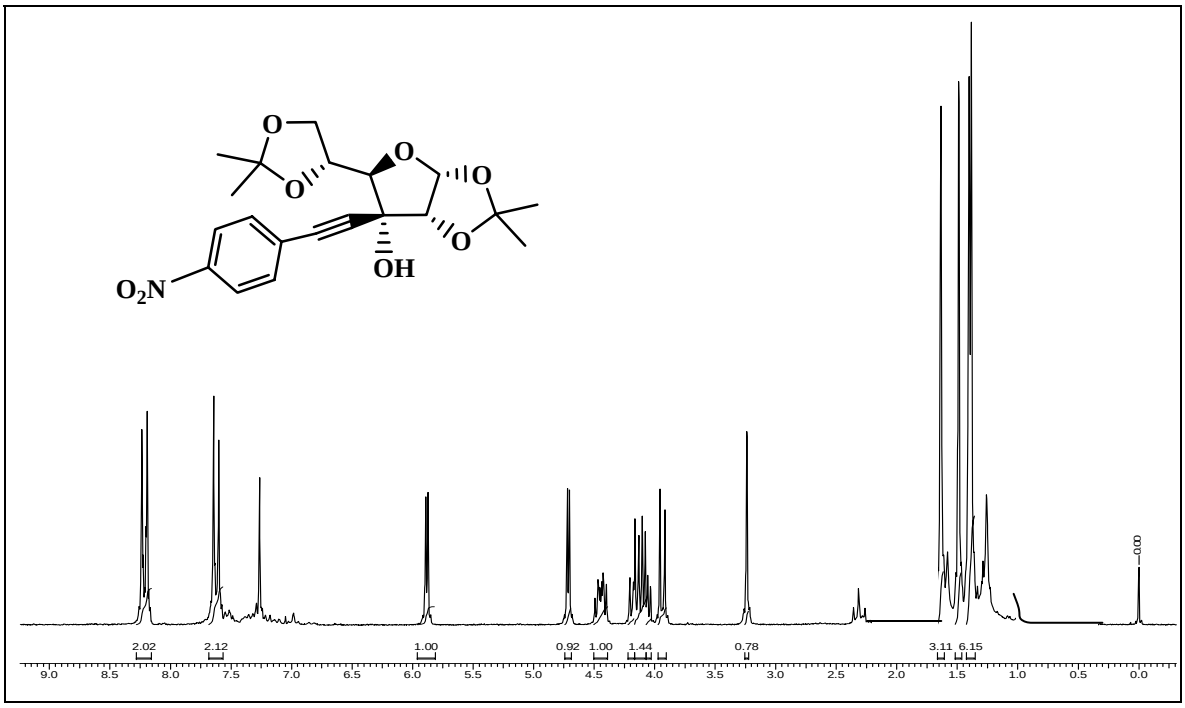

Spectral data for Compound no. 41

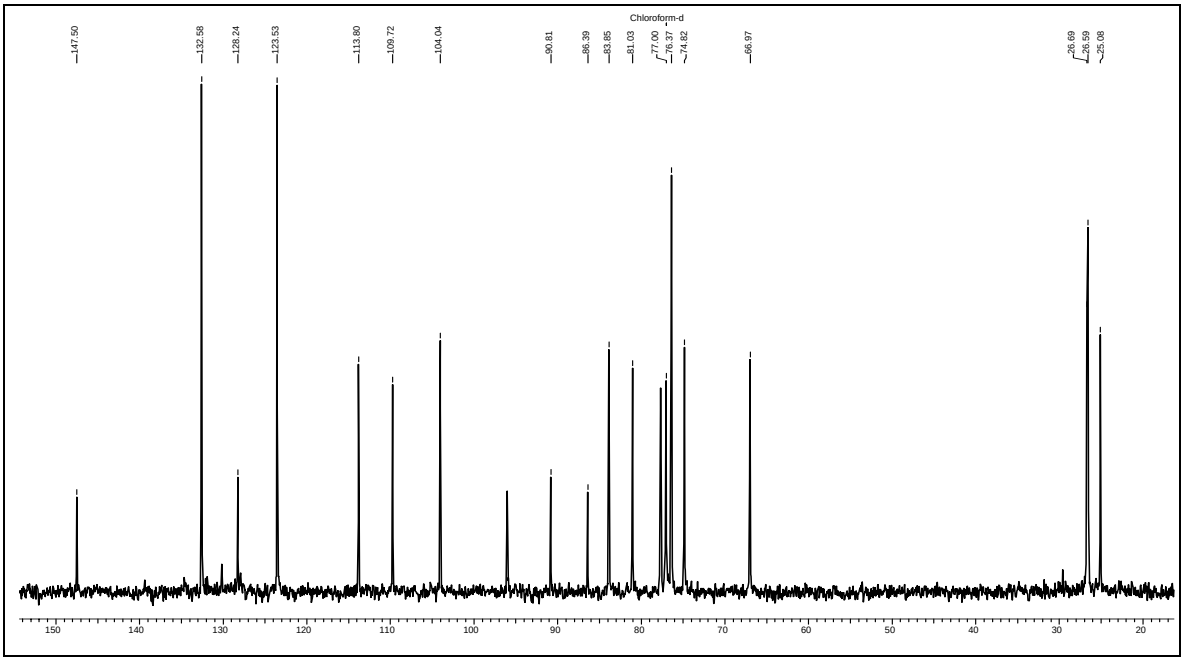

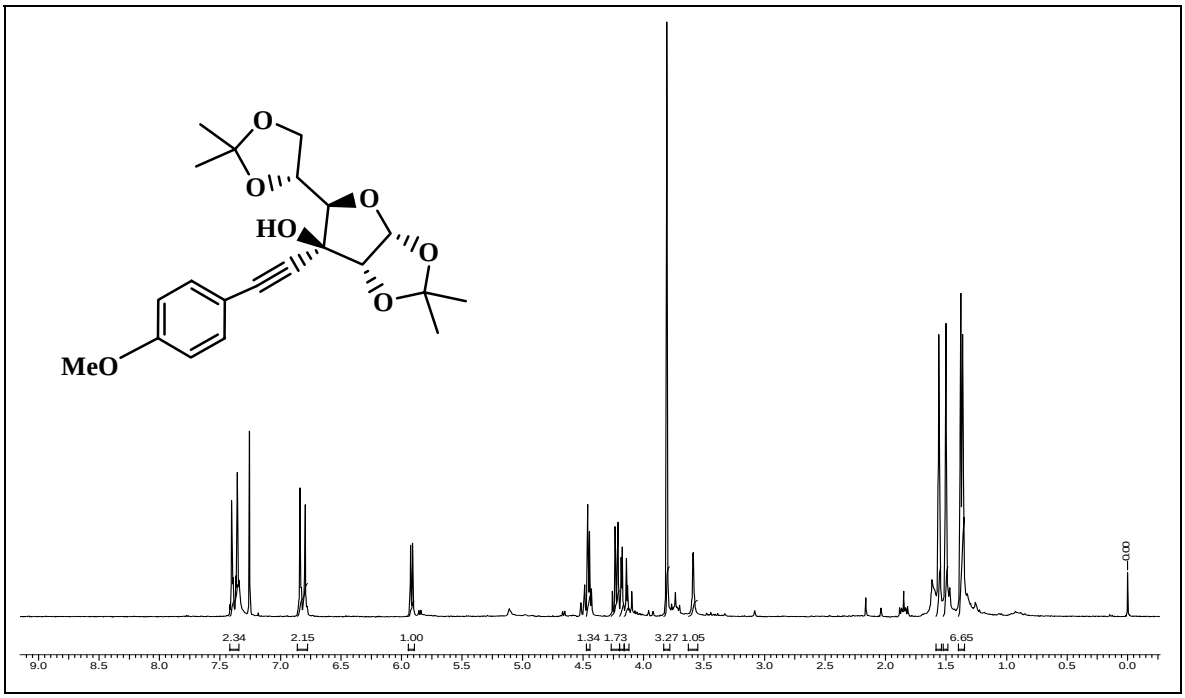

Spectral data for Compound no. 42

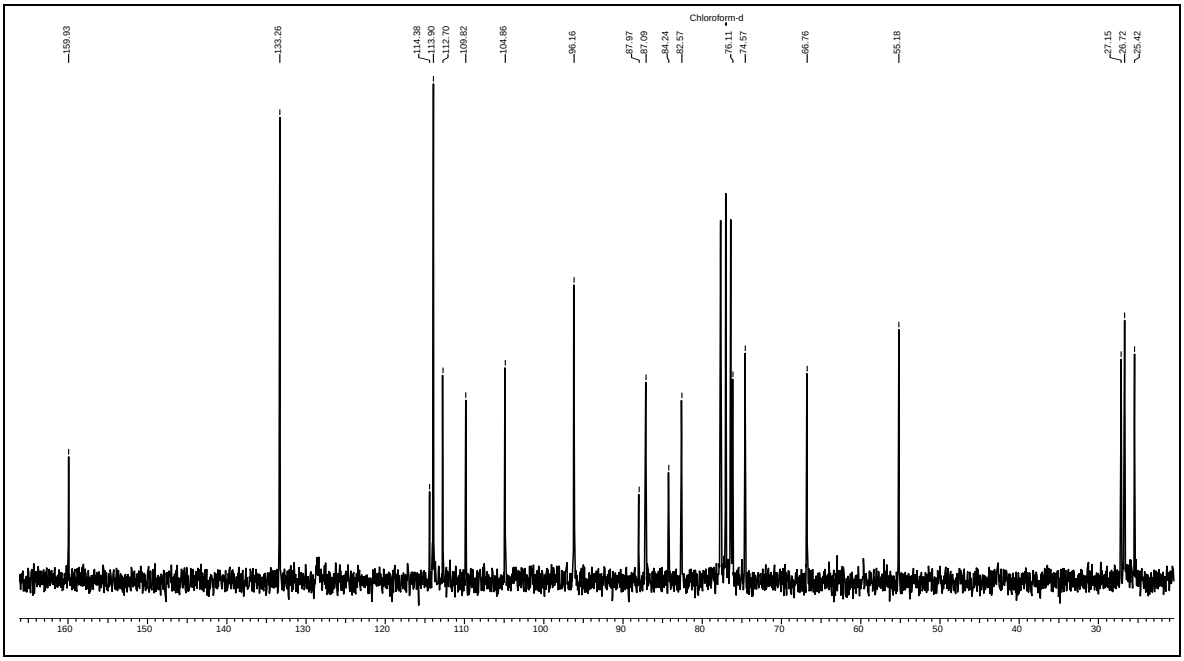

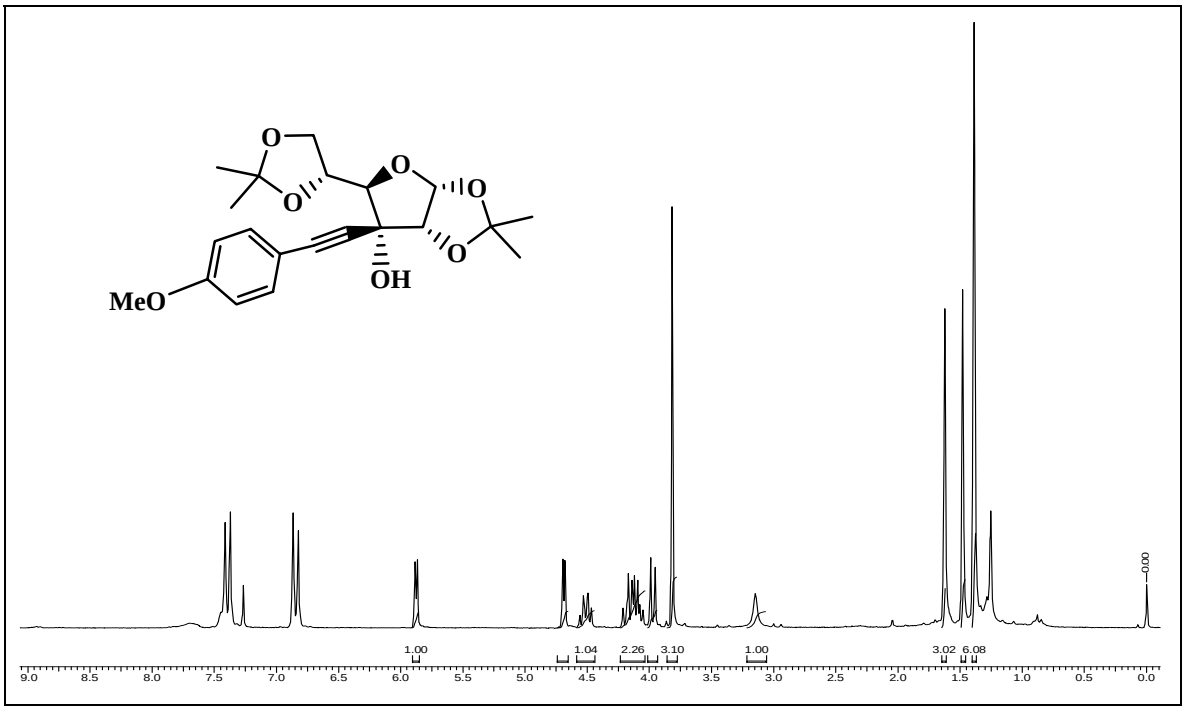

Spectral data for Compound no. 43

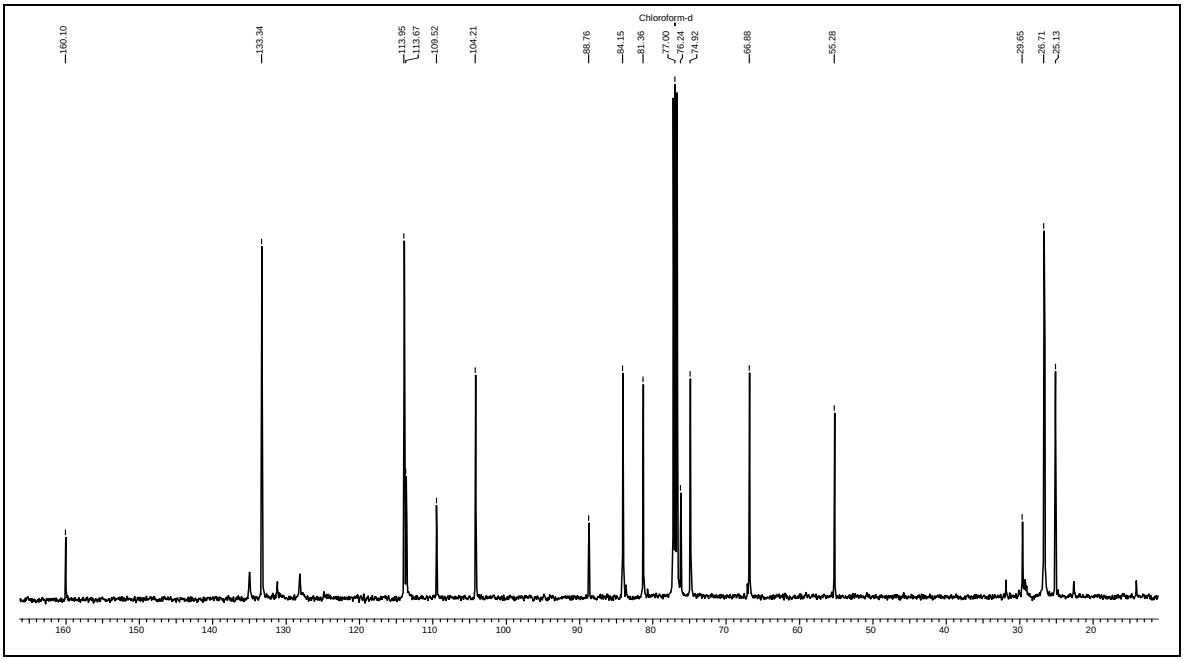

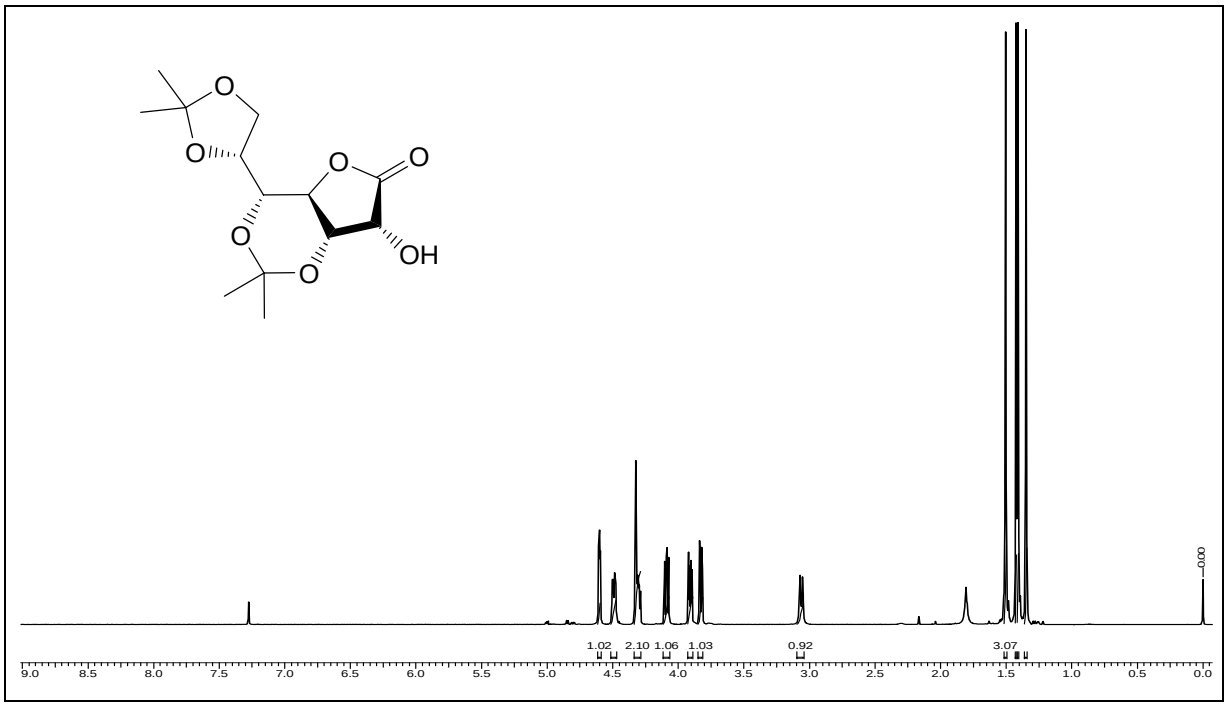

Spectral data for Compound no. 45

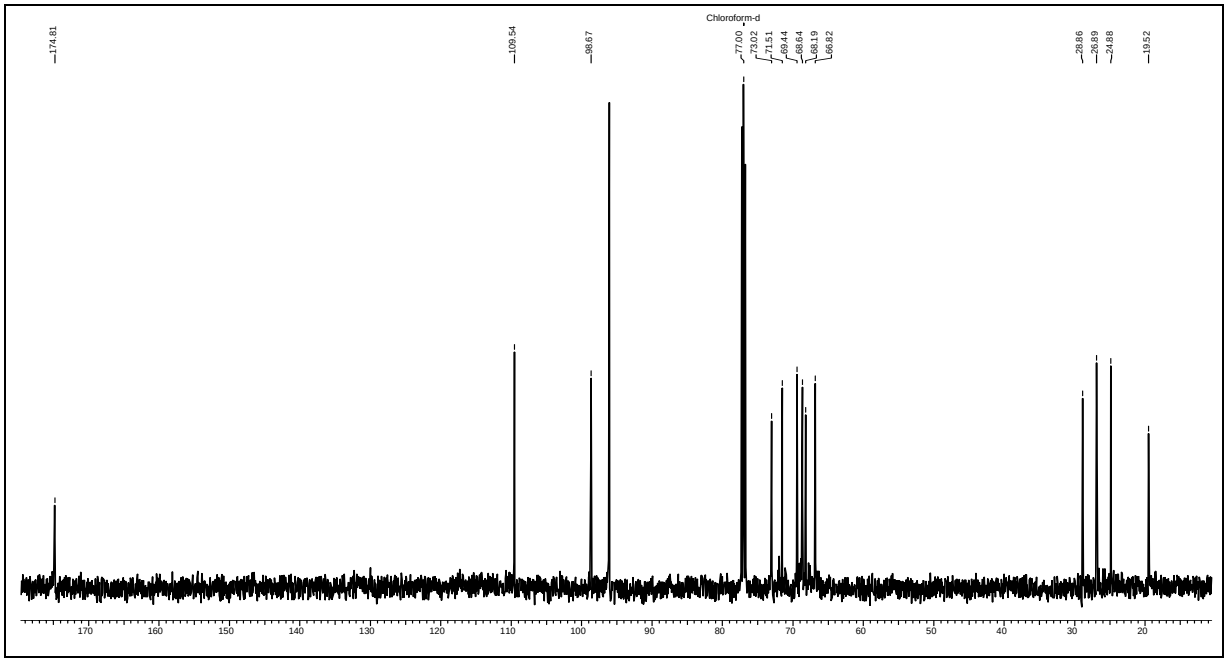

Synopsis

Chapter I: Solid acid Catalysts Mediated Organic Transformations

Section I: Synthesis of Chiral Morpholins using Beckmann Rearrangement

Apart from their use as chiral auxiliaries in asymmetric synthesis, morpholins and morpholinones are widely used scaffolds in the medicinal chemistry. One of the significant uses of morpholine skeleton is in the area of anti-thrombotics. There are several methods for the syntheses of chiral morphlinones and in general are synthesized from respective amino acids. Considering their potential medicinal importance, were interested to develop new methods for the synthesis of chiral morpholinones. Our basic approach in this regard is to use the easily available sugar derivatives as precursors (**Scheme 1**). As indicated in the **Scheme 1**, we are interested to explore the possibility of Beckmann rearrangement on sugar ketoximes where in one can address the synthesis of chiral morpholinones. To the best of our knowledge, there is no report concerning the Beckmann rearrangement of sugar oximes. However, the possibility of formation of a regiomeric product during the Beckmann process is not ruled out.

Scheme 1. Intended Beckmann Rearrangement on Sugar Oximes

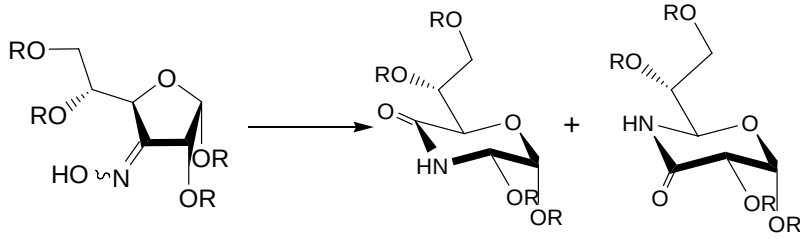

The Beckmann rearrangement is a well-known transformation of keto-oximes to *N*-substituted amides in the presence of an acid. Generally, strong Brønstead/Lewis acids ranging from stoichiometric to catalytic amounts are employed in order to accomplish the Beckmann rearrangement. To circumvent the harsh reaction conditions generally used for the Beckmann rearrangement coupled with a desire to use clean and environmentally benign reusable catalysts, we selected two different catalyst conditions i.e. beta zeolite cat. **1** and MoO_3 on SiO_2 with 20% molybdenum cat. **2**. To check the application of the

new and unexplored catalysts, initially it was decided to test these catalyst systems with the known substrates. A comprehensive listing of various substrates and the yields with respect to the two different catalysts used in this regard is given in Table 1.

Table 1 Beckmann rearrangement using solid acid catalysts 1 and 2.

Entry	Starting Material	Product	Yield (%)	
			Beta-Zeolite	MoO_3/ SiO_2
1	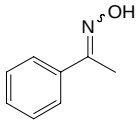	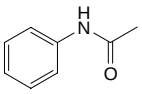	92	95
2	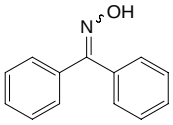	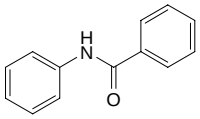	94	97
3	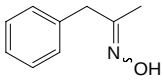	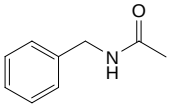	81	91
4	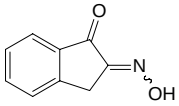	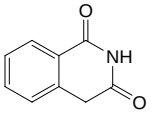	83	87
5	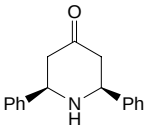	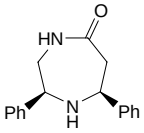	79	89
6	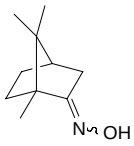	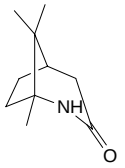	83	96

These results obtained with aromatic as well as aliphatic oximes encouraged us to try this newly developed catalyst systems on various sensitive substrates having acid sensitive protecting groups and compare those results with both catalyst systems. In order to apply the scope of these reagents to the synthesis of chiral morpholinones, the oximes **3** – **6** which can be easily derived from glucose (Table 2; **3** and **4**) and xylose (Table 2; **5** and **6**) are selected. The rearrangement of sugar-oxime **3** was carried out in the presence of catalyst **1** as well as **2** in refluxing ethanol. With both catalysts, the reactions are clean and resulted in an inseparable regioisomeric mixture. The presence of non epimeric but regioisomeric mixture was confirmed by various NMR studies of the mixture **7** and **8**.

The amides **7** and **8** are obtained in very good yields and with moderate regioselectivity (3: 2). We next focused on oximes **4** – **6**. As indicated in Table 2, with oximes **4** and **5**, the rearrangement was smooth and resulted in regiomeric mixtures.

Table 2 Beckmann rearrangement of sugar oximes

Sr. No.	Starting Material	Products	Yield (%)	
			Beta-Zeolite	MoO_3/ SiO_2
1	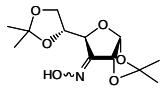 **3**	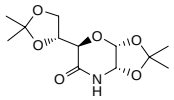 **7** 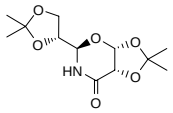 **8**	85 (3: 2)	82 (3: 2)
2	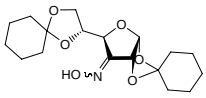 **4**	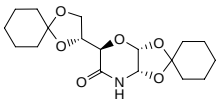 **9** 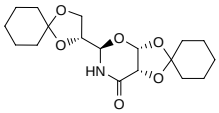 **10**	84 (3: 2)	87 (3: 2)
3	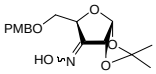 **5**	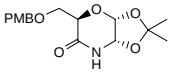 **11** 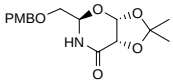 **12**	71 (3: 1)	70 (3: 1)
4	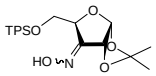 **6**	Complex Reaction Mixture		

In the case of the TPS oxime **6** (Table 2, entry **4**), we encountered a complex reaction mixture presumably because of the cleavage of TPS under these conditions. The regioselectivity for oximes **3** – **5** was found to be independent of the catalyst used. This indicated that both catalysts can facilitate the rearrangement but the regioselectivity is governed by stereoelectronic factors. Also, the protecting groups employed *i.e* ketals (isopropylidine and cyclohexylidine) and benzyl ether are stable under the reaction conditions.

Section II: Epoxidation of internal olefins catalyzed by solid acid catalysts: A Systematic Investigation

Hydrogen peroxide is probably the best terminal oxidant after oxygen with respect to environmental and economic considerations. Indeed in certain circumstances it is better than oxygen in so far as O_2 / organic mixtures can sometimes spontaneously ignite. There are various reports on epoxidation using H_2O_2 as a potent oxygen supplier. Various

inorganic salts of metals like manganese, hydrotalcites, tungsten, molybdenum, titanium, rhenium, niobium, selenides & arsenides, iron and so on have been already employed for such reactions. These epoxidation systems that use hydrogen peroxide in conjunction with catalytic amounts of cheap relatively nontoxic metals are potentially viable for large-scale production of inexpensive products and for specialized applications in process development and research. H_2O_2 in combination with base like NaOH, bicarbonates generates the peroxy species like OOH^-, and these species are known to carry out epoxidation of conjugated olefins i.e. Payne reaction. CV Rode et.al. have shown that this system in conjugation with TS-1 catalyst is a potent viable epoxidation medium for styrene.

Scheme 1

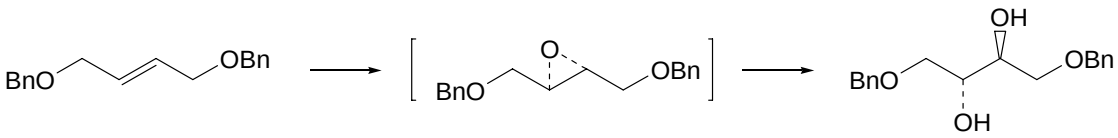

As a possible extension, we have explored application of the two solid acid catalysts we have in our hands as heterogenous catalyst systems and ammonium molybdate as homogenous catalyst for epoxidation of the internal olefins. The 1,4 di *O*-benzyloxy 2-butene was as used as a model substrate to optimize various parameters like reaction time, temperature, additives (di-butyl tin oxide) and their concentrations and so on. DBTO is investigated in comparison with BTAC. Also evaluation of quantity used for H_2O_2 is determined. The solvent effect is also investigated by comparing two different solvent systems viz. dichloromethane vs. Methanol: Acetonitrile in 3:1 ratio

Various reactions are carried out for all possible combinations of reagents mentioned. Reaction samples taken at an interval of 4 hrs upto 12 hrs are analyzed by HPLC to get conversion, selectivity and turn over frequency (TOF). The actual products are confirmed by isolation and NMR analysis and the results of this study are as follows.

- The catalysts used efficiently catalyze this reaction and it follows the Payne reaction route.
- TS-1 is the better catalyst system for epoxidation overall giving 99% conversion with 93% selectivity towards epoxide.
- Chlorinated solvents are better solvents for epoxidation.

- DBTO is used as a promoter in this reaction and is found to be better medium over BTAC.

Chapter II: Synthesis of a novel bis-furan UAA template for peptiodomimetic studies

Figure 1 A designed bis-furan template

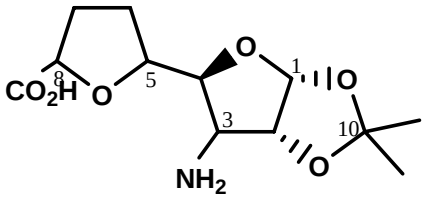

An important objective in modern bioorganic and medicinal chemistry concerns the design of synthetic models that mimic various aspects of biologically active molecules. Detailed study of such models could lead to the development of better chemotherapeutic agents, novel artificial restriction enzymes and molecular biological and diagnostic tools. There is currently considerable interest in the design and synthesis of various templates that can be used as structural mimicking portions of biologically active molecules.

Scheme 1 Retrosynthetic plan

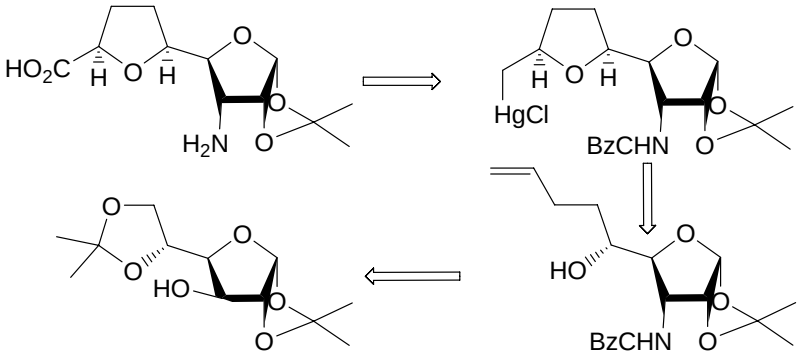

A careful examination of various templates that so far used revealed that they will be either rigid aromatic rings or posses certain stereochemical factors which strongly direct the orientation of attached oligomers. In this context, we are interested to synthesize flexible molecules with little directional influence and their further exploration as nucleating agents for mimicking the secondary structures of proteins and peptides. As shown in Figure 1, after a careful examination of the crystal structures of various bis-furan containing natural products, it has been noticed that this moiety has a potential in using peptidomimetics as helix inducers and beta-turn mimics.

Thus we decide to synthesize the simple looking substrate with absolute stereochemistry of RRRRSR. The computational study revealed that since the two furan rings in this structure form a trans fusion, they also give rise to relative trans geometry to the amine center and the acid center which is a good sign towards achieving the said activity we were interested. The retrosynthetic plan for the same is shown in **scheme 1**

Scheme 2

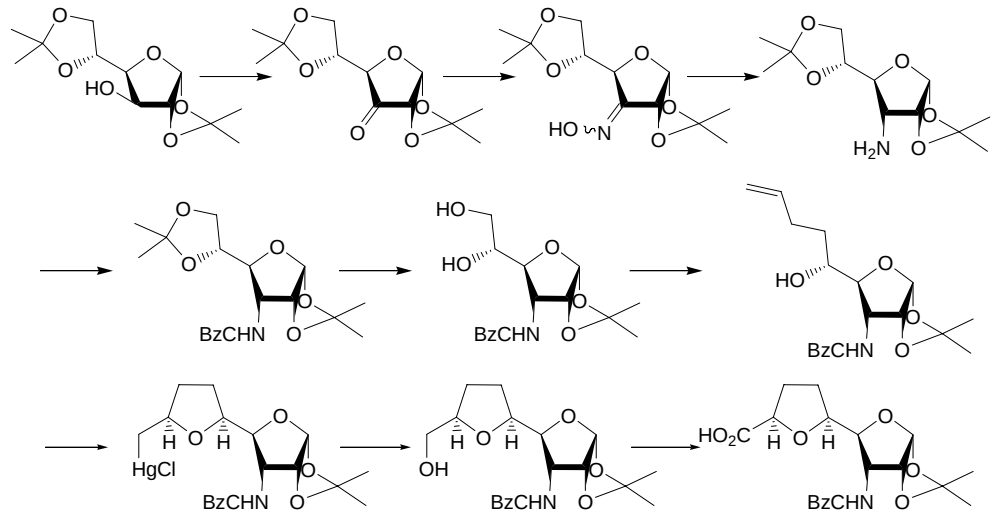

The synthesis started with D-glucose. The diacetonide derivative of glucose is oxidized by PDC and the ketone is converted to oxime followed by LAH reduction gives the desired amine in good yields. This amine on protection followed by selective hydrolysis afforded the diol. Periodate cleavage of the diol followed by treatment with butenyl magnesium bromide gives the secondary alcohol as shown in **scheme 2**.

Scheme 3

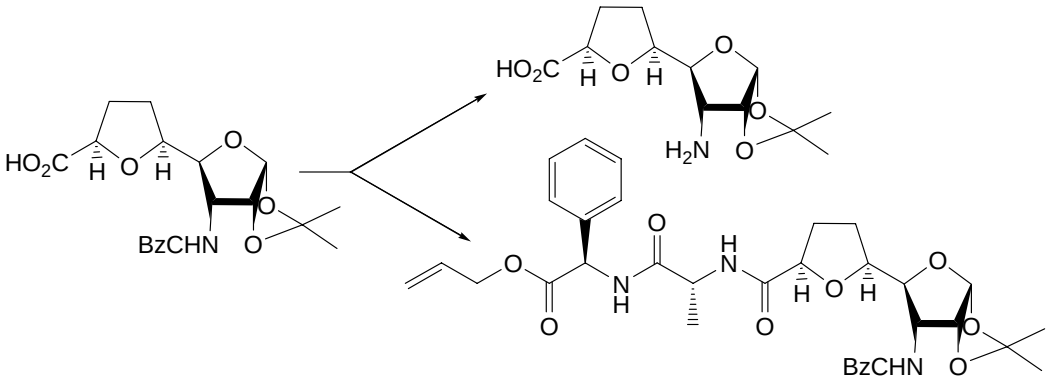

This alcohol is subjected to mercuriation reaction. Chromatographic separation of resulting mercury complex followed by demercuriation of particular complex gives the primary alcohol. This alcohol is oxidized by $RuCl_3$ to achieve the acid functionality at the desired position. The free amino acid is achieved by deprotection of benzyl oxy carbonyl group by hydrogenation conditions. The acid is coupled with a dipeptide obtained from phenyl glycine and alanine to obtain one of the desired products in appreciable yield. All the compounds are confirmed by spectroscopic methods and the activity testing and further investigation of this peptide is under progress.

Chapter III Hydrogen bonding in various carbohydrate systems

Non-covalent interactions underlie all aspects of supramolecular chemistry, including molecular recognition, host–guest chemistry and self-assembly, of synthetic and natural, especially in vivo, systems. One such interaction, hydrogen bonding, has attracted particular attention because of its ubiquity, magnitude, specificity and directionality. Hydrogen bonding in compounds containing hindered alcohol has been an issue of great interest.

Figure 1. Designed Alkynols to Study the Hydrogen Bonding Motifs in Solid State

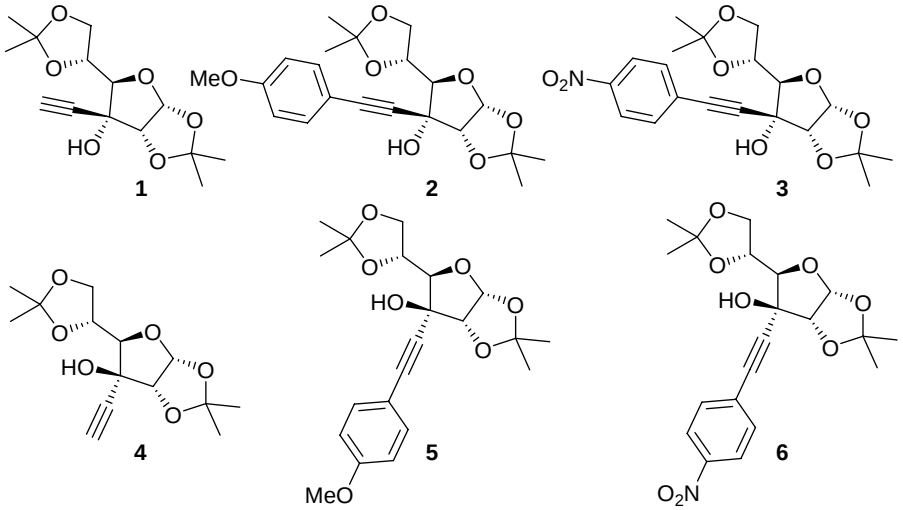

The interplay between the orientation of donor/acceptors and the stability arising due to hydrogen bonding have been fascinating and studied in detail on simple naturally

available bicycles. However, such examinations in carbohydrates systems (where one can anticipate a competition between intra- and intermolecular hydrogen bonding depending upon the relative orientation of the donor/acceptor) are scarce.

Scheme 1

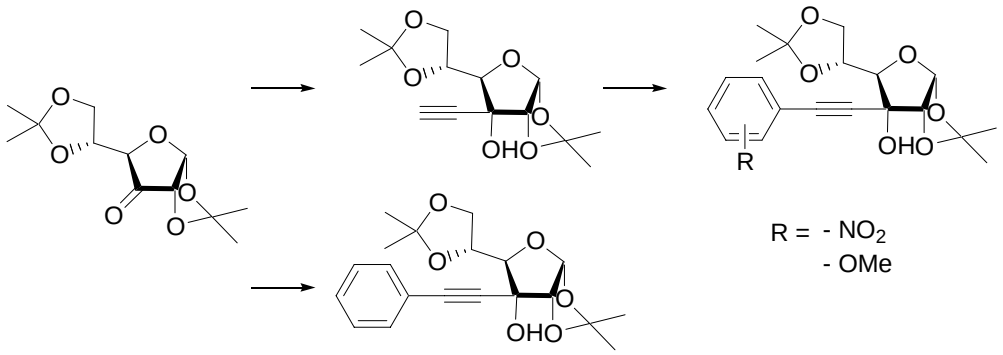

The objective of the present investigation is to understand the relationship between the hydrogen bonding motifs displayed by monoalcohols and the properties of the solids that contain these motifs. The hydrogen bonding motifs displayed by monoalcohols in many systems excluding carbohydrates are described briefly by Bernstein *et. al* and more comprehensively in terms of graph set theory by Brock and Duncan. The free hydroxyl groups in carbohydrate derivatives are unique in being appended on an electron deficient cyclic ether framework, and closely located near to good hydrogen-bond donors as well hydrogen-bond acceptors. As shown in Figure 1, we have designed three pairs of epimeric tertiary alcohols (1 – 6). The D-*allo* configured alcohols 1 – 3 are synthesized according to the reported procedures (scheme 1) and a novel route for the synthesis of D-*gluco* configured alkynols 4 – 6 was developed (Scheme 2).

These four substrates are selected because when the alkyne is attached to the said position the +I effect partially stabilizes the system. The phenyl ring further attached to this alkyne happens to supply extra electrons available with it in its π-clowd. Further this phenyl ring is functionalized with functionality at appropriate position that either destabilize the π-clowd by means of –R effect (-NO_2 group) or stabilize further the π-cloud by +R effect (-OMe group). The synthesis of these derivatives is achieved in good yields as shown in scheme 1 and 2. The repeating pattern of chemical shift in NMR for the free hydroxyl groups is observed in case of both the distereoisomers. Interestingly

when the free hydroxyl group is flanked by 1,2 isopropylidine (allo conformer), the hydrogen bonding for hydroxyl oxygen and isopropylidine methyls is not observed on the contrary they cause inter electronic repulsion and this causes the shielding of free hydroxyl group by almost 0.5 ppm δ value. This trend is observed in case of substituted aromatic protons as well. In some cases the hydrogen bonding is observed between C3 - OH and isopropylidine oxygen and in some cases with furanose oxygen. No hydrogen bonding is observed with side chain oxygens. Various structures form sheet like structure with the hydrogen-bonding framework and few of them form helical network. Only in some cases dimer formation is observed.

Scheme 2

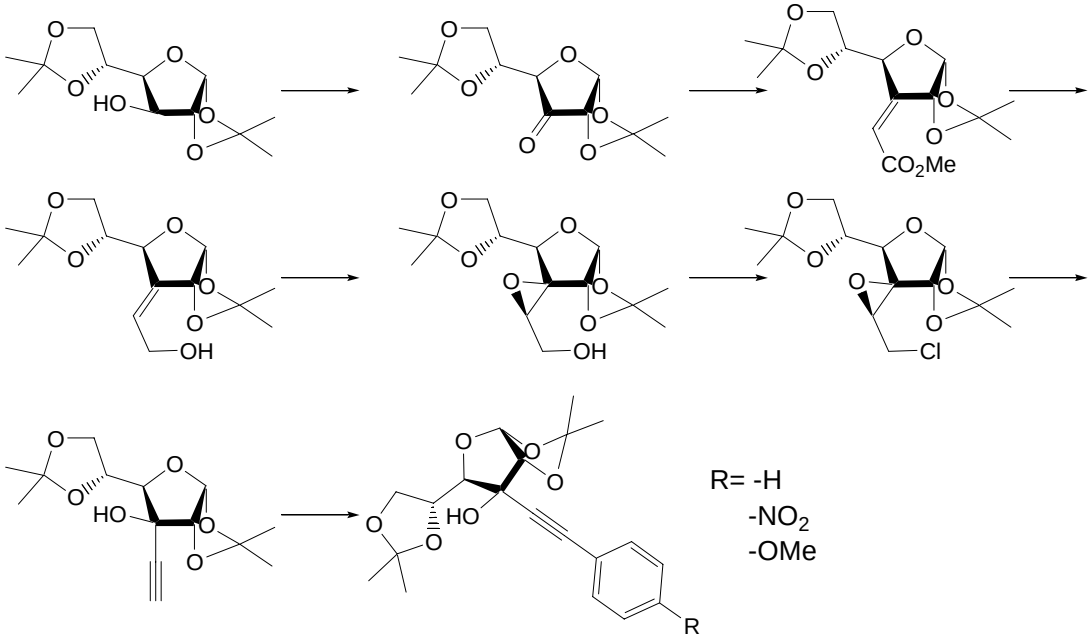

In this connection we investigated the compound named as 3, 5, 6, 7-di-*O*-isopropylidene - D-*glycero* - D-*gulo* - heptono 1, 4 - lactone and here also we observe the same trend of intermolecular hydrogen bonding. Strong helical pattern of crystallization by means of O-H…O intermolecular hydrogen bonding is observed when the molecule is viewed along c axis.